Towards control relevant system design and constrained order controller synthesis

Towards Control Relevant System Design and Constrained Order Controller Synthesis

with a Thermal Control Application in Immersion Lithography

Ruben Merks

Towards Control Relevant System Design and Constrained Order Controller Synthesis

with a Thermal Control Application in Immersion Lithography

PROEFSCHRIFT

ter verkrijging van de graad van doctor aan de
Technische Universiteit Eindhoven, op gezag van de
rector magnificus prof.dr.ir. F.P.T. Baaijens, voor een
commissie aangewezen door het College voor Promoties,
in het openbaar te verdedigen op

woensdag 25 september 2019 om 16:00 uur

door

Ruben Wouterus Henricus Merks

geboren te Eindhoven

Dit proefschrift is goedgekeurd door de promotoren en de samenstelling van de promotiecommisie is als volgt:

voorzitter:	prof.dr.ir. A.B. Smolders
1^e promotor:	prof.dr. S. Weiland
2^e promotor:	prof.dr.ir. H. Butler
leden:	prof.dr.ir. N. van de Wouw
	prof.dr.ir. A.W. Heemink (TU Delft)
	prof.dr.ir. J. Stoustrup (Aalborg University)
adviseurs:	dr.ir. B. Besselink (Rijksuniversiteit Groningen)
	dr.ir. M.E.C. Mutsaers (ASML)

Het onderzoek dat in dit proefschrift wordt beschreven is uitgevoerd in overeenstemming met de TU/e Gedragscode Wetenschapsbeoefening.

This dissertation has been completed in fulfilment of the requirements of the Dutch Institute of Systems and Control (DISC) for graduate study.

This work is part of the Impuls 1 research program with project number 6, which is financed by ASML Netherlands B.V.

Cover Design: Robert den Harink.

Printing: Ridderprint B.V.

A catalogue record is available from the Eindhoven University of Technology Library.

ISBN: 978-90-386-4836-1

Summary

Towards Control Relevant System Design and Constrained Order Controller Synthesis

Photolithographic machines are responsible for a key step in the production of integrated circuits. The societal demand for additional functionality and faster computing is leading to ever increasing requirements on the precision of these machines. A dominant factor that currently limits this precision is the thermally induced deformation of several machine components; and in fact, it is predicted that this problem is one of the main hurdles in the years to come.

The control solutions that are developed in order to deal with this problem, currently rely on so-called classical controller designs. These solutions are, however, reaching the limits of their capabilities. To meet future performance requirements, it is often proposed to utilise optimal control instead. Results have shown—in several applications—that the design of these controllers requires a substantial amount of time and effort, while in many of these applications only a moderate to small increase in performance is achieved. For this reason, optimal control is often regarded as cost-ineffective and rarely applied in industrial applications.

The performance in any optimal control application is determined by the *combined effect* of the system design, the modelling procedure and the control design. These three aspects are in most applications viewed as separate fields of research and it is hypothesised in the introduction that such a separation limits performance. We therefore propose to acquire a better understanding of the relation between these fields, in order to improve both the performance and cost-effectiveness of optimal control.

For each field we will investigate one problem with the aim of bringing us closer to coordinating these three aspects. These three problems, together with the results for a thermal control application, will now briefly be discussed.

Closed-Loop Optimal Actuator and Sensor Selection:

Actuators and sensors are essential components that directly contribute towards the performance in a control system. The question of how many actuators or sensors to use and where to place them is therefore important in many applications. This question is closely related to so-called actuator and sensor selection problems, for which the allowed actuators and sensors must be chosen from a large sets of possible control inputs and measured outputs, respectively. In this way, the placement

problem becomes a combinatorial optimisation problem in which optimal subsets of actuators and sensors need to be determined.

We will consider the problem of selecting the actuators and sensors that maximise closed-loop performance when optimal control is considered. It will be shown that the controller must, indeed, be taken into account with such a selection problem. Therefore, the problem of designing an optimal actuator configuration for a fixed sensor configuration is investigated. In addition, the dual problem of designing an optimal sensor configuration for a fixed actuator configuration is discussed.

Control Relevant Order Reduction:

For the control of thermally induced deformations, it is required to build models that commonly contain well over $10,000$ states. It is often not possible to directly design an optimal controller on the basis of such a model due to computational constraints. A common method to overcome this problem, is to utilise model and controller order reduction.

For this reason, the use of order reduction in combination with optimal controller design is investigated. It is shown that several existing (control relevant) order reduction techniques do not provide sufficient guarantees on performance when optimal control is considered. In fact, it is shown that—in some cases—the absence of control leads to a better performance than the reduced order control design techniques that are advocated in literature. Improvements to these techniques are therefore proposed.

Minimal Order Optimal Control:

As explained above, the problem of constructing a low order controller for a high order system is solved in practice by utilising model order reduction techniques. Such an "indirect" approach is taken, because there does not exist a solution that directly addresses the problem from an optimal control perspective.

In this thesis we will discuss "direct" control design methods, which aim to construct a controller of minimal order that achieves optimal closed-loop performance for a given high order system. By investigating the so-called disturbance decoupling problems, it is shown that there exist H_2 optimal controllers of reduced order; i.e. the controller order can, in general, be smaller than the system order. Furthermore, preliminary results on the numerical construction of these reduced order optimal controllers are discussed.

The Results for a Thermal Control Application:

Finally, the importance of coordinating the system design, the modelling procedure and control design is demonstrated on a numerical model that describes the thermally induced deformations of a specific machine component. For this model, the relatively simple classical control solutions are able to reduce imaging errors from approximately 15 nm to 1.8 nm in magnitude. In the future it will be required to reduce these errors below 1 nm. For this type of controller, however, the introduc-

tion of additional sensors and actuators does not lead to a significant improvement in performance.

By considering H_2 optimal control without improving the system, a significant improvement in performance cannot be achieved either. At the same time, the introduction of H_2 optimal control is accompanied by additional freedom in the system design. It is shown that the imaging errors can (significantly) be reduced to 0.4 nm in magnitude when H_2 optimal control is introduced and this additional freedom is exploited.

Contents

Summary **vii**

List of Abbreviations **xiii**

1 Introduction **1**

1.1 Motivation and Background Information 2
1.2 The Control of Thermally Induced Deformations 9
1.3 Control Relevant Modelling and System Design 18
1.4 Research Questions 20
1.5 Outline of the Thesis 23

2 Mathematical Preliminaries **27**

2.1 Mathematical Notation 28
2.2 Basic Notions from Systems and Control Theory 34
2.3 Linear Matrix Inequalities in Control 42
2.4 H_2 Optimal Control 43
2.5 Geometric Control Theory 61

3 Actuator and Sensor Selection for Control **69**

3.1 Introduction 70
3.2 Modularity and Greedy Algorithms 75
3.3 Sparsity Promoting Controller Design 86
3.4 Performance Analysis on a Practical Example 93

4 Control Relevant Order Reduction **101**

4.1 Introduction 102
4.2 Balancing-Based Order Reduction Techniques for Control 107
4.3 The Non-Optimality of Closed-Loop Order Reduction for Constrained Order Control 122

4.4 Proposed Improvements 124
4.5 Fixed Order Optimisation 127

5 Minimal Order Optimal Estimation and Control 135
5.1 Introduction 136
5.2 The Disturbance Decoupled Estimation Problem with a Constrained Order Estimator 139
5.3 The Disturbance Decoupling Problem with Measurement Feedback using a Constrained Order Controller 150
5.4 H_2 Optimal Estimation and Control with a Constrained Order . . . 169

6 Results for a Thermal Control Application 185
6.1 The Control of Thermally Induced Deformations 186
6.2 Controller Design 190
6.3 Improved System Design 193
6.4 Constrained Order Controller Design 199

7 To Conclude this Thesis 203
7.1 Conclusions and Future Work 204
7.2 Implications for Industry and Academia 209

A Mathematical Proofs 213
A.1 Proofs for Chapter 2 214
A.2 Proofs for Chapter 3 219
A.3 Proofs for Chapter 5 220

B Additional Equations for Chapter 5 231

Bibliography 235

List of Publications 247

Acknowledgements/Dankwoord 251

About the Author 257

List of Abbreviations

ADMM	Alternating Direction Method of Multipliers
ARE	Algebraic Riccati Equation
BES	Bubble Extraction System
BIBO	Bounded-Input Bounded-Output
BT	Balanced Truncation
CD	Critical Dimension
COR	Controller Order Reduction
DDEP(S)(-CO)	Disturbance Decoupled Estimation Problem (with Stability)(using a Constrained Order Estimator)
DDP(S)	Disturbance Decoupling Problem (with Stability)
DDPM(S)(-CO)	Disturbance Decoupling Problem with Measurement Feedback (and Stability)(using a Constrained Order Controller)
DOF	Depth of Focus
DUV	Deep Ultraviolet
EUV	Extreme Ultraviolet
FEM	Finite Element Method
FVM	Finite Volume Method
HIFOO	H_∞-H_2 Fixed Order Optimisation
IC	Integrated Circuit
LMI	Linear Matrix Inequality
LQG(-BT)	Linear Quadratic Gaussian (Balanced Truncation)
LTI	Linear and Time-Invariant
MIMO	Multiple-Input Multiple-Output
MOR	Model Order Reduction

NA	Numerical Aperture
ODE	Ordinary Differential Equation
PDE	Partial Differential Equation
PID	Proportional-Integral-Derivative
ROM	Reduced Order Model
SISO	Single-Input Single-Output
SVD	Singular Value Decomposition
WOR	Weighted Order Reduction

The true function of philosophy is to educate us in the principles of reasoning and not to put an end to further reasoning by the introduction of fixed conclusions.

George Henry Lewes

1 Introduction

Lithographic machines are responsible for a key step in the production of integrated circuits. The societal demand for additional functionality and faster computing is leading to ever increasing requirements on the precision of these machines. A dominant factor that currently limits this precision is the thermally induced deformation of several machine components; and in fact, it is predicted that this problem is one of the main hurdles in the years to come.

The control solutions that are developed in order to deal with this problem, currently rely on so-called classical controller designs. These solutions are, however, reaching the limits of their capabilities. To meet future performance requirements, it is often proposed to utilise optimal control instead. Results have shown—in several applications—that the design of these controllers requires a substantial amount of time and effort, while in many of these applications only a moderate to small increase in performance is achieved. For this reason, optimal control is often regarded as cost-ineffective and rarely applied in industrial applications.

The performance in any optimal control application is determined by the *combined effect* of the system design, modelling procedure and control design. These three aspects are in most applications viewed as separate fields of research and it is hypothesised in this chapter that such a separation limits its performance. We therefore propose to acquire a better understanding of the relation between these fields, in order to improve both the performance and cost-effectiveness of optimal control.

1.1 Motivation and Background Information

In 1990—the year that I was born—navigation of a car could cause a lot of stress in an otherwise happy marriage. At that time, a person could probably not imagine that a pocket-size device would soon be capable of performing such a complex task. Nowadays, most people cannot imagine life without their smartphone which is capable of navigation, taking photos, several types of communication and showing live television. As users we often take these technological developments for granted and it is easy to overlook the incredibly complex problems that have to be overcome in order to develop these devices.

Improvements in the performance of digital computers have been at the heart of nearly all of these technological breakthroughs. With these improvements, the production of computers has become an extremely high precision process and the companies involved are therefore facing ever increasing performance requirements—as reported in the Semiconductor Industry Association [2015] roadmap.

The research as presented in this thesis is funded by ASML Netherlands B.V. ASML produces (photo)lithographic machines that are responsible for a key step in the production of digital computers. A major factor that currently limits the precision of these machines, is the thermally induced deformation of several machine components; for example, deformation of the mirrors in the optical system as explained by Bikcora et al. [2014] and Habets et al. [2015]. In fact, it is predicted that these thermal effects are one of the main hurdles that the company will face in the years to come.

At this moment, a set of relatively simple control solutions is applied in order to deal with these problems. These solutions are, however, reaching the limits of their capabilities and it remains unclear how further improvements can be made. The research as presented in this thesis is therefore directly aiming to get a better understanding of these problems and, based on this knowledge, to improve the control solutions that are currently in place. Before addressing the control of thermally induced deformations, let us first establish how and why the production of computers has become such a high-precision process.

1.1.1 Moore's Law

A typical computer consists of several integrated circuits (ICs)—better known as "chips". Such an IC contains a large number of transistors that determine its speed and efficiency, which is explained in great detail by Toumazou et al. [2002, Ch. 3]. The speed of an IC relates to the amount of instructions (i.e. calculations) that can be performed per second; efficiency relates to power consumption of and heat generation within the IC.

A fast IC is created by performing tasks in parallel, which requires the use of a large number of transistors. IC manufacturers are therefore continuously making efforts to increase this number. In 1965—before the introduction of the first commercially available IC—it was observed by Moore [1965] that the number of transistors on

an IC approximately doubles every year. Ten years later Moore [1975] re-evaluated this observation and predicted a doubling per two years for the future.

This prediction has become self fulfilling to some extend and today it is best known as "Moore's law". A more detailed description of this law and its implications for other industries can be found in many on-line sources such as Wikipedia [2018b]. As a result of this law, the amount of transistors on an IC has increased from $10,000$ up to $10,000,000,000$ in less than 50 years of time; this continuous and enormous increase is graphically depicted in figure 1.1.

In the engineering world, almost everything comes at a price. An increase in the amount of transistors on an IC therefore comes with a number of challenges as well. First of all, each individual transistor consumes a certain amount of power and will generate heat. A larger number of transistors will therefore consume more power in total and will generate more heat, which both have a negative impact on the speed of an IC—as explained by Toumazou et al. [2002, Ch. 3]. Furthermore, the velocity at which information travels along a wire imposes an upper limit on the size of an IC and therefore also on the number of transistors. To put this into perspective, a typical IC is nowadays capable of performing over $50,000,000,000$ instructions per second. Assuming that this information travels at the speed of light, a maximum distance of 0.6 cm can be covered in the timespan of one instruction.

The amount of transistors and the number of instructions per second can therefore only be increased simultaneously, if the transistors themselves are reduced in size. Another advantage of smaller transistors is that they are typically faster, require less power and will generate less heat—as explained by Toumazou et al. [2002, Ch. 3]. The overall size of a typical IC has, as a consequence, remained nearly constant over the past 50 years and the *area* per transistor is therefore inversely related to the amount of transistors per IC. This implies that the *size* of a transistor halves every four years, as is shown in figure 1.2.

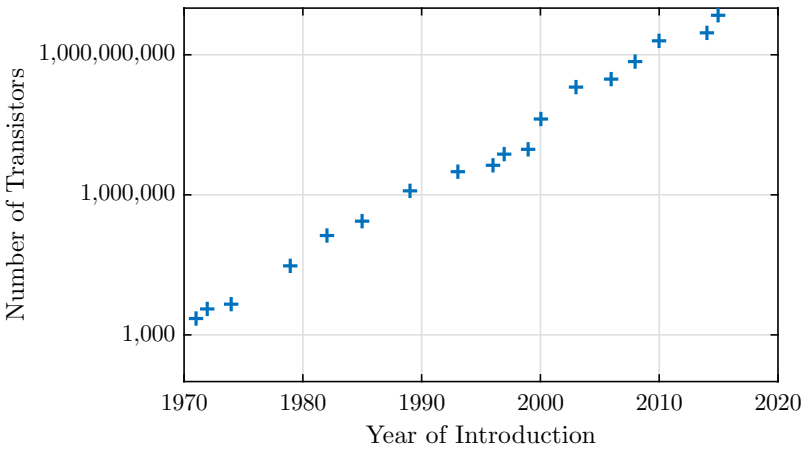

Figure 1.1: The number of transistors as a function of the introduction date for several ICs.

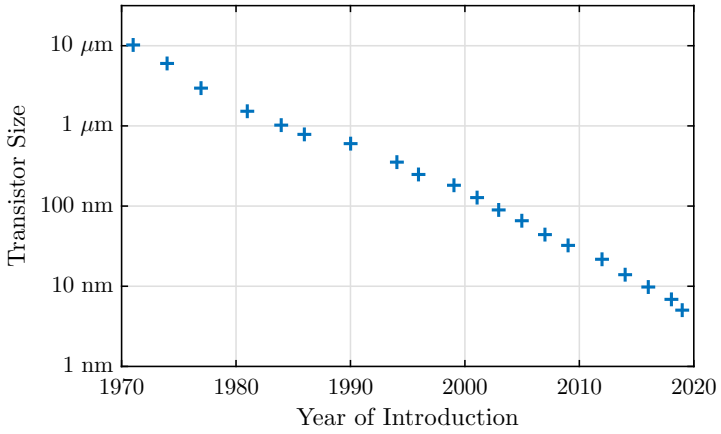

Figure 1.2: The transistor size as a function of the introduction date for several technology nodes in IC production.

1.1.2 Manufacturing of Integrated Circuits

Now let us briefly discuss the main steps that are taken in the IC production process. For this purpose, consider the schematic overview in figure 1.3. Please note that a more detailed description of all steps involved is given by Mack [2007, Ch. 1].

The production of an IC starts with a silicon boule that is sliced into so-called wafers. Several ICs—which are a three dimensional structure that is built up by 20 to 30 layers—are created on the top surface of such a wafer. After this entire structure is built, the wafer is cut into separate ICs that are ready for packaging.

For each layer, the wafer surface is first coated with a light-sensitive material that is called a photoresist. An illumination pattern is then applied to this coated surface during the exposure step, which changes certain material properties of the photoresist—e.g. the photoresist hardens under the influence of light. In this way, the light and photoresist are combined in order to protect certain areas on the wafer surface from processes like etching and ion implantation. The layer is finalised by removing the remaining photoresist afterwards.

1.1.3 Photolithography

The (photo)lithographic machines that ASML produces are responsible for the exposure step in figure 1.3. During this step an illumination pattern is created on the top surface of a wafer, as described above. It is explained by Ito and Okazaki [2000] that the performance of these machines is the driving force behind Moore's Law, because smaller transistors can only be created when the features of the illumination pattern become smaller.

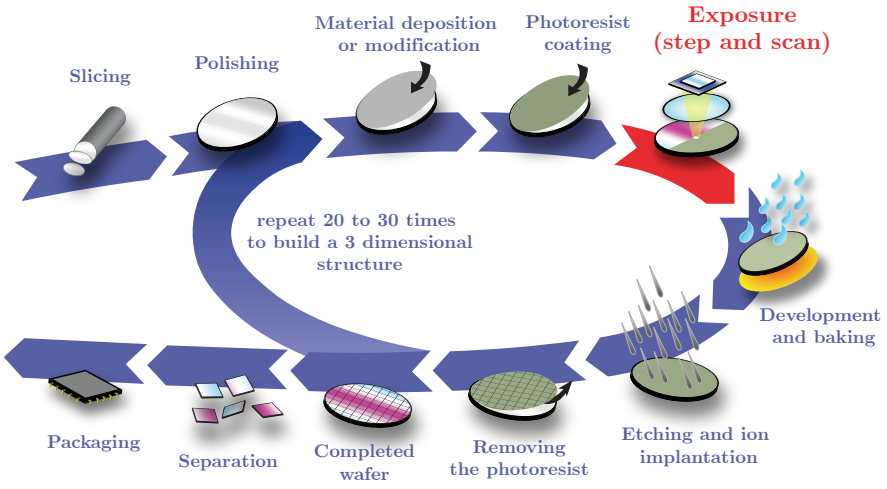

Figure 1.3: A schematic overview of the production process for ICs. (Courtesy of ASML Netherlands B.V.)

The performance of these lithographic machines is measured in terms of throughput and the critical dimension (CD). These measures are therefore addressed in great detail at public presentations by Van den Brink [2016]—the company's chief technical officer. Throughput is often measured by the amount of wafer layers that can be exposed per hour, which is an important measure for the industry since lithographic machines are used for mass production of ICs. The CD is a measure for the minimum feature size within the illumination pattern at the wafer. This CD is strongly related to the minimum size of a transistor and therefore limits the amount of transistors on an IC[1].

In lithography, a pattern is created on the wafer surface by illuminating the so-called photomask as depicted at the top of figure 1.4. This mask is in essence a larger version of the desired illumination pattern at the wafer, while an optical system is used to scale this pattern down to the desired size. Diffraction of light imposes a theoretical limit on the CD of such a process, as is discussed in great detail by Mack [2007, Sec. 10.1]. This limit is approximately given by

$$CD = k_1 \frac{\lambda}{NA},$$

where k_1 describes several process-related effects, λ is the wavelength of the light (in vacuum) that is used and NA is the numerical aperture of the optical system.

ASML is continuously making efforts to minimise this fundamental limit on the CD of their machines, while maintaining a sufficiently high throughput. Over the

[1] Multiple patterning technique, as explained by Drapeau et al. [2007], are currently used to create features that are smaller than the CD. A reduction in the CD therefore allows transistors to become smaller; these numbers are, however, not a *directly* related.

past decades, state of the art machines have utilised immersion lithography and deep ultraviolet (DUV) light with a wavelength of $\lambda = 193$ nm. These machines currently have a throughput of 275 wafers per hour and a critical dimension of $CD = 38$ nm. The fact that water has a higher refractive index than air is used in immersion lithography to raise the NA of the system—as explained by Mack [2007, sec. 3.7]. In this way a numerical aperture of $NA = 1.35$ is achieved, which is well above the theoretical limit of 1.0 that can be achieved with an infinitely large optical system in "dry" lithography.

In order to further reduce the CD in the future, the use of extreme ultraviolet light (EUV) with a wavelength of $\lambda = 13.5$ nm is proposed—as explained by Lin [2018]. The introduction of EUV light does, however, come with many technical challenges and it has taken approximately 15 years to develop the first commercially viable EUV machine. Current state of the art EUV machines have a critical dimension of $CD = 13$ nm, which is a substantial improvement with respect to the DUV machines. Nevertheless, these machines should still be improved since their throughput is currently limited to 125 wafers per hour.

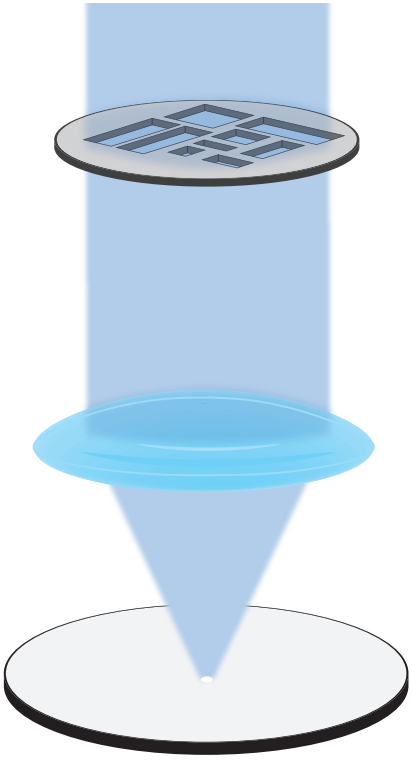

Figure 1.4: A simplified visualisation of the (photo)lithographic process.

1.1.4 Focus and Overlay Errors

Reducing the theoretical limit on the CD is not the only challenge in lithography. For example, incorrect alignment of several components in a machine could shift and deform the illumination pattern at the wafer, which leads to undesired imaging errors. These errors are often categorised as overlay errors and focus errors.

So-called in-plane errors are caused by a shift or deformation of the illumination pattern that is tangential to the wafer surface. This type of error is not directly problematic when a layer is added to the wafer, because the pattern itself remains nearly unchanged. However, a misalignment could arise between subsequent layers when these shifts and deformations vary over time. Alignment errors between the layers of an IC are called overlay errors and it is important that these errors are several factors smaller than the CD, as explained by Megens [2007].

Out-of-plane errors are, on the other hand, caused by a shift or deformation of the illumination pattern that is orthogonal to the wafer surface. This type of error is the main cause of focus errors, which lead to undesired smoothing effects at the corners of features[1]. Mack and Lin [1988] explain in great detail how the requirements on orthogonal alignment of the wafer surface are determined by Rayleigh depth of focus (DOF). This quantity is approximately given by

$$DOF = k_2 \frac{\lambda}{NA^2},$$

where k_2 is another process dependent constant. It is important to note that the CD and the DOF are typically similar in order. This implies that the requirements on focus are often less strict than the requirements on overlay, since the latter should be several orders smaller in magnitude.

1.1.5 Thermally Induced Deformations

So far we have seen that it is important for ASML to create a sharp, undeformed and correctly aligned illumination pattern on the surface of a wafer. It is therefore also required that the wafer surface itself is correctly aligned by a positioning system. Vibration effects of the wafer and this positioning system have been a substantial source of imaging errors in the past. Nowadays, however, thermal disturbances have become a substantial source of errors. These disturbances come from several sources, such as

- dissipation energy which is generated by electrical currents in the linear motors of the wafer positioning system.
- evaporation of water in the immersion system.
- the absorption of DUV or EUV light by the wafer.

During exposure, the wafer is clamped onto a wafer table as depicted in figure 1.5. Thermal disturbances do, however, cause temperature variations of around 1 K in the wafer and wafer table, which—due to thermal expansion—lead to wafer surface

[1] Theoretically speaking, some degree of smoothing is always expected due to the diffraction of light; focus errors are therefore increasing this undesired effect.

deformations in the order of 10 nm. As a rule of thumb, these deformations lead to imaging errors that are similar magnitude when no corrective measure is taken. In lithography the performance requirements have become so demanding that this effect is considered to be one of the dominant factors that limits precision.

To put this into perspective, Van den Brink [2016] predicted that mass production of ICs with features in the order of 7 nm should have started at the end of 2018; according to Wikipedia [2018a] this prediction was correct. In order to create these ICs, it is important that overlay errors are smaller than 3 nm in magnitude. This is approximately a factor 3 smaller than the "uncontrolled" thermally induced wafer surface deformations of 10 nm. We can therefore conclude that the imaging errors as a result of these deformations must be reduced by several orders in magnitude; for example, by implementing a number of preventive and corrective measures.

Preventive measures aim at directly minimising the wafer surface deformations during operation. This could, for example, be achieved by introducing heaters, coolers or thermal isolation with the aim of minimising temperature changes in the system. With a corrective measure on the other hand, the wafer surface deformations remain unchanged, while an improvement is made by reducing the imaging errors as a result of these deformations. An example of this is calibration, which utilises wafer alignment to compensate for the imaging errors that each machine produces on average.

The research as presented in this thesis is mainly focussed on the development of tools and theory that can be used to create the next generation of preventive and corrective measures for this type of application. More specifically, the focus will be on system, estimator and measurement feedback controller design.

Figure 1.5: A wafer table (Source: Amcoss [2019]).

1.2 The Control of Thermally Induced Deformations

In section 1.1 it is explained why preventive and corrective measures are required in order to reduce imaging errors as a result of thermally induced deformations of the wafer surface. Such measures aim at minimising the effect that unknown disturbances have on certain quantities, which in control theory is referred to as "disturbance rejection". Measurement feedback controllers are well-suited for dealing with type of control problem, as explained by Franklin et al. [2015, Ch. 1].

In this section we will fist introduce the application and some basic notions from systems and control theory. The rationale behind the theory involved is explained later in chapter 2. Secondly, we will take a closer look at the system design methodology and the controllers that are currently used in the application; followed by a discussion on improvements that are proposed for the future. It is, however, important to note that a similar methodology is applied in a wide range of applications. E.g. electronic power steering (Mehrabi [2014]), vibration control (Verkerk [2018]) and several systems in the process industry (Subawalla et al. [1996]). For this reason the analysis will be performed by using the generic systems and control framework.

1.2.1 The Application

As application, we will consider the design of a controller in DUV lithography, which aims at minimising the imaging errors caused by a thermal disturbance that is introduced by the immersion system. In order to introduce this disturbance, consider a cross section of the wafer, wafer table and immersion system as depicted in figure 1.6.

A potential problem arises during exposure, when the immersion system crosses the wafer edge. Namely, a pocket of air is trapped by water which leads to the formation of air bubbles; these bubbles could—due to the scattering of light as explained by Davis [1955]—cause severe imaging errors. A bubble extraction system (BES) is therefore used, which essentially creates a low pressure in the gap between the wafer and wafer table in order to draw the bubbles away from the immersion system—as explained by Hanema [2018].

Within the BES, however, air with a low relative humidity is flowing in a channel that contains water. This causes some water to evaporate, which is an endothermic process (Gold [2014]) and heat is removed from the system. The wafer table and the wafer cool down by approximately 0.8 K as a result of this thermal disturbance, which causes wafer surface deformations in the order of 11 nm.

Wafer surface deformations are strongly related to imaging errors. To explain this relation, we start by observing from figure 1.6 that only a small section of the wafer surface is exposed to light at any time instance. Imaging errors are therefore caused by deformations at the location of illumination. More specifically, overlay errors are caused by in-plane deformations (i.e. in the x and y direction) and focus

errors by out-of plane deformations (i.e. in the z direction) at this so-called point of interest.

In order to minimise imaging errors, preventive measures should therefore aim at minimising the wafer surface deformations around this moving point of interest. Deformations at other locations could, however, also cause other undesired effects; for example, the wafer could start slipping with respect to the wafer table. In order to avoid this type of effect, it is for this application decided to not take the location of illumination into account and to minimise all wafer surface deformations instead.

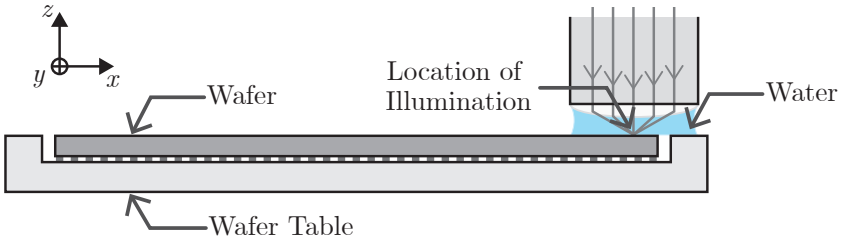

Figure 1.6: A cross section of the wafer, wafer table, immersion system and bubble extraction system.

1.2.2 Linear and Time-invariant Systems and Controllers

With controller design for disturbance rejection problems, a feedback interconnection as depicted in figure 1.7 is typically considered. In this figure, the system is denoted by Σ, the controller by Σ_c and the quantities of interest are denoted by signals $w(t)$, $u(t)$, $y(t)$ and $z(t)$, which are functions of time t. The interconnection between Σ and Σ_c is called the closed-loop system, which is denoted by Σ_{cl}.

The disturbance $w(t)$ represents all unknown external quantities that cannot be affected or controlled, but which do influence the system. Examples are the evaporative load as explained above and noise that affects the measured output $y(t)$.

The control input $u(t)$, on the other hand, represents all external quantities that can be utilised in order to manipulate the system during operation. Examples are the heating power generated by a heater and the flow rate of water in a cooling channel.

The measured output $y(t)$ represents all internal quantities of the system which are measured by sensors during operation. Examples are hall sensors that measure electrical currents and temperature sensors that measure temperature at a specific location. These measurements are in practice affected by noise, which is often described as an external disturbance $w(t)$ that directly affects these measurements.

Finally, the control output $z(t)$ represents all internal quantities of the system which should be altered by the controller. Examples are the wafer surface deformations and the resulting imaging errors, which both should be reduced in magnitude.

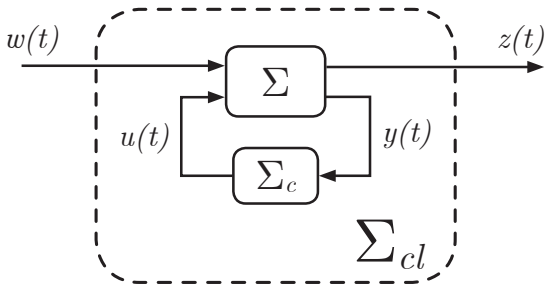

Figure 1.7: The closed-loop interconnection between the system Σ and a measurement feedback controller Σ_c.

A norm is often used to describe the magnitude of a time dependent quantity with a single number—for more information about norms, consider reading the work by Kreyszig [1989, Ch. 2,3]. Norms are denoted by $\| \cdot \|$, for example $\|z(t)|_{t=t_0}\|$ denotes the norm of z at time t_0 and $\|z(t)\|$ denotes the norm of the entire signal[1].

At this moment a conceptual definition for system, controller and closed-loop system have been given. However, we still require a mathematical formulation that describes the relation between the signals of interest. In control applications, linear and time-invariant (LTI) continuous-time state-space systems are often considered, which are defined as

$$\Sigma = \begin{cases} \dot{x}(t) = Ax(t) + B_u u(t) + B_w w(t) \\ y(t) = C_y x(t) + D_{wy} w(t) \\ z(t) = C_z x(t) + D_{uz} u(t), \end{cases} \tag{1.1}$$

where $\dot{x}(t)$ denotes the derivative of $x(t)$ with respect to time t. The quantities $w(t)$, $u(t)$, $y(t)$ and $z(t)$ as depicted in figure 1.7 are represented mathematically by vector signals of dimension n_w, n_u, n_y and n_z, respectively. In addition, the internal state of the system is described by $x(t)$, which is a vector signal of dimension n_x; this state dimension is also called the *system order*. Finally, the dynamical relation between all signals is described by real-valued matrices of appropriate dimension.

For this type of system it is often considered to use an LTI controller, which is mathematically defined as

$$\Sigma_{c,n_c} = \begin{cases} \dot{x}_c(t) = Jx_c(t) + Ky(t) \\ u(t) = Mx_c(t) + Ny(t). \end{cases} \tag{1.2}$$

The dimensions of the inputs and outputs of such a controller are determined by Σ (1.1). Its internal state is described by the vector signal $x_c(t)$ of dimension n_c; this dimension is called the *controller order* and the dynamical relation between all signals is again defined by real-valued matrices of appropriate dimension.

[1] Norms will formally be defined in chapter 2 and at this moment it suffices to know that the norm of a signal describes its magnitude.

Finally, Σ (1.1) can be interconnected with Σ_{c,n_c} (1.2) in order to mathematically define the closed-loop system as

$$\Sigma_{cl,n_c} = \left\{ \begin{array}{rcl} \begin{pmatrix} \dot{x}(t) \\ \dot{x}_c(t) \end{pmatrix} & = & \begin{pmatrix} A + B_u N C_y & B_u M \\ K C_y & J \end{pmatrix} \begin{pmatrix} x(t) \\ x_c(t) \end{pmatrix} + \begin{pmatrix} B_w + B_u N D_{wy} \\ K D_{wy} \end{pmatrix} w(t) \\ z(t) & = & \begin{pmatrix} C_z + D_{uz} N C_y & D_{uz} M \end{pmatrix} \begin{pmatrix} x(t) \\ x_c(t) \end{pmatrix} + \left(D_{uz} N D_{wy} \right) w(t). \end{array} \right. \tag{1.3}$$

The aim with disturbance rejection by measurement feedback is to design a controller Σ_{c,n_c} (1.2) such that the effect of $w(t)$ on $z(t)$ is reduced for the closed-loop system Σ_{cl,n_c} (1.3). A system norm is often used in order to quantify with one number how much $w(t)$ affects $z(t)$; for Σ_{cl,n_c} (1.3) this norm is denoted by $\|\Sigma_{cl,n_c}\|$[1].

In addition to reducing $\|\Sigma_{cl,n_c}\|$, it is in practice required that the closed-loop system is internally stable. Σ_{cl,n_c} (1.3) is said to be internally stable if for all initial conditions $x(0) = x_0$, $x_c(0) = x_{c,0}$ and all bounded signals $w(t)$, the states $x(t)$ and $x_c(t)$ also remain bounded for all $t \geq 0$.

1.2.3 Classical Control

Feedback controllers have successfully been applied in many applications where some degree of disturbance rejection is required—see for example the works by Liu et al. [2016] Yang et al. [2018] Zhao et al. [2015]. In order to reduce the potential for problems and the resulting delay during development, it is often viewed as good engineering practice to start with a relatively simple solution. For the considered application, it is therefore decided to first apply classical controller designs such as Proportional-Integral-Derivative (PID) controllers.

With classical controller design, the aim is to control a quantity that is directly measured during operation. This is equivalent to requiring that $y(t) = z(t)$—i.e. you measure what you want to control—which in this application requires the deformations to be measured. It is, however, technically not possible to continuously measure around 10 nm accuracy and a different physical quantity must be measured instead. To determine what quantities could be considered, let us first establish how the dynamics in this application can mathematically be described.

The dynamics behind thermally induced deformations are physically governed by thermal diffusion and convection, combined with with mechanical elasticity—as explained by Van den Hurk et al. [2018]. Both the thermal and the mechanical behaviour is mathematically described by linear partial differential equations (PDEs), which are coupled though (linear) thermal expansion. These coupled PDEs can be transformed into a, potentially large, set of linear ordinary differential equations (ODEs) with the separation of variables technique as discussed by Renardy and Rogers [2004, Sec. 1.2]. The dynamical behaviour for this application can therefore be described mathematically by Σ (1.1).

[1]System norms will formally be defined in chapter 2 and at this moment it suffices to know that such a norm quantifies how much $w(t)$ affects $z(t)$.

It has also been shown by Van den Hurk et al. [2018] that the thermal behaviour is much slower than the mechanical behaviour in this type of application. The latter can therefore be considered to be an instantaneous effect (i.e. without dynamics). The state of the system is, as a consequence, described by temperature variations with respect to some reference temperature[2], while the deformations are described by linear combinations of this state. In this way, the dynamical behaviour of the system can be interpreted as follows. The thermal disturbances $w(t)$ directly affect the state $x(t)$, while the wafer surface deformations $z(t)$ are a linear function of state.

Sensors and Actuators

In terms of magnitude, a relation between deformations and temperature variations can now be established for Σ (1.1), which is given by

$$\|z(t)\| = \|C_z x(t)\| \leq \|C_z\| \, \|x(t)\| \, .$$

From this inequality we can observe that the deformations are reduced in magnitude by reducing the temperature variations in the system. It is therefore decided to minimise temperature variations at specific locations that are measured using temperature sensors. This also implies that actuation must be performed in the thermal domain and, because the main disturbance in the considered application is a cooling load, it is therefore decided to utilise heaters.

The next step is to determine the location for and the amount of sensors and actuators that are used for control. A common design philosophy is to place both the sensors and actuators close to where the disturbances enter the system. The disturbances are mainly located at the outer edge of the wafer table, which implies that the sensors and actuators are—as depicted in figure 1.8—placed at the outer edge as well.

Finally, it is important to mention that single-input single-output (SISO) controller architectures are often considered in classical control, which implies that each measured output $y(t)$ is paired with a control input $u(t)$. A typical system design therefore has an equal amount of sensors and actuators, as can be observed in figure 1.8 as well. However, the interaction between these SISO controllers—which is not taken into account in the controller design—could lead to stability issues that limit performance[3]. This potential loss of performance is often minimised by limiting the amount of sensors and actuators; and by collocating each sensor with an actuator.

[2] By considering temperature variations with respect to some reference, it is essentially assumed that there are no deformations at this temperature.

[3] Several techniques—such as sequential loop closing as introduced by Bernstein [1987]—have been developed in order to reduce this loss of performance. These techniques could potentially allow the introduction of additional pairs of sensors and actuators as well; however, their placement is preferably still performed according to these rules.

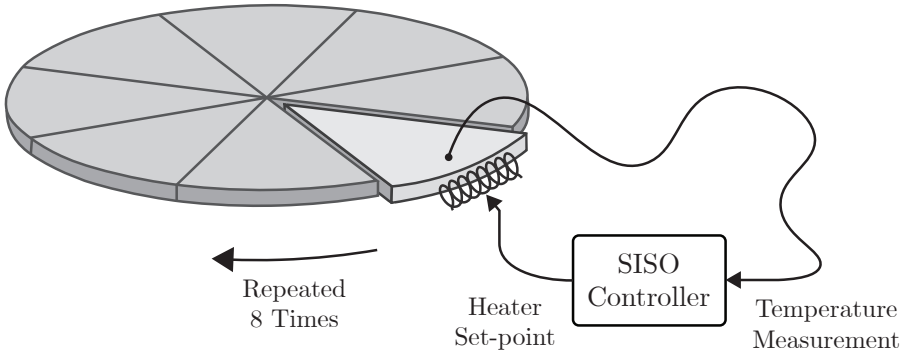

Figure 1.8: A typical SISO controller configuration that is used for classical control.

Modelling and Controller Design

The theory regarding classical controller design is well-documented in numerous textbooks; for example the books by Franklin et al. [2015], Åström and Murray [2012]. For these controllers, models are utilised that accurately describe the system behaviour for each sensor-actuator pair. One often considers transfer functions and state-space models such as Σ (1.1) for this purpose. For the control of thermally induced deformation with classical controllers, the aim is to minimise the measured temperature changes as a result of the disturbances that act on the system. However, during the design of such a controller it is also important to guarantee that sensor noise does not introduce unnecessary temperature variations, which leads to a design trade-off.

Models are typically used in classical control to decide on an initial controller design, while the parameters of this controller are optimised for the real system—for example, on the basis of data from experiments. This data is typically gathered from frequency response measurements, or by measuring impulse and step responses. The model accuracy does therefore not completely determine the control performance and a relatively simple model is often used for this type of controller design.

1.2.4 Optimal Control

Classical control has successfully been used in order to reduce the imaging errors as a result of the BES from approximately 11 nm to 1.8 nm in magnitude[1]. For the future, however, this accuracy should meet values below 1 nm.

Currently there are numerous factors that introduce conservatism in the controller design. For example, it is assumed that the system behaves linearly, does not

[1]These numbers follow from an example system in chapter 6 and are only an indication for the relative increase in performance.

change over time, modelling errors are not considered and the location of illumination is not taken into account. Furthermore, the decision to consider classical controllers implies that temperature must be controlled instead of deformations and that the coupling between SISO controllers is not explicitly taken into account. For this reason, optimal control is regarded as a potential solution for the future. Furthermore, changes in control can be viewed as a software update that requires only minor adjustments in the system, which makes them preferable over hardware changes.

Controller Design

The aim with classical controller design is to control a measured quantity. For the considered application, however, we did see that it is not always possible to measure all quantities of interest. One method of dealing with this limitation is to utilise a model that describes the relation between the known quantities $u(t)$ and $y(t)$ and which, in addition, describes their relation to the unknown quantities $w(t)$ and $z(t)$.

Such a model can be used by a controller that, similarly to classical control design, determines $u(t)$ on the basis of $y(t)$; but this time in such a way that—according to the model—the magnitude of $z(t)$ as a result of unknown disturbances $w(t)$ is reduced. In addition, it is possible to introduce a notion of optimality when this model is described by Σ (1.1), which leads to the following well-known optimal control problem.

Problem 1.1 *Construct a stabilising optimal controller $\Sigma^\star_{c,n_c}$ of the form* (1.2) *and of any order $n_c \in \mathbb{N}$, which is a solution to*

$$\Sigma^\star_{c,n_c} = \arg \min_{n_c \in \mathbb{N}, \Sigma_{c,n_c}} \|\Sigma_{cl,n_c}\| \quad \text{s.t.} \quad \Sigma_{cl,n_c} \text{ is internally stable.}$$

This optimal control problem has received a considerable amount of attention in the second half of the 20$^{\text{th}}$ century and today its solution is well-known for several norms—for example the H_2 and H_∞ norms[2]. These optimal multiple-input multiple-output (MIMO) controllers utilise a so-called observer based architecture[2], which has the same order as the system; that is, $n_c = n_x$.

Because the solution is well known for $n_c = n_x$, Problem 1.1 is often defined in literature without explicitly including n_c as an optimisation variable. However, in this thesis we will distinguish between optimal control problems with and without a constraint on the controller order.

Modelling of the System

Relatively simple models are used in classical controller design to create a initial controller, which is then optimised on the actual system. In contrast, optimal

[2]These norms and the controller architecture will formally be introduced in chapter 2.

controllers are entirely based on a model of the system. It is often assumed that the performance of such a controller is completely determined by the quality of the model—as explained by Obinata and Anderson [2001, Ch. 1]—and optimal control is therefore also known as model based control.

The modelling of systems is typically performed by utilising a mixture of two philosophies; namely "first principles modelling" and "data driven modelling" as explained by Ljung [1999]. A first principles model consists of equations that describe the physical behaviour of a system such as Newton's second law and the heat equation. With data driven modelling, the system is essentially regarded as a black box and the dynamical relations between inputs and outputs are determined completely on the basis of data. These philosophies can, however, be mixed get the best of both worlds. For example, data can be used to estimate certain physical parameters (e.g. the density and thermal capacity of a material) within a first principles model.

For the considered thermal control application, only a limited amount of information can be gathered about the thermal disturbances $w(t)$ and the deformations $z(t)$. This makes it infeasible to accurately model all relevant dynamics on the basis of data only and it is therefore decided to construct a first principles model. A subset of the physical parameters can, however, be estimated on the basis of data.

In section 1.2.3 it was mentioned that the physical behaviour in the considered application is described by coupled PDEs. For such a system, a model of the form Σ (1.1) can be created by utilising the finite element method (FEM) or the finite volume method (FVM), as is explained in great detail by Bathe [1996]. With both methods, the spatial domain is discretised using a mesh as depicted in figure 1.9. With this mesh, the entire temperature distribution and deformation profile of the system is replaced by a finite set of temperatures and deformations that are defined at the nodes of this mesh.

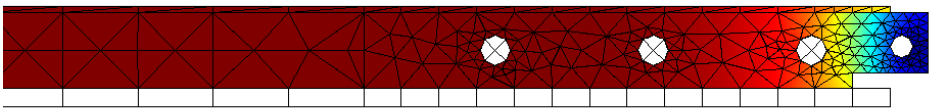

Figure 1.9: A two dimensional FEM model in which a domain is discretised by using a mesh.

Order Reduction

In thermal control applications, much effort is made to create an accurate model using the FEM. It is often required to use a fine mesh to achieve a sufficiently high degree of accuracy, which leads to a high order model. For example, a two dimensional model as depicted in figure 1.9 will typically contain $100-1,000$ states,

while model orders in the range of $10,000 - 1,000,000$ states are no exception when three dimensional models are considered.

Models of such high order cannot directly be used for controller synthesis, as explained by Obinata and Anderson [2001, Ch. 1]. First of all, computational hardware limitations like the amount of memory available could make it infeasible to perform the required numerical calculations. Secondly, issues with numerical conditioning will potentially make the results of these calculations unreliable.

Furthermore, for several norms the solution to the optimal control Problem 1.1 is described by a controller with $n_c = n_x$. A high order controller does require a large number of calculations to determine $u(t)$ on the basis of $y(t)$, which results in a relatively large computational time. However, the control inputs $u(t)$ must be produced in real-time, which therefore imposes an upper bound on the controller order.

To bridge the gap between the original model order, the required model order for controller synthesis and the maximum controller order for real-time implementation, model order reduction (MOR) and controller reduction (COR) techniques are often applied—as explained in great detail by Wortelboer [1994].

In many applications, much effort is made to construct an accurate model Σ (1.1) of (potentially large) order n_x. We would therefore prefer to use the input to output behaviour of this model for controller synthesis. With MOR, the aim is therefore to find a new model $\widehat{\Sigma}$, which is of much lower order $n_{\hat{x}} \ll n_x$; and which is similar to Σ (1.1) in terms of the input to output behaviour.

When MOR is used for low order controller design, it is essentially assumed that a low order approximation of the original model can safely be used for controller synthesis when both models are "similar enough" in terms of their input to output behaviour. Likewise, a controller can be viewed as a model with input $y(t)$ and output $u(t)$. Under the same assumption we can therefore also utilise any MOR technique to find a low order approximation $\widehat{\Sigma}_{c,n_{\hat{c}}}$ of a controller Σ_{c,n_c} (1.2), which is called COR.

1.2.5 Why Optimal Control is Rarely Applied in Practice

For the considered thermal control application, current solutions rely on classical controllers that are designed according to the method as explained in section 1.2.3. These relatively simple SISO controllers reduce deformations and imaging errors as a result of the BES from approximately 11 nm to 1.8 nm in magnitude[1]. In the future it will be required to further reduce this value to a number below 1 nm.

In order to meet the future performance requirements, it is proposed to improve the control solution by introducing an optimal controller that is designed according to section 1.2.4. These MIMO controllers are based on a reduced order model of

[1] These numbers follow from an example system in chapter 6 and are only an indication for the relative increase in performance.

the system, which essentially is used to virtually control the unmeasurable deformations. This solution has been investigated for the example system as well and a performance increase of approximately 0.1 nm is achieved.

This number is much lower than expected; especially if we consider that a considerable amount of time, effort and expertise is required to go from the relatively simple classical control designs to optimal controllers. At the same time, a similar increase in performance can be achieved by simply adding extra sensors, actuators and by applying classical control instead. We must therefore conclude that there exist other solutions that are more attractive when both the potential gain and the required effort are considered; this makes these solutions financially speaking more cost-effective. To put this into a broader perspective, similar numbers are reported in numerous other applications—for example, the applications mentioned at the beginning of section 1.2—and optimal control is therefore rarely applied in practice.

1.3 Control Relevant Modelling and System Design

The invention of optimal control originates from the desire to achieve the best possible closed-loop performance for any given system. In section 1.2 we saw that a substantial amount of time and effort is required to design such a controller, while the resulting increase in performance is relatively small in practice. The industry is primarily driven by economic gains, which implies that the cost-effectiveness of a solution becomes an important factor when alternative solutions exist that achieve a similar degree of improvement. In industry, this type of solution is therefore viewed as a "nice to have" instead of a necessity.

From both an academic and industrial perspective, it is interesting to investigate if the cost-effectiveness and performance can be improved for optimal control. In this section we will therefore investigate whether and how the entire development process could be improved.

1.3.1 Control Relevant System Design

In section 1.2.3 it is explained that classical control is considered first in the considered application. This control-related decision does, however, also directly impact the design of the system itself. Namely,

- temperature is controlled instead of deformations, which implies that measurements are taken and actuation is performed in the thermal domain.
- SISO controllers are considered, which implies that the sensors and actuators are paired.

Some of these decisions could be reconsidered to improve the performance when optimal control is introduced. For example, the deformations are controlled with optimal control, which implies that the wafer positioning system can be used as a

control input as well. Furthermore, for optimal control it is not required to pair sensors and actuators.

The introduction of optimal control is therefore accompanied with additional freedom in the system design, which is not exploited when only the controller is replaced. In addition, the well-defined mathematical framework of optimal control can be used to numerically optimise the sensor locations to further increase closed-loop performance. Such an automated procedure will also reduce the time, effort and expertise required for system design.

We can therefore hypothesise that there is a potential to increase the closed-loop performance and to reduce the effort required for system design, when automated procedures for control relevant system design are considered. It is important to note that this hypothesis will directly lead to the research questions in section 1.4. A metaphor will now be used to clarify why it is decided to investigate this topic.

As a metaphor, consider the problem of winning a Formula 1 race. In the thermal application it is decided to first design a relatively simple controller, which is represented by a qualified driver that is capable of driving a car on public roads. The system design is represented by the selection of an appropriate car for this driver. Such a car should obviously be as fast as possible; however, not any qualified driver will be able to drive a Formula 1 car[1]. For an average driver it is therefore more appropriate to select a fast road car instead—a Lotus Elise for example. In other words, the choice of driver does affect what car is chosen.

It is safe to assume that this combination of driver and car will not be able to seriously compete in a Formula 1 race and a substantial improvement is therefore required. Now, by considering optimal control without changing the system, we are essentially hiring a talented and very expensive Formula 1 driver that will drive the same car. This solution will absolutely improve the lap-times; however, this combination of driver and car will still finish last in any race. At the same time, it is likely that a similar improvement can be achieved by simply giving the original driver some time to train and by spending some money on a slightly faster car. The considered car does therefore also affect the choice of driver.

It could indeed happen that an average driver will eventually become good enough to operate the Formula 1 car and even to compete in a race. In a similar fashion, it can be argued for the thermal control application that the desired performance could eventually be met after spending enough time and effort on the classical controllers and on iteratively improving the system design. We can, however, also argue that the full potential of optimal control will never be observed—and to some degree it is overshadowed by the required effort—when the additional freedom in the system design is not exploited. Similarly, the Formula 1 driver will simply not be able to demonstrate all his talents in a fast road car. By considering control relevant system design, we essentially want to assure that the car and driver are improved together.

[1] As evidence for this claim, please consider the following video from Top Gear [2007].

1.3.2 Control Relevant Modelling

In the design of an optimal controller, much effort is typically made in order to model all system aspects with the highest possible accuracy. At the same time, it should be accepted that a linear model with an upper bound on the state dimension cannot always capture all relevant system dynamics. In a similar fashion to system design, it can therefore be hypothesised that an increase in closed-loop performance—and a reduction of the required effort—could be achieved by better understanding what system aspects are important to model from a control perspective.

For this reason, it is decided to investigate control relevant modelling as well. This topic has the potential to increase closed-loop performance and to reduce effort during all steps in the modelling procedure—that is, the development of the high order model and the use of MOR in combination with COR. Let us consider the same metaphor in order to clarify this argument.

As a metaphor, the model is represented by a simulator which is used to train the driver. The current modelling procedures essentially aim at replicating all aspects of driving. This includes driving in traffic, driving in snow, replacing a tyre, replicating the noise that the car makes etcetera. In order to win a race, however, it is mainly required to model the technical aspects of driving on a Formula 1 circuit. By investigating control relevant modelling, we essentially aim at creating a relatively simple simulator that is capable of maximising the driver's performance on the circuit.

1.4 Research Questions

In section 1.2 it is mentioned that optimal controllers are considered for the control of thermally induced deformations—and several other applications—in order to meet future performance requirements. Results, however, have shown that such a solution is at this moment only capable of achieving a marginal improvement. In section 1.3 it is hypothesised that the full potential of optimal control is actually not observed because the system design, modelling procedure and controller synthesis are viewed as separate problems. This hypothesis will therefore be tested in this thesis, by investigating whether these problems can be coordinated in order to achieve the desired performance. This leads to the main research question:

Main Research Question:

How can the system design, modelling procedure and optimal controller synthesis be coordinated with the aim of meeting a given set of closed-loop performance requirements?

To answer this question, it is essentially required to combine three separate fields of research. However, it is necessary to first acquire a better understanding of the

relation between these fields in order to address this problem. For each field we will therefore investigate one problem, in combination with a set of research questions that aim at bringing us closer to this main goal.

Closed-loop Optimal Actuator and Sensor Selection

For the control of thermally induced deformations, it is required to utilise temperature sensors. The question of how many sensors to use and where to place them is therefore relevant for control. Likewise, from a control perspective it is equally interesting to investigate these questions in terms of actuators; there is, however, less freedom in their design for the considered application.

These questions are closely related to actuator and sensor selection problems as discussed by Van de Wal and de Jager [2001]. In these problems, the allowed actuator and sensor locations are characterised as a large set of possible control inputs and measured outputs, respectively. The actual placement problem is hereby replaced by selecting—from these sets—smaller subsets of control inputs and measured outputs. To formally define this problem, let us consider the following mathematical operator.

For a set $\mathbb{V} = \{v_1, v_2, \cdots, v_m\}$ with elements $v_i \in \mathbb{R}^{n_{v_i} \times n_w}$, define the following operator that "stacks" these elements in one matrix $\mathrm{col}(\mathbb{V}) = \begin{pmatrix} v_1^\top & v_2^\top & \cdots & v_m^\top \end{pmatrix}^\top$.

The optimal selection problem now amounts to finding the subsets of control inputs and measured outputs that achieve the best closed-loop performance. This so-called "closed-loop optimal actuator and sensor selection problem" is mathematically defined as follows:

Problem 1.2 *For a given system, let* $\mathbb{U} = \{u_1, u_2, \cdots u_{N_u}\}$ *and* $\mathbb{Y} = \{y_1, y_2, \cdots y_{N_y}\}$, *with* $u_i \in \mathbb{R}^{n_{u_i}}$ *and* $y_i \in \mathbb{R}^{n_{y_i}}$, *denote sets that contain all possible control inputs and measured outputs, respectively. Furthermore, let* $\mathbb{U}_{n_u} \subseteq \mathbb{U}$ *and* $\mathbb{Y}_{n_y} \subseteq \mathbb{Y}$ *be subsets of cardinality* n_u *and* n_y *respectively; and let* Σ (1.1) *be a mathematical representation of the system with* $u = \mathrm{col}(\mathbb{U}_{n_u})$ *and* $y = \mathrm{col}(\mathbb{Y}_{n_y})$, *which after interconnection with* Σ_{c,n_c} (1.2) *results in a closed-loop system* Σ_{cl,n_c} (1.3).

Then, for predefined numbers $n_u \in \mathbb{N}$ *and* $n_y \in \mathbb{N}$, *find the subsets* $\mathbb{U}^\star_{n_u}$ *and* $\mathbb{Y}^\star_{n_y}$, *which are a solution to*

$$(\mathbb{U}^\star_{n_u}, \mathbb{Y}^\star_{n_y}) = \arg \min_{\substack{\mathbb{U}_{n_u} \subseteq \mathbb{U} \\ \mathbb{Y}_{n_y} \subseteq \mathbb{Y}}} \min_{n_c \in \mathbb{N}, \Sigma_{c,n_c}} \|\Sigma_{cl,n_c}\| \quad \text{s.t. } \Sigma_{cl,n_c} \text{ is internally stable.}$$

This type of selection problem has received a considerable amount of attention in literature. It is therefore relevant to investigate these existing techniques and, if necessary, to make improvements. This leads to the first set of research questions:

Research Questions for the System Design:

Does a solution to Problem 1.2 exist for specific norms?
If not, how well do existing selection methods perform and can these be improved?

Constrained Order Controller Design

In section 1.2.4 it is discussed that high order model are required for the control of thermally induced deformations. For several norms, the solution to the optimal control Problem 1.1 is given by a controller which is of the same order as the model order—that is, $n_c = n_x$. In practice it may therefore not be possible to numerically construct such a controller due to computational constraints. Furthermore, real-time application of such a controller requires this order to be even lower. For this reason the design of a low order controller that is optimal for the high order system, is an important problem. This results in the "constrained order optimal control problem", which is mathematically defined as follows:

Problem 1.3 *For a predefined order $n_c \in \mathbb{N}$, construct a stabilising optimal controller $\Sigma^\star_{c,n_c}$ of the form* (1.2)*, which is a solution to*

$$\Sigma^\star_{c,n_c} = \arg \min_{\Sigma_{c,n_c}} \|\Sigma_{cl,n_c}\| \quad \text{s.t. } \Sigma_{cl,n_c} \text{ is internally stable.}$$

The constrained order optimal control problem is often replaced by a modelling approach that utilises MOR and COR to construct a low order approximation of the system and the corresponding optimal controller, respectively. It is, however, at this moment unclear whether such an approach could provide any guarantees on the interconnection of the low order controller with the original high order system. This leads to the second set of research questions:

Research Questions for the Modelling Procedure:

Does a solution to Problem 1.3 exist for specific norms?
If not, how well do existing methods for constrained order controller design perform and can an improvement be achieved?

Minimal Order Optimal Control

As mentioned above, there exist controller synthesis algorithms that, for several norms, solve Problem 1.3 with $n_c = n_x$. For orders $n_c < n_x$, however, this remains an open problem. As a first step towards finding such a solution, it could therefore

be relevant to determine the smallest controller order that can be used to solve the original optimal control Problem 1.1. This leads to the "minimal order optimal control problem", which is mathematically defined as:

Problem 1.4 *Construct a stabilising optimal controller* $\Sigma^\star_{c,n_c^-}$ *of the form* (1.2) *and of minimal order* $n_c^- \in \mathbb{N}$*, which is a solution to*

$$(n_c^-, \Sigma^\star_{c,n_c^-}) = \arg \min_{n_c \in \mathbb{N}} \min_{\Sigma_{c,n_c}} \|\Sigma_{cl,n_c}\| \quad \text{s.t. } \Sigma_{cl,n_c} \text{ is internally stable.}$$

Before finding a solution to this problem, we must first determine whether there could exist a controller that solves the optimal control Problem 1.1 for orders $n_p < n_x$ in the first place. This leads to the final set of research questions:

Research Questions for Controller Synthesis:

Does a solution to Problem 1.4 exist for specific norms?
If so, can n_c^- be characterised and how is $\Sigma^\star_{c,n_c^-}$ constructed?
Furthermore, can this solution satisfy $n_c^- < n_x$ for the H_2 norm[1]?

1.5 Outline of the Thesis

In this thesis, we will investigate Problems 1.2–1.4 and the corresponding research questions, with the aim of bringing us closer to answering the main research question. An overview of the chapters is now presented.

Chapter 2 introduces the mathematical notation and describes basic notions from systems and control theory, linear matrix inequalities, H_2 optimal control and geometric control theory. The chapter can be treated as a reference; it is therefore not required to completely read it before proceeding to the subsequent chapters.

Chapters 3–5 are concerned with Problems 1.2–1.4 and the corresponding research questions, respectively. These chapters can be read individually and in any given order, while references to chapter 2 are added where necessary. They are self-contained in the sense that each chapter contains an introduction, an overview of existing literature, formal problem definitions and its own (system) definitions.

Chapter 6 is used to demonstrate the results from chapters Chapters 3–5 on a numerical model for the thermal control application. In addition, the numerical model will directly show the importance of the main research question.

Chapter 7 contains the conclusions and future work that follow from Chapters 3–5. The chapter is concluded by presenting the implications for industry and academia that follow from this thesis.

[1] This norm will formally be introduced in chapter 2.

Finally, it is important to note that:

- any mathematical proof is included in appendix A, if it is significant in size.
- the list of publications is included on page 247. Throughout this thesis, a reference is added for all chapters and sections that are based on submitted or published papers.
- the software that is used to generate all numerical results in this thesis is available upon request.

Mathematics is the art of giving the same name to different things.

Henri Poincare

2

Mathematical Preliminaries

Several well-known concepts from mathematics, systems and control will be introduced in this chapter. It is assumed that all readers are to some degree familiar with these concepts. However, existing literature is referenced throughout for clarity and for completeness.

First, in section 2.1 the general notation and several elementary mathematical concepts are introduced. This is followed by a short summary on the basic notions from systems and control in section 2.2.

In section 2.3, the use of linear matrix inequalities (LMIs) in control is discussed. Then, an extensive treatment of—and a full derivation for the solution to—the H_2 optimal control problem is provided in section 2.4.

The chapter is finalised in section 2.5 by introducing the main concepts from geometric control theory. In addition, a short discussion is presented on the relation between geometric control theory and disturbance decoupling.

2.1 Mathematical Notation

In section 2.1, the mathematical notation is defined and a number of basic concepts from mathematics is briefly summarised. It is assumed that all readers are—at least, to some degree—familiar with these concepts.

2.1.1 General Notation

The following definitions are used throughout this thesis:

- $\mathbb{N}$ The set of non-negative integers (including 0).
- $\mathbb{N}_+$ The set of positive integers (excluding 0).
- $\mathbb{R}$ The set of real numbers.
- $\mathbb{C}$ The set of complex numbers that are expressed as $z = a + jb$, with $a, b \in \mathbb{R}$.
- $\mathbb{C}_-$ The open left half complex plane, which contains all complex numbers $z = a + jb$ with $a < 0$.
- $\mathbb{C}_g$ A stability domain $\mathbb{C}_g \subseteq \mathbb{C}$ is a subset that is symmetric with respect to the real axis, while $\mathbb{C}_g \cap \mathbb{R}$ is non-empty.
- $\|\cdot\|$ Any norm of a vector, matrix, function or system.
- I_k The identity matrix of dimension $k \times k$.
- $e_k(i, j)$ An indicator vector of dimension k, with $0 < i \leq j \leq k$. Entries $i, \cdots, j$ of this vector contain a value of 1, while all other entries are 0.
- $e_k(i)$ The i^{th} unit basis vector of dimension k, with $0 < i \leq k$. Entry i of this vector contains a value of 1, while all other entries are 0.
- $\dot{x}(t)$ The derivative of a function $x(t)$ with respect to (time) t.
- $\delta(t)$ The Dirac function.

2.1.2 Numbers and Vectors

Consider the following definitions for any complex number $z \in \mathbb{C}$ of the form $z = a + jb$, with $a, b \in \mathbb{R}$:

- $\mathrm{Re}(z)$ The real part of z is defined as $\mathrm{Re}(z) \coloneqq a$.
- $\mathrm{Im}(z)$ The imaginary part of z is defined as $\mathrm{Im}(z) \coloneqq b$.
- z^* The conjugate of z is defined as $z^* \coloneqq a - jb$.
- $|z|$ The modulus of z is defined as $|z| \coloneqq \sqrt{a^2 + b^2}$.

And consider the following definitions for column vectors $x, y \in \mathbb{C}^p$ with p rows:

- x_i The element of x in row i.
- $x^\top$ The transpose of x.
- x^* The conjugate transpose of x.
- $\langle x, y \rangle$ The inner product between x and y is defined as $\langle x, y \rangle = x^* y$.

- $\|x\|_k$ The k-norm of x is defined as

$$\|x\|_k \coloneqq \begin{cases} \left(\sum_{i=1}^{p} |x_i|^k\right)^{\frac{1}{k}} & \text{for } k \in \mathbb{N}_+, \\ \max_{i \in \{1,2,\cdots,p\}} |x_i| & \text{for } k = \infty. \end{cases} \tag{2.1}$$

2.1.3 Linear Mappings and Matrices

Every matrix $A \in \mathbb{C}^{p \times q}$ defines a linear mapping $T(A) : \mathbb{C}^q \to \mathbb{C}^p$ that is typically denoted by A. That is, we directly identify the matrix A with the mapping $T(A)$.

Matrices

Consider the following definitions for any matrix $A \in \mathbb{C}^{p \times q}$ with p rows and q columns:

- $A_{i,j}$ The element of A in row i and column j.[1]
- $A^\top$ The transpose of A.
- A^* The conjugate—or Hermitian—transpose of A.
- $\ker(A)$ The kernel of A is defined as $\ker(A) \coloneqq \{x \in \mathbb{C}^q \mid Ax = 0\}$.
- $\mathrm{im}(A)$ The image of A is defined as
$$\mathrm{im}(A) \coloneqq \{y \in \mathbb{C}^p \mid y = Ax \text{ for some } x \in \mathbb{C}^q\}.$$
- $\mathrm{rank}(A)$ The rank of A. This describes the number of independent row or columns. For any matrix A we have that $\mathrm{rank}(A) \leq \min(p, q)$ and A is called full rank if $\mathrm{rank}(A) = \min(p, q)$.
- $\mathrm{card}(A)$ The cardinality of A. This describes the number of non-zero elements.
- $\|A\|_{k,l}$ The (k, l)-induced-norm of A is defined as $\|A\|_{k,l} \coloneqq \sup_{x \neq 0} \frac{\|Ax\|_k}{\|x\|_l}$.
- $\|A\|_F$ The Frobenius norm of A is defined as $\|A\|_F \coloneqq \sqrt{\sum_{i=1}^{p} \sum_{j=1}^{q} |A_{i,j}|^2}$.

Square Matrices

Consider the following definitions for a square matrix $A \in \mathbb{C}^{p \times p}$ with p rows and columns:

- $\lambda \in \mathbb{C}$ is an eigenvalue of A if $Av = \lambda v$ for some $v \in \mathbb{C}^p$.
- The vector $v \in \mathbb{C}^p$—with $\|v\|_2 = 1$—is called a normalised (right) eigenvector of A corresponding to the eigenvalue $\lambda \in \mathbb{C}$ if $Av = \lambda v$.
- The vector $w \in \mathbb{C}^p$—with $\|w\|_2 = 1$—is called a normalised left eigenvector of A corresponding to the eigenvalue $\lambda \in \mathbb{C}$ if $w^* A = \lambda w^*$.
- The matrix A is called Hermitian if $A = A^*$ and symmetric if $A = A^\top$.

[1] Subscripts without a comma are used to describe matrix partitions that consist of multiple rows and columns.

- $\mathrm{tr}(A)$ The trace of A is defined as $\mathrm{tr}(A) \coloneqq \sum_{i=1}^{p} A_{i,i}$.
- $\det(A)$ The determinant of A, which is discussed in great detail by Lay and Lay [2015, Ch. 3]. The determinant of A is non-zero if the matrix is full rank.
- A^{-1} The inverse of A is a matrix that satisfies $AA^{-1} = I_p$. A is called non-singular—or invertible—if A^{-1} exists. A is nonsingular if it is full rank, or equivalently if the determinant is non-zero.
- $\lambda(A)$ The spectrum of A is defined as
$$\lambda(A) \coloneqq \{\lambda \in \mathbb{C} \mid Ax = \lambda x \text{ for some } x \in \mathbb{C}^p\}.$$

A Hermitian matrix A will satisfy $\lambda(A) \subset \mathbb{R}$. Such a matrix is called positive (or negative) definite when the eigenvalues $\lambda_i \in \lambda(A)$ satisfy $\lambda_i > 0$ (or $\lambda_i < 0$), which is denoted by $A \succ 0$ (or $A \prec 0$). Similarly, an Hermitian matrix A is called positive (or negative) semidefinite when the eigenvalues $\lambda_i \in \lambda(A)$ satisfy $\lambda_i \geq 0$ (or $\lambda_i \leq 0$), which is denoted by $A \succeq 0$ (or $A \preceq 0$).

The Singular Value Decomposition

The Singular Value Decomposition (SVD)—as discussed in great detail by Antoulas [2005, Sec. 3.2]—essentially generalises the concept of eigenvalues to non-square matrices.

The SVD of a (potentially non-square) matrix $A \in \mathbb{C}^{p\times q}$ of rank r is a factorisation of the form $A = USV^*$, where:

- $U \in \mathbb{C}^{p\times p}$ is a matrix satisfying $UU^* = I_p$.
- $V \in \mathbb{C}^{q\times q}$ is a matrix satisfying $VV^* = I_q$.
- $S \in \mathbb{C}^{p\times q}$ is a matrix with elements $S_{i,i} = \sigma_i > 0$ for $i \leq r$ and with zeros elsewhere.

The columns u_i and v_i of U and V, respectively, are called the left and right singular vectors corresponding to the singular value σ_i, respectively. These vectors satisfy $Av_i = \sigma_i u_i$ and we get that $A = \sum_{i=1}^{r} \sigma_i v_i u_i^*$.

Furthermore, the singular values are ordered in the sense that $\sigma_1 \geq \sigma_2 \geq \cdots \geq \sigma_r > 0$. In a similar fashion to the eigenvalues of a matrix, the following set is considered:

$$\sigma(A) \coloneqq \left\{ \sigma_i > 0 \;\middle|\; A = \sum_{i=1}^{r} \sigma_i v_i u_i^* \right\}$$

and $\sigma_i(A)$ denotes the i^{th} singular value of A.

Matrix Norms

The (k, l)-induced norm of A is called the k-induced norm if $k = l$. In other words $\|A\|_k \coloneqq \|A\|_{k,k}$.

For a matrix $A \in \mathbb{C}^{p\times q}$, the following norms are often considered:

$$\|A\|_1 = \max_{1\le j\le q} \sum_{i=1}^{p} |A_{i,j}|,$$

$$\|A\|_2 = \max(\sigma(A)),$$

$$\|A\|_\infty = \max_{1\le i\le p} \sum_{j=1}^{q} |A_{i,j}|.$$

2.1.4 Subspaces

Let us define two finite-dimensional vector spaces $\mathcal{X}$ and $\mathcal{Y}$ of dimension n_x and n_y, respectively. Furthermore, let us consider the following definitions for the subspaces $\mathcal{R}$ and $\mathcal{S}$ of the vector space $\mathcal{X}$ and for the linear mappings $A : \mathcal{R} \to \mathcal{S}$, $B : \mathcal{X} \to \mathcal{Y}$ and $C : \mathcal{X} \to \mathcal{X}$:

- $\dim(\mathcal{R})$ The dimension of $\mathcal{R}$.
- $\mathcal{R} \subseteq \mathcal{S}$ $\mathcal{R}$ is a subspace of $\mathcal{S}$. This implies that any $r \in \mathcal{X}$ which satisfies $r \in \mathcal{R}$, must satisfy $r \in \mathcal{S}$ as well. A strict inclusion $\mathcal{R} \subset \mathcal{S}$ is used if there exists at least one element in $\mathcal{S}$ that is not an element in $\mathcal{R}$; i.e. there exists an $s \in \mathcal{S}$ such that $s \notin \mathcal{R}$.
- $\mathcal{R} \cap \mathcal{S}$ The intersection of $\mathcal{R}$ and $\mathcal{S}$ is defined as
$$\mathcal{R} \cap \mathcal{S} \coloneqq \{t \in \mathcal{X} \mid t \in \mathcal{R},\ t \in \mathcal{S}\}.$$
- $\mathcal{R} + \mathcal{S}$ The sum of $\mathcal{R}$ and $\mathcal{S}$ is defined as
$$\mathcal{R} + \mathcal{S} \coloneqq \{t \in \mathcal{X} \mid t = r + s \text{ for some } r \in \mathcal{R},\ s \in \mathcal{S}\}.$$
- $\mathcal{R} \oplus \mathcal{S}$ The direct sum of $\mathcal{R}$ and $\mathcal{S}$ denotes the sum of these subspaces if $\mathcal{R}$ and $\mathcal{S}$ are disjoint—i.e. if $\mathcal{R} \cap \mathcal{S} = 0$.
- $\mathcal{R}_c$ An arbitrary complement of $\mathcal{R}$ is a subspace $\mathcal{R}_c \subseteq \mathcal{X}$ that satisfies $\mathcal{R} \oplus \mathcal{R}_c = \mathcal{X}$.
- $\mathcal{R}^\perp$ The orthogonal complement of $\mathcal{R}$ is defined as
$$\mathcal{R}^\perp \coloneqq \{t \in \mathcal{X} \mid \langle r, t\rangle = 0 \text{ for any } r \in \mathcal{R}\}.$$
- $A\mathcal{R}$ A linear transformation A applied to the subspace $\mathcal{R}$ is defined as
$$A\mathcal{R} \coloneqq \{s \in \mathcal{S} \mid s = Ar \text{ for some } r \in \mathcal{R}\}.$$
- $A^{-1}\mathcal{S}$ [1] An inverse linear transformation A^{-1} applied to the subspace $\mathcal{S}$ is defined as $A^{-1}\mathcal{S} \coloneqq \{r \in \mathcal{R} \mid s = Ar \text{ for some } s \in \mathcal{S}\}$.
- $B|\mathcal{R}$ The restriction of B to the subspace $\mathcal{R}$. We say that a mapping $\underline{B} : \mathcal{R} \to \mathcal{Y}$ that satisfies $\underline{B}r = Br$ for any $r \in \mathcal{R}$ is the restriction of B to $\mathcal{R}$, which is denoted by $B|\mathcal{R}$.
- $\Pi(\mathcal{R}, \mathcal{S})$ The oblique projection onto $\mathcal{R}$ along $\mathcal{S}$, which is denoted by a linear transformation $\Pi(\mathcal{R}, \mathcal{S}) : \mathcal{R} + \mathcal{S} \to \mathcal{R}$. For a subspace $\mathcal{T} \subseteq \mathcal{R} + \mathcal{S}$ this linear transformation is defined as $\Pi(\mathcal{R}, \mathcal{S})\mathcal{T} =$
$\{r \in \mathcal{R} \mid \text{there exists an } s \in \mathcal{S} \text{ such that } r = s + t \text{ for any } t \in \mathcal{T}\}$.
The transformation is single valued—i.e. for any $t \in \mathcal{T}$ the projection of t: $\Pi(\mathcal{R}, \mathcal{S})t$ is described by exactly one point—if $\mathcal{R} \cap \mathcal{S} = 0$.

[1] This so-called set inverse is defined for a mapping A and does not require that the corresponding matrix is full rank.

When a complement of $\mathcal{R}$ is used, we get that $\Pi(\mathcal{R}, \mathcal{R}_c) : \mathcal{X} \to \mathcal{R}$; and $\Pi(\mathcal{R}, \mathcal{R}^\perp) : \mathcal{X} \to \mathcal{R}$ is called an orthogonal projection onto $\mathcal{R}$.

- $\mathcal{X}$ mod $\mathcal{R}$ The quotient space $\mathcal{X}$ modulo $\mathcal{R}$. A subspace $\mathcal{R}$ imposes an equivalence relation between elements $x_1, x_2 \in \mathcal{X}$ in the sense that $x_1 \simeq x_2$ if $x_1 - x_2 \in \mathcal{R}$. The set of all equivalence classes is called the quotient space $\mathcal{X}$ modulo $\mathcal{R}$, which is denoted by $\mathcal{X}$ mod $\mathcal{R}$. For any $x \in \mathcal{X}$, the equivalence class is denoted by $\bar{x} \coloneqq \{y \mid x - y \in \mathcal{R}\}$.
- The subspace $\mathcal{R}$ is called invariant under C, or simply C-invariant, if $C\mathcal{R} \subseteq \mathcal{R}$.
- If $\mathcal{R}$ is invariant under C, we have that $C|(\mathcal{X} \text{ mod } \mathcal{R}) : \mathcal{X} \text{ mod } \mathcal{R} \to \mathcal{X} \text{ mod } \mathcal{R}$ in the sense that $\bar{y} = C\bar{x}$ where $\bar{y}$ is the equivalence class of $y = Cx$ for any x in the equivalence class $\bar{x}$.

Please note that subspace algebra is discussed in more detail by Basile and Marro [1992]. Equivalence classes and modulo relations are discussed by Trentelman et al. [2001] and more information about oblique projections is provided by Saad [2003, 2011].

Numerical Representations for Subspaces

Again, let us consider the subspace $\mathcal{R}$—with $n_r = \dim(\mathcal{R})$—of the vector space $\mathcal{X}$ with $n_x = \dim(\mathcal{X})$. Then the subspace $\mathcal{R}$ can numerically be described by a set of vectors in $\mathbb{R}^{n_x}$ that span this subspace. I.e. we say that a matrix $R \in \mathbb{R}^{n_x \times n_q}$ is an (image) representation for $\mathcal{R}$ if $\text{im}(R) = \mathcal{R}$; it is called a minimal (image) representation if $n_q = n_r$.

All subspace operations as described above are numerically implemented by Marro [2018] and explained by Basile and Marro [1992, sec. 3.1]; except for the projector $\Pi(\cdot, \cdot)$, which is—according to Saad [2003, Sec. 1.12]—defined as follows:

Let $\mathcal{R}_1$ and $\mathcal{R}_2$ of dimension r_1 and r_2, respectively, be subspaces of the vector space $\mathcal{R}_1 \oplus \mathcal{R}_2$. Furthermore, let the matrices of $R_1 \in \mathbb{R}^{(r_1+r_2)\times r_1}$ and $R_2 \in \mathbb{R}^{(r_1+r_2)\times r_2}$ be minimal representations for the subspaces $\mathcal{R}_1$ and $\mathcal{R}_2$, respectively. Finally, let $R_{2p} \in \mathbb{R}^{(r_1+r_2)\times r_1}$ be a minimal representation for $\mathcal{R}_2^\perp$.

Then the projection *onto* $\mathcal{R}_1$ and along $\mathcal{R}_2$ is numerically described by

$$\Pi(\mathcal{R}_1, \mathcal{R}_2) = R_1 (R_{2p}^\top R_1)^{-1} R_{2p}^\top = P \in \mathbb{R}^{(r_1+r_2)\times(r_1+r_2)}.$$

Furthermore, the projection *to* $\mathcal{R}_1$ and along $\mathcal{R}_2$ is numerically described by

$$\Pi_s(\mathcal{R}_1, \mathcal{R}_2) = R_1^\top R_1 (R_{2p}^\top R_1)^{-1} R_{2p}^\top = P_s \in \mathbb{R}^{r_1 \times (r_1+r_2)}.$$

2.1.5 Functions

For any (matrix) function $f : \mathbb{R} \to \mathbb{C}^{p\times q}$, the L_k-norm is defined as

$$\|f\|_{L_k} \coloneqq \begin{cases} \left(\int_{t=-\infty}^{\infty} \|f(t)\|_k^k \, dt \right)^{\frac{1}{k}} & \text{for } k \in \mathbb{N}_+, \\ \sup\limits_{t\in\mathbb{R}} \|f(t)\|_\infty & \text{for } k = \infty. \end{cases} \tag{2.2}$$

We say that the function f is L_k-bounded if there exists a number $\gamma > 0$ such that $\|f\|_{L_k} \leq \gamma < \infty$.

2.1.6 Sets and Set Functions

Consider the following definitions for a set $\mathbb{V} = \{v_1, v_2, \cdots, v_m\}$:

- $\text{card}(\mathbb{V})$ The cardinality of $\mathbb{V}$. This describes the number of elements in the set; i.e. $\text{card}(\mathbb{V}) = m$.
- $\text{row}(\mathbb{V})$ For a set that contains elements $v_i \in \mathbb{C}^{n_w \times n_{v_i}}$ with an equal amount of rows, $\text{row}(\mathbb{V})$ "joins" these elements in a matrix:
$$\text{row}(\mathbb{V}) \coloneqq \begin{pmatrix} v_1 & v_2 & \cdots & v_m \end{pmatrix}.$$
- $\text{col}(\mathbb{V})$ For a set that contains elements $v_i \in \mathbb{C}^{n_{v_i} \times n_w}$ with an equal amount of columns, $\text{col}(\mathbb{V})$ "stacks" these elements in a matrix:
$$\text{col}(\mathbb{V}) \coloneqq \begin{pmatrix} v_1 \\ v_2 \\ \vdots \\ v_m \end{pmatrix}.$$
- $\text{diag}(\mathbb{V})$ For a set that contains elements $v_i \in \mathbb{C}^{n_{v_{i1}} \times n_{v_{i2}}}$ of arbitrary dimension, $\text{diag}(\mathbb{V})$ creates a block diagonal matrix with these elements on the diagonal:
$$\text{diag}(\mathbb{V}) \coloneqq \begin{pmatrix} v_1 & 0 & \cdots & 0 \\ 0 & v_2 & & 0 \\ \vdots & & \ddots & \vdots \\ 0 & 0 & \cdots & v_m \end{pmatrix}.$$

Consider the following definitions for the subsets $\mathbb{V}_1, \mathbb{V}_2 \subseteq \mathbb{V}$:

- $\mathbb{V}_1 \subseteq \mathbb{V}_2$ $\mathbb{V}_1$ is a subset of $\mathbb{V}_2$. This implies that any $v \in \mathbb{V}_1$ satisfies $v \in \mathbb{V}_2$. A strict inclusion $\mathbb{V}_1 \subset \mathbb{V}_2$ is used if there exists at least one element in $\mathbb{V}_2$ that is not an element in $\mathbb{V}_1$; i.e. there exists a $v \in \mathbb{V}_2$ such that $v \notin \mathbb{V}_1$.
- $\mathbb{V}_1 \cap \mathbb{V}_2$ The intersection of $\mathbb{V}_1$ and $\mathbb{V}_2$ is defined as
$$\mathbb{V}_1 \cap \mathbb{V}_2 \coloneqq \{v \in \mathbb{V} \mid v \in \mathbb{V}_1 \text{ and } v \in \mathbb{V}_2\}.$$
- $\mathbb{V}_1 \cup \mathbb{V}_2$ The union of $\mathbb{V}_1$ and $\mathbb{V}_2$ is defined as
$$\mathbb{V}_1 \cup \mathbb{V}_2 \coloneqq \{v \in \mathbb{V} \mid v \in \mathbb{V}_1 \text{ or } v \in \mathbb{V}_2\}.$$
- $\mathbb{V}_1 \setminus \mathbb{V}_2$ The subtraction of elements in $\mathbb{V}_2$ from $\mathbb{V}_1$ is defined as
$$\mathbb{V}_1 \setminus \mathbb{V}_2 \coloneqq \{v \in \mathbb{V}_1 \mid v \notin \mathbb{V}_2\}.$$

For a set $\mathbb{V} = \{v_1, v_2, \cdots, v_m\}$, a *set function* $f : 2^{\mathbb{V}} \to \mathbb{R}$ is a function that assigns a real-valued number to each subset of $\mathbb{V}$. Consider the following definitions for such a function and subsets $\mathbb{V}_i, \mathbb{V}_j \subseteq \mathbb{V}$:

- The function f is called monotone increasing in $\mathbb{V}$ if
$$\mathbb{V}_i \subseteq \mathbb{V}_j \Rightarrow f(\mathbb{V}_i) \leq f(\mathbb{V}_j).$$
- The function f is called monotone decreasing in $\mathbb{V}$ if
$$\mathbb{V}_i \subseteq \mathbb{V}_j \Rightarrow f(\mathbb{V}_i) \geq f(\mathbb{V}_j).$$

- The function f is called submodular in $\mathbb{V}$ if for all subsets $\mathbb{V}_i, \mathbb{V}_j \subseteq \mathbb{V}$ we have that
$$f(\mathbb{V}_i) + f(\mathbb{V}_j) \geq f(\mathbb{V}_i \cup \mathbb{V}_j) + f(\mathbb{V}_i \cap \mathbb{V}_j).$$
- The function f is called supermodular in $\mathbb{V}$ if for all subsets $\mathbb{V}_i, \mathbb{V}_j \subseteq \mathbb{V}$ we have that
$$f(\mathbb{V}_i) + f(\mathbb{V}_j) \leq f(\mathbb{V}_i \cup \mathbb{V}_j) + f(\mathbb{V}_i \cap \mathbb{V}_j).$$
- The function f is called modular in $\mathbb{V}$ if it is both supermodular and submodular in $\mathbb{V}$. For all subsets $\mathbb{V}_i, \mathbb{V}_j \subseteq \mathbb{V}$ we therefore have that
$$f(\mathbb{V}_i) + f(\mathbb{V}_j) = f(\mathbb{V}_i \cup \mathbb{V}_j) + f(\mathbb{V}_i \cap \mathbb{V}_j).$$

2.2 Basic Notions from Systems and Control Theory

2.2.1 Internal and External System Descriptions

A system Σ (1.1) with two types of inputs and two types of outputs is introduced in chapter 1. A number of notions from systems and control will now be discussed in section 2.2, for which this distinction is not required. Therefore, let us consider the simplified system

$$\Sigma_s = \begin{cases} \dot{x}(t) &= Ax(t) + Bu(t) \\ y(t) &= Cx(t) + Du(t), \end{cases} \tag{2.3}$$

with vector signals $x(t)$, $u(t)$ and $y(t)$ that represent the state, input and output. These signals assume values in finite-dimensional vector spaces $\mathcal{X} = \mathbb{R}^{n_x}$, $\mathcal{U} = \mathbb{R}^{n_u}$ and $\mathcal{Y} = \mathbb{R}^{n_y}$, respectively. The dynamical relation between the signals is described by real-valued matrices A, B, C and D of appropriate dimension.

Σ_s (2.3) is called an internal, or state-space, system representation. We say that such a representation is *strictly proper* if $D = 0$.

External, or input to output, system representations are often considered as well. For example, Σ_s (2.3) defines a transfer function

$$\Gamma_s(s) = \left[C(sI_{n_x} - A)^{-1}B + D\right]$$

that relates the Laplace transforms $U(s)$ and $Y(s)$ of the signals $u(t)$ and $y(t)$—provided that $x(0) = 0$—by $Y(s) = \Gamma_s(s)U(s)$.

The transfer function $\Gamma_{s,i,j}(s)$ between input $u_j(t)$ and output $y_i(t)$ is often expressed as

$$\Gamma_{s,i,j}(s) = K\frac{(s - z_1)(s - z_2)\cdots(s - z_{m-1})(s - z_m)}{(s - p_1)(s - p_2)\cdots(s - p_{n-1})(s - p_n)} = \frac{Z(s)}{P(s)},$$

where we assume that all common factors of $Z(s)$ and $P(s)$ are removed in order to obtain polynomial functions of minimal degree—i.e. there do not exist values i, j such that $z_i = p_j$.

The solutions to the equation $Z(s) = 0$—i.e. the values $s = z_i$ for $i = 1, 2, \cdots, m$—are called the zeros of $\Gamma_{s,i,j}(s)$. Similarly, the solutions to the equation $P(s) = 0$—i.e. the values $s = p_i$ for $i = 1, 2, \cdots, n$—are called the poles of $\Gamma_{s,i,j}(s)$.

The poles of the entire transfer function $\Gamma_s(s)$ are simply the union of the poles for each transfer function $\Gamma_{s,i,j}(s)$ as defined above. The extension of zeros to the entire system $\Gamma_s(s)$ is more complicated—as explained by Bosgra et al. [2007]; it is, however, not necessary to discuss this extension.

Finally, it is important to note that the state $x(t)$ of Σ_s (2.3) is not uniquely determined by the input to output behaviour. In other words, we can define a non-singular state transformation $T : \mathcal{X} \to \mathcal{X}$ to define a new system—with the state $\bar{x}(t) = Tx(t)$—that describes the same transfer function. By applying a state transformation T to Σ_s (2.3), the *equivalent* system

$$\bar{\Sigma}_s = \begin{cases} \dot{\bar{x}}(t) &= \bar{A}\bar{x}(t) + \bar{B}u(t) \\ y(t) &= \bar{C}\bar{x}(t) + Du(t), \end{cases} \tag{2.4}$$

with $\bar{A} = TAT^{-1}$, $\bar{B} = TB$ and $\bar{C} = CT^{-1}$ is obtained.

2.2.2 Stability

Stability is an important system property; let us now define two types of stability.

Definition 2.1 *The system Σ_s (2.3) is "bounded-input, bounded-output (BIBO) stable" if any L_∞-bounded input signal $u(t)$ results in an L_∞-bounded output signal $y(t)$ for initial condition $x(0) = 0$.*

The system Σ_s (2.3) is "internally stable" if the states $x(t)$ remain L_∞-bounded for all initial conditions $x(0) = x_0 \in \mathbb{R}^{n_x}$ and for all L_∞-bounded signals $u(t)$.

It is a well-known fact that these types of stability are mathematically expressed as requirements on the eigenvalues of A and the poles of $\Gamma_s(s)$, for which all common factors in the numerator and denominator polynomials are removed.

Proposition 2.2 *Consider the system Σ_s (2.3) and the corresponding transfer function $\Gamma_s(s)$, for which all common factors in the numerator and denominator polynomials are removed.*

Then Σ_s (2.3) is BIBO stable if and only if any pole p_i of $\Gamma_s(s)$ satisfies $p_i \in \mathbb{C}_-$.

Furthermore, Σ_s (2.3) is internally stable if and only if $\lambda(A) \subset \mathbb{C}_-$.

Proof: The proof is given by Trentelman et al. [2001, Sec. 3.7]. □

It is important to note that internal stability of a system is invariant under state transformations. In other words, Σ_s (2.3) is internally stable if and only if $\bar{\Sigma}_s$ (2.4) is internally stable, because $\lambda(\bar{A}) = \lambda(TAT^{-1}) = \lambda(A)$.

Finally, it might be possible to stabilise or destabilise the system Σ_s (2.3) with the signal $u(t)$. Let us therefore consider the following definition.

Definition 2.3 *For Σ_s (2.3), an input signal $u(t)$ stabilises the state $x_0 \in \mathcal{X}$ if with this input signal $u(t)$ and for $x(0) = x_0$ we have that $\lim_{t\to\infty} x(t) = 0$.*

Furthermore, let $\mathbb{U}(x_0)$ denote the set of signals $u(t)$ that stabilise x_0.

2.2.3 Reachability and Observability

An internally stable system is BIBO stable. A BIBO stable system is, however, not necessarily internally stable. For example, certain inputs $u(t)$ could, for a BIBO stable system, result in unbounded state trajectories $x(t)$ as long as these unbounded states do not affect the output $y(t)$.

It is therefore important to determine which states are affected by the input $u(t)$ and what states affect the output $y(t)$. This leads to the concepts of reachability and observability of states, which are formally defined as follows.

Definition 2.4 *For a system Σ_s (2.3), the state $\underline{x} \in \mathcal{X}$ is called*

- *reachable if for $x(0) = 0$ there exists an input signal $u(t)$ and a time $T < \infty$ such that $x(T) = \underline{x}$.*
- *unobservable if for $x(0) = \underline{x}$ and $u(t) = 0$ we get that $y(t) = 0$ for $t \geq 0$.*

The subspaces $\mathcal{R}(A, B) \subseteq \mathcal{X}$ and $\mathcal{N}(C, A) \subseteq \mathcal{X}$ are the sets of all reachable and unobservable states, respectively.

Finally, Σ_s (2.3) is called reachable if $\mathcal{R}(A, B) = \mathcal{X}$, observable if $\mathcal{N}(C, A) = 0$ and minimal if it is both reachable and observable.

Now let us consider a state transformation T_k that partitions the state-space of Σ_s (2.3) in the so-called Kalman canonical form, which is explained in more detail by Polderman and Willems [1998]. In this representation the state-space is partitioned as $\mathcal{X} = \mathcal{X}_1 \oplus \mathcal{X}_2 \oplus \mathcal{X}_3 \oplus \mathcal{X}_4$, with $\mathcal{R}(T_k A T_k^{-1}, T_k B) = \mathcal{X}_1 \oplus \mathcal{X}_2$ and $\mathcal{N}(T_k^{-1} C, T_k A T_k^{-1}) = \mathcal{X}_1 \oplus \mathcal{X}_3$.

This implies that the states $x \in \mathcal{X}_1$ are reachable and observable, the states $x \in \mathcal{X}_2$ are reachable and unobservable, the states $x \in \mathcal{X}_3$ are not reachable and unobservable, while the states $x \in \mathcal{X}_4$ are not reachable and observable. With such a partitioning, the system Σ_s (2.3) is described by

$$\Sigma_k = \left\{ \begin{array}{rcl} \begin{pmatrix} \dot{x}_1(t) \\ \dot{x}_2(t) \\ \dot{x}_3(t) \\ \dot{x}_4(t) \end{pmatrix} & = & \begin{pmatrix} A_{11} & A_{12} & A_{13} & A_{14} \\ 0 & A_{22} & 0 & A_{24} \\ 0 & 0 & A_{33} & A_{34} \\ 0 & 0 & 0 & A_{44} \end{pmatrix} \begin{pmatrix} x_1(t) \\ x_2(t) \\ x_3(t) \\ x_4(t) \end{pmatrix} + \begin{pmatrix} B_1 \\ B_2 \\ 0 \\ 0 \end{pmatrix} u(t) \\ y(t) & = & \begin{pmatrix} 0 & C_2 & 0 & C_4 \end{pmatrix} \quad x(t) \quad + \quad \begin{pmatrix} D \end{pmatrix} \; u(t). \end{array} \right. \tag{2.5}$$

The distinction between BIBO stability and internal stability becomes more intuitive by considering the system Σ_k (2.5), which will be demonstrated in the following proposition.

Proposition 2.5 *The system Σ_k (2.5) is BIBO stable if and only if $\lambda(A_{22}) \subset \mathbb{C}_-$. Furthermore, Σ_k (2.5) is internally stable if and only if $\lambda(A) \subset \mathbb{C}_-$.*

Proof: Internal stability follows directly from Proposition 2.2.

For BIBO stability, let us consider the transfer function of Σ_k (2.5). The structure of Σ_k (2.5) implies that this transfer function is described by

$$\Gamma_k(s) = C_2(sI_{n_{x_2}} - A_{22})^{-1}B_2 + D.$$

Therefore, the reachable and observable system

$$\Sigma_{2,2} = \begin{cases} \dot{x}_2(t) &= A_{22}x(t) + B_2u(t) \\ y(t) &= C_2x_2(t). + Du(t) \end{cases}$$

is equivalent to Σ_k (2.5) in terms of input to output behaviour. Finally, Trentelman et al. [2001, Thm. 3.20] have shown that the eigenvalues of A_{22} are equal to the poles of $\Gamma_k(s)$, if all common factors in the numerator and denominator polynomials are removed, which completes the proof. □

The concepts of reachability and observability are used to determine whether a state is affected by the input $u(t)$ and whether it can be observed in the output $y(t)$, respectively. It is, however, often desired to quantify how reachable or how observable a state is. Let us consider the following definition for this purpose.

Definition 2.6 *For an internally stable system Σ_s (2.3) and the state $\underline{x} \in \mathbb{R}^{n_x}$*

- *we define the minimal energy to reach $\underline{x}$ as*

$$\begin{aligned} \mathcal{E}_R(\underline{x}) \coloneqq \inf_{u(t)} \quad & \int_{t=-\infty}^{0} \|u(t)\|_2^2 \, dt \\ s.t. \quad & u(t) \text{ is } L_2\text{-bounded}, \\ & \lim_{t\to-\infty} x(t) = 0 \text{ and } x(0) = \underline{x}. \end{aligned}$$

- *we define the observation energy associated with $\underline{x}$ as*

$$\mathcal{E}_O(\underline{x}) \coloneqq \int_{t=0}^{\infty} \|y(t)\|_2^2 \, dt, \text{ with } x(0) = \underline{x} \text{ and } u(t) = 0.$$

These energies can—by assuming internal stability for Σ_s (2.3)—be expressed in terms of the so-called Gramians, which are discussed in great detail by Antoulas [2005]. The reachability and observability Gramians are defined as

$$\mathcal{P}(A, B) \coloneqq \int_{t=0}^{\infty} e^{At}BB^\top e^{A^\top t} dt, \tag{2.6}$$

$$\mathcal{Q}(C, A) \coloneqq \int_{t=0}^{\infty} e^{A^\top t}C^\top Ce^{At} dt, \tag{2.7}$$

respectively. Each Gramian is dual to the other, in the sense that $\mathcal{P}(A, B) = \mathcal{Q}(B^\top, A^\top)$ and $\mathcal{Q}(C, A) = \mathcal{P}(A^\top, C^\top)$.

When Σ_s (2.3) is internally stable, the Gramians are the unique positive semidefinite solutions to the following Lyapunov equations:

$$\mathcal{P} \succeq 0 \text{ such that } A\mathcal{P} + \mathcal{P}A^\top + BB^\top = 0, \tag{2.8}$$

$$\mathcal{Q} \succeq 0 \text{ such that } A^\top\mathcal{Q} + \mathcal{Q}A + C^\top C = 0. \tag{2.9}$$

Furthermore, $\mathcal{P} \succ 0$ if and only if Σ_s (2.3) is reachable, while $\mathcal{Q} \succ 0$ if and only if Σ_s (2.3) is observable.

Now, let us relate the Gramians to the energies $\mathcal{E}_R$ and $\mathcal{E}_O$ as defined above. If Σ_s (2.3) is internally stable and reachable, the minimal energy to reach the state $\underline{x}$ is described in terms of the reachability Gramian by

$$\mathcal{E}_R(\underline{x}) = \underline{x}^\top \mathcal{P}^{-1} \underline{x}.$$

If the system is internally stable, the minimal observation energy associated with $\underline{x}$ is described in terms of the observability Gramian by

$$\mathcal{E}_O(\underline{x}) = \underline{x}^\top \mathcal{Q} \underline{x}.$$

2.2.4 System norms

In chapter 1 it is mentioned that system norms are used to quantify, for example for Σ_s (2.3), how much the input $u(t)$ affects the output $y(t)$. The H_2 and H_∞ norms are typically considered; these norms are discussed in great detail by Scherer and Weiland [2015].

The H_2 Norm of a System

Let us consider a formal definition for the H_2 norm, which is defined for the transfer function of a system Σ_s (2.3):

Definition 2.7 *Let $\Gamma_s(s)$ be the transfer function of a strictly proper—i.e. with $D = 0$—BIBO stable system Σ_s (2.3).*

Then the H_2 norm (squared) for $\Gamma_s(s)$ is defined as

$$\|\Gamma_s(s)\|_{H_2}^2 := \frac{1}{2\pi} \mathrm{tr} \left(\int_{\omega=-\infty}^{\infty} \Gamma_s(j\omega) \Gamma_s^*(j\omega) d\omega \right).$$

The notation $\|\Sigma_s\|_{H_2}$ is used to denote the H_2 norm of the transfer function $\Gamma_s(s)$.

In the frequency domain, the H_2 norm is an integral over the frequency response of a system. A time domain interpretation of the H_2 norm can be obtained by utilising Parseval's theorem, as explained by Scherer and Weiland [2015, Sec. 2.3].

In the time domain, the H_2 norm of Σ_s (2.3) essentially describes the output energy associated with the impulse response of the system.

Now, let us consider the impulse response matrix $\Phi(t) = Ce^{At}B$ for the system Σ_s (2.3) and for $t \geq 0$—i.e. $\Phi(t) = 0$ for $t < 0$. The entries $\Phi_{i,j}(t)$ of this matrix describe the response for the i^{th} output $y_i(t)$ of Σ_s (2.3), provided that $x(0) = 0$ and that an impulse is applied to the j^{th} input $u_j(t)$ at $t = 0$, i.e. $u(t) = \delta(t)e_{n_u}(j)$.

From this time domain interpretation, a direct relation can be established between the H_2 norm of Σ_s (2.3) and its Gramians.

Lemma 2.8 *Consider a strictly proper internally stable system Σ_s (2.3) and let $\mathcal{P}$ and $\mathcal{Q}$ be the Gramians as defined in (2.6) and (2.7), respectively.*

Then the H_2 norm of Σ_s (2.3) is described by

$$\begin{aligned}\|\Sigma_s\|_{H_2}^2 = \sum_{i,j} \|\Phi_{i,j}(t)\|_{L_2}^2 &= \operatorname{tr} \int_{t=0}^{\infty} B^\top e^{A^\top t} C^\top C e^{At} B dt \\ &= \operatorname{tr} \int_{t=0}^{\infty} C e^{At} B B^\top e^{A^\top t} C^\top dt \\ &= \operatorname{tr}(C\mathcal{P}C^\top) = \operatorname{tr}(B^\top \mathcal{Q} B).\end{aligned}$$

Proof: The proof is given by Scherer and Weiland [2015, Sec. 3.3]. □

A similar relation can, however, also be observed if Σ_s (2.3) is only BIBO stable. In order to establish this relation, an equivalent system of the form Σ_k (2.5) is utilised.

Proposition 2.9 *Consider a strictly proper BIBO stable system Σ_s (2.3) and a state transformation T_k that is used to construct an equivalent system of the form Σ_k (2.5). Furthermore, let $\mathcal{P}_{22,k} = \mathcal{P}(A_{22}, B_u)$ and $\mathcal{Q}_{22,k} = \mathcal{Q}(C_2, A_{22})$ denote (partial) Gramians for Σ_k (2.5) as defined in (2.6) and (2.7), respectively.*

Then the H_2 norm of Σ_s (2.3) is described by

$$\|\Sigma_s\|_{H_2}^2 = \|\Sigma_k\|_{H_2}^2 = \operatorname{tr}(C_2 \mathcal{P}_{k,22} C_2^\top) = \operatorname{tr}(B_2^\top \mathcal{Q}_{k,22} B_2).$$

Proof: The proof can be found in appendix A.1. □

Finally, duality of the Gramians—i.e. $\mathcal{P}(A, B) = \mathcal{Q}(B^\top, A^\top)$ and $\mathcal{Q}(C, A) = \mathcal{P}(A^\top, C^\top)$—implies that the *dual system*

$$\Sigma_s^\top = \begin{cases} \dot{x}'(t) = A^\top x'(t) + C^\top y'(t) \\ u'(t) = B^\top x'(t) + D^\top y'(t) \end{cases} \tag{2.10}$$

satisfies $\|\Sigma_s\|_{H_2} = \left\|\Sigma_s^\top\right\|_{H_2}$.

The H_∞ Norm of a System

Let us now consider a formal definition for the H_∞ norm, which is defined for the transfer function of a system Σ_s (2.3):

Definition 2.10 *Let $\Gamma_s(s)$ be the transfer function of a BIBO stable system Σ_s (2.3). Then the H_∞ norm is for $\Gamma_s(s)$ defined as*

$$\|\Gamma_s(s)\|_{H_\infty} \coloneqq \sup_{\omega\in\mathbb{R}} \sigma_1(\Gamma_s(j\omega)).$$

The notation $\|\Sigma_s\|_{H_\infty}$ is used to denote the H_∞ norm of the transfer function $\Gamma_s(s)$.

In the frequency domain, the H_∞ norm is the peak value in the frequency response of a system. Similarly to the H_2 norm, a time domain interpretation of this norm exists as well. In the time domain, the H_∞ norm of Σ_s (2.3) essentially describes the output energy associated with the "worst case" input. This interpretation is formally described as follows.

Lemma 2.11 *The H_∞ norm of a BIBO stable system Σ_s (2.3) satisfies*

$$\begin{aligned}\|\Sigma_s\|_{H_\infty} = \sup_{u(t)\neq 0} \ & \frac{\|y(t)\|_{L_2}}{\|u(t)\|_{L_2}} \\ s.t. \ & u(t) \text{ is } L_2\text{-bounded}, \\ & u(t) = 0 \text{ and } x(t) = 0 \text{ for } t \leq 0.\end{aligned}$$

Proof: The proof is given by Scherer and Weiland [2015, Sec. 3.3]. □

Finally, by observing that the singular values of $\Gamma_s(s)$ are equal to the singular values of $\Gamma_s^\top(s)$, we can also conclude that $\|\Sigma_s\|_{H_\infty} = \left\|\Sigma_s^\top\right\|_{H_\infty}$.

2.2.5 System Properties for Control

In control it is often desired to achieve stability in combination with a certain degree of performance; for example, the states of Σ_s (2.3) should converge to the origin at some predetermined minimal convergence rate when $u(t) = 0$. In order to capture a combination of stability and performance requirements, a stability domain $\mathbb{C}_g$ as defined in section 2.1.1 can be considered. For a stability domain $\mathbb{C}_g$ we will consider the following definitions:

Definition 2.12 *Consider a stability domain $\mathbb{C}_g$, a system Σ_s (2.3) and the corresponding transfer function $\Gamma_s(s)$, for which all common factors in the numerator and denominator polynomials are removed.*

Then Σ_s (2.3) is "externally $\mathbb{C}_g$-stable" if any pole p_i of $\Gamma_s(s)$ satisfies $p_i \in \mathbb{C}_g$.

Furthermore, Σ_s (2.3) is "internally $\mathbb{C}_g$-stable" if

$$\lambda(A_{11}) \cup \lambda(A_{22}) \cup \lambda(A_{33}) \cup \lambda(A_{44}) \subseteq \mathbb{C}_g.$$

This type of stability is a generalisation of the stability concepts that were introduced in section 2.2.2. Namely, external $\mathbb{C}_-$-stability is equivalent to BIBO stability and internal $\mathbb{C}_-$-stability is equivalent to internal stability.

A state feedback $u(t) = Fx(t)$ is often considered in control problems. Applying such a feedback to Σ_s (2.3), results in the closed-loop state equation

$$\dot{x}(t) = \big(A + BF\big)\, x(t).$$

Now, from a control perspective, it is important to determine whether there exists a state feedback $u(t) = Fx(t)$ such that this closed-loop state equation is internally $\mathbb{C}_g$-stable. This leads to the concept of $\mathbb{C}_g$-stabilisability.

Definition 2.13 *The pair (A, B) is $\mathbb{C}_g$-stabilisable if there exists a mapping $F : \mathcal{X} \to \mathcal{U}$ such that $\lambda(A + BF) \subseteq \mathbb{C}_g$.*

Furthermore, we say that (A, B) is stabilisable if it is $\mathbb{C}_-$-stabilisable.

The dual problem—which is called a state observation problem—consists of finding an appropriate mapping $L : \mathcal{Y} \to \mathcal{X}$ for the state equation

$$\dot{\tilde{x}}(t) = \big(A + LC\big)\, \tilde{x}(t).$$

In a dual fashion to state feedback design, the concept of $\mathbb{C}_g$-detectability is now introduced.

Definition 2.14 *The pair (C, A) is $\mathbb{C}_g$-detectable if there exists a mapping $L : \mathcal{Y} \to \mathcal{X}$ such that $\lambda(A + LC) \subseteq \mathbb{C}_g$.*

Furthermore, we say that (C, A) is detectable if it is $\mathbb{C}_-$-detectable.

It can easily be verified whether Σ_s (2.3) is $\mathbb{C}_g$-stabilisability and $\mathbb{C}_g$-detectable by considering an equivalent system of the form Σ_k (2.5); this will be shown in the following proposition.

Proposition 2.15 *Consider a stability domain $\mathbb{C}_g$, the system Σ_s (2.3) and a state transformation T_k that is used to construct an equivalent system of the form Σ_k (2.5).*

Then Σ_s (2.3) is $\mathbb{C}_g$-stabilisable if and only if $\lambda(A_{33}) \subseteq \mathbb{C}_g$ and $\lambda(A_{44}) \subseteq \mathbb{C}_g$.

Furthermore, Σ_s (2.3) is $\mathbb{C}_g$-detectable if and only if $\lambda(A_{11}) \subseteq \mathbb{C}_g$ and $\lambda(A_{33}) \subseteq \mathbb{C}_g$.

Proof: The proof is given by Trentelman et al. [2001, Theorem. 3.38], when it is observed that the unreachable eigenvalues of Σ_k (2.5) are described by A_{33} and A_{44}, while the unobservable eigenvalues are described by A_{11} and A_{33}. □

2.3 Linear Matrix Inequalities in Control

The concepts of $\mathbb{C}_g$-stabilisabilty and $\mathbb{C}_g$-detectability are introduced to establish whether there exist mappings F and L that are $\mathbb{C}_g$-stabilising for the system Σ_s (2.3). In this section, we will introduce two algorithms that utilise an LMI in order to construct these stabilising mappings for stability domain $\mathbb{C}_-$. As explained by Henrion and Arzelier [2004], these algorithms can be extended in order to consider a larger class of stability domains.

The following proposition will be utilised in order to construct these LMIs.

Proposition 2.16 *Consider a nonsingular matrix $T \in \mathbb{R}^{n_x \times n_x}$.*

Then the following properties are obtained:

- *the spectrum of any matrix $A \in \mathbb{R}^{n_x \times n_x}$ is invariant under similarity transformations; i.e. $\lambda(A) = \lambda(TAT^{-1})$.*
- *the definiteness of a symmetric matrix $A \in \mathbb{R}^{n_x \times n_x}$ is invariant under congruence transformations; i.e. $A \succ 0$ if and only if $T^\top AT \succ 0$.*

Proof: To prove the first property, observe that for any $\lambda_i \in \lambda(A)$ there exists a vector $x \in \mathbb{C}^{n_x}$ such that $Ax = \lambda_i x$. By observing that $T^{-1}T = I_{n_x}$, by left multiplying this equation with T and by defining $\bar{x} = Tx$, we obtain $TAT^{-1}\bar{x} = \lambda_i \bar{x}$. Therefore, for any $\lambda_i \in \lambda(A)$ we get that $\lambda_i \in \lambda(TAT^{-1})$ and vice versa.

For the second property, it must be noted that $A \succ 0$ implies for any vector $x \in \mathbb{R}^{n_x}$ that $x^\top Ax > 0$. Now, let us define the transformation $x = Tz$ in order to conclude $z^\top T^\top ATz > 0$ for any vector $z \in \mathbb{R}^{n_x}$, which implies that $T^\top AT \succ 0$. The converse statement is proven in the same way. □

Let us first establish how stability is characterised in terms of an LMI. It is explained by Scherer and Weiland [2015, Sec. 1.4.3] that a matrix $A \in \mathbb{R}^{n_x \times n_x}$ satisfies $\lambda(A) \subset \mathbb{C}_-$ if and only if there exists a matrix $X = X^\top \succ 0 \in \mathbb{R}^{n_x \times n_x}$ such that $A^\top X + XA \prec 0$.

Then, let us consider the construction of a matrix $F \in \mathbb{R}^{n_u \times n_x}$ that achieves $\lambda(A + BF) \subset \mathbb{C}_-$. This is—by utilising the LMI as defined above—equivalent to finding the matrices F and $X = X^\top \succ 0$ such that

$$(A + BF)^\top X + X(A + BF) \prec 0.$$

This equation is, however, not linear in the variables F and X.

The problem can be converted into an equivalent LMI by applying the congruence transformation X^{-1}; and by defining $Y = Y^\top = X^{-1} \succ 0$ and $K = FY$ in order to obtain

$$\begin{aligned} X^{-1}(A + BF)^\top + (A + BF)X^{-1} &\prec 0, \\ X^{-1}A^\top + AX^{-1} + X^{-1}F^\top B^\top + BFX^{-1} &\prec 0, \\ YA^\top + AY + K^\top B^\top + BK &\prec 0. \end{aligned}$$

In this way, all stabilising matrices $F = KY^{-1}$ are essentially characterised by solutions to an LMI in the variables K and $Y \succ 0$.

Similarly, the construction of a matrix $L \in \mathbb{R}^{n_x \times n_y}$ that achieves $\lambda(A+LC) \subset \mathbb{C}_-$ is equivalent to finding the matrices L and $Z = Z^\top \succ 0$ such that

$$(A+LC)^\top Z + Z(A+LC) \prec 0.$$

This equation is also not linear in the variables L and Z. However, the problem can be converted into an equivalent LMI by, again, utilising $Z \succ 0$ and by defining $J = ZL$ in order to obtain

$$A^\top Z + ZA + C^\top J^\top + JC \prec 0.$$

In this way, all stabilising matrices $L = Z^{-1}J$ are essentially characterised by solutions to an LMI in the variables J and $Z \succ 0$.

2.4 H_2 Optimal Control

The optimal control problem is defined in Problem 1.1 for an arbitrary system norm that quantifies performance. In order to mathematically solve this type of problem, a specific norm must be chosen; typically, the H_2 and H_∞ norms are considered. These so-called H_2 and H_∞ optimal control problems have received a considerable amount of attention over the past decades and their solution is well-documented in several textbooks, such as [Saberi et al., 1995a],[Zhou et al., 1996], [Trentelman et al., 2001] and [Bosgra et al., 2007].

A specific derivation—which is directly based on the approach taken by Trentelman et al. [2001]—for the H_2 optimal control problem will now be discussed. As a generalisation for the system Σ (1.1) that is defined in chapter 1, let us consider an LTI system of the form

$$\Sigma_f = \begin{cases} \dot{x}(t) = Ax(t) + B_u u(t) + B_w w(t) \\ y(t) = C_y x(t) + D_{uy} u(t) + D_{wy} w(t) \\ z(t) = C_z x(t) + D_{uz} u(t) + D_{wz} w(t), \end{cases} \tag{2.11}$$

with vector signals $x(t)$, $u(t)$, $w(t)$, $y(t)$ and $z(t)$ that represent the state, known input, unknown disturbance, measured output and the control output, respectively. These signals assume values in finite-dimensional vector spaces $\mathcal{X} = \mathbb{R}^{n_x}, \mathcal{U} = \mathbb{R}^{n_u}$, $\mathcal{W} = \mathbb{R}^{n_w}$, $\mathcal{Y} = \mathbb{R}^{n_y}$ and $\mathcal{Z} = \mathbb{R}^{n_z}$, respectively. The dynamical relation between the signals is described by real-valued matrices A, B_u, B_w, C_y, C_z,D_{uy}, D_{wy}, D_{uz} and D_{wz} of appropriate dimension.

Then, let us consider applying a controller of the form

$$\Sigma_{c,n_c} = \begin{cases} \dot{x}_c(t) = Jx_c(t) + Ky(t) \\ u(t) = Mx_c(t) + Ny(t) \end{cases} \tag{2.12}$$

to Σ_f (2.11), in order to obtain the following closed-loop system:

$$\Sigma_{f,cl,n_c} = \begin{cases} \dot{x}_{cl}(t) = A_{cl}x_{cl}(t) + B_{cl}w(t) \\ z(t) = C_{cl}x_{cl}(t) + D_{cl}w(t), \end{cases} \tag{2.13}$$

with

$$\begin{aligned} A_{cl} &= \begin{pmatrix} A + B_u(I_{n_u} - ND_{uy})^{-1}NC_y & B_u(I_{n_u} - ND_{uy})^{-1}M \\ K(I_{n_u} - D_{uy}N)^{-1}C_y & J + K(I_{n_u} - D_{uy}N)^{-1}D_{uy}M \end{pmatrix}, \\ B_{cl} &= \begin{pmatrix} B_w + B_u(I_{n_u} - ND_{uy})^{-1}ND_{wy} \\ K(I_{n_u} - D_{uy}N)^{-1}D_{wy} \end{pmatrix}, \\ C_{cl} &= \begin{pmatrix} C_z + D_{uz}(I_{n_u} - ND_{uy})^{-1}NC_y & D_{uz}(I_{n_u} - ND_{uy})^{-1}M \end{pmatrix}, \\ D_{cl} &= D_{wz} + D_{uz}(I_{n_u} - ND_{uy})^{-1}ND_{wy} \quad \text{and} \quad x_{cl}(t) = \begin{pmatrix} x(t) \\ x_c(t) \end{pmatrix}. \end{aligned}$$

The mapping D_{uy} of Σ_f (2.11) is a direct mapping from input $u(t)$ to output $y(t)$, while the mapping N of Σ_{c,n_c} (2.12) is direct mapping from output $y(t)$ to input $u(t)$. These direct mappings might result in an *ill-posed* closed-loop interconnection if the matrix $(I_{n_u} - ND_{uy})$ is non-singular, because the signals $u(t)$ and $y(t)$ are then not—or non-uniquely—defined for some signals $w(t)$ and initial conditions $x(0) = x_0$, $x_c(0) = x_{c,0}$; this is explained in more detail by Trentelman et al. [2001, Sec. 3.13]. It is therefore required that the closed-loop interconnection of Σ_f (2.11) with Σ_{c,n_c} (2.12) is *well-posed*.

We say that this interconnection is well-posed if the signals $x(t)$, $x_c(t)$, $u(t)$, $y(t)$ and $z(t)$ are uniquely defined for any disturbance signal $w(t)$ and any initial condition $x(0) = x_0$ and $x_c(0) = x_{c,0}$. This is equivalent to requiring that the inverse $(I_{n_u} - ND_{uy})^{-1}$—or equivalently $(I_{n_y} - D_{uy}N)^{-1}$—exists.

With the H_2 optimal control problem, the aim is to minimise $\|\Sigma_{f,cl,n_c}\ (2.13)\|_{H_2}$ by appropriate selection of the controller mappings J, K, M and N. In order to solve these problems, it is required that the closed-loop interconnection of Σ_f (2.11) with Σ_{c,n_c} (2.12) is well-posed, internally stable and that the norm $\|\Sigma_{f,cl,n_c}\ (2.13)\|_{H_2/H_\infty}$ is well-defined. These requirements lead to the concept of admissibility, which is defined as follows.

Definition 2.17 *The controller Σ_{c,n_c} (2.12) is called*

- *H_∞-admissible for Σ_f (2.11) if for Σ_{f,cl,n_c} (2.13) we have that $\lambda(A_{cl}) \subset \mathbb{C}_-$ and that $(I_{n_u} - ND_{uy})$ is non-singular.*
- *H_2-admissible for Σ_f (2.11) if for Σ_{f,cl,n_c} (2.13) we have that $\lambda(A_{cl}) \subset \mathbb{C}_-$, $D_{cl} = 0$ and that $(I_{n_u} - ND_{uy})$ is non-singular.*

For the H_2 optimal control problem, let us consider the following assumption.

Assumption 2.1 *It is assumed that*

1a) (A, B_u) is stabilisable.
1b) (C_y, A) is detectable.

2a) $\begin{pmatrix} A - j\omega I_{n_x} & B_u \\ C_z & D_{uz} \end{pmatrix}$ *is full column rank for all* $\omega \in \mathbb{R}$.
2b) $\begin{pmatrix} A - j\omega I_{n_x} & B_w \\ C_y & D_{wy} \end{pmatrix}$ *is full row rank for all* $\omega \in \mathbb{R}$.
3a) D_{uz} *is full column rank.*
3b) D_{wy} *is full row rank.*

Item 1 in this assumption is a necessary requirement for the existence of a stabilising controller, item 2 is sufficient to guarantee that an optimal controller exists which generates bounded signals, while item 3 is a technical condition that guarantees the existence of stabilising solutions to so-called algebraic Riccati equations (AREs). The assumption should therefore not be viewed as a restriction.

For example, the assumption that D_{uz} is full column rank implies that all input signals $u(t)$ are directly visible on the control output $z(t)$. This implies that a bounded signal $u(t)$ is required in order to obtain a bounded norm for Σ_{f,cl,n_c} (2.13); as a result, an optimal controller will generate bounded input signals.

In addition, we will consider a second assumption for notational convenience. The solution to the H_2 optimal control problem will first be derived under this assumption and a generalisation that does not require this assumption will be presented afterwards.

Assumption 2.2 *It is assumed that*
1) $D_{uz}^\top \begin{pmatrix} C_z & D_{uz} \end{pmatrix} = \begin{pmatrix} 0 & I_{n_u} \end{pmatrix}$.
2) $D_{wy} \begin{pmatrix} B_w^\top & D_{wy}^\top \end{pmatrix} = \begin{pmatrix} 0 & I_{n_y} \end{pmatrix}$.

The following lemma shows that, without loss of generality, it can be assumed that the matrices D_{uy} and D_{wz} are equal to zero.

Lemma 2.18 *Consider a system* Σ_f (2.11) *that satisfies assumption 2.1.*

Then there exists an H_2*-admissible controller* Σ_{c,n_c} (2.12) *for* Σ_f (2.11) *if and only if there exists a mapping* $N : \mathcal{Y} \to \mathcal{U}$ *such that* $D_{cl} = D_{wz} + D_{uz}(I_{n_u} - ND_{uy})^{-1}ND_{wy} = 0$.

If this mapping exists, the design of an H_2*-admissible controller for* Σ_f (2.11) *can be transformed into the design of a strictly proper* H_2*-admissible controller—i.e. with* $N = 0$*—for a system of the form*

$$\Sigma = \begin{cases} \dot{x}(t) = Ax(t) + B_u u(t) + B_w w(t) \\ y(t) = C_y x(t) + D_{wy} w(t) \\ z(t) = C_z x(t) + D_{uz} u(t), \end{cases} \tag{2.14}$$

which satisfies assumption 2.1 as well.

Proof: The proof can be found in appendix A.1. □

Now let us discuss the approach that is typically considered in solving the H_2 optimal control problem for Σ (2.14). With this approach, a strictly proper Luenberger

observer-based controller is utilised; this controller is of the form

$$\Sigma_{c,sp} = \begin{cases} \dot{\tilde{x}}(t) = \left(A + B_u F + LC_y\right)\tilde{x}(t) - Ly(t) \\ u(t) = F\tilde{x}(t). \end{cases} \tag{2.15}$$

The design of such a controller consists of finding appropriate mappings $F : \mathcal{X} \to \mathcal{U}$ and $L : \mathcal{Y} \to \mathcal{X}$. Please note that the controller state $\tilde{x}(t)$—which is called the observed state—is an estimate of the system state $x(t)$.

Interconnecting Σ (2.14) with $\Sigma_{c,sp}$ (2.15) yields—when a state observation error $e(t) = x(t) - \tilde{x}(t)$ is defined—the closed-loop system

$$\Sigma_{cl,sp} = \left\{ \begin{array}{rcl} \begin{pmatrix} \dot{x}(t) \\ \dot{e}(t) \end{pmatrix} & = & \begin{pmatrix} A + B_u F & -B_u F \\ 0 & A + LC_y \end{pmatrix} \begin{pmatrix} x(t) \\ e(t) \end{pmatrix} + \begin{pmatrix} B_w \\ B_w + LD_{wy} \end{pmatrix} w(t) \\ z(t) & = & \begin{pmatrix} C_z + D_{uz}F & -D_{uz}F \end{pmatrix} \begin{pmatrix} x(t) \\ e(t) \end{pmatrix} + \begin{pmatrix} 0 \end{pmatrix} w(t). \end{array} \right. \tag{2.16}$$

By utilising a controller of the form $\Sigma_{c,sp}$ (2.15), the optimal control problem in Problem 1.1 is solved with a controller of order $n_c = n_x$, by appropriately selecting the mappings F and L. The H_2 optimal control problem is therefore typically formulated in the following manner.

Problem 2.1 *Construct an H_2-admissible controller $\Sigma^\star_{c,sp}$ of the form* (2.15) *for* Σ (2.14)*, which is parametrised in the mappings $F^\star$ and $L^\star$ that are a solution to*

$$\begin{aligned} (F^\star, L^\star) = \arg \quad & \min_{F,L} \left\| \Sigma_{cl,sp} \text{ (2.16)} \right\|_{H_2} \\ & \text{s.t. } \Sigma_{c,sp} \text{ (2.15) is } H_2\text{-admissible for } \Sigma \text{ (2.14)}. \end{aligned}$$

Under assumption 2.1, it is a well-known fact that the solution to this problem is obtained by separately solving a state feedback problem—which constructs the mapping $F^\star$—and an estimation problem, which constructs the mapping $L^\star$. This fact is called the *separation principle*, as explained by Trentelman et al. [2001, Sec. 11.5].

To solve Problem 2.1, let us first discuss the H_2 optimal state feedback problem and, subsequently, the H_2 optimal estimation problem by utilising the method that is presented by Trentelman et al. [2001, Ch. 10-11]. The solution to these problems is then combined in order to present a solution to the H_2 optimal (measurement feedback) control problem. Please note that each of these problems is first solved under assumption 2.2 and a generalisation is presented afterwards.

2.4.1 State Feedback Design

The aim for H_2 optimal control is to construct an input signal $u(t)$ that—if this norm is interpreted according to Lemma 2.8—minimises the norm $\|z(t)\|_{L_2}$ of

Σ (2.14), when an impulse is applied to each disturbance $w(t)$. An impulse on $w(t)$ at time $t = 0$ essentially generates some initial condition $x(0) = x_0$; this problem is therefore equivalent to minimising $\|z(t)\|_{L_2}$ for a given set of specific initial conditions.

For this reason, let us quantify the L_2 (squared) performance for each initial condition $x(0) = x_0$ and input signal $u(t)$ by

$$\begin{aligned}\gamma_{L_2}(x_0, u(t)) = & \int_{t=0}^{\infty} \|C_z x(t) + D_{uz} u(t)\|_2^2 \, dt \\ \text{s.t. } & \dot{x}(t) = Ax(t) + B_u u(t) \\ & x(0) = x_0.\end{aligned}$$

With optimal control, the aim is therefore to minimise this performance measure by finding a suitable stabilising input signals $u(t) \in \mathbb{U}(x_0)$ (stabilising input signals are formally defined in section 2.2.2) in order to obtain the optimal L_2 optimal (squared) performance

$$\gamma^\star_{L_2}(x_0) = \min_{u \in \mathbb{U}(x_0)} \gamma_{L_2}(x_0, u(t)).$$

As explained by Trentelman et al. [2001, Sec. 10.2], it is expected that this optimal performance is a quadratic function of x_0; i.e. $\gamma^\star_{L_2}(x_0) = x_0^\top P_s x_0$ for some matrix $P_s \succeq 0$.

By assuming items 1a, 2a and 3a in assumption 2.1 and item 1 in assumption 2.2, by exploiting the fact that $\lim_{t\to\infty} x(t) = 0$ for a stabilising input signal $u(t)$ and by utilising the fundamental theorem of calculus, we can obtain the expression

$$\gamma_{L_2}(x_0, u(t)) = x_0^\top P_s x_0 + \int_{t=0}^{\infty} x(t)^\top C_z^\top C_z x(t) + u(t)^\top u(t) + \frac{d}{dt}(x(t)^\top P_s x(t)) dt.$$

Then, by observing that

$$\frac{d}{dt}(x(t)^\top P_s x(t)) = (Ax(t) + B_u u(t))^\top P_s x(t) + x(t)^\top P_s (Ax(t) + B_u u(t)),$$

it can be shown that

$$\gamma_{L_2}(x_0, u(t)) = x_0^\top P_s x_0 + \int_{t=0}^{\infty} \left\|u(t) + B_u^\top P_s x(t)\right\|_2^2 dt + \int_{t=0}^{\infty} x(t)^\top S x(t) dt, \quad (2.17)$$

with $S = A^\top P_s + P_s A + C_z^\top C_z - P_s B_u B_u^\top P_s$. This equation is called the completion of squares formula.

If P_s is chosen such that $S = 0$, the following ARE is obtained:

$$A^\top P_s + P_s A + C_z^\top C_z - P_s B_u B_u^\top P_s = 0. \quad (2.18)$$

This ARE can then be used to obtain the following well-known result.

Lemma 2.19 *Consider a system* Σ (2.14) *that satisfies items 1a, 2a and 3a in assumption 2.1 and item 1 in assumption 2.2, with* $w(t) = 0$ *and an initial condition* $x_0 \in \mathcal{X}$*. Furthermore, let* P_s *be a solution to the ARE in* (2.18)*.*

Then, the completion of squares formula in (2.17) *reduces to*

$$\gamma_{L_2}(x_0, u(t)) = x_0^\top P_s x_0 + \int_{t=0}^{\infty} \left\| u(t) + B_u^\top P_s x(t) \right\|_2^2 dt$$

Proof: The proof is given by Trentelman et al. [2001, Chp. 10]. □

From this lemma it is directly clear that a minimum is obtained for $\gamma_{L_2}(x_0, u(t))$ by setting $u(t) = -B_u^\top P_s x(t)$, because it sets the only term that depends on the input signal $u(t)$ to zero. This solution does, however, not guarantee that $u(t) \in \mathbb{U}(x_0)$; furthermore, the input signal depends on a mapping P_s that is not uniquely defined.

Trentelman et al. [2001, Lem. 10.14] did show that both of these problems are solved by considering the unique stabilising solution P_s^+ to the ARE in (2.18), which leads to the following result.

Lemma 2.20 *Consider a system* Σ (2.14) *that satisfies items 1a, 2a and 3a in assumption 2.1 and item 1 in assumption 2.2, with* $w(t) = 0$ *and an initial condition* $x_0 \in \mathcal{X}$*.*

Furthermore, let $P_s^+ \succeq 0$ *be the unique stabilising solution to the ARE in* (2.18)*. This positive semidefinite solution satisfies* $P_s^+ \succeq P_s$*, for any real and symmetric solution* P_s *to the ARE in* (2.18)*.*

Then the L_2 *optimal (squared) performance for* x_0 *is described by*

$$\gamma_{L_2}^\star(x_0) = x_0^\top P_s^+ x_0,$$

In addition, the optimal input can be generated with the state feedback $u(t) = -B_u^\top P_s^+ x(t)$*.*

Proof: The proof is given by Trentelman et al. [2001, Lem. 10.14]. □

From this lemma, it is important to observe that the optimal input signal $u(t)$ for a given initial condition $x(0) = x_0$ is generated by a static state feedback. Furthermore, there exists a unique stabilising state feedback $u(t) = F^\star x(t) = -B_u^\top P_s^+ x(t)$ that is optimal for all initial conditions, in the sense that $u^\star(t) = F^\star \exp\left((A + B_u F^\star)t\right) x_0 \in \mathbb{U}(x_0)$ and $\gamma_{L_2}^\star(x_0) = \gamma_{L_2}(x_0, u^\star(t))$. For any initial condition, an optimal input signal $u(t)$ is therefore generated by the static state feedback that is based on the unique stabilising solution to an ARE.

Let us now formulate this problem in terms of the H_2 norm. An H_2 optimal state feedback essentially minimises the L_2 performance for the initial conditions that

are generated by an impulse on each disturbance $w(t)$. Apply a state feedback $u(t) = Fx(t)$ to Σ (2.14) in order to obtain the closed-loop system

$$\Sigma_{cl,F} = \begin{cases} \dot{x}(t) = \Big(A + B_u F \Big) x(t) + B_w w(t) \\ z(t) = \Big(C_z + D_{uz} F \Big) x(t). \end{cases} \tag{2.19}$$

Because this state feedback should stabilise $\Sigma_{cl,F}$ (2.19), let us consider the following definition for admissibility.

Definition 2.21 *The state feedback $u(t) = Fx(t)$ is called H_2-admissible for Σ (2.14) if for $\Sigma_{cl,F}$ (2.19) we have that $\lambda(A + B_u F) \subset \mathbb{C}_-$.*

Then, for an H_2-admissible state feedback, the H_2 (squared) performance is quantified as

$$\gamma_{H_2,F}(\Sigma \text{ (2.14)}, F) = \|\Sigma_{cl,F} \text{ (2.19)}\|_{H_2}^2 .$$

Furthermore, an H_2-admissible state feedback is H_2 optimal for Σ (2.14) if $\gamma_{H_2,F}(\Sigma \text{ (2.14)}, F) = \gamma^\star_{H_2,F}(\Sigma \text{ (2.14)})$, with

$$\begin{aligned} \gamma^\star_{H_2,F}(\Sigma \text{ (2.14)}) = \quad & \min_F \ \gamma_{H_2,F}(\Sigma \text{ (2.14)}, F) \\ & \text{s.t.} \quad u(t) = Fx(t) \text{ is } H_2\text{-admissible for } \Sigma \text{ (2.14)}. \end{aligned}$$

In terms of H_2 performance, we obtain the following result.

Theorem 2.22 *Consider a state feedback $u(t) = Fx(t)$ applied to the system Σ (2.14) that satisfies items 1a, 2a and 3a in assumption 2.1 and item 1 in assumption 2.2, which results in the closed-loop system $\Sigma_{cl,F}$ (2.19).*

Furthermore, let $P_s^+ \succeq 0$ be the unique stabilising solution to the ARE in (2.18)*. This positive semidefinite solution satisfies $P_s^+ \succeq P_s$, for any real and symmetric solution P_s to the ARE in* (2.18)*.*

Then the H_2 optimal (squared) performance is described by

$$\gamma^\star_{H_2,F}(\Sigma \text{ (2.14)}) = \operatorname{tr}\left(B_w^\top P_s^+ B_w \right).$$

In addition, an H_2 optimal state feedback is given by $u(t) = -B_u^\top P_s^+ x(t)$.

Proof: The result follows directly from Lemma 2.20, when it is observed that the initial conditions x_0 are—for the H_2 norm—generated by impulses on each disturbance $w(t)$. This implies that

$$\gamma^\star_{H_2,F}(\Sigma \text{ (2.14)}) = \sum_{i=1}^{n_w} B_{w,i}^\top P_s^+ B_{w,i} = \operatorname{tr}\left(B_w^\top P_s^+ B_w \right).$$

□

It is, however, also desired to quantify the performance of any H_2-admissible feedback for Σ (2.14). For this purpose, let us consider the state and input trajectories

of $\Sigma_{cl,F}$ (2.19) as a result of impulses on each disturbance $w(t)$. These trajectories are described for $t \geq 0$ by

$$X(t) = \exp\left(\left(A + B_u F\right) t\right) B_w, \quad U(t) = F \exp\left(\left(A + B_u F\right) t\right) B_w.$$

In addition, it can be noted that

$$\frac{d}{dt} X(t) = AX(T) + B_u U(t), \quad X(0) = B_w.$$

Then, by assuming items 1a, 2a and 3a in assumption 2.1 and item 1 in assumption 2.2, by exploiting the fact that an internally stabilising feedback implies that $\lim_{t\to\infty} X(t) = 0$ and that $\lim_{t\to\infty} U(t) = 0$; and by utilising the fundamental theorem of calculus, we obtain the expression

$$\begin{aligned} -B_w^\top P_s^+ B_w &= \int_{t=0}^{\infty} \tfrac{d}{dt}\left(X(t)^\top P_s^+ X(t)\right) dt \\ &= \int_{t=0}^{\infty} (B_u^\top P_s^+ X(t) + U(t))^\top (B_u^\top P_s^+ X(t) + U(t)) dt \\ &\quad - \int_{t=0}^{\infty} (C_z X(t) + D_{uz} U(t))^\top ((C_z X(t) + D_{uz} U(t)) dt. \end{aligned}$$

By defining the transformed system

$$\Sigma_{P,s} = \left\{ \begin{array}{rcl} \dot{x}(t) &=& Ax(t) + B_u u(t) + B_w w(t) \\ y(t) &=& C_y x(t) + D_{wy} w(t) \\ z(t) &=& B_u^\top P_s^+ x(t) + u(t), \end{array} \right. \tag{2.20}$$

it can be shown that this expression is equivalent to

$$-\mathrm{tr}\left(B_w^\top P_s^+ B_w\right) = \gamma_{H_2,F}(\Sigma_{P,s}\ (2.20), F) - \gamma_{H_2,F}(\Sigma\ (2.14), F),$$

which leads to the following main result.

Theorem 2.23 *Consider a state feedback $u(t) = Fx(t)$ applied to the system Σ (2.14) that satisfies items 1a, 2a and 3a in assumption 2.1 and item 1 in assumption 2.2, which results in the closed-loop system $\Sigma_{cl,F}$ (2.19); and consider the transformed system $\Sigma_{P,s}$ (2.20).*

Furthermore, Let $P_s^+ \succeq 0$ be the unique stabilising solution to the ARE in (2.18). This positive semidefinite solution satisfies $P_s^+ \succeq P_s$, for any real and symmetric solution P_s to the ARE in (2.18). Then

- *The state feedback $u(t) = Fx(t)$ is H_2-admissible for Σ (2.14) if and only if it is H_2-admissible for $\Sigma_{P,s}$ (2.20).*
- *For any H_2-admissible state feedback we have that $\gamma_{H_2,F}(\Sigma\ (2.14), F) = \mathrm{tr}\left(B_w^\top P_s^+ B_w\right) + \gamma_{H_2,F}(\Sigma_{P,s}\ (2.20), F)$.*
- *Any H_2 optimal (and admissible) state feedback $u(t) = F^\star x(t)$ achieves $\gamma_{H_2,F}(\Sigma\ (2.14), F^\star) = \gamma^\star_{H_2,F}(\Sigma\ (2.14)) = \mathrm{tr}\left(B_w^\top P_s^+ B_w\right)$.*

Proof: The proof is given by Trentelman et al. [2001, Sec. 11.2]. □

To finalise the topic of H_2 optimal state feedback design, let us generalise these results by removing the assumption 2.2.

Corollary 2.24 *Consider a state feedback $u(t) = Fx(t)$ applied to the system Σ (2.14) that satisfies items 1a, 2a and 3a in assumption 2.1, which results in the closed-loop system $\Sigma_{cl,F}$ (2.19).*

Furthermore, let $P^+ \succeq 0$ be the unique stabilising solution to the following ARE:

$$A^\top P + PA + C_z^\top C_z - (PB_u + C_z^\top D_{uz})(D_{uz}^\top D_{uz})^{-1}(PB_u + C_z^\top D_{uz})^\top = 0. \quad (2.21)$$

This positive semidefinite solution satisfies $P^+ \succeq P$, for any real and symmetric solution P to the ARE in (2.21).

Then the H_2 optimal (squared) performance is described by

$$\gamma^\star_{H_2,F}(\Sigma\ (2.14)) = \operatorname{tr}\left(B_w^\top P^+ B_w\right).$$

In addition, an H_2 optimal state feedback is given by
$u(t) = -(D_{uz}^\top D_{uz})^{-1}(B_u^\top P^+ + D_{uz}^\top C_z)x(t)$.

Proof: The proof can be found in appendix A.1. □

Furthermore, consider the transformed system

$$\Sigma_P = \begin{cases} \dot{x}(t) = Ax(t) + B_u u(t) + B_w w(t) \\ y(t) = C_y x(t) + D_{wy} w(t) \\ z(t) = (D_{uz}^\top D_{uz})^{-\frac{1}{2}}(B_u^\top P^+ + D_{uz}^\top C_z)x(t) + (D_{uz}^\top D_{uz})^{\frac{1}{2}} u(t). \end{cases}$$

in order to obtain the following result.

Corollary 2.25 *Consider a state feedback $u(t) = Fx(t)$ applied to the system Σ (2.14) that satisfies items 1a, 2a and 3a in assumption 2.1, which results in the closed-loop system $\Sigma_{cl,F}$ (2.19); and consider the transformed system Σ_P (2.4.1).*

Furthermore, let $P^+ \succeq 0$ be the unique stabilising solution to the ARE in (2.21). This positive semidefinite solution satisfies $P^+ \succeq P$, for any real and symmetric solution P to the ARE in (2.21). Then

- *The state feedback $u(t) = Fx(t)$ is H_2-admissible for Σ (2.14) if and only if it is H_2-admissible for Σ_P (2.4.1).*
- *For any H_2-admissible state feedback we have that $\gamma_{H_2,F}(\Sigma\ (2.14), F) = \operatorname{tr}\left(B_w^\top P^+ B_w\right) + \gamma_{H_2,F}(\Sigma_P\ (2.4.1), F)$.*
- *Any H_2 optimal (and admissible) state feedback $u(t) = F^\star x(t)$ achieves $\gamma_{H_2,F}(\Sigma\ (2.14), F^\star) = \gamma^\star_{H_2,F}(\Sigma\ (2.14)) = \operatorname{tr}\left(B_w^\top P^+ B_w\right)$.*

Proof: This is Theorem 2.23 combined with Corollary 2.24. □

2.4.2 Estimator Design

Now, let us consider the design of an estimator

$$\Sigma_{e,n_e} = \begin{cases} \dot{x}_e(t) = Jx_e(t) + Ky(t) + K_u u(t) \\ \tilde{z}(t) = Mx_e(t) + Ny(t) + N_u u(t). \end{cases} \quad (2.22)$$

of order n_e that produces an estimated output $\tilde{z}(t)$ for the "to-be-estimated output" $z(t)$ of the system Σ (2.14). This estimator creates the signal $\tilde{z}(t)$ by utilising the known input $u(t)$ and the measured output $y(t)$.

By defining an output estimation error $\epsilon_z(t) = z(t) - \tilde{z}(t)$ and by applying this estimator Σ_{e,n_e} (2.22) to the system Σ_f (2.11), we obtain the so-called error system

$$\Sigma_{f,\epsilon,n_e} = \begin{cases} \dot{x}^{f,\epsilon}(t) = A^{f,\epsilon}x^{f,\epsilon}(t) + B_u^{f,\epsilon}u(t) + B_w^{f,\epsilon}w(t) \\ \epsilon_z(t) \;\; = C_z^{f,\epsilon}x^{f,\epsilon}(t) + D_{uz}^{f,\epsilon}u(t) + D_{wz}^{f,\epsilon}w(t), \end{cases} \tag{2.23}$$

with

$$\begin{aligned} x^{f,\epsilon}(t) &= \begin{pmatrix} x(t) \\ x_e(t) \end{pmatrix}, & A^{f,\epsilon} &= \begin{pmatrix} A & 0 \\ KC_y & J \end{pmatrix}, \\ B_u^{f,\epsilon} &= \begin{pmatrix} B_u \\ KD_{uy} + K_u \end{pmatrix}, & B_w^{f,\epsilon} &= \begin{pmatrix} B_w \\ KD_{wy} \end{pmatrix}, \\ C_z^{f,\epsilon} &= \begin{pmatrix} C_z - NC_y & -M \end{pmatrix}, & D_{uz}^{f,\epsilon} &= \begin{pmatrix} D_{uz} - ND_{uy} - N_u \end{pmatrix}, \\ D_{wz}^{f,\epsilon} &= \begin{pmatrix} D_{wz} - ND_{wy} \end{pmatrix} \end{aligned}$$

and with the extended state-space $\mathcal{X}^{f,\epsilon}$. The interconnection between Σ_{e,n_e} (2.22) and Σ_f (2.11) is depicted in figure 2.1.

The H_2 optimal estimation problem, essentially consists of appropriately selecting the mappings J, K, K_u, M, N and N_u of Σ_{e,n_e} (2.22) with the aim of minimising—in the H_2 norm—the effect of the external signals $u(t)$ and $w(t)$ on the estimation error $\epsilon_z(t)$. In a similar fashion to controller design, let us define when such an estimator is H_2-admissible.

Definition 2.26 *Let $\mathcal{N} \subseteq \mathcal{X}^{f,\epsilon}$ denote the unobservable subspace of Σ_{f,ϵ,n_e} (2.23) for a given estimator Σ_{e,n_e} (2.22).*

Then the estimator Σ_{e,n_e} (2.22) is called H_2-admissible for Σ_f (2.11) if for Σ_{f,ϵ,n_e} (2.23) we have that $D_{uz}^{f,\epsilon} = 0$, $D_{wz}^{f,\epsilon} = 0$ and $\lambda(A^{f,\epsilon}|(\mathcal{X}^{f,\epsilon} \bmod \mathcal{N})) \subset \mathbb{C}_-$.

Please note that for estimation problems it is not required that the system Σ_f (2.11) is internally stable, which implies that the error system Σ_{f,ϵ,n_e} (2.23) might not be internally stable. Instead, stability is added to guarantee that $\lim_{t\to\infty} \epsilon_z(t) = 0$ for $w(t) = 0$ and $u(t) = 0$ and for any initial condition; therefore it is only required that the observable dynamics of Σ_{f,ϵ,n_e} (2.23) are stable.

Furthermore, it is important to note that $\lambda(A^{f,\epsilon}|(\mathcal{X}^{f,\epsilon} \bmod \mathcal{N}))$ is well-defined, because the unobservable subspace $\mathcal{N}$ satisfies $A^{f,\epsilon}\mathcal{N} \subseteq \mathcal{N}$.

With this definition, it is possible to formally define the H_2 optimal estimation problem in the following manner.

Problem 2.2 *Construct an H_2-admissible estimator $\Sigma_{e,n_e}^\star$ of the form (2.22) for Σ (2.14), which is a solution to*

$$\begin{aligned} \Sigma_{e,n_e}^\star \;=\; \arg \min_{\Sigma_{e,n_e}\ (2.22)} \; & \|\Sigma_{f,\epsilon,n_e}\ (2.23)\|_{H_2} \\ \text{s.t.} \quad & \Sigma_{e,n_e}\ (2.22) \text{ is } H_2\text{-admissible for } \Sigma\ (2.14). \end{aligned}$$

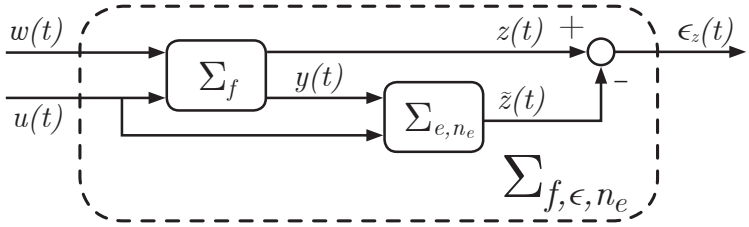

Figure 2.1: The interconnection between Σ_f (2.11) and Σ_{e,n_e} (2.22).

The following lemma shows for estimator design that it can also be assumed, without loss of generality, that the matrices D_{uy} and D_{wz} are equal to zero.

Lemma 2.27 *Consider a system Σ_f (2.11) that satisfies items 1b, 2b and 3b in assumption 2.1.*

Then there exists an H_2-admissible estimator Σ_{e,n_e} (2.22) for Σ_f (2.11) if and only if there exists a mapping $N : \mathcal{Y} \to \mathcal{U}$ such that $D_{wz}^{f,\epsilon} = D_{wz} - ND_{wy} = 0$.

If this mapping exists, the design of an H_2-admissible estimator for Σ_f (2.11) can be transformed into the design of an H_2-admissible estimator with $N = 0$, for a system of the form Σ (2.14) that satsifies items 1b, 2b and 3b in assumption 2.1 as well.

Proof: The proof can be found in appendix A.1. □

We can therefore solve the H_2 optimal estimation problem for a system of the form Σ (2.14) and by utilising an estimator Σ_{e,n_e} (2.22) with $N = 0$. In addition, it will be shown in Proposition 2.32 that any H_2 optimal (and admissible) estimator $\Sigma_{e,n_e}^\star$ can make the output estimation error $\epsilon_z(t)$ independent of the signal $u(t)$; the signal $u(t)$ will therefore be omitted for notational convenience.

Now, let us consider an estimator Σ_{e,n_e} (2.22) with $N = 0$ that is applied to the system Σ (2.14) in order to obtain an error system—without input $u(t)$—of the form

$$\Sigma_{\epsilon,n_e,sp} = \left\{ \begin{array}{rcl} \begin{pmatrix} \dot{x}(t) \\ \dot{x}_e(t) \end{pmatrix} & = & \begin{pmatrix} A & 0 \\ KC_y & J \end{pmatrix} \begin{pmatrix} x(t) \\ x_e(t) \end{pmatrix} + \begin{pmatrix} B_w \\ KD_{wy} \end{pmatrix} w(t) \\ \epsilon_z(t) & = & \begin{pmatrix} C_z & -M \end{pmatrix} \begin{pmatrix} x(t) \\ x_e(t) \end{pmatrix} + \begin{pmatrix} 0 \end{pmatrix} w(t). \end{array} \right. \tag{2.24}$$

It has been shown in section 2.2.4 that the H_2 norm of any system is equal to the H_2 norm of the corresponding dual system. In order to solve the H_2 optimal

estimation problem, we can therefore also consider the dual error system

$$\Sigma^{\top}_{\epsilon,n_e,sp} = \left\{ \begin{array}{rcl} \begin{pmatrix} \dot{x}'(t) \\ \dot{x}'_e(t) \end{pmatrix} & = & \begin{pmatrix} A^{\top} & C_y^{\top} K^{\top} \\ 0 & J^{\top} \end{pmatrix} \begin{pmatrix} x'(t) \\ x'_e(t) \end{pmatrix} + \begin{pmatrix} C_z^{\top} \\ -M^{\top} \end{pmatrix} \epsilon'_z(t) \\ w'(t) & = & \begin{pmatrix} B_w^{\top} & D_{wy}^{\top} K^{\top} \end{pmatrix} \begin{pmatrix} x'(t) \\ x'_e(t) \end{pmatrix} + \begin{pmatrix} 0 \end{pmatrix} \epsilon'_z(t). \end{array} \right. \tag{2.25}$$

This dual error system—for which the input $u(t)$ is not taken into consideration—consists the interconnection of the dual system

$$\Sigma^{\top} = \left\{ \begin{array}{l} \dot{x}'(t) = A^{\top} x'(t) + C_y^{\top} y'(t) + C_z^{\top} z'(t) \\ u'(t) = B_u^{\top} x'(t) + D_{uz}^{\top} z'(t) \\ w'(t) = B_w^{\top} x'(t) + D_{wy}^{\top} y'(t), \end{array} \right. \tag{2.26}$$

with the dual estimator

$$\Sigma^{\top}_{e,n_e} = \left\{ \begin{array}{l} \dot{x}'_e(t) = J^{\top} x'_e(t) + M^{\top} \tilde{z}'(t) \\ y'(t) = K^{\top} x'_e(t) + N^{\top} \tilde{z}'(t) \\ u'(t) = K_u^{\top} x'_e(t) + N_u^{\top} \tilde{z}'(t). \end{array} \right. \tag{2.27}$$

The dual interconnection that describes $\Sigma^{\top}_{\epsilon,n_e,sp}$ (2.25) is depicted in figure 2.2.

For an H_2-admissible estimator and for $u(t) = 0$, the H_2 (squared) performance is quantified as

$$\gamma_{H_2,e}(\Sigma \text{ (2.14)}, \Sigma_{e,n_e} \text{ (2.22)}) = \|\Sigma_{\epsilon,n_e,sp} \text{ (2.24)}\|^2_{H_2} = \left\|\Sigma^{\top}_{\epsilon,n_e,sp} \text{ (2.25)}\right\|^2_{H_2}.$$

Furthermore, an H_2-admissible estimator is H_2 optimal for Σ (2.14) and $u(t) = 0$ if $\gamma_{H_2,e}(\Sigma \text{ (2.14)}, \Sigma_{e,n_e} \text{ (2.22)}) = \gamma^{\star}_{H_2,e}(\Sigma \text{ (2.14)})$, with

$$\begin{array}{rl} \gamma^{\star}_{H_2,e}(\Sigma \text{ (2.14)}) = & \min\limits_{\Sigma_{e,n_e} \text{ (2.22)}} \gamma_{H_2,e}(\Sigma \text{ (2.14)}, \Sigma_{e,n_e} \text{ (2.22)}) \\ & \text{s.t.} \quad \Sigma_{e,n_e} \text{ (2.22) is } H_2\text{-admissible for } \Sigma \text{ (2.14)}. \end{array}$$

A similar approach to the state feedback design problem is now considered by utilising the dual error system $\Sigma^{\top}_{\epsilon,n_e,sp}$ (2.25) and the dual ARE, which is given by

$$AQ_s + Q_s A^{\top} + B_w B_w^{\top} - Q_s C_y^{\top} C_y Q_s = 0. \tag{2.28}$$

In addition, it is again expected that the optimal performance is of the form $\gamma^{\star}_{H_2,e}(\Sigma \text{ (2.14)}) = \text{tr}\left(C_z Q_s^{+} C_z^{\top}\right)$, where Q_s^{+} is the unique stabilising solution to the ARE in (2.28). This positive semidefinite solution satisfies $Q_s^{+} \succeq Q_s$, for any real and symmetric solution Q_s to the ARE in (2.28).

In order to quantify the performance of any H_2-admissible estimator for Σ (2.14), let us consider the dual state and measured output trajectories of $\Sigma^{\top}_{\epsilon,n_e,sp}$ (2.25) as a result of impulses on each dual disturbance $\epsilon'_z(t)$. These trajectories are described by

$$\begin{pmatrix} X'(t) \\ X'_e(t) \end{pmatrix} = \exp\left(\begin{pmatrix} A^{\top} & C_y^{\top} K^{\top} \\ 0 & J^{\top} \end{pmatrix} t \right) \begin{pmatrix} C_z^{\top} \\ -M^{\top} \end{pmatrix}, \quad Y'(t) = K^{\top} X'_e(t).$$

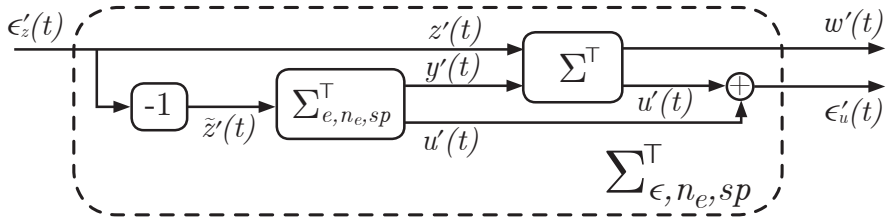

Figure 2.2: The interconnection between the dual system $\Sigma^\top$ (2.26) and the dual estimator $\Sigma^\top_{e,n_e}$ (2.27).

Furthermore, it can be noted that

$$\frac{d}{dt}X'(t) = A^\top X'(T) + C_y^\top Y'(t), \quad X'(0) = C_z^\top.$$

By assuming items 1b, 2b and 3b in assumption 2.1 and item 2 in assumption 2.2, by utilising the fundamental theorems of calculus; and by exploiting the fact that all observable states of $\Sigma^\top_{\epsilon,n_e,sp}$ (2.25) should converge to the origin and therefore that $\lim_{t\to\infty} X'(t)^\top Q_s^+ X'(t) = 0$, we obtain the expression

$$\begin{aligned} -C_z Q_s^+ C_z^\top &= \int_{t=0}^{\infty} \tfrac{d}{dt}\left(X'(t)^\top Q_s^+ X'(t)\right) dt \\ &= \int_{t=0}^{\infty} (C_y Q_s^+ X'(t) + Y'(t))^\top (C_y Q_s^+ X'(t) + Y'(t)) dt \\ &\quad - \int_{t=0}^{\infty} (B_w^\top X'(t) + D_{wy}^\top Y'(t))^\top (B_w^\top X'(t) + D_{wy}^\top Y'(t)) dt. \end{aligned}$$

By defining the transformed system

$$\Sigma_{Q,s} = \begin{cases} \dot{x}(t) = Ax(t) + B_u u(t) + Q_s^+ C_y^\top w(t) \\ y(t) = C_y x(t) + w(t) \\ z(t) = C_z x(t) + D_{uz} u(t). \end{cases} \tag{2.29}$$

it can be shown that this expression is equivalent to

$$-\left(C_z Q_s^+ C_z^\top\right) = \gamma_{H_2,e}(\Sigma_{Q,s}\ (2.29), \Sigma_{e,n_e}\ (2.22)) - \gamma_{H_2,e}(\Sigma\ (2.14), \Sigma_{e,n_e}\ (2.22)),$$

which leads to the following main result.

Theorem 2.28 *Consider an estimator* Σ_{e,n_e} (2.22) *with* $N = 0$ *applied to the system* Σ (2.14) *that satisfies items 1b, 2b and 3b in assumption 2.1 and item 2 in assumption 2.2, which results in the error system* $\Sigma_{\epsilon,n_e,sp}$ (2.24)*; and consider the transformed system* $\Sigma_{Q,s}$ (2.29)*.*

Furthermore, let $Q_s^+ \succeq 0$ *be the unique stabilising solution to the ARE in* (2.28)*. This positive semidefinite solution satisfies* $Q_s^+ \succeq Q_s$*, for any real and symmetric solution* Q_s *to the ARE in* (2.28)*. Then*

- *The estimator* Σ_{e,n_e} (2.22) *is* H_2*-admissible for* Σ (2.14) *if and only if it is* H_2*-admissible for* $\Sigma_{Q,s}$ (2.29)*.*

- *For any H_2-admissible estimator we have that* $\gamma_{H_2,e}(\Sigma\ (2.14), \Sigma_{e,n_e}\ (2.22)) = \mathrm{tr}\left(C_z Q_s^+ C_z^\top\right) + \gamma_{H_2,e}(\Sigma_{Q,s}\ (2.29), \Sigma_{e,n_e}\ (2.22))$.
- *Any H_2 optimal (and admissible) estimator $\Sigma^\star_{e,n_e}$ achieves* $\gamma_{H_2,e}(\Sigma\ (2.14), \Sigma^\star_{e,n_e}) = \gamma^\star_{H_2,e}(\Sigma\ (2.14)) = \mathrm{tr}\left(C_z Q_s^+ C_z^\top\right)$.

Proof: This theorem is completely dual to Theorem 2.23 and mathematically explained above after imposing $u(t) = 0$ and $N = 0$. Lemma 2.27 and Proposition 2.32 state that these conditions do not affect optimality. □

The typical solution to the H_2 optimal estimation problem utilises a Luenberger state observer. It will now be shown that such an observer can, indeed, be considered. In addition, it will be derived how optimality can be achieved with this observer.

Theorem 2.29 *Consider an estimator Σ_{e,n_e} (2.22) with $N = 0$ applied to the system Σ (2.14) that satisfies items 1b, 2b and 3b in assumption 2.1 and item 2 in assumption 2.2, which results in the error system $\Sigma_{\epsilon,n_e,sp}$ (2.24).*

Furthermore, let $Q_s^+ \succeq 0$ be the unique stabilising solution to the ARE in (2.28). This positive semidefinite solution satisfies $Q_s^+ \succeq Q_s$, for any real and symmetric solution Q_s to the ARE in (2.28).

Then the H_2 optimal (squared) performance is described by

$$\gamma^\star_{H_2,e}(\Sigma\ (2.14)) = \mathrm{tr}\left(C_z Q_s^+ C_z^\top\right).$$

In addition, a Luenberger state observer—with estimated output—of the form

$$\Sigma_o = \begin{cases} \dot{\tilde{x}}(t) = \left(A + LC_y\right)\tilde{x}(t) - Ly(t) + B_u u(t) \\ \tilde{z}(t) = C_z\tilde{x}(t) + D_{uz}u(t), \end{cases} \tag{2.30}$$

is H_2 optimal for Σ (2.14) if $L^\star = -Q_s^+ C_y^\top$.

Proof: The H_2 optimal performance follows directly from Theorem 2.28.

Furthermore, is easy to show that the observer Σ_o (2.30) will achieve $\gamma_{H_2,e}(\Sigma_{Q,s}\ (2.29), \Sigma_{e,n_e}\ (2.22)) = 0$, it will satisfy the stability requirement and it will render $\epsilon_z(t)$ independent of $u(t)$; therefore it must be H_2 optimal. □

To finalise the topic of H_2 optimal estimator design, let us generalise these results by removing the assumption 2.2. Therefore, consider the transformed system

$$\Sigma_Q = \begin{cases} \dot{x}(t) = Ax(t) + B_u u(t) + (Q^+ C_y^\top + B_w D_{wy}^\top)(D_{wy} D_{wy}^\top)^{-\frac{1}{2}} w(t) \\ y(t) = C_y x(t) + (D_{wy} D_{wy}^\top)^{\frac{1}{2}} w(t) \\ z(t) = C_z x(t) + D_{uz} u(t) \end{cases} \tag{2.31}$$

in order to obtain the following result.

Corollary 2.30 *Consider an estimator* Σ_{e,n_e} (2.22) *with* $N = 0$ *applied to the system* Σ (2.14) *that satisfies items 1b, 2b and 3b in assumption 2.1, which results in the error system* $\Sigma_{\epsilon,n_e,sp}$ (2.24)*; and consider the transformed system* Σ_Q (2.31)*.*

Furthermore, let $Q^+ \succeq 0$ *be the unique stabilising solution to the ARE*

$$AQ+QA^\top+B_wB_w^\top-(QC_y^\top+B_w^\top D_{wy})(D_{wy}D_{wy}^\top)^{-1}(QC_y^\top+B_w^\top D_{wy})^\top = 0. \quad (2.32)$$

This positive semidefinite solution satisfies $Q^+ \succeq Q$*, for any real and symmetric solution* Q *to the ARE in* (2.32)*. Then*

- *The estimator* Σ_{e,n_e} (2.22) *is* H_2*-admissible for* Σ (2.14) *if and only if it is* H_2*-admissible for* Σ_Q (2.31)*.*
- *For any* H_2*-admissible estimator we have that* $\gamma_{H_2,e}(\Sigma \text{ (2.14)}, \Sigma_{e,n_e} \text{ (2.22)}) = \operatorname{tr}\left(C_zQ^+C_z^\top\right)+\gamma_{H_2,e}(\Sigma_Q \text{ (2.31)}, \Sigma_{e,n_e} \text{ (2.22)})$*.*
- *Any* H_2 *optimal (and admissible) estimator* $\Sigma^\star_{e,n_e}$ *achieves* $\gamma_{H_2,e}(\Sigma \text{ (2.14)}, \Sigma^\star_{e,n_e}) = \gamma^\star_{H_2,e}(\Sigma \text{ (2.14)}) = \operatorname{tr}\left(C_zQ^+C_z^\top\right)$*.*

Proof: The proof can be found in appendix A.1. □

And, again, let us show that a Luenberger state observer can be considered.

Corollary 2.31 *Consider an estimator* Σ_{e,n_e} (2.22) *with* $N = 0$ *applied to the system* Σ (2.14) *that satisfies items 1b, 2b and 3b in assumption 2.1, which results in the error system* $\Sigma_{\epsilon,n_e,sp}$ (2.24)*.*

Furthermore, let $Q^+ \succeq 0$ *be the unique stabilising solution to the ARE in* (2.32)*. This positive semidefinite solution satisfies* $Q^+ \succeq Q$*, for any real and symmetric solution* Q *to the ARE in* (2.32)*.*

Then the H_2 *optimal (squared) performance is described by*

$$\gamma^\star_{H_2,e}(\Sigma \text{ (2.14)}) = \operatorname{tr}\left(C_zQ^+C_z^\top\right).$$

In addition, a Luenberger state observer Σ_o (2.30) *is* H_2 *optimal for* Σ (2.14) *if* $L^\star = -(Q^+C_y^\top + B_w^\top D_{wy})(D_{wy}D_{wy}^\top)^{-1}$*.*

Proof: This is Theorem 2.29 combined with Corollary 2.30. □

Finally, for a state observer Σ_o (2.30) it can be noted that the input signal $u(t)$ does not affect the output estimation error $\epsilon_z(t)$ for any mapping L. It will now be shown that a similar property holds for any estimator that is H_2 optimal for Σ (2.14), which is designed under the assumption that $u(t) = 0$.

Theorem 2.32 *Consider a system* Σ (2.14) *that satisfies items 1b, 2b and 3b in assumption 2.1.*

Then, any H_2*-admissible estimator* Σ_{e,n_e} (2.22) *that achieves* $\gamma_{H_2,e}(\Sigma \text{ (2.14)}, \Sigma_{e,n_e} \text{ (2.22)}) = \gamma^\star_{H_2,e}(\Sigma \text{ (2.14)})$ *with the estimator mappings* J*,* K*,* M *and* N *can, in addition, make* $\epsilon_z(t)$ *independent of* $u(t)$ *by appropriate construction of the mappings* K_u *and* N_u*.*

Proof: The proof can be found in appendix A.1. □

2.4.3 Measurement Feedback Controller Design

We have seen that general H_2 optimal performance—i.e. when any input signal $u(t)$ can be chosen in order to minimise the effect of the disturbance $w(t)$ on the control output $z(t)$—can be obtained by a state feedback $u(t) = Fx(t)$. Such a feedback does, however, require complete information about the state of the system. Furthermore, it has been shown that the H_2 optimal estimation problem is solved by a Luenberger state observer of the form Σ_o (2.30).

At the beginning of section 2.4 a controller of the form $\Sigma_{c,sp}$ (2.15) is introduced in order to solve the H_2 optimal control problem in Problem 2.1. This controller, essentially combines the observer Σ_o (2.30) with the state feedback $u(t) = Fx(t)$. In this section, first the H_2 performance of any measurement feedback controller Σ_{c,n_c} (2.12) is characterised. Subsequently, it will be shown that a controller of the form $\Sigma_{c,sp}$ (2.15) can indeed be considered and a derivation for the H_2 optimal controller mappings $F^\star$ and $L^\star$ will be presented.

In Lemma 2.18 it is established that the design of a strictly proper H_2-admissible controller Σ_{c,n_c} (2.12) for a system of the form Σ (2.14) can be considered without loss of generality. We can therefore consider a closed-loop system, which is described by

$$\Sigma_{cl,n_c,sp} = \left\{ \begin{array}{rcl} \begin{pmatrix} \dot{x}(t) \\ \dot{x}_c(t) \end{pmatrix} & = & \begin{pmatrix} A & B_u M \\ KC_y & J \end{pmatrix} \begin{pmatrix} x(t) \\ x_c(t) \end{pmatrix} + \begin{pmatrix} B_w \\ KD_{wy} \end{pmatrix} w(t) \\ z(t) & = & \begin{pmatrix} C_z & D_{uz} M \end{pmatrix} \begin{pmatrix} x(t) \\ x_c(t) \end{pmatrix} + \begin{pmatrix} 0 \end{pmatrix} w(t). \end{array} \right. \tag{2.33}$$

For an H_2-admissible controller, the H_2 (squared) performance is quantified as

$$\gamma_{H_2}(\Sigma \text{ (2.14)}, \Sigma_{c,n_c} \text{ (2.12)}) = \|\Sigma_{cl,n_c,sp} \text{ (2.33)}\|_{H_2}^2 .$$

Furthermore, an H_2-admissible controller is H_2 optimal for Σ (2.14) if $\gamma_{H_2}(\Sigma \text{ (2.14)}, \Sigma_{c,n_c} \text{ (2.12)}) = \gamma^\star_{H_2}(\Sigma \text{ (2.14)})$, with

$$\begin{array}{rll} \gamma^\star_{H_2}(\Sigma \text{ (2.14)}) = & \min\limits_{\Sigma_{c,n_c} \text{ (2.12)}} & \gamma_{H_2}(\Sigma \text{ (2.14)}, \Sigma_{c,n_c} \text{ (2.12)}) \\ & \text{s.t.} & \Sigma_{c,n_c} \text{ (2.12) is } H_2\text{-admissible for } \Sigma \text{ (2.14)}. \end{array}$$

Then, in order to quantify the performance of any strictly proper H_2-admissible controller, let us consider the state and input trajectories of $\Sigma_{cl,n_c,sp}$ (2.33) as a result of impulses on each disturbance $w(t)$. These trajectories are described by

$$\begin{pmatrix} X(t) \\ X_c(t) \end{pmatrix} = \exp\left(\begin{pmatrix} A & B_u M \\ KC_y & J^\top \end{pmatrix} t \right) \begin{pmatrix} B_w \\ KD_{wy} \end{pmatrix}, \quad U(t) = MX_c(t).$$

Furthermore, it can be noted that

$$\frac{d}{dt} X(t) = AX(T) + B_u U(t), \quad X(0) = B_w.$$

Under assumptions 2.1 and 2.2, we obtain equivalently to state feedback design, the expression

$$\gamma_{H_2}(\Sigma\ (2.14), \Sigma_{c,n_c}\ (2.12)) = \mathrm{tr}(B_w^\top P_s^+ B_w) + \gamma_{H_2}(\Sigma_{P,s}\ (2.20), \Sigma_{c,n_c}\ (2.12)),$$

for which P_s^+ is the unique stabilising solution to the ARE in (2.18).

With H_2 optimal state feedback design we were able to find a solution that achieves $\gamma_{H_2}(\Sigma_{P,s}\ (2.20), \Sigma_{c,n_c}\ (2.12))$, which should therefore be an optimal solution. This can, however, not be achieved with a controller of the form $\Sigma_{c,sp}$ (2.15) and it is therefore not directly clear which controller will be able to minimise this expression. In order to overcome this problem, let us consider the dual of the closed-loop interconnection between $\Sigma_{P,s}$ (2.20) and Σ_{c,n_c} (2.12), which is defined as follows.

$$\Sigma_{cl,n_c,sp,P,s}^\top = \left\{ \begin{array}{rcl} \begin{pmatrix} \dot{x}'(t) \\ \dot{x}_c'(t) \end{pmatrix} & = & \begin{pmatrix} A^\top & C_y^\top K^\top \\ M^\top B_u^\top & J^\top \end{pmatrix} \begin{pmatrix} x'(t) \\ x_c'(t) \end{pmatrix} + \begin{pmatrix} P_s^+ B_u \\ M^\top \end{pmatrix} z'(t) \\ w'(t) & = & \begin{pmatrix} B_w^\top & D_{wy}^\top K^\top \end{pmatrix} \begin{pmatrix} x'(t) \\ x_c'(t) \end{pmatrix} + \begin{pmatrix} 0 \end{pmatrix} z'(t). \end{array} \right. \tag{2.34}$$

Then, let us consider the dual state and measured output trajectories of this system, as a result of disturbances on each dual disturbance $z'(t)$. These trajectories are described by

$$\begin{pmatrix} X'(t) \\ X_c'(t) \end{pmatrix} = \exp\left(\begin{pmatrix} A^\top & C_y^\top K^\top \\ M^\top B_u^\top & J^\top \end{pmatrix} t \right) \begin{pmatrix} P_s^+ B_u \\ M^\top \end{pmatrix}, \quad Y'(t) = K^\top X_c'(t).$$

In addition, it can be noted that

$$\frac{d}{dt} X'(t) = A^\top X'(T) + C_y^\top Y'(t), \quad X'(0) = P_s^+ B_u.$$

Then, under assumptions 2.1 and 2.2, we obtain equivalently to estimator design, the expression

$$\begin{aligned} \gamma_{H_2}(\Sigma_{P,s}\ (2.20), \Sigma_{c,n_c}\ (2.12)) = \mathrm{tr}(B_u^\top P_s^+ Q_s^+ P_s^+ B_u) \\ + \gamma_{H_2}(\Sigma_{PQ,s}\ (2.35), \Sigma_{c,n_c}\ (2.12)), \end{aligned}$$

for which P_s^+ and Q_s^+ are the unique stabilising solutions to the AREs in (2.18) and (2.28), respectively. Furthermore, the following transformed system is obtained:

$$\Sigma_{PQ,s} = \left\{ \begin{array}{rcl} \dot{x}(t) & = & Ax(t) + B_u u(t) + Q_s^+ C_y^\top w(t) \\ y(t) & = & C_y x(t) + w(t) \\ z(t) & = & B_u^\top P_s^+ x(t) + u(t). \end{array} \right. \tag{2.35}$$

Finally, by inserting the expression for $\gamma_{H_2}(\Sigma_{P,s}\ (2.20), \Sigma_{c,n_c}\ (2.12))$ in the expression for $\gamma_{H_2}(\Sigma\ (2.14), \Sigma_{c,n_c}\ (2.12))$, the following result is obtained.

Theorem 2.33 *Consider a controller* Σ_{c,n_c} (2.12) *with* $N = 0$ *applied to the system* Σ (2.14) *that satisfies assumptions 2.1 and 2.2, which results in the closed-loop system* $\Sigma_{cl,n_c,sp}$ (2.33)*; and consider the transformed system* $\Sigma_{PQ,s}$ (2.35)*.*

Furthermore, let $P_s^+ \succeq 0$ *and* $Q_s^+ \succeq 0$ *be the unique stabilising solutions to the AREs in* (2.18) *and* (2.28)*, respectively. These positive semidefinite solutions satisfy* $P_s^+ \succeq P_s$ *and* $Q_s^+ \succeq Q_s$*, for any real and symmetric solution* P_s *and* Q_s *to the AREs in* (2.18) *and* (2.28)*, respectively. Then*

- *The controller* Σ_{c,n_c} (2.12) *is* H_2*-admissible for* Σ (2.14) *if and only if it is* H_2*-admissible for* $\Sigma_{PQ,s}$ (2.35)*.*
- *For any* H_2*-admissible controller we have that*

$$\begin{aligned}
&\gamma_{H_2}(\Sigma\ (2.14), \Sigma_{c,n_c}\ (2.12)) = \\
&\quad tr(B_w^\top P_s^+ B_w) + \mathrm{tr}(B_u^\top P_s^+ Q_s^+ P_s^+ B_u) + \gamma_{H_2}(\Sigma_{PQ,s}\ (2.35), \Sigma_{c,n_c}\ (2.12)) \\
&= \mathrm{tr}(C_z Q_s^+ C_z^\top) + \mathrm{tr}(C_y Q_s^+ P_s^+ Q_s^+ C_y^\top) + \gamma_{H_2}(\Sigma_{PQ,s}\ (2.35), \Sigma_{c,n_c}\ (2.12)).
\end{aligned}$$

- *Any* H_2 *optimal (and admissible) controller* $\Sigma_{c,n_c}^\star$ *achieves*

$$\begin{aligned}
\gamma_{H_2}(\Sigma\ (2.14), \Sigma_{c,n_c}^\star) = \gamma_{H_2}^\star(\Sigma\ (2.14)) &= \mathrm{tr}(B_w^\top P_s^+ B_w) + \mathrm{tr}(B_u^\top P_s^+ Q_s^+ P_s^+ B_u) \\
&= \mathrm{tr}(C_z Q_s^+ C_z^\top) + \mathrm{tr}(C_y Q_s^+ P_s^+ Q_s^+ C_y^\top).
\end{aligned}$$

- *A controller of the form* $\Sigma_{c,sp}$ (2.15) *is* H_2 *optimal for* Σ (2.14) *if* $F^\star = -B_u^\top P_s^+$ *and* $L^\star = -Q_s^+ C_y^\top$*.*

Proof: The proof is given by Trentelman et al. [2001, Sec. 11.3]. □

To finalise the topic of H_2 optimal controller design, let us generalise these results by removing the assumption 2.2. For this purpose, consider the transformed system

$$\Sigma_{PQ} = \left\{ \begin{array}{rcl} \dot{x}(t) &=& Ax(t) + B_u u(t) + \tilde{B}_w w(t) \\ y(t) &=& C_y x(t) + (D_{wy} D_{wy}^\top)^{\frac{1}{2}} w(t) \\ z(t) &=& \tilde{C}_z x(t) + (D_{uz}^\top D_{uz})^{\frac{1}{2}} u(t), \end{array} \right. \tag{2.36}$$

with $\tilde{C}_z = (D_{uz}^\top D_{uz})^{-\frac{1}{2}}(B_u^\top P^+ + D_{uz}^\top C_z)$ and $\tilde{B}_w = (Q^+ C_y^\top + B_w D_{wy}^\top)(D_{wy} D_{wy}^\top)^{-\frac{1}{2}}$, in order to obtain the following result.

Corollary 2.34 *Consider a controller* Σ_{c,n_c} (2.12) *with* $N = 0$ *applied to the system* Σ (2.14) *that satisfies assumption 2.1, which results in the closed-loop system* $\Sigma_{cl,n_c,sp}$ (2.33)*; and consider the transformed system* $\Sigma_{PQ,s}$ (2.35)*.*

Furthermore, let $P^+ \succeq 0$ *and* $Q^+ \succeq 0$ *be the unique stabilising solutions to the AREs in* (2.21) *and* (2.32)*, respectively. These positive semidefinite solutions satisfy* $P^+ \succeq P$ *and* $Q^+ \succeq Q$*, for any real and symmetric solution* P *and* Q *to the AREs in* (2.21) *and* (2.32)*, respectively. Then*

- *The controller* Σ_{c,n_c} (2.12) *is* H_2*-admissible for* Σ (2.14) *if and only if it is* H_2*-admissible for* Σ_{PQ} (2.36)*.*

- *For any H_2-admissible controller we have that*

$$\begin{aligned}&\gamma_{H_2}(\Sigma\ (2.14), \Sigma_{c,n_c}\ (2.12)) = \\ &\quad \operatorname{tr}(B_w^\top P^+ B_w) + \operatorname{tr}(B_u^\top P^+ Q^+ P^+ B_u) + \gamma_{H_2}(\Sigma_{PQ}\ (2.36), \Sigma_{c,n_c}\ (2.12)) \\ &= \operatorname{tr}(C_z Q^+ C_z^\top) + \operatorname{tr}(C_y Q^+ P^+ Q^+ C_y^\top) + \gamma_{H_2}(\Sigma_{PQ}\ (2.36), \Sigma_{c,n_c}\ (2.12)).\end{aligned}$$

- *Any H_2 optimal (and admissible) controller $\Sigma^\star_{c,n_c}$ achieves*

$$\begin{aligned}\gamma_{H_2}(\Sigma\ (2.14), \Sigma^\star_{c,n_c}) = \gamma^\star_{H_2}(\Sigma\ (2.14)) &= \operatorname{tr}(B_w^\top P^+ B_w) + \operatorname{tr}(B_u^\top P^+ Q^+ P^+ B_u) \\ &= \operatorname{tr}(C_z Q^+ C_z^\top) + \operatorname{tr}(C_y Q^+ P^+ Q^+ C_y^\top).\end{aligned}$$

- *A controller of the form $\Sigma_{c,sp}$ (2.15) is H_2 optimal for Σ (2.14) if $F^\star = -(D_{uz}^\top D_{uz})^{-1}(B_u^\top P^+ + D_{uz}^\top C_z)$ and $L^\star = -(Q^+ C_y^\top + B_w^\top D_{wy})(D_{wy} D_{wy}^\top)^{-1}$.*

Proof: This is Theorem 2.33 with the extensions as discussed in Corollaries 2.24 and 2.30. □

2.5 Geometric Control Theory

In this section, several concepts from geometric control theory and their relation to disturbance decoupling problems are discussed. A more extensive treatment of these concepts is provided by Wonham [1985], Basile and Marro [1992] and Trentelman et al. [2001].

2.5.1 Disturbance Decoupling

Let us first formally define what is meant by the term *disturbance decoupling.*

Definition 2.35 *The system Σ (2.14) is "disturbance decoupled" if the control output $z(t)$ is independent of the disturbance $w(t)$.*

Geometric control theory relies heavily on invariant subspaces. We will now see that there exists a direct relation between disturbance decoupling and these subspaces.

Lemma 2.36 *Consider the system Σ (2.14) with $u(t) = 0$.*

Then Σ (2.14) is disturbance decoupled if and only if there exists a subspace $\mathcal{S}^A \subseteq \mathcal{X}$ such that $\operatorname{im}(B_w) \subseteq \mathcal{S}^A \subseteq \ker(C_z)$ and $A\mathcal{S}^A \subseteq \mathcal{S}^A$.

Proof: The proof is given by Trentelman et al. [2001, Thm. 4.6]. □

Lemma 2.36 can intuitively be interpreted in the following manner. The inclusion $A\mathcal{S}^A \subseteq \mathcal{S}^A$ guarantees that any state trajectory starting within the subspace $\mathcal{S}^A$ will remain in $\mathcal{S}^A$ when $u(t) = 0$ and $w(t) = 0$, which is graphically depicted in figure 2.3. Combining this with $\operatorname{im}(B_w) \subseteq \mathcal{S}^A$, implies that the effect of the

disturbance $w(t)$ on all state trajectories is restricted to the subspace $\mathcal{S}^A$—i.e. only the states within this subspace are affected by the disturbance. The output $z(t)$ is therefore completely independent of the disturbance $w(t)$ when these state trajectories are not visible on the output $z(t)$, which is implied by $\mathcal{S}^A \subseteq \ker(C_z)$.

It has been shown by Trentelman et al. [2001, Cor. 3.3] that there exists a unique subspace, which can be used to verify whether Σ (2.14) is disturbance decoupled with $u(t) = 0$.

Lemma 2.37 *Consider the system* Σ (2.14) *with* $u(t) = 0$.

Then there exists a unique smallest subspace $\mathcal{S}^{A\star} \subseteq \mathcal{X}$ *that satisfies* $\operatorname{im}(B_w) \subseteq \mathcal{S}^{A\star}$ *and* $A\mathcal{S}^{A\star} \subseteq \mathcal{S}^{A\star}$. *Specifically:*

$$\mathcal{S}^{A\star} = \operatorname{im}\begin{pmatrix} B_w & AB_w & \cdots & A^{n_x-1}B_w \end{pmatrix}.$$

This subspace is the "smallest" in the sense that $\mathcal{S}^{A\star} \subseteq \mathcal{S}^A$, *for any subspace* $\mathcal{S}^A \subseteq \mathcal{X}$ *that satisfies* $\operatorname{im}(B_w) \subseteq \mathcal{S}^A$ *and* $A\mathcal{S}^A \subseteq \mathcal{S}^A$.

Proof: The proof is given by Trentelman et al. [2001, Cor. 3.3]. □

Because this specific subspace is the smallest, we can equivalently say that Σ (2.14) is disturbance decoupled with $u(t) = 0$ if and only if $\mathcal{S}^{A\star} \subseteq \ker(C_z)$.

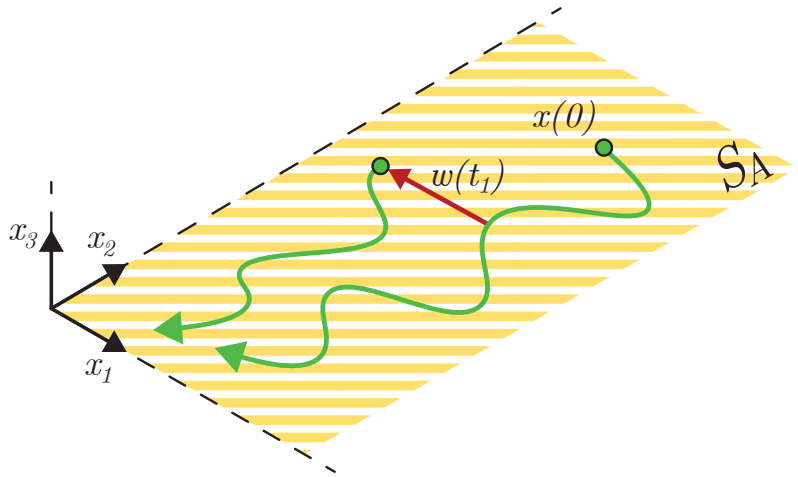

Figure 2.3: A graphical representation for the properties of the subspace $\mathcal{S}^A$ as defined in Lemma 2.36.

2.5.2 Output-Nulling Stabilisability Subspaces

In a situation where Σ (2.14) is not disturbance decoupled with $u(t) = 0$, we can consider the problem of finding a state feedback $u(t) = Fx(t)$ for the system to achieve disturbance decoupling and internal $\mathbb{C}_g$-stability in closed-loop.

By combining the closed-loop system $\Sigma_{cl,F}$ (2.19) with Lemma 2.36, we can conclude that disturbance decoupling can be achieved with a state feedback $u(t) = Fx(t)$ if and only if there exists a pair $(\mathcal{S}^A, F)$ such that $\mathrm{im}(B_w) \subseteq \mathcal{S}^A \subseteq \ker(C_z + D_{uz}F)$ and $(A + B_uF)\mathcal{S}^A \subseteq \mathcal{S}^A$. Furthermore, internal $\mathbb{C}_g$-stability adds the requirement that $\lambda(A + B_uF) \subseteq \mathbb{C}_g$.

By utilising Lemma 2.37, it is possible to construct a subspace $\mathcal{S}^A$ when the mapping F is given. Similarly, it is possible to construct the mapping F when the subspace $\mathcal{S}^A$ is given. It is, however, not obvious how to appropriately construct the subspace $\mathcal{S}^A$ or the mapping F without knowing the other.

In order to overcome this problem, we will now introduce controlled invariant and $\mathbb{C}_g$-stabilisability subspaces. These subspaces and the underlying concepts are discussed in more detail by Hautus [1979]; we will, however, only consider their mathematical characterisation.

Lemma 2.38 *Consider a system Σ (2.14), the subspaces $\mathcal{V}^C, \mathcal{V}_g^C \subseteq \mathcal{X}$ and a stability domain $\mathbb{C}_g$. Then the following statements are equivalent:*

(i) $\mathcal{V}^C$ is a controlled invariant subspace.
(ii) $A\mathcal{V}^C \subseteq \mathcal{V}^C + \mathrm{im}(B_u)$.
(iii) there exists a mapping $F : \mathcal{X} \to \mathcal{U}$ such that $(A + B_uF)\mathcal{V}^C \subseteq \mathcal{V}^C$.

Furthermore, the following statements are equivalent:

(i) $\mathcal{V}_g^C$ is a $\mathbb{C}_g$-stabilisability subspace.
(ii) for any $\lambda_i \in \lambda(A)$ that satisfies $\lambda_i \notin \mathbb{C}_g$ we have $(\lambda_i I_{n_x} - A)\mathcal{V}_g^C + \mathrm{im}(B_u) = \mathcal{V}_g^C + \mathrm{im}(B_u)$.
(iii) there exists a mapping $F : \mathcal{X} \to \mathcal{U}$ such that $(A + B_uF)\mathcal{V}_g^C \subseteq \mathcal{V}_g^C$ and $\lambda((A + B_uF)|\mathcal{V}_g^C) \subseteq \mathbb{C}_g$.

Proof: The proof is given by Trentelman et al. [2001, Thm. 4.2 and 4.22]. □

By considering these subspaces, we essentially obtain a characterisation for all possible $(A + B_uF)$-invariant subspaces. In addition, item (ii) provides a mathematical description that does not depend on the mapping F. Next, we will include the requirement that these subspaces should lie in the subspace $\ker(C_z + D_{uz}F)$.

Lemma 2.39 *Consider a system Σ (2.14), the subspaces $\mathcal{V}, \mathcal{V}_g \subseteq \mathcal{X}$ and a stability domain $\mathbb{C}_g$. Then the following statements are equivalent:*

(i) $\mathcal{V}$ is an output-nulling controlled invariant subspace.
(ii) $A\mathcal{V} \subseteq \mathcal{V} + \mathrm{im}(B_u)$ and $C_z\mathcal{V} \subseteq \mathrm{im}(D_{uz})$.
(iii) there exists a mapping $F : \mathcal{X} \to \mathcal{U}$ such that $(A + B_uF)\mathcal{V} \subseteq \mathcal{V}$ and $(C_z + D_{uz}F)\mathcal{V} = 0$.

Furthermore, the following statements are equivalent:

(i) $\mathcal{V}_g$ is an output-nulling $\mathbb{C}_g$-stabilisability subspace.
(ii) for any $\lambda_i \in \lambda(A)$ that satisfies $\lambda_i \notin \mathbb{C}_g$ we have $(\lambda_i I_{n_x} - A)\mathcal{V}_g + \mathrm{im}(B_u) = \mathcal{V}_g + \mathrm{im}(B_u)$ and $C_z\mathcal{V}_g \subseteq \mathrm{im}(D_{uz})$.
(iii) there exists a mapping $F : \mathcal{X} \to \mathcal{U}$ such that $(A + B_uF)\mathcal{V}_g \subseteq \mathcal{V}_g$, $(C_z + D_{uz}F)\mathcal{V}_g = 0$ and $\lambda((A + B_uF)|\mathcal{V}_g) \subseteq \mathbb{C}_g$.

Proof: The proof is given by Trentelman et al. [2001, Sec. 7.3 and 7.4]. □

By utilising this lemma, we obtain a characterisation for all possible $(A + B_u F)$-invariant subspaces that are contained in the subspace $\ker(C_z + D_{uz}F)$. In addition, item (ii) provides a mathematical description that does not depend on the mapping F. The stability requirement does, however, only guarantee that $\lambda((A + B_u F)|\mathcal{V}_g) \subseteq \mathbb{C}_g$ can be achieved.

Remark 2.1 *This stability guarantee is, however, sufficient if the system* Σ (2.14) *is* $\mathbb{C}_g$*-stabilisable. Because then, for any output-nulling* $\mathbb{C}_g$*-stabilisability subspace* $\mathcal{V}_g$ *we have that there exists a mapping* $F : \mathcal{X} \to \mathcal{U}$ *such that* $(A + B_u F)\mathcal{V}_g \subseteq \mathcal{V}_g$, $(C_z + D_{uz}F)\mathcal{V}_g = 0$ *and* $\lambda(A + B_u F) \subseteq \mathbb{C}_g$. *This is explained in more detail by Basile and Marro [1992, Prop. 4.1.16].*

As a final step, we must verify whether there exists a subspace $\mathcal{V}_{(g)}$ that contains the subspace $\mathrm{im}(B_w)$. For this purpose, it will now be shown that there exists a unique *largest* output-nulling controlled invariant—and a $\mathbb{C}_g$-stabilisability—subspace.

Theorem 2.40 *For a system* Σ (2.14)*, there exists a unique largest output-nulling controlled invariant subspace, which is called the "weakly unobservable subspace". This subspace is denoted by* $\mathcal{V}^\star$ *and it satisfies* $\mathcal{V} \subseteq \mathcal{V}^\star$*, for any output-nulling controlled invariant subspace* $\mathcal{V}$*.*

Furthermore, there exists a unique largest output-nulling $\mathbb{C}_g$*-stabilisability subspace, which is called the "*$\mathbb{C}_g$*-stabilisable weakly unobservable subspace". This subspace is denoted by* $\mathcal{V}_g^\star$ *and it satisfies* $\mathcal{V}_g \subseteq \mathcal{V}_g^\star$*, for any output-nulling* $\mathbb{C}_g$*-stabilisability subspace* $\mathcal{V}_g$*.*

Proof: The proof is given by Trentelman et al. [2001, Sec. 7.3]. □

In this theorem, it is essentially shown that—for a $\mathbb{C}_g$-stabilisable system—there exists a unique largest subspace that—for an appropriate mapping F—satisfies $\mathcal{V}_{(g)}^\star \subseteq \ker(C_z + D_{uz}F)$, $(A + B_u F)\mathcal{V}_{(g)}^\star \subseteq \mathcal{V}_{(g)}^\star$ and $\lambda(A + B_u F) \subseteq \mathbb{C}_{(g)}$. The system Σ (2.14) can therefore be disturbance decoupled (and internally stabilised when it is $\mathbb{C}_g$-stabilisable) with some state feedback $u(t) = Fx(t)$ if and only if $\mathrm{im}(B_w) \subseteq \mathcal{V}_{(g)}^\star$.

Furthermore, there exist several algorithms that can be used to numerically construct the subspace $\mathcal{V}_{(g)}^\star$ in combination with an appropriate mapping F; these algorithms are created by Marro [2018] and by Chen [2018].

2.5.3 Input-Containing Detectability Subspaces

In a dual fashion, we can also consider disturbance decoupled output estimation. For this purpose, let us apply the observer Σ_o (2.30) to the system Σ (2.14) in order

to obtain an error system that—with $e(t) = x(t) - \tilde{x}(t)$ and $\epsilon_z(t) = z(t) - \tilde{z}(t)$—is described by

$$\Sigma_{\epsilon,o} = \begin{cases} \dot{e}(t) = \left(A + LC_y\right) e(t) + \left(B_w + LD_{wy}\right) w(t) \\ \epsilon_z(t) = C_z\ e(t). \end{cases} \tag{2.37}$$

The question now is, whether there exists a mapping L such that the output estimation error $\epsilon_z(t)$ becomes independent of the disturbance $w(t)$ and such that the error system is internally $\mathbb{C}_g$-stable. By combining $\Sigma_{\epsilon,o}$ (2.37) with Lemma 2.36, we can conclude that this requires the existence of a pair $(\mathcal{S}^A, L)$ such that $\mathrm{im}(B_w + LD_{wy}) \subseteq \mathcal{S}^A \subseteq \ker(C_z)$ and $(A+LC_y)\mathcal{S}^A \subseteq \mathcal{S}^A$. Furthermore, internal $\mathbb{C}_g$-stability adds the requirement that $\lambda(A + LC_y) \subseteq \mathbb{C}_g$.

Similarly to the state feedback problem, let us first characterise all $(A + LC_y)$-invariant subspaces.

Lemma 2.41 *Consider a system Σ (2.14), the subspaces $\mathcal{S}^C, \mathcal{S}_g^C \subseteq \mathcal{X}$ and a stability domain $\mathbb{C}_g$. Then the following statements are equivalent:*

(i) $\mathcal{S}^C$ is a conditioned invariant subspace.
(ii) $A(\mathcal{S}^C \cap \ker(C_y)) \subseteq \mathcal{S}^C$.
(iii) there exists a mapping $L : \mathcal{Y} \to \mathcal{X}$ such that $(A + LC_y)\mathcal{S}^C \subseteq \mathcal{S}^C$.

Furthermore, the following statements are equivalent:

(i) $\mathcal{S}_g^C$ is a $\mathbb{C}_g$-detectability subspace.
(ii) for any $\lambda_i \in \lambda(A)$ that satisfies $\lambda_i \notin \mathbb{C}_g$ we have $(A - \lambda_i I_{n_x})^{-1}(\mathcal{S}_g^C \cap \ker(C_y)) = \mathcal{S}_g^C \cap \ker(C_y)$.
(iii) there exists a mapping $L : \mathcal{Y} \to \mathcal{X}$ such that $(A + LC_y)\mathcal{S}_g^C \subseteq \mathcal{S}_g^C$ and $\lambda((A + LC_y)|(\mathcal{X} \bmod \mathcal{S}_g^C)) \subseteq \mathbb{C}_g$.

Proof: The proof is given by Trentelman et al. [2001, Thm. 5.5 and 5.11]. □

Next, we will characterise the class of conditioned invariant and $\mathbb{C}_g$-detectability subspaces that contain the subspace $\mathrm{im}(B_w + LD_{wy})$.

Lemma 2.42 *Consider a system Σ (2.14), the subspaces $\mathcal{S}, \mathcal{S}_g \subseteq \mathcal{X}$ and a stability domain $\mathbb{C}_g$. Then the following statements are equivalent:*

(i) $\mathcal{S}$ is input-containing conditioned invariant.
(ii) $A(\mathcal{S} \cap \ker(C_y)) \subseteq \mathcal{S}$ and $\ker(D_{wy}) \subseteq B_w^{-1}\mathcal{S}$.
(iii) there exists a mapping $L : \mathcal{Y} \to \mathcal{X}$ such that $(A + LC_y)\mathcal{S} \subseteq \mathcal{S}$ and $\mathrm{im}(B_w + LD_{wy}) \subseteq \mathcal{S}$.

Furthermore, the following statements are equivalent:

(i) $\mathcal{S}_g$ is an input-containing $\mathbb{C}_g$-detectability subspace.
(ii) for any $\lambda_i \in \lambda(A)$ that satisfies $\lambda_i \notin \mathbb{C}_g$ we have $(A-\lambda_i I_{n_x})^{-1}(\mathcal{S}_g \cap \ker(C_y)) = \mathcal{S}_g \cap \ker(C_y)$ and $\ker(D_{wy}) \subseteq B_w^{-1}\mathcal{S}_g$.
(iii) there exists a mapping $L : \mathcal{Y} \to \mathcal{X}$ such that $(A + LC_y)\mathcal{S}_g \subseteq \mathcal{S}_g$, $\mathrm{im}(B_w + LD_{wy}) \subseteq \mathcal{S}_g$ and $\lambda((A + LC_y)|(\mathcal{X} \bmod \mathcal{S}_g)) \subseteq \mathbb{C}_g$.

Proof: The duality to Lemma 2.39 is explained by Aling and Schumacher [1984, Sec. 2]. □

Remark 2.2 *If the system* Σ (2.14) *is* $\mathbb{C}_g$*-detectable, then for any input-containing* $\mathbb{C}_g$*-detectability subspace* $\mathcal{S}_g$ *we have that there exists a mapping* $L : \mathcal{Y} \to \mathcal{X}$ *such that* $(A + LC_y)\mathcal{S}_g \subseteq \mathcal{S}_g$, $\mathrm{im}(B_w + LD_{wy}) \subseteq \mathcal{S}_g$ *and* $\lambda(A + LC_y) \subseteq \mathbb{C}_g$. *This is explained in more detail by Basile and Marro [1992, Prop. 4.1.19].*

Finally, it will be shown that there exists a unique smallest input-containing conditioned invariant—and a $\mathbb{C}_g$-detectability—subspace.

Theorem 2.43 *For a system* Σ (2.14)*, there exists a unique smallest input-containing conditioned invariant subspace, which is called the "strongly reachable subspace". This subspace is denoted by* $\mathcal{S}^\star$ *and it satisfies* $\mathcal{S}^\star \subseteq \mathcal{S}$*, for any input-containing conditioned invariant subspace* $\mathcal{S}$.

Furthermore, there exists a unique smallest input-containing $\mathbb{C}_g$*-detectability subspace, which is called the "*$\mathbb{C}_g$*-detectable strongly reachable subspace". This subspace is denoted by* $\mathcal{S}_g^\star$ *and it satisfies* $\mathcal{S}_g^\star \subseteq \mathcal{S}_g$*, for any input-containing* $\mathbb{C}_g$*-detectability subspace* $\mathcal{S}_g$.

Proof: The proof is given by Trentelman et al. [2001, Sec. 8.4]. □

In this theorem, it is essentially shown that—for a $\mathbb{C}_g$-detectable system—there exists a unique smallest subspace that—for an appropriate mapping L—satisfies $\mathrm{im}(B_w + LD_{wy}) \subseteq \mathcal{S}_{(g)}^\star$, $(A + LC_y)\mathcal{S}_{(g)}^\star \subseteq \mathcal{S}_{(g)}^\star$ and $\lambda(A + LC_y) \subseteq \mathbb{C}_{(g)}$. The error system $\Sigma_{\epsilon,o}$ (2.37) can therefore be disturbance decoupled (and internally stabilised when it is $\mathbb{C}_g$-stabilisable) with some mapping L if and only if $\mathcal{S}_{(g)}^\star \subseteq \ker(C_z)$.

Furthermore, the algorithms that construct the subspace $\mathcal{V}_{(g)}^\star$, can also be used to construct the subspace $\mathcal{S}_{(g)}^\star$ and to construct an appropriate mapping L.

2.5.4 $(\mathcal{S}, \mathcal{V})$-Pairs

The final concept in this section combines $\mathbb{C}_g$-stabilisability subspaces with $\mathbb{C}_g$-detectability subspaces.

Definition 2.44 *Consider the system* Σ (2.14) *and a stability domain* $\mathbb{C}_g$.

Then a pair of subspaces $(\mathcal{S}_g^C, \mathcal{V}_g^C)$ *is called an* $(\mathcal{S}, \mathcal{V})$-pair *if* $\mathcal{S}_g^C \subseteq \mathcal{V}_g^C$, $\mathcal{S}_g^C$ *is a* $\mathbb{C}_g$*-detectability subspace and* $\mathcal{V}_g^C$ *is a* $\mathbb{C}_g$*-stabilisability subspace.*

An $(\mathcal{S}, \mathcal{V})$-pair introduces a "partial invariance" that can be achieved by the mapping N of the controller Σ_{c,n_c} (2.12).

Proposition 2.45 *Consider the system* Σ (2.14)*, a stability domain* $\mathbb{C}_g$ *and let* $(\mathcal{S}_g^C, \mathcal{V}_g^C)$ *be an* $(\mathcal{S}, \mathcal{V})$*-pair.*

Then there exists a mapping $N : \mathcal{Y} \to \mathcal{U}$ *such that* $(A + B_u N C_y)\mathcal{S}_g^C \subseteq \mathcal{V}_g^C$.

Proof: The proof is given by Trentelman et al. [2001, Lem. 6.3]. □

We have decommissioned natural selection and must now look deep within ourselves and decide what we wish to become.

Edward Osborne Wilson

3

Actuator and Sensor Selection for Control

Actuators and sensors are essential components in a control system that have a direct impact on the performance that can be achieved in closed-loop. The question of how many actuators or sensors to use and where to place them is therefore important in many applications, which closely relates to actuator and sensor selection problems such as Problem 1.2.

In this chapter we will investigate a number of selection techniques for the purpose of maximising closed-loop H_2 performance with a limited number of actuators and sensors. First, the use of several optimisation algorithms in combination with modularity properties is investigated, which has been an active field of research in recent years. It will, however, be shown that the performance guarantees for these methods do not apply to closed-loop selection problems.

Secondly, sparsity promoting controller design methods are considered. These methods attempt to maximise closed-loop performance while simultaneously introducing (block) sparsity in a controller, which can equivalently be interpreted as an actuator or sensor selection problem.

The chapter is finalised by analysing and comparing the performance of these methods on a practical example.

3.1 Introduction

Controllers aim to improve performance by utilising actuators to affect a system, on the basis of available sensor information. Consequently, these actuators and sensors are essential components in a control system that have a direct impact on the performance that can be achieved in closed-loop. Appropriately selecting the type and number of actuators and sensors, in combination with their placement, is therefore important in many control applications.

As mentioned in section 1.2.3, SISO controller architectures are often considered in classical control. For this type of control architecture, each actuator is often paired with a sensor and typical system designs therefore contain an equal number of actuators and sensors. A common design philosophy is to place the actuators close to where the disturbances enter the system, while each sensor is collocated with one actuator. Furthermore, the sensors and actuators are often placed with the aim of reducing the interaction between the SISO controllers—e.g. each sensors is placed far away from the other actuators in the application as discussed in section 1.2.1.

Decoupling for control is often considered in practice to further reduce this interaction, as explained by Wang [2006]. It is important to note that this type of approach originates from the desire to apply classical SISO control designs to a MIMO system.

Optimal controllers, on the other hand, can directly be designed for MIMO systems, which introduces additional freedom in the system design. For example, any number of actuators and sensors can be used, while it is not required to pair actuators with sensors or to use decoupling. This additional freedom can be utilised to improve closed-loop performance.

In general, it is not obvious where the actuators and sensors should be placed in order to maximise closed-loop performance. The development of an automated procedure that is capable of producing an—in some sense—optimal actuator and sensor configuration has therefore received a considerable amount of attention.

Existing methods can be categorised into open-loop and closed-loop methods. Open-loop methods typically aim to improve reachability and observability properties of the system; e.g. the trace of a Gramian is maximised. Closed-loop methods, on the other hand, aim to directly improve certain closed-loop performance measure. For a complete overview of this field of research, we refer to the survey paper by Van de Wal and de Jager [2001].

3.1.1 H_2 Optimal Actuator and Sensor Selection

In this chapter we will investigate the problem of constructing a combined actuator and sensor configuration that—for a given number of actuators and a given number of sensors—maximises the best achievable closed-loop H_2 performance for a system. For this problem, the starting point is an actuator-free and sensor-free system that

is assumed to be given throughout this chapter. This system is of the from

$$\Sigma_{wz} = \begin{cases} \dot{x}(t) &= Ax(t) + \widetilde{B}_w \widetilde{w}(t) \\ \tilde{z}(t) &= \widetilde{C}_z x(t), \end{cases} \tag{3.1}$$

where vector signals $x(t)$, $\widetilde{w}(t)$ and $\tilde{z}(t)$ represent the state, unknown disturbance and control output, respectively. These signals assume values in finite-dimensional vector spaces $\mathcal{X} = \mathbb{R}^{n_x}$, $\widetilde{\mathcal{W}} = \mathbb{R}^{n_{\tilde{w}}}$ and $\widetilde{\mathcal{Z}} = \mathbb{R}^{n_{\tilde{z}}}$, respectively. The dynamical relation between the signals is described by real-valued matrices A, $\widetilde{B}_w$ and $\widetilde{C}_z$ of appropriate dimension.

The construction of a combined actuator and sensor configuration amounts to the introduction of control inputs $u(t)$ and measured outputs $y(t)$ for Σ_{wz} (3.1). The construction of such a configuration is often described as a selection problem, where small subsets of actuators and sensors are selected from sets that contain all "allowed" actuators and sensors. For this purpose, let us define the sets that describe all allowed actuators and sensors:

$$\mathbb{U} = \{(B_{u1}, D_{u\tilde{z}1}, D_{uz_u1}),\ \cdots,\ (B_{uN_u}, D_{u\tilde{z}N_u}, D_{uz_uN_u})\}, \tag{3.2}$$

$$\mathbb{Y} = \{(C_{y1}, D_{\tilde{w}y1}, D_{w_yy1}),\ \cdots,\ (C_{yN_y}, D_{\tilde{w}yN_y}, D_{w_yyN_y})\}, \tag{3.3}$$

with $B_{ui} \in \mathbb{R}^{n_x \times n_{u_i}}$, $D_{u\tilde{z}i} \in \mathbb{R}^{n_{\tilde{z}} \times n_{u_i}}$ and $D_{uz_ui} \in \mathbb{R}^{n_{u_i} \times n_{u_i}}$ for $1 \leq i \leq N_u$; and with $C_{yj} \in \mathbb{R}^{n_{y_j} \times n_x}$, $D_{\tilde{w}yj} \in \mathbb{R}^{n_{y_j} \times n_{\tilde{w}}}$ and $D_{w_yyj} \in \mathbb{R}^{n_{y_j} \times n_{y_j}}$ for $1 \leq j \leq N_y$.

The idea is that each potential measured output $y_i(t)$ is described by a triple $(C_{yi}, D_{\tilde{w}yi}, D_{w_yyi})$. The state information that can be obtained with $y_i(t)$ is described by matrix C_{yi}, while the effect of the disturbance $\widetilde{w}(t)$ on $y_i(t)$ is described by $D_{\tilde{w}y}$. Furthermore, the introduction of a sensor is often accompanied by the introduction of an additional disturbance that directly affects $y_i(t)$—e.g. measurement noise is introduced. The effect of this disturbance on the measured output $y_i(t)$ is described by the matrix $D_{w_yy_i}$.

Each potential control input $u_i(t)$ is, in a similar fashion, described by a triple $(B_{ui}, D_{u\tilde{z}i}, D_{uz_ui})$. The matrix B_{ui} describes how the control input $u_i(t)$ affects the system states, while the effect of this control input on the control output $\tilde{z}(t)$ is described by $D_{u\tilde{z}i}$. Furthermore, the introduction of an actuator is—for optimal control—often accompanied by the introduction of additional control outputs. The matrix D_{uz_ui} describes the effect of the control input $u_i(t)$ on those outputs. Please note that these additional control outputs are introduced in optimal control problems, for the purpose of limiting the control input $u_i(t)$ in magnitude.

Remark 3.1 *It is important to observe that an actuator could add multiple control inputs to $u(t)$, while a sensor can add multiple measured outputs to $y(t)$. For example, an inertial measurement unit is a sensor that typically describes the orientation of an object in three angles, which correspond to three measured outputs. The triples $(B_{ui}, D_{u\tilde{z}i},\ D_{uz_ui})$ and $(C_{yi}, D_{\tilde{w}yi}, D_{w_yyi})$ are therefore described by matrices that can contain multiple column and rows, respectively.*

Then for $n_u, n_y \in \mathbb{N}$, let us define the subsets of actuators and sensors $\mathbb{U}_{n_u} \subseteq \mathbb{U}$ and $\mathbb{Y}_{n_y} \subseteq \mathbb{Y}$, which are of cardinality $n_u \leq N_u$ and $n_y \leq N_y$, respectively. In

addition, these subsets are described by the Cartesian products $\mathbb{U}_{n_u} = \mathbb{U}_{B,n_u} \times \mathbb{U}_{\tilde{D},n_u} \times \mathbb{U}_{D_u,n_u}$ and $\mathbb{Y}_{n_y} = \mathbb{Y}_{C,n_y} \times \mathbb{U}_{\tilde{D},n_y} \times \mathbb{U}_{D_y,n_y}$. This in the sense that, for example, the i^{th} element of $\mathbb{U}_{n_u}$ is described by the i^{th} elements of $\mathbb{U}_{B,n_u}$, $\mathbb{U}_{\widetilde{D},n_u}$ and $\mathbb{U}_{D_u,n_u}$.

Finally, let the control inputs and measured outputs be described by the subsets $\mathbb{U}_{n_u} \subseteq \mathbb{U}$ and $\mathbb{Y}_{n_y} \subseteq \mathbb{Y}$, in order to obtain a system of the form

$$\Sigma(\mathbb{U}_{n_u}, \mathbb{Y}_{n_y}) = \left\{ \begin{array}{rcl} \dot{x}(t) &=& Ax(t) + \operatorname{row}(\mathbb{U}_{B,n_u})u(t) + \begin{pmatrix} \tilde{B}_w & 0 \end{pmatrix} \begin{pmatrix} \tilde{w}(t) \\ w_y(t) \end{pmatrix} \\ y(t) &=& \operatorname{col}(\mathbb{Y}_{C,n_y})x(t) + \begin{pmatrix} \operatorname{col}(\mathbb{Y}_{\widetilde{D},n_y}) & \operatorname{diag}(\mathbb{Y}_{D_y,n_y}) \end{pmatrix} \begin{pmatrix} \tilde{w}(t) \\ w_y(t) \end{pmatrix} \\ \begin{pmatrix} \tilde{z}(t) \\ z_u(t) \end{pmatrix} &=& \begin{pmatrix} \tilde{C}_z \\ 0 \end{pmatrix} x(t) + \begin{pmatrix} \operatorname{row}(\mathbb{U}_{\widetilde{D},n_u}) \\ \operatorname{diag}(\mathbb{U}_{D_u,n_u}) \end{pmatrix} u(t), \end{array} \right. \tag{3.4}$$

with the additional vector signals $u(t)$, $z_u(t)$, $y(t)$ and $w_y(t)$ that represent the control input, additional control output, measured output and additional disturbance, respectively. These signals assume values in finite-dimensional vector spaces $\mathcal{U} = \mathbb{R}^{n_u}$, $\mathcal{W}_y = \mathbb{R}^{n_{w_y}}$, $\mathcal{Y} = \mathbb{R}^{n_y}$ and $\mathcal{Z}_u = \mathbb{R}^{n_{z_u}}$, respectively. The dynamical relation between the signals is described by the real-valued matrices A, $B_u = \operatorname{row}(\mathbb{U}_{B,n_u})$, $B_w = \begin{pmatrix} \tilde{B}_w & 0 \end{pmatrix}$, $C_y = \operatorname{col}(\mathbb{Y}_{C,n_y})$, $D_{wy} = \begin{pmatrix} \operatorname{col}(\mathbb{Y}_{\widetilde{D},n_y}) & \operatorname{diag}(\mathbb{Y}_{D_y,n_y}) \end{pmatrix}$, $C_z = \begin{pmatrix} \tilde{C}_z \\ 0 \end{pmatrix}$ and $D_{uz} = \begin{pmatrix} \operatorname{row}(\mathbb{U}_{\widetilde{D},n_u}) \\ \operatorname{diag}(\mathbb{U}_{D_u,n_u}) \end{pmatrix}$ of appropriate dimension. Finally, the functional dependence on $\mathbb{U}_{n_u}$ and $\mathbb{Y}_{n_y}$ is omitted when it is clear from the context what subsets are used to construct Σ (3.4).

It is important to note that the absence of the direct mappings D_{uy} and D_{wz} can, as established in Lemma 2.18, be assumed without loss of generality for the H_2 optimal control problem. For actuator and sensor selection problems, on the other hand, the absence of these mappings is used to avoid technical issues regarding H_2-admissibility of controllers and well-posedness of the closed-loop interconnection.

Now let us consider to apply a controller of the form

$$\Sigma_{c,n_c} = \left\{ \begin{array}{rl} \dot{x}_c(t) &= Jx_c(t) + Ky(t) \\ u(t) &= Mx_c(t) + Ny(t)) \end{array} \right. \tag{3.5}$$

and of order n_c to Σ (3.4), which results in a closed-loop interconnection that is described by

$$\Sigma_{cl,n_c} = \left\{ \begin{array}{rl} \begin{pmatrix} \dot{x}(t) \\ \dot{x}_c(t) \end{pmatrix} &= \begin{pmatrix} A + B_u N C_y & B_u M \\ KC_y & J \end{pmatrix} \begin{pmatrix} x(t) \\ x_c(t) \end{pmatrix} + \begin{pmatrix} B_w + B_u N D_{wy} \\ KD_{wy} \end{pmatrix} w(t) \\ z(t) &= \begin{pmatrix} C_z + D_{uz} N C_y & D_{uz} M \end{pmatrix} \begin{pmatrix} x(t) \\ x_c(t) \end{pmatrix} + \begin{pmatrix} D_{uz} N D_{wy} \end{pmatrix} w(t), \end{array} \right. \tag{3.6}$$

with $w(t) = \begin{pmatrix} \tilde{w}(t) \\ w_y(t) \end{pmatrix}$ and $z(t) = \begin{pmatrix} \tilde{z}(t) \\ z_u(t) \end{pmatrix}$. This closed-loop system has an extended state $x^{cl,n_c} = \begin{pmatrix} x(t) \\ x_c(t) \end{pmatrix}$ and extended matrices A^{cl,n_c}, B_w^{cl,n_c}, C_z^{cl,n_c} and D_{wz}^{cl,n_c}, while the extended state-space is characterised by the vector space $\mathcal{X}^{cl,n_c}$.

Then, let us define the H_2 (squared) performance for Σ (3.4)—with a given actuator and sensor configuration that is characterised by the subsets $\mathbb{U}_{n_u}$, $\mathbb{Y}_{n_y}$—and a given H_2-admissible controller as

$$\gamma_{H_2}(\Sigma_{c,n_c}\ (3.5), \mathbb{U}_{n_u}, \mathbb{Y}_{n_y}) = \|\Sigma_{cl,n_c}\ (3.6)\|_{H_2}^2 . \tag{3.7}$$

Furthermore, the *best achievable* H_2 (squared) performance for Σ (3.4) with this actuator and sensor configuration is described by

$$\begin{aligned} \gamma_{H_2}^\star(\mathbb{U}_{n_u}, \mathbb{Y}_{n_y}) = \min_{n_c \in \mathbb{N}, \Sigma_{c,n_c}\ (3.5)} \quad & \|\Sigma_{cl,n_c}\ (3.6)\|_{H_2}^2 \\ \text{s.t.} \quad & \Sigma_{c,n_c}\ (3.5) \text{ is } H_2\text{-admissible for } \Sigma\ (3.4). \end{aligned} \tag{3.8}$$

Remark 3.2 *These performance measures are, formally speaking, a function of* $\Sigma(\mathbb{U}_{n_u}, \mathbb{Y}_{n_y})$ (3.4). *The notation* $\gamma_{H_2}(\Sigma\ (3.4), \Sigma_{c,n_c}\ (3.5), \mathbb{U}_{n_u}, \mathbb{Y}_{n_y})$, $\gamma_{H_2}^\star(\Sigma\ (3.4), \mathbb{U}_{n_u}, \mathbb{Y}_{n_y})$ *will therefore be used when it is not directly clear from the context which system is considered.*

The closed-loop H_2 optimal actuator and sensor selection problem amounts to minimising $\gamma_{H_2}^\star$ by appropriate selection of the subsets $\mathbb{U}_{n_u}$ and $\mathbb{U}_{n_y}$ of a given cardinality. This problem is formally defined as follows.

Problem 3.1 *For* Σ (3.4)*, let* $\mathbb{U}$ *and* $\mathbb{Y}$ *be sets that contain all allowed actuators and sensors as defined in* (3.2) *and* (3.3)*, respectively. Furthermore, consider the numbers* $n_u \in \mathbb{N}$ *and* $n_y \in \mathbb{N}$*, with* $n_u \leq N_u$ *and* $n_u \leq N_y$*.*

Then, construct optimal subsets $\mathbb{U}_{n_u}^\star \subseteq \mathbb{U}$ *and* $\mathbb{Y}_{n_y}^\star \subseteq \mathbb{Y}$ *of cardinality* n_u *and* n_y*, respectively, which are a solution to*

$$\begin{aligned} (\mathbb{U}_{n_u}^\star, \mathbb{Y}_{n_y}^\star) = \quad \arg \min_{\substack{\mathbb{U}_{n_u} \subseteq \mathbb{U} \\ \mathbb{Y}_{n_y} \subseteq \mathbb{Y}}} \min_{n_c \in \mathbb{N}, \Sigma_{c,n_c}\ (3.5)} \quad & \|\Sigma_{cl,n_c}\ (3.6)\|_{H_2}^2 \\ \text{s.t.} \quad & \Sigma_{c,n_c}\ (3.5) \text{ is } H_2\text{-admissible for } \Sigma\ (3.4). \end{aligned}$$

This is a combinatorial optimisation problem that can be solved by evaluating all possible subsets $\mathbb{U}_{n_u} \subseteq \mathbb{U}$, $\mathbb{Y}_{n_y} \subseteq \mathbb{Y}$ of the appropriate cardinality. Such a brute force approach will, however, become computationally infeasible when large sets of allowed actuators and sensors are provided. In most practical situations, it is therefore required to take a different approach.

3.1.2 Exploiting Modularity

Early actuator and sensor selection methods, such as the work by Morari and Stephanopoulos [1980], aimed at creating a completely reachable and observable system. These methods, however, interpret reachability and observability of states in a binary sense—i.e. a state is reachable or it is not reachable—while performance is often described by a quantitative measure such as the H_2 norm. In the 1990s it was therefore proposed by several authors—e.g. Hać and Liu [1993], Gawronski and Lim [1996] and Georges [1995]—to utilise Gramians as a quantitative measure for the selection of actuators and sensors.

Recently, it has been shown by Summers et al. [2016], Summers [2016] that certain Gramian-based actuator and sensor selection problems can be solved for large sets of allowed actuators and sensors. For example, it is shown that the observability Gramian of a system is modular in the subset $\mathbb{Y}_{n_y}$. This implies that the trace of this Gramian for several sensors is directly characterised by the traces of the Gramians for each individual sensor. A minimisation or maximisation of this trace can therefore be performed by separately analysing the effect of each allowed sensor.

When reachability and observability properties of a system are optimised, it is essentially assumed that the resulting actuator and sensor configuration provides a viable—although, not necessarily optimal—solution to Problem 3.1; as explained by Taylor et al. [2017]. It has, however, never been established that such an approach could provide any guarantees on the obtained closed-loop performance measure in (3.8).

As a first step towards closed-loop optimal selection of sensors, it is investigated by Chamon et al. [2017] and by Singh et al. [2017] whether similar results can be obtained for the interconnection of a system with an optimal time-varying Kalman filter in discrete time. The results have shown that (approximate) performance guarantees can be obtained under certain conditions. It is, however, not established that similar guarantees can be obtained for the H_2 optimal estimation or control as described in section 2.4.

3.1.3 Sparsity Promoting Methods

In recent years, distributed control problems for networked systems have received a considerable amount of attention. These problems essentially amount to minimising the norm of Σ_{cl,n_c} (3.6) by appropriately constructing a controller Σ_{c,n_c} (3.5), while simultaneously introducing (block) sparsity in the controller. This type of control problem has been addressed by several authors; e.g. by Schuler et al. [2011], Lin et al. [2013] and Wang et al. [2014].

It is observed by Vaidya and Fardad [2013], Dhingra et al. [2014] and Argha et al. [2016] that the introduction of specific types of block sparsity in a controller, is equivalent to an actuator and sensor selection problem. For example, the i^{th} measured output of a system is not used by the controller Σ_{c,n_c} (3.5), if the i^{th} column of K in (3.5) is identically equal to zero. Similarly, the j^{th} control input of a system

is not used by the controller Σ_{c,n_c} (3.5), if the j^{th} row of M in (3.5) is identically equal to zero.

By utilising these sparsity promoting controller design methods, we therefore address Problem 3.1 directly. It is important to note that existing solutions to the distributed control problem—and therefore to the corresponding actuator and sensor selection problems—do not guarantee that an optimal solution is obtained. The potential of these methods for the purpose of closed-loop optimal sensor selection is, however, demonstrated by Dhingra et al. [2014] and by Liu et al. [2014].

3.1.4 Chapter Outline

In this chapter, we will investigate the problem of constructing a combined actuator and sensor configuration that maximises the best achievable closed-loop H_2 performance with a limited number of actuators and sensors. First, we will investigate the use of modularity and greedy algorithms in section 3.2. It will, however, be shown that the performance guarantees for these methods do not apply to the closed-loop selection problem.

Sparsity promoting controller design methods are considered in section 3.3. These methods attempt to maximise closed-loop performance while simultaneously introducing (block) sparsity in a controller, which can equivalently be interpreted as an actuator or sensor selection problem. We will extend an existing solution to address the problem of constructing an actuator configuration that maximises closed-loop H_2 performance for a fixed sensor configuration. In addition, the dual problem of designing an optimal sensor configuration for a fixed actuator configuration is addressed.

The chapter is finalised by analysing and comparing the performance of these methods on a practical example in section 3.4. The conclusions and future work are discussed in chapter 7.

3.2 Modularity and Greedy Algorithms

3.2.1 Mathematical Background

In Problem 3.1, the aim is to minimise the set function $\gamma^\star_{H_2}$ in (3.8) over the arguments $\mathbb{U}_{n_u} \subseteq \mathbb{U}$, $\mathbb{Y}_{n_y} \subseteq \mathbb{Y}$ of a given cardinality, which could be solved by evaluating all possible subsets. Such a brute force approach will, as mentioned above, become computationally infeasible if large sets of allowed actuators and sensors are provided. For this type of optimisation problem, we should therefore aim to exploit certain structural properties of the set function to solve the problem more efficiently, as proposed by Summers et al. [2016].

To discuss these properties, let us consider a finite set $\mathbb{V} = \{v_1, v_2, \cdots, v_m\}$ of cardinality $m \in \mathbb{N}$, a set function $f : 2^{\mathbb{V}} \to \mathbb{R}$ and a number $n \in \mathbb{N}$ with $n \leq m$ to

define the following minimisation problem:

$$\begin{aligned} f^{\star}_{n-} = & \min_{\mathbb{A}\subseteq\mathbb{V}} f(\mathbb{A}) \\ & \text{s.t. } \operatorname{card}(\mathbb{A}) = n. \end{aligned} \tag{3.9}$$

Similarly, the maximisation problem is defined as

$$\begin{aligned} f^{\star}_{n+} = & \max_{\mathbb{A}\subseteq\mathbb{V}} f(\mathbb{A}) \\ & \text{s.t. } \operatorname{card}(\mathbb{A}) = n. \end{aligned} \tag{3.10}$$

A *modular* set function f has the property that all elements in $\mathbb{V}$ have an individual and independent contribution to the value of f; this is formally defined in section 2.1.6. To clarify this property, modularity of f implies that $f(\{v_1, v_2\}) = f(\{v_1\}) + f(\{v_2\}) - f(\emptyset)$ for any pair of elements $v_1, v_2 \in \mathbb{V}$, with $v_1 \neq v_2$. A modular function can therefore be optimised by individually analysing the contribution of each element in $\mathbb{V}$, which is established in the following lemma.

Lemma 3.1 *Consider a finite set $\mathbb{V} = \{v_1, v_2, \cdots, v_m\}$ of cardinality $m \in \mathbb{N}$, a set function $f : 2^{\mathbb{V}} \to \mathbb{R}$ and a number $n \in \mathbb{N}$ with $n \leq m$.*

Furthermore, let $f^{\star}_{n-}$ be a solution to (3.9) *and let Algorithm 3.1 be used to numerically obtain the subset $\mathbb{V}_{mn-} = \text{Modularmin}(f, \mathbb{V}, n)$. Finally, let $f^{\star}_{n+}$ be a solution to* (3.10) *and let Algorithm 3.1 be used to numerically obtain the subset $\mathbb{V}_{mn+} = \text{Modularmin}(-f, \mathbb{V}, n)$.*

If f is modular, then $f^{\star}_{n-} = f(\mathbb{V}_{mn-})$ and $f^{\star}_{n+} = f(\mathbb{V}_{mn+})$.

Proof: It is proven by Summers et al. [2016] that, for any subset $\mathbb{V}_n \subseteq \mathbb{V}$, a modular set function can be expressed as

$$f(\mathbb{V}_n) = f(\emptyset) + \sum_{v_i \in \mathbb{V}_n} w(v_i)$$

for some weight function $w : \mathbb{V} \to \mathbb{R}$.

The optimisation problem in (3.9) is therefore solved by evaluation f for each element in $\mathbb{V}$ and then choosing the n elements that result in the smallest function value, which is implemented in Algorithm 3.1. As a result, it can be concluded that $f^{\star}_{n-} = f(\mathbb{V}_{mn-})$.

Finally, maximisation of f is equivalent to minimisation of $-f$, while it can be observed that this change in sign does not affect modularity. This implies that $f^{\star}_{n+} = f(\mathbb{V}_{mn+})$. □

On the other hand, minimisation of a *supermodular and monotone decreasing* set function—as defined in section 2.1.6—is an NP-hard problem; this is explained by Summers et al. [2016]. In order to solve this type of problem with an upper bound on the degree of non-optimality, a greedy search algorithm such as Algorithm 3.2 can be used. This is established in the following theorem.

Theorem 3.2 *Consider a set* $\mathbb{V} = \{v_1, v_2, \cdots, v_m\}$*, a set function* $f : 2^{\mathbb{V}} \to \mathbb{R}$ *and a number* $n \in \mathbb{N}$ *with* $n \leq m$*. Furthermore, let* $f^\star_{n-}$ *be the solution to* (3.9) *and let Algorithm 3.2 be used to numerically obtain the subset* $\mathbb{V}_{gn} = \text{Greedymin}(f, \mathbb{V}, n)$*.*

If f *is supermodular and monotone decreasing, then*

$$\frac{f^\star_{n-} - f(\mathbb{V}_{gn})}{f^\star_{n-} - f(\emptyset)} = \frac{1}{e} \approx 0.37.$$

Proof: The proof is given by Nemhauser et al. [1978]. □

Although it is not considered in this chapter, it is important to note that a similar upper bound can be obtained for the maximisation problem in (3.10), when a *submodular and monotone increasing* set function—as defined in section 2.1.6—is considered. This stems from the fact that f is supermodular and monotone decreasing if and only if $-f$ is submodular and monotone increasing.

Algorithm 3.1 Modular Minimisation

```
1: procedure MODULARMIN(f, {v_1, v_2, ··· , v_m}, n)
2:     if n ≥ m then
3:         return {v_1, v_2, ··· , v_m}
4:     else
5:         for i = 1, 2, ··· , m do
6:             f_i = f(v_i).
7:         end for
8:         Order the function values f_i such that:
9:         f_{i,1} ≤ f_{i,2} ≤ ··· ≤ f_{i,m}
10:        return {v_{i,1}, v_{i,2}, ··· , v_{i,n}}
11:    end if
12: end procedure
```

3.2.2 Control Relevant Selection on the Basis of Open-Loop System Properties

In order to use these algorithms for "open-loop selection" of actuators and sensors, let us consider the subsets $\mathbb{U}_{n_u} \subseteq \mathbb{U}$ and $\mathbb{Y}_{n_y} \subseteq \mathbb{Y}$ of all allowed actuators and sensors in (3.2) and (3.3) to define—for $\lambda(A) \subset \mathbb{C}_-$—the Gramians as the set functions

$$\mathcal{P}(A, \mathbb{U}_{n_u}) \coloneqq \int_{t=0}^{\infty} e^{At} \text{row}(\mathbb{U}_{B,n_u}) \text{row}(\mathbb{U}_{B,n_u})^\top e^{A^\top t} dt, \tag{3.11}$$

$$\mathcal{Q}(\mathbb{Y}_{n_y}, A) \coloneqq \int_{t=0}^{\infty} e^{A^\top t} \text{col}(\mathbb{Y}_{C,n_y})^\top \text{col}(\mathbb{Y}_{C,n_y}) e^{At} dt, \tag{3.12}$$

It will now be shown that the trace of these Gramians is a modular function in $\mathbb{U}$ and $\mathbb{Y}$, respectively.

Algorithm 3.2 Greedy Minimisation

```
procedure GREEDYMIN(f, {v_1, v_2, ··· , v_m}, n)
    if n ≥ m then
        return {v_1, v_2, ··· , v_m}
    else
        V_1 = ∅, V_c = {v_1, v_2, ··· , v_m}
        for i = 1, ··· , n do
            for j = 1, ··· , card(V_c) do
                f_j = f(v_cj), where v_cj is the j^th element in V_c.
            end for
            Find a value k such that f_k ≤ f_l for all l ≠ k
            V_{i+1} = V_i ∪ v_ck, V_c = V_c \ v_ck
        end for
        return V_{i+1}
    end if
end procedure
```

Theorem 3.3 *For an internally stable system* Σ (3.4)*—i.e. with* $\lambda(A) \subset \mathbb{C}_-$*—let* $\mathbb{U}_{n_u} \subseteq \mathbb{U}$ *and* $\mathbb{Y}_{n_y} \subseteq \mathbb{Y}$ *be subsets of all allowed actuators and sensors as defined in* (3.2) *and* (3.3)*, respectively. Let* $\mathcal{P}$ *and* $\mathcal{Q}$ *be the Gramians as defined in* (3.11) *and* (3.12)*, respectively. Finally, consider the real-valued matrices* $C \in \mathbb{R}^{p \times n_x}$ *and* $B \in \mathbb{R}^{n_x \times q}$*.*

Then the set function $f_u(\mathbb{U}_{n_u}) = \operatorname{tr}(C\mathcal{P}C^\top)$ *is modular in* $\mathbb{U}$*.*

Furthermore, the set function $f_y(\mathbb{Y}_{n_y}) = \operatorname{tr}(B^\top \mathcal{Q} B)$ *is modular in* $\mathbb{Y}$*.*

Proof: The proof is given by Summers et al. [2016, Thm. 4]. □

As established in Lemma 3.1, this modularity property implies that the optimisation problems in (3.9) and (3.10) can be solved efficiently for f_u and f_y with Algorithm 3.1.

State Feedback Design

The question now arises whether the functions f_u and f_y in Theorem 3.3—which relate to the open-loop reachability and observability properties of a system—can be used to obtain a control relevant actuator and sensor configuration. To answer this question, let us first consider the design of a static state feedback $u(t) = Fx(t)$.

State feedback design is equivalent to controller design as discussed in section 3.1.1 if $y(t) = x(t)$; i.e. $\mathbb{Y}_{n_y} = \mathbb{Y}_{full} = \{(I_{n_x}, 0, 0)\}$ is used to construct Σ (3.4). As explained in section 2.4, in such a situation the dynamic controller Σ_{c,n_c} (3.5) can be replaced by a static mapping $u(t) = Ny(t)$ that for this specific situation is denoted by $u(t) = Fx(t)$.

Therefore, let us consider a state feedback $u(t) = Fx(t)$ applied to Σ (3.4) for a given subset of actuators $\mathbb{U}_{n_u}$ to obtain—when $y(t)$ is eliminated—the closed-loop

system

$$\Sigma_{cl,F} = \begin{cases} \dot{x}(t) = \left(A + \operatorname{row}(\mathbb{U}_{B,n_u})F \right) x(t) + \widetilde{B}_w \widetilde{w}(t) \\ \begin{pmatrix} \tilde{z}(t) \\ z_u(t) \end{pmatrix} = \left(\begin{pmatrix} \tilde{C}_z \\ 0 \end{pmatrix} + \begin{pmatrix} \operatorname{row}(\mathbb{U}_{\widetilde{D},n_u}) \\ \operatorname{diag}(\mathbb{U}_{D_u,n_u}) \end{pmatrix} F \right) x(t). \end{cases} \tag{3.13}$$

In addition, let us define the H_2 (squared) performance for Σ (3.4)—with a given actuator configuration that is characterised by the subset $\mathbb{U}_{n_u}$—and an H_2-admissible state feedback as

$$\gamma_{H_2,F}(F, \mathbb{U}_{n_u}) = \|\Sigma_{cl,F} \ (3.13)\|_{H_2}^2 . \tag{3.14}$$

When the design of a state feedback is considered, the best achievable H_2 (squared) performance for Σ (3.4) with this actuator configuration (and $\mathbb{Y}_{full} = \{(I_{n_x}, 0, 0)\}$) is therefore described by

$$\begin{aligned} \gamma^\star_{H_2,F}(\mathbb{U}_{n_u}) = \min_F \ & \|\Sigma_{cl,F} \ (3.13)\|_{H_2}^2 \\ \text{s.t. } & F \text{ is } H_2\text{-admissible for } \Sigma(\mathbb{U}_{n_u}, \mathbb{Y}_{full}) \ (3.4). \end{aligned} \tag{3.15}$$

Remark 3.3 *These performance measures are, formally speaking, a function of* $\Sigma(\mathbb{U}_{n_u}, \mathbb{Y}_{full})$ (3.4)*. The notation* $\gamma_{H_2,F}(\Sigma \ (3.4), F, \mathbb{U}_{n_u})$*,* $\gamma^\star_{H_2,F}(\Sigma \ (3.4), \mathbb{U}_{n_u})$ *will therefore be used when it is not directly clear from the context which system is considered.*

The closed-loop H_2 optimal actuator selection problem for state feedback amounts design to minimising $\gamma^\star_{H_2,F}$ by appropriate selection of the subset $\mathbb{U}_{n_u}$ of a given cardinality. This problem is formally defined as follows.

Problem 3.2 *For* Σ (3.4)*, consider the set* $\mathbb{Y}_{full} = \{(I_{n_x}, 0, 0)\}$ *and let* $\mathbb{U}$ *be a set that contains all allowed actuators as defined in* (3.2)*. Furthermore, consider the number* $n_u \in \mathbb{N}$*, with* $n_u \leq N_u$*.*

Then, construct an optimal subset $\mathbb{U}^\star_{n_u} \subseteq \mathbb{U}$ *of cardinality* n_u*, which is a solution to*

$$\begin{aligned} \mathbb{U}^\star_{n_u} = \ & \arg \min_{\mathbb{U}_{n_u} \subseteq \mathbb{U}} \ \min_F \ \|\Sigma_{cl,F} \ (3.13)\|_{H_2}^2 \\ & \text{s.t. } F \text{ is } H_2\text{-admissible for } \Sigma(\mathbb{U}_{n_u}, \mathbb{Y}_{full}) \ (3.4). \end{aligned}$$

As explained in section 3.1, it is generally claimed that improved reachability properties of a system will improve the best achievable performance $\gamma^\star_{H_2}$. From this perspective, it can be argued that Problem 3.2 might be solved if reachability through the control inputs $u(t)$ is maximised for the states that are—on average—most affected by $\widetilde{w}(t)$ and most observable in $\tilde{z}(t)$.

For Σ (3.4), let us therefore consider the set function

$$f_{u,g}(\mathbb{U}_{n_u}, \alpha_u) = \alpha_u \operatorname{tr}(\widetilde{C}_z \mathcal{P} \widetilde{C}_z^\top) + (1 - \alpha_u) \operatorname{tr}(\widetilde{B}_w^\top \mathcal{P} \widetilde{B}_w), \tag{3.16}$$

with the design parameter $0 \leq \alpha_u \leq 1$ and where $\mathcal{P}$ is the reachability Gramian as defined in (3.11).

It will first be shown that the function $f_{u,g}$ is modular in $\mathbb{U}$.

Proposition 3.4 *For Σ (3.4), let $\mathbb{U}_{n_u} \subseteq \mathbb{U}$ be a subset of all allowed actuators as defined in* (3.2) *and let $\mathcal{P}$ be the Gramian as defined in* (3.11).

Then, the function $f_{u,g}$ in (3.16) *is modular in $\mathbb{U}$ for any $0 \leq \alpha_u \leq 1$.*

Proof: The proof can be found in appendix A.2. □

Since $f_{u,g}$ is a modular set function, the following optimisation problem can efficiently be solved with Algorithm 3.1 for some pair $0 \leq \alpha_u \leq 1$, $n_u \leq N_u$:

$$\begin{aligned} \mathbb{U}_{n_u}^{\star} = \arg \max_{\mathbb{U}_{n_u} \subseteq \mathbb{U}} & f_{u,g}(\mathbb{U}_{n_u}, \alpha_u) \\ \text{s.t.} \quad & \operatorname{card}(\mathbb{U}_{n_u}) = n_u. \end{aligned} \tag{3.17}$$

The solution to this optimisation problem provides an actuator configuration for Σ (3.4). This configuration maximises a reachability trade-off for the states that are visible on the control output $\tilde{z}(t)$ and states that are affected by the disturbance $\widetilde{w}(t)$.

For example, a maximisation of this function with $\alpha_u = 0$ corresponds to maximising reachability through the control input $u(t)$, for the states that are affected the most by the disturbance $\widetilde{w}(t)$. Similarly, a maximisation of this function with $\alpha_u = 1$ corresponds to maximising reachability through the control input $u(t)$, for the states that are most visible in the control output $\tilde{z}(t)$.

Let us now investigate whether maximisation of $f_{u,g}$ could provide a viable—although, not necessarily optimal—solution to Problem 3.2. For this purpose, consider the system

$$\Sigma_{ce,1} = \left\{ \begin{array}{l} \begin{pmatrix} \dot{x}_1(t) \\ \dot{x}_2(t) \end{pmatrix} = \begin{pmatrix} -1 & 0 \\ 0 & -1 \end{pmatrix} \begin{pmatrix} x_1(t) \\ x_2(t) \end{pmatrix} + \operatorname{row}(\mathbb{U}_{B,n_u}) u(t) + \begin{pmatrix} 1 & 0 \\ 0 & 0 \end{pmatrix} \begin{pmatrix} \widetilde{w}_1(t) \\ \widetilde{w}_2(t) \end{pmatrix} \\ \left(\begin{array}{c} \tilde{z}_1(t) \\ \tilde{z}_2(t) \\ \hline z_u(t) \end{array} \right) = \left(\begin{array}{cc} 1 & 0 \\ 0 & 10 \\ \hline 0 & 0 \end{array} \right) \begin{pmatrix} x_1(t) \\ x_2(t) \end{pmatrix} + \left(\begin{array}{c} \operatorname{row}(\mathbb{U}_{\widetilde{D},n_u}) \\ \hline \operatorname{diag}(\mathbb{U}_{D_u,n_u}) \end{array} \right) u(t), \end{array} \right. \tag{3.18}$$

with two allowed actuators that are described by the set

$$\mathbb{U} = \{u_1, u_2\} = \left\{ \left(\begin{pmatrix} 1 \\ 0 \end{pmatrix}, \begin{pmatrix} 0 \\ 0 \end{pmatrix}, 1 \right) \ , \ \left(\begin{pmatrix} 0 \\ 1 \end{pmatrix}, \begin{pmatrix} 0 \\ 0 \end{pmatrix}, 1 \right) \right\}.$$

When we consider the value $\alpha_u = 0.5$, we obtain $f_{u,g}(\{u_1\}, 0.5) = 0.5$ and $f_{u,g}(\{u_2\}, 0.5) = 12.5$. The solution to (3.17) for $n_u = 1$ is therefore given by $\mathbb{U}_1^{\star} = \{u_2\}$.

However, the best achievable closed-loop performance for $\Sigma_{ce,1}$ with each actuator is given by $\gamma_{H_2,F}^{\star}(\{u_1\}) = 0.41$ and $\gamma_{H_2,F}^{\star}(\{u_2\}) = 0.5$. Problem 3.2 is therefore solved by considering the actuator $\{u_1\}$ instead. Furthermore, it is important to observe that $\gamma_{H_2,F}^{\star}(\emptyset) = 0.5$, which implies that the actuator u_2 does not improve performance.

From this example, we can therefore observe that the optimisation problem in (3.17) does not necessarily solve Problem 3.2. In addition, a solution to the former problem might even contain actuators that do not improve the closed-loop performance measure $\gamma^{\star}_{H_2,F}$ at all. It is, however, important to emphasise that the optimisation problem in (3.17) does not necessarily produce actuator configurations with poor closed-loop performance in a more practical situation.

Observer Design

The measured output $y(t)$ is not taken into consideration with the state feedback design problem as described above, which implies that $\gamma^{\star}_{H_2,F}$ is only affected by the selected actuators. To select the sensors, we will now investigate the (dual) estimation problem.

For this type of problem, a given actuator configuration $\mathbb{U}_f = \{(B_{uf}, D_{u\tilde{z}f}, D_{uz_uf})\}$ and a given subset of sensors $\mathbb{Y}_{n_y}$ we can—as discussed in section 2.4—consider a Luenberger state observer of the form

$$\Sigma_o = \begin{cases} \dot{\tilde{x}}(t) = \left(A + L\mathrm{col}(\mathbb{Y}_{C,n_y})\right)\tilde{x}(t) - Ly(t) + B_{uf}u(t) \\ \tilde{z}(t) = \begin{pmatrix}\tilde{C}_z \\ 0\end{pmatrix}\tilde{x}(t) + \begin{pmatrix}D_{u\tilde{z}f} \\ D_{uz_uf}\end{pmatrix}u(t). \end{cases} \tag{3.19}$$

When this observer is connected to Σ (3.4), we obtain an error system of the form

$$\Sigma_{\epsilon,o} = \begin{cases} \dot{e}(t) = \left(A + L\mathrm{col}(\mathbb{Y}_{C,n_y})\right)e(t) + \left(B_w + LD_{wy}\right)\begin{pmatrix}\tilde{w}(t) \\ w_y(t)\end{pmatrix} \\ \epsilon_z(t) = \begin{pmatrix}\tilde{C}_z \\ 0\end{pmatrix}e(t), \end{cases} \tag{3.20}$$

with $e(t) = x(t) - \tilde{x}(t)$, $\epsilon_z(t) = z(t) - \tilde{z}(t)$, $B_w = \begin{pmatrix}\tilde{B}_w & 0\end{pmatrix}$ and $D_{wy} = \left(\mathrm{col}(\mathbb{Y}_{\tilde{D},n_y}) \ \mathrm{diag}(\mathbb{Y}_{D_y,n_y})\right)$. It is important to note that the control input $u(t)$—and therefore the selected actuators—do not affect this error system.

In a dual fashion to state feedback design, let us define the H_2 (squared) performance for Σ (3.4)—with a given sensor configuration that is characterised by the subset $\mathbb{Y}_{n_y}$—and an H_2-admissible observer as

$$\gamma_{H_2,e}(\Sigma_o \ (3.19), \mathbb{Y}_{n_y}) = \left\|\Sigma_{\epsilon,o} \ (3.20)\right\|^2_{H_2}. \tag{3.21}$$

With the design of an observer, the best achievable H_2 (squared) performance for Σ (3.4) with this sensor configuration (and any actuator configuration that is described by the subset $\mathbb{U}_f$) is therefore given by

$$\begin{aligned} \gamma^{\star}_{H_2,e}(\mathbb{Y}_{n_y}) = \min_{L} \ & \left\|\Sigma_{\epsilon,o} \ (3.20)\right\|^2_{H_2} \\ \text{s.t. } & \Sigma_o \ (3.19) \text{ is } H_2\text{-admissible for } \Sigma(\mathbb{U}_f, \mathbb{Y}_{n_y}) \ (3.4). \end{aligned} \tag{3.22}$$

Remark 3.4 *These performance measures are, formally speaking, a function of* $\Sigma(\mathbb{U}_f, \mathbb{Y}_{n_y})$ (3.4). *The notation* $\gamma_{H_2,e}(\Sigma\ (3.4), L, \mathbb{Y}_{n_y})$, $\gamma^\star_{H_2,e}(\Sigma\ (3.4), \mathbb{Y}_{n_y})$ *will therefore be used when it is not directly clear from the context which system is considered.*

The closed-loop H_2 optimal sensor selection problem for observer design amounts to minimising $\gamma^\star_{H_2,e}$ by appropriate selection of the subset $\mathbb{Y}_{n_y}$ of a given cardinality. This problem is formally defined as follows.

Problem 3.3 *For* Σ (3.4), *consider the set* $\mathbb{U}_f = \{(B_{uf}, D_{u\tilde{z}f}, D_{uz_uf})\}$ *and let* $\mathbb{Y}$ *be a set that contains all allowed sensors as defined in* (3.3). *Furthermore, consider the number* $n_y \in \mathbb{N}$, *with* $n_y \leq N_y$.

Then, construct an optimal subset $\mathbb{Y}^\star_{n_y} \subseteq \mathbb{Y}$ *of cardinality* n_y, *which is a solution to*

$$\begin{aligned}\mathbb{Y}^\star_{n_y} = \quad & \arg\min_{\mathbb{Y}_{n_Y}\subseteq\mathbb{Y}} \min_{L} \|\Sigma_{\epsilon,o}\ (3.20)\|^2_{H_2} \\ & \text{s.t. } \Sigma_o\ (3.19) \text{ is } H_2\text{-admissible for } \Sigma(\mathbb{U}_f, \mathbb{Y}_{n_y})\ (3.4).\end{aligned}$$

As before, it can be argued that Problem 3.3 might be solved if observability in the measured outputs $y(t)$ is maximised for the states that are—on average—most affected by $\widetilde{w}(t)$ and most visiblein $\tilde{z}(t)$.

Let us therefore consider the set function

$$f_{y,g}(\mathbb{Y}_{n_y}, \alpha_y) = \alpha_y \mathrm{tr}(\widetilde{C}_z \mathcal{Q} \widetilde{C}_z^\top) + (1-\alpha_y)\mathrm{tr}(\widetilde{B}_w^\top \mathcal{Q} \widetilde{B}_w), \tag{3.23}$$

with the design parameter $0 \leq \alpha_y \leq 1$ and where $\mathcal{Q}$ is the observability Gramian as defined in (3.12).

It will now be shown that the function $f_{y,g}$ is modular in $\mathbb{Y}$.

Corollary 3.5 *For* Σ (3.4), *let* $\mathbb{Y}_{n_y} \subseteq \mathbb{Y}$ *be a subset of all allowed sensors as defined in* (3.3) *and let* $\mathcal{Q}$ *be the Gramian as defined in* (3.12).

Then, the function $f_{y,g}$ *in* (3.23) *is modular in* $\mathbb{Y}$ *for any* $0 \leq \alpha_y \leq 1$.

Proof: This corollary is dual to Proposition 3.4. □

Therefore, the following optimisation problem can be solved efficiently with Algorithm 3.1 for some pair $0 \leq \alpha_y \leq 1$, $n_y \leq N_y$:

$$\begin{aligned}\mathbb{Y}^\star_{n_y} = \arg\max_{\mathbb{Y}_{n_y}\subseteq\mathbb{Y}} & f_{y,g}(\mathbb{Y}_{n_y}, \alpha_y) \\ \text{s.t.} \quad & \mathrm{card}(\mathbb{Y}_{n_y}) = n_y.\end{aligned} \tag{3.24}$$

The observer design is a dual problem to state feedback design, which implies that the conclusions for the latter—as described above—will hold for observer design as well.

As a consequence, the optimisation problem in (3.24) does not necessarily solve Problem 3.3. In addition, a solution to the former problem might even contain sensors that do not affect the closed-loop performance measure $\gamma^\star_{H_2,e}$ at all. It is, again, important to emphasise that the optimisation problem in (3.24) does not necessarily produce sensor configuration with poor closed-loop performance in a more practical situation.

3.2.3 Directly Maximising Closed-Loop H_2 Performance

In section 3.2.2 it has been shown that selection of actuators and sensors on the basis of Gramians—which are open-loop system properties—does not provide any guarantees with regards to the best achievable closed-loop performance. This conclusion emphasises the importance of the main research question in chapter 1. Namely, it is important to take the controller into consideration during the selection of actuators and sensors—i.e. during system design.

In order to improve the best achievable closed-loop performance, let us now investigate whether the set functions $\gamma^\star_{H_2}$, $\gamma^\star_{H_2,F}$ and $\gamma^\star_{H_2,e}$ satisfy similar structural properties; for example, monotonicity as defined in section 2.1.6.

Lemma 3.6 *For a system* Σ (3.4)*, let* $\mathbb{U}_{n_u} \subseteq \mathbb{U}$ *and* $\mathbb{Y}_{n_y} \subseteq \mathbb{Y}$ *be subsets of all allowed actuators and sensors as defined in* (3.2) *and* (3.3)*, respectively.*

Then, the set function

(a) $\gamma^\star_{H_2}(\mathbb{U}_{n_u}, \mathbb{Y}_{n_y})$ *in* (3.8) *is monotone decreasing in* $\mathbb{U}$ *and in* $\mathbb{Y}$*.*
(b) $\gamma^\star_{H_2,F}(\mathbb{U}_{n_u})$ *in* (3.15) *is monotone decreasing in* $\mathbb{U}$*.*
(c) $\gamma^\star_{H_2,e}(\mathbb{Y}_{n_y})$ *in* (3.22) *is monotone decreasing in* $\mathbb{Y}$*.*

Proof: A proof will be given for $\gamma^\star_{H_2,F}$, while a similar argument can directly be applied to $\gamma^\star_{H_2}$ and $\gamma^\star_{H_2,e}$.

Consider the subsets $\mathbb{U}_1 \subseteq \mathbb{U}_2 \subseteq \mathbb{U}$ and let $u_i(t) = F_i^\star x(t)$ be the H_2 optimal state feedback for $\mathbb{U}_i$ that achieves $\gamma^\star_{i,F} = \gamma^\star_{H_2,F}(\mathbb{U}_i)$, with $i = 1, 2$.

Since $\mathbb{U}_1 \subseteq \mathbb{U}_2$, it is proven that the function $\gamma^\star_{H_2,F}$ is monotone decreasing if it is shown that $\gamma^\star_{1,F} \geq \gamma^\star_{2,F}$. In addition, any state feedback $u_2(t) = F_2 x(t)$ can—after a suitable ordering of the control inputs—be decomposed as

$$u_2(t) = \begin{pmatrix} u_1(t) \\ u_{2e}(t) \end{pmatrix} = \begin{pmatrix} F_1 \\ F_{2e} \end{pmatrix} x(t).$$

Now, we can directly conclude from an optimality argument that

$$\gamma^\star_{1,F} = \gamma_{H_2,F}\left(\begin{pmatrix} F_1^\star \\ 0 \end{pmatrix}, \mathbb{U}_2\right) \geq \gamma_{H_2,F}\left(F_2^\star, \mathbb{U}_2\right) = \gamma^\star_{2,F},$$

which completes the proof. □

These properties therefore follow directly from an optimality argument. Namely, a controller does not have to use all sensors and actuators, a state feedback does

not have to use all actuators and an observer does not have to use all sensors. The addition of actuators and sensors can therefore not decrease optimal performance, which corresponds to an increase in $\gamma^\star_{H_2,(F/e)}$.

According to Theorem 3.2, a greedy algorithm such as Algorithm 3.2 can be used to minimise these functions with explicit guarantees on the obtained result, if $\gamma^\star_{H_2}$, $\gamma^\star_{H_2,F}$ and $\gamma^\star_{H_2,e}$ are supermodular. Let us therefore investigate whether this is indeed the case.

First, in section 2.4 it has been shown that there exist unique stabilising solutions to the AREs for certain actuator and sensor configurations. Let us now define for which actuator and sensor configurations these solutions exist.

Definition 3.7 *For Σ (3.4), let $\mathbb{U}_{n_u} \subseteq \mathbb{U}$ and $\mathbb{Y}_{n_y} \subseteq \mathbb{Y}$ be subsets of all allowed actuators and sensors as defined in (3.2) and (3.3), respectively.*

We then say that the subset $\mathbb{U}_{n_u}$ is ARE-admissible for Σ (3.4) if

- $(A, \mathrm{row}(\mathbb{U}_{B,n_u}))$ *is stabilisable.*
- $\begin{pmatrix} A - j\omega I_{n_x} & \mathrm{row}(\mathbb{U}_{B,n_u}) \\ \tilde{C}_z & \mathrm{row}(\mathbb{U}_{\tilde{D},n_u}) \\ 0 & \mathrm{diag}(\mathbb{U}_{D_u,n_u}) \end{pmatrix}$ *is full column rank for all $\omega \in \mathbb{R}$.*
- $\begin{pmatrix} \mathrm{row}(\mathbb{U}_{\tilde{D},n_u}) \\ \mathrm{diag}(\mathbb{U}_{D_u,n_u}) \end{pmatrix}$ *is full column rank,*

Furthermore, we say that the subset $\mathbb{Y}_{n_y}$ is ARE-admissible for Σ (3.4) if

- $(\mathrm{col}(\mathbb{Y}_{C,n_y}), A)$ *is detectable.*
- $\begin{pmatrix} A - j\omega I_{n_x} & \tilde{B}_w & 0 \\ \mathrm{col}(\mathbb{Y}_{C,n_y}) & \mathrm{col}(\mathbb{Y}_{\tilde{D},n_y}) & \mathrm{diag}(\mathbb{Y}_{D_y,n_y}) \end{pmatrix}$ *is full row rank for all $\omega \in \mathbb{R}$.*
- $\begin{pmatrix} \mathrm{col}(\mathbb{Y}_{\tilde{D},n_y}) & \mathrm{diag}(\mathbb{Y}_{D_y,n_y}) \end{pmatrix}$ *is full row rank.*

For a system Σ (3.4) and the ARE-admissible subsets $\mathbb{U}_{n_u}$ and $\mathbb{Y}_{n_y}$, we can now define the AREs as the following set functions:

$$P(\Sigma\ (3.4), \mathbb{U}_{n_u}) \text{ such that } A^\top P + PA + C_z^\top C_z - (PB_u + C_z^\top D_{uz})(D_{uz}^\top D_{uz})^{-1}(PB_u + C_z^\top D_{uz})^\top = 0, \tag{3.25}$$

$$Q(\Sigma\ (3.4), \mathbb{Y}_{n_y}) \text{ such that } AQ + QA^\top + B_w B_w^\top - (QC_y^\top + B_w^\top D_{wy})(D_{wy} D_{wy}^\top)^{-1}(QC_y^\top + B_w^\top D_{wy})^\top = 0. \tag{3.26}$$

Then, let us utilise the unique stabilising solutions $P^+(\Sigma\ (3.4), \mathbb{U}_{n_u})$ and $Q^+(\Sigma\ (3.4), \mathbb{Y}_{n_y})$ to these AREs in order to write the optimisation problem in Problem 3.1 as

$$\begin{aligned} (\mathbb{U}^\star_{n_u}, \mathbb{Y}^\star_{n_y}) = \ & \arg \min_{\substack{\mathbb{U}_{n_u} \subseteq \mathbb{U} \\ \mathbb{Y}_{n_y} \subseteq \mathbb{Y}}} \gamma^\star_{H_2}(\mathbb{U}_{n_u}, \mathbb{Y}_{n_y}) \\ & \text{s.t. } \mathbb{U}_{n_u}, \mathbb{Y}_{n_y} \text{ are ARE-admissible for } \Sigma\ (3.4), \end{aligned} \tag{3.27}$$

$$\begin{aligned} \text{with} \quad \gamma^\star_{H_2}(\mathbb{U}_{n_u}, \mathbb{Y}_{n_y}) &= \mathrm{tr}(B_w^\top P^+ B_w) + \mathrm{tr}(B_u^\top P^+ Q^+ P^+ B_u) \\ &= \mathrm{tr}(C_z Q^+ C_z^\top) + \mathrm{tr}(C_y Q^+ P^+ Q^+ C_y^\top). \end{aligned}$$

It will now be shown that this set function is generally not supermodular and not submodular in its arguments. To see this, we consider again a state feedback design problem by introducing $\mathbb{Y}_{full} = \{(I_{n_x}, 0, 0)\}$ in combination with $n_y = 1$. In this way, we can prove that $\gamma^\star_{H_2}$ is not supermodular and not submodular if we can show this for the function

$$\gamma^\star_{H_2}(\mathbb{U}_{n_u}, \mathbb{Y}_{full}) = \gamma^\star_{H_2,F}(\mathbb{U}_{n_u}) = \mathrm{tr}(B_w^\top P^+ B_w).$$

Let us therefore consider the design of a state feedback $u(t) = Fx(t)$ for the system

$$\Sigma_{ce,2} = \left\{ \begin{array}{rcl} \begin{pmatrix} \dot{x}_1(t) \\ \dot{x}_2(t) \end{pmatrix} & = & \begin{pmatrix} -1 & 0 \\ 0 & -0.01 \end{pmatrix} \begin{pmatrix} x_1(t) \\ x_2(t) \end{pmatrix} + \mathrm{row}(\mathbb{U}_{B,n_u}) u(t) + \widetilde{B}_w \widetilde{w}(t) \\ \left(\begin{array}{c} \tilde{z}_1(t) \\ \tilde{z}_2(t) \\ \hline z_u(t) \end{array}\right) & = & \left(\begin{array}{cc} 1 & 1 \\ 1 & -1 \\ \hline 0 & 0 \end{array}\right) \begin{pmatrix} x_1(t) \\ x_2(t) \end{pmatrix} + \left(\begin{array}{c} \mathrm{row}(\mathbb{U}_{\widetilde{D},n_u}) \\ \hline \mathrm{diag}(\mathbb{U}_{D_u,n_u}) \end{array}\right) u(t), \end{array} \right. \tag{3.28}$$

with two allowed actuators that are described by the set

$$\mathbb{U} = \{u_1, u_2\} = \left\{ \left(\begin{pmatrix} -1 \\ 1 \end{pmatrix}, \begin{pmatrix} 0 \\ 0 \end{pmatrix}, 0.1 \right) \ , \ \left(\begin{pmatrix} -1 \\ -1 \end{pmatrix}, \begin{pmatrix} 0 \\ 0 \end{pmatrix}, 0.1 \right) \right\}.$$

Then, for $\widetilde{B}_w = \begin{pmatrix} 1 \\ 0 \end{pmatrix}$ we obtain

$$\gamma^\star_{H_2,F}(\{u_1\}) = \gamma^\star_{H_2,F}(\{u_2\}) \approx 0.92, \qquad \gamma^\star_{H_2,F}(\{u_1, u_2\}) \approx 0.31, \qquad \gamma^\star_{H_2,F}(\emptyset) = 1.$$

This implies that the function $\gamma^\star_{H_2,F}$ is not supermodular, because

$$\gamma^\star_{H_2,F}(\{u_1\}) + \gamma^\star_{H_2,F}(\{u_2\}) \not\leq \gamma^\star_{H_2,F}(\{u_1, u_2\}) + \gamma^\star_{H_2,F}(\emptyset).$$

Similarly, for $\widetilde{B}_w = \begin{pmatrix} 0 \\ 1 \end{pmatrix}$ we obtain

$$\gamma^\star_{H_2,F}(\{u_1\}) = \gamma^\star_{H_2,F}(\{u_2\}) \approx 0.96, \qquad \gamma^\star_{H_2,F}(\{u_1, u_2\}) \approx 0.32, \qquad \gamma^\star_{H_2,F}(\emptyset) = 10.$$

This implies that the function $\gamma^\star_{H_2,F}$ is not submodular either, because

$$\gamma^\star_{H_2,F}(\{u_1\}) + \gamma^\star_{H_2,F}(\{u_2\}) \not\geq \gamma^\star_{H_2,F}(\{u_1, u_2\}) + \gamma^\star_{H_2,F}(\emptyset).$$

From this example we therefore infer the following main result.

Theorem 3.8 *For Σ (3.4), let $\mathbb{U}_{n_u} \subseteq \mathbb{U}$ and $\mathbb{Y}_{n_y} \subseteq \mathbb{Y}$ be subsets of all allowed actuators and sensors as defined in (3.2) and (3.3), respectively. Furthermore, let these subsets be ARE-admissible for Σ (3.4).*

Then, the set functions $\gamma^\star_{H_2}(\mathbb{U}_{n_u}, \mathbb{Y}_{n_y})$ in (3.8), $\gamma^\star_{H_2,F}(\mathbb{U}_{n_u})$ in (3.15) and $\gamma^\star_{H_2,e}(\mathbb{Y}_{n_y})$ in (3.22) are, in general, not supermodular and not submodular in the sets $\mathbb{U}$ and $\mathbb{Y}$.

Proof: This is shown for $\gamma^{\star}_{H_2}$ and for $\gamma^{\star}_{H_2,F}$ by using the system $\Sigma_{ce,2}$ (3.28) as described above. Furthermore, the state feedback problem is dual to the estimator design problem, which implies that the same property holds for $\gamma^{\star}_{H_2,e}$. □

It has now been proven that the structural properties of the open-loop Gramian-based set functions, do not hold for the closed-loop performance measures $\gamma^{\star}_{H_2,(F/e)}$. We can therefore conclude that closed-loop optimal selection of actuators and sensors is a significantly more complicated problem that cannot be solved with Algorithm 3.1.

A greedy search algorithm such as Algorithm 3.2 can be applied in practice to find an upper bound for $\gamma^{\star}_{H_2,(F/e)}$ by appropriate selection of the actuators and sensors. Such an approach will, however, not provide any guarantees with regards to optimality of the obtained result,. This, because the considered closed-loop performance measures are, in general, not supermodular.

3.3 Sparsity Promoting Controller Design

3.3.1 Mathematical Background

In recent years, sparsity promoting controller design methods have been used as a solution to closed-loop actuator or sensor selection problems. In order to explain this approach, consider the system Σ (3.4) and the ARE-admissible sets that contain all allowed actuators and sensors $\mathbb{U}$ and $\mathbb{Y}$ as defined in (3.2) and (3.3), respectively.

Then, let *all allowed* control inputs and measured outputs be used to obtain the system $\Sigma(\mathbb{U},\mathbb{Y})$ (3.4). These control inputs and measured outputs are partitioned according to the elements of $\mathbb{U}$ and $\mathbb{Y}$; i.e. $u_i(t) \in \mathbb{R}^{n_{u_i}}$ and $y_i(t) \in \mathbb{R}^{n_{y_i}}$, where n_{u_i} and n_{y_i} are described by the i^{th} block elements in $\mathbb{U}$ and $\mathbb{Y}$, respectively.

By Lemma 2.18, we can for $\Sigma(\mathbb{U},\mathbb{Y})$ (3.4) consider the design of a strictly proper controller of the form

$$\Sigma_{c,n_c,sp,N} = \begin{cases} \dot{x}_c(t) = Jx_c(t) + \begin{pmatrix} K_1 \cdots K_{N_y} \end{pmatrix} \begin{pmatrix} y_1(t) \\ \vdots \\ y_{N_y}(t) \end{pmatrix} \\ \begin{pmatrix} u_1(t) \\ \vdots \\ u_{N_u}(t) \end{pmatrix} = \begin{pmatrix} M_1 \\ \vdots \\ M_{N_u} \end{pmatrix} x_c(t), \end{cases} \tag{3.29}$$

with the partitioning $K_i \in \mathbb{R}^{n_c \times n_{y_i}}$ and $M_i \in \mathbb{R}^{n_{u_i} \times n_c}$.

Since all allowed actuators and sensors are available to $\Sigma_{c,n_c,sp,N}$ (3.29), the selection problem is now equivalent to imposing block sparsity in the matrices K and M. I.e. the i^{th} actuator in $\mathbb{U}$ is not used by the controller if M_i is identically zero, while the i^{th} sensor in $\mathbb{Y}$ is not used by the controller if K_i is identically zero.

To formulate the closed-loop optimal selection of actuators and sensors as a sparse optimisation problem, let us consider the H_2 (squared) performance γ_{H_2} in (3.7). Then the optimisation problem in Problem 3.1 is equivalent to

$$\begin{aligned}\Sigma^\star_{c,n_c,sp,N} = \quad \arg \min_{n_c\in\mathbb{N},\Sigma_{c,n_c,sp,N}\ (3.29)} \quad & \gamma_{H_2}(\Sigma_{c,n_c,sp,N}\ (3.29),\mathbb{U},\mathbb{Y}) \\ \text{s.t.} \quad & \Sigma_{c,n_c,sp,N}\ (3.29) \text{ is } H_2\text{-admissible for} \\ & \Sigma(\mathbb{U},\mathbb{Y})\ (3.4). \\ & \sum_{i=1}^{N_u} \operatorname{card}(\|M_i\|) = n_u,\ \sum_{i=1}^{N_y} \operatorname{card}(\|K_i\|) = n_y,\end{aligned} \tag{3.30}$$

in the sense that $(B_{ui}, D_{u\tilde{z}i}, D_{uz_ui}) \in \mathbb{U}^\star_{n_u}$ if for $\Sigma^\star_{c,n_c,sp,N}$ we have that $M_i^\star \neq 0$, while $(C_{yi}, D_{\tilde{w}yi}, D_{w_yyi}) \in \mathbb{Y}^\star_{n_y}$ if $K_i^\star \neq 0$. Please note that the cardinality of a *matrix* describes the number of non-zero elements.

This is again a combinatorial optimisation problem that requires the evaluation of all possible subsets $\mathbb{U}_{n_u} \subseteq \mathbb{U}$, $\mathbb{Y}_{n_y} \subseteq \mathbb{Y}$ of the appropriate cardinality. Such an approach is, as explained before, computationally infeasible when a large sets of allowed actuators and sensors are provided. To overcome this problem, it is proposed by several authors—such as Dhingra et al. [2014] and Argha et al. [2016]—to include convex approximations of the cardinality constraints in the cost function of the optimisation problem.

In this way, a *sparsity promoting* controller design problem is formulated as

$$\begin{aligned}&\widetilde{\Sigma}^\star_{c,n_c,sp,N} = \\ &\arg \min_{n_c\in\mathbb{N},\Sigma_{c,n_c,sp,N}\ (3.29)} \gamma_{H_2}(\Sigma_{c,n_c,sp,N}\ (3.29),\mathbb{U},\mathbb{Y}) + \alpha_u \sum_{i=1}^{N_u} \|M_i\|_F + \alpha_y \sum_{i=1}^{N_y} \|K_i\|_F \\ &\qquad \text{s.t.} \qquad \Sigma_{c,n_c,sp,N}\ (3.29) \text{ is } H_2\text{-admissible for } \Sigma(\mathbb{U},\mathbb{Y})\ (3.4),\end{aligned}$$

with the design parameters $\alpha_u, \alpha_y \in \mathbb{R}$ that satisfy $\alpha_u \geq 0$ and $\alpha_y \geq 0$.

In this sparsity promoting problem, the non-convex constraints

$$\sum_{i=1}^{N_u} \operatorname{card}(\|M_i\|) = n_u,\ \sum_{i=1}^{N_y} \operatorname{card}(\|K_i\|) = n_y$$

are approximated by a convex function of the form

$$\alpha_u \sum_{i=1}^{N_u} \|M_i\|_F + \alpha_y \sum_{i=1}^{N_y} \|K_i\|_F .$$

With such an approach, these cardinality constraints are essentially approximated by including two L_1-norm regularisation terms in the cost function. Furthermore, α_u and α_y can be viewed as sparsity promoting parameters that allow a trade-off between the best achievable closed-loop H_2 performance and the number of actuators or sensors, respectively. This is discussed in more detail by Lin et al. [2012] and by Jovanović and Dhingra [2016].

For example, the optimal control problem without sparsity promotion is solved if $\alpha_u = \alpha_y = 0$ are considered. An increase in the value of these parameters will reduce the number of actuators and sensors, at the cost of an increase in $\gamma^\star_{H_2}$—which corresponds to a reduction in performance.

Finally, this sparsity promoting controller design problem is formulated as an LMI by Argha et al. [2016] and by Singh et al. [2018]. The LMI can numerically be solved by well-known numerical optimisation tools such as Yalmip and CVX—as developed by Löfberg [2004] and by Grant and Boyd [2014, 2008], respectively. This type of solution that directly aims to solve Problem 3.1 does, however, not scale well with the cardinality of $\mathbb{U}$ or $\mathbb{Y}$ and can only be considered for problems with $N_u \leq 10$ and $N_y \leq 10$.

To solve this problem for larger sets, it is proposed by Dhingra et al. [2014] to utilise the alternating direction method of multipliers (ADMM)—as introduced by Boyd [2010]. With this type of solution, it is required to separately solve the actuator selection problem for state feedback design in Problem 3.2 and the sensor selection problem for estimator design in Problem 3.3; instead of the combined actuator and sensor selection problem in Problem 3.1.

We have seen in section 3.2.2 the selection of actuators and the selection of sensors is, indeed, independent when state feedback design and estimator design are considered. However, it will now be shown that the selection of sensors does rely on the allowed actuators and vice versa in Problem 3.1; i.e. for a situation where we consider measurement feedback controller design.

For this purpose, let us consider the system $\Sigma_{ce,3}(\mathbb{U}_{n_u}, \mathbb{Y}_{n_y}) =$

$$\begin{cases} \begin{pmatrix} \dot{x}_1(t) \\ \dot{x}_2(t) \end{pmatrix} = \begin{pmatrix} -1 & 0 \\ 0 & -0.1 \end{pmatrix} \begin{pmatrix} x_1(t) \\ x_2(t) \end{pmatrix} + \operatorname{row}(\mathbb{U}_{B,n_u}) u(t) + \begin{pmatrix} 1 & 0 & 0 \\ 0 & 1 & 0 \end{pmatrix} \begin{pmatrix} \widetilde{w}_1(t) \\ \widetilde{w}_2(t) \\ w_y(t) \end{pmatrix} \\ y(t) = \operatorname{col}(\mathbb{Y}_{C,n_y}) \begin{pmatrix} x_1(t) \\ x_2(t) \end{pmatrix} + \left(\operatorname{col}(\mathbb{Y}_{\widetilde{D},n_y}) \operatorname{diag}(\mathbb{Y}_{D_y,n_y}) \right) \begin{pmatrix} \widetilde{w}_1(t) \\ \widetilde{w}_2(t) \\ w_y(t) \end{pmatrix} \\ \begin{pmatrix} \tilde{z}_1(t) \\ \tilde{z}_2(t) \end{pmatrix} = \begin{pmatrix} 1 & 0 \\ 0 & 1 \end{pmatrix} \begin{pmatrix} x_1(t) \\ x_2(t) \end{pmatrix} + \begin{pmatrix} \operatorname{row}(\mathbb{U}_{\widetilde{D},n_u}) \\ \operatorname{diag}(\mathbb{U}_{D_u,n_u}) \end{pmatrix} u(t), \end{cases} \tag{3.31}$$

with two allowed actuators that are described by the set

$$\mathbb{U} = \{u_1, u_2\} = \left\{ \left(\begin{pmatrix} 1 \\ 0 \end{pmatrix}, \begin{pmatrix} 0 \\ 0 \end{pmatrix}, 1 \right) \ , \ \left(\begin{pmatrix} 0 \\ 1 \end{pmatrix}, \begin{pmatrix} 0 \\ 0 \end{pmatrix}, 1 \right) \right\}.$$

First, let us consider the selection of one actuator from the set $\mathbb{U}$ for a fixed sensor configuration that is described by $\mathbb{Y} = \mathbb{Y}_{full} = \{(I_2, 0, 0)\}$; i.e. the combined selection problem for controller design in Problem 3.1 is replaced by the actuator selection problem for state feedback design in Problem 3.2.

For the system without control, the values in the A matrix indicate that the state $x_2(t)$ has the largest contribution towards the H_2 norm. For state feedback design

it is therefore easy to show that $\gamma^\star_{H_2,F}(\{u_2\}) < \gamma^\star_{H_2,F}(\{u_1\})$, which implies that the actuator u_2 should be selected when $\mathbb{Y}_{full}$ is considered.

Then, let us consider the same actuator selection problem for a different sensor configuration that is described by $\mathbb{Y} = \mathbb{Y}_2 = \left\{\begin{pmatrix}1 & 0\end{pmatrix}, \begin{pmatrix}0 & 0\end{pmatrix}, 1\right\}$. For the design of a controller of the form Σ_{c,n_c} (3.5) we now obtain $\gamma^\star_{H_2}(\{u_1\}, \mathbb{Y}_2) < \gamma^\star_{H_2}(\{u_2\}, \mathbb{Y}_2) = \gamma^\star_{H_2}(\emptyset, \mathbb{Y}_2)$—i.e. the selection of actuator u_2 does not improve performance at all—since only the state $x_1(t)$ is available through the measured output $y(t)$. The (other) actuator u_1 should therefore be selected when the sensor configuration is described by $\mathbb{Y}_2$.

We have now seen that the selection of actuators does depend on the available sensors, if controller design is considered instead of state feedback design. In addition, an actuator configuration that is obtained for the latter problem might even contain actuators that do not improve closed-loop performance when we synthesise a controller. Finally, it is important to note that these conclusions will also hold for the selection of sensors, since both selection problems are dual.

We can therefore not regard the selection of actuators and sensors as two independent problems in Problem 3.1. As a first step towards solving this combined selection problem, it will now be shown how the solution to Problem 3.2 can be used to design an optimal actuator configuration in Problem 3.1 for a fixed sensor configuration. The dual problem of designing an optimal sensor configuration for a fixed actuator configuration is discussed thereafter.

3.3.2 Optimal Actuator Selection for a Fixed Sensor Configuration

Actuator Selection for H_2 Optimal State Feedback Design

Let us first formulate Problem 3.2 as a sparsity promoting state feedback design problem. Please note that a solution to this problem has been developed by Dhingra et al. [2014], which has been implemented in a toolbox by Lin et al. [2014].

For this purpose, let all allowed actuators $\mathbb{U}$ and $\mathbb{Y}_{full} = \{(I_{n_x}, 0, 0)\}$ be used to obtain the system $\Sigma(\mathbb{U}, \mathbb{Y}_{full})$ (3.4), with the control inputs partitioned according to the elements of $\mathbb{U}$; i.e. $u_i(t) \in \mathbb{R}^{n_{u_i}}$ where n_{u_i} are described by the i^{th} block elements in $\mathbb{U}$. For $\Sigma(\mathbb{U}, \mathbb{Y}_{full})$ (3.4) we consider the design of a state feedback that is partitioned as

$$u(t) = F_N x(t) = \begin{pmatrix} F_1 \\ \vdots \\ F_{N_u} \end{pmatrix} x(t), \tag{3.32}$$

with $F_i \in \mathbb{R}^{n_{u_i} \times n_x}$.

As before, the selection of actuators is equivalent to the introduction of block sparsity in F_N (3.32). Therefore, let us consider the H_2 squared performance of a state feedback $\gamma_{H_2,F}$ in (3.14) to equivalently formulate Problem 3.2 as the

following sparse state feedback design problem:

$$F^\star_{N,F} = \arg \min_{F_N} \gamma_{H_2,F}(F_N, \mathbb{U}) \quad \text{s.t. } u(t) = F_N x(t) \text{ (3.32) is } H_2\text{-admissible for } \Sigma(\mathbb{U}, \mathbb{Y}_{full}) \text{ (3.4)}, \ \sum_{i=1}^{N_u} \operatorname{card}(\|F_i\|) = n_u. \tag{3.33}$$

These problems are equivalent in the sense that $(B_{ui}, D_{u\tilde{z}i}, D_{uz_ui}) \in \mathbb{U}^\star_{n_u}$ if for $F^\star_{N,F}$ we have that $F^\star_i \neq 0$.

In a similar fashion to (3.30), let us include convex approximations of the cardinality constraint in the cost function to formulate a *sparsity promoting* state feedback design problem as

$$\widetilde{F}^\star_{N,F} = \arg \min_{F_N} \gamma_{H_2,F}(F_N, \mathbb{U}) + \alpha_u \sum_{i=1}^{N_u} \|F_i\|_F \quad \text{s.t. } u(t) = F_N x(t) \text{ (3.32) is } H_2\text{-admissible for } \Sigma(\mathbb{U}, \mathbb{Y}_{full}) \text{ (3.4)}, \tag{3.34}$$

with the design parameter $\alpha_u \in \mathbb{R}$ that satisfies $\alpha_u \geq 0$.

Control Relevant Actuator Selection

Now we will address the following problem of designing an optimal actuator configuration in Problem 3.1 for a fixed sensor configuration.

Problem 3.4 *For* Σ (3.4)*, let* $\mathbb{U}$ *be a set that contains all allowed actuators as defined in* (3.2)*. Furthermore, consider a fixed sensor configuration that is described by* $\mathbb{Y}_f = \{(C_{yf}, D_{\tilde{w}yf}, D_{w_yyf})\}$ *and a number* $n_u \in \mathbb{N}$ *with* $n_u \leq N_u$*.*

Then, construct an optimal subset $\mathbb{U}^\star_{n_u} \subseteq \mathbb{U}$ *of cardinality* n_u*, which is a solution to*

$$\mathbb{U}^\star_{n_u} = \arg \min_{\mathbb{U}_{n_u} \subseteq \mathbb{U}} \min_{n_c \in \mathbb{N}, \Sigma_{c,n_c} \text{ (3.5)}} \gamma_{H_2}(\Sigma_{c,n_c} \text{ (3.5)}, \mathbb{U}_{n_u}, \mathbb{Y}_f) \quad \text{s.t. } \Sigma_{c,n_c} \text{ (3.5) is } H_2\text{-admissible for } \Sigma(\mathbb{U}_{n_u}, \mathbb{Y}_f) \text{ (3.4)}.$$

In order to numerically solve this problem with the toolbox by Lin et al. [2014], we will now show that Problem 3.4 can be transformed into Problem 3.2.

Theorem 3.9 *For* Σ (3.4)*, let* $\mathbb{U}$ *be a set that contains all allowed actuators as defined in* (3.2)*, consider a fixed ARE-admissible sensor configuration* $\mathbb{Y}_f = \{(C_{yf}, D_{\tilde{w}yf}, D_{w_yyf})\}$ *and a number* $n_u \leq N_u$*. Furthermore, let the unique stabilising solution* $Q^+(\Sigma \text{ (3.4)}, \mathbb{Y}_f) \succeq 0$ *to the ARE in* (3.26) *be used to construct—for any sensor configuration that is described by the set* $\mathbb{Y}_{n_y}$*—the transformed system*

$\Sigma_Q(\mathbb{U}_{n_u}, \mathbb{Y}_{n_y}) =$

$$\begin{cases} \dot{x}(t) = & Ax(t) + \operatorname{row}(\mathbb{U}_{B,n_u})u(t) \\ & \quad + \begin{pmatrix} (Q^+ C_{yf}^\top + B_w D_{wyf}^\top)(D_{wyf} D_{wyf}^\top)^{-\frac{1}{2}} & 0 \end{pmatrix} \begin{pmatrix} \widetilde{w}(t) \\ w_y(t) \end{pmatrix} \\ y(t) = \operatorname{col}(\mathbb{Y}_{C,n_y})x(t) & \quad + \begin{pmatrix} \operatorname{col}(\mathbb{Y}_{\widetilde{D},n_y}) & \operatorname{diag}(\mathbb{Y}_{D_y,n_y}) \end{pmatrix} \begin{pmatrix} \widetilde{w}(t) \\ w_y(t) \end{pmatrix} \\ \begin{pmatrix} \tilde{z}(t) \\ z_u(t) \end{pmatrix} = & \begin{pmatrix} \tilde{C}_z \\ 0 \end{pmatrix} x(t) + \begin{pmatrix} \operatorname{row}(\mathbb{U}_{\widetilde{D},n_u}) \\ \operatorname{diag}(\mathbb{U}_{D_u,n_u}) \end{pmatrix} u(t), \end{cases} \tag{3.35}$$

with $B_w = \begin{pmatrix} \widetilde{B}_w & 0 \end{pmatrix}$ *and* $D_{wyf} = \begin{pmatrix} D_{\widetilde{w}yf} & D_{w_yf} \end{pmatrix}$.

Finally, for Σ (3.4) *let* $\mathbb{U}_{n_u}^\star$ *be a solution to Problem 3.4 and for* Σ_Q (3.35) *let* $\mathbb{U}_{n_u,F}^\star$ *be a solution to Problem 3.2. Then* $\mathbb{U}_{n_u}^\star = \mathbb{U}_{n_u,F}^\star$.

Proof: The proof can be found in appendix A.2. □

It is therefore shown that solving Problem 3.4 for Σ (3.4) is equivalent to solving Problem 3.2 for Σ_Q (3.35). The solution to Problem 3.2—as developed by Dhingra et al. [2014]—can therefore be used to solve Problem 3.4 by considering the transformed system Σ_Q (3.35).

3.3.3 Optimal Sensor Selection for a Fixed Actuator Configuration

Sensor Selection for H_2 Optimal Observer Design

Sensor selection for observer design is dual to actuator selection for state feedback design. Let us therefore first formulate Problem 3.3 as a sparsity promoting observer gain design problem. Again, a solution this sparsity promoting problem has been developed by Dhingra et al. [2014] and is implemented in a toolbox by Lin et al. [2014].

For this purpose, let a given actuator configuration $\mathbb{U}_f = \{(B_{uf}, D_{u\tilde{z}f}, D_{uz_uf})\}$ and all allowed sensors $\mathbb{Y}$ be used to obtain the system $\Sigma(\mathbb{U}_f, \mathbb{Y})$ (3.4), with the measured outputs partitioned according to the elements of $\mathbb{Y}$; i.e. $y_i(t) \in \mathbb{R}^{n_{y_i}}$ where n_{y_i} are described by the i^{th} block elements in $\mathbb{Y}$.

For $\Sigma(\mathbb{U}_f, \mathbb{Y})$ (3.4)—and the corresponding observer Σ_o (3.19)—we consider the design of an observer gain that is partitioned as

$$L_N = \begin{pmatrix} L_1 & \cdots & L_{N_y} \end{pmatrix}, \tag{3.36}$$

with $L_i \in \mathbb{R}^{n_x \times n_{y_i}}$.

As before, the selection of sensors is equivalent to the introduction of block sparsity in L_N (3.32). Therefore, let us consider the H_2 squared performance for an observer $\gamma_{H_2,e}$ in (3.21) to equivalently formulate Problem 3.3 as the following sparse

observer gain design problem:

$$\begin{aligned} L^\star_{N,e} = \quad \arg \quad & \min_{L_N} \quad \gamma_{H_2,e}(\Sigma_o\ (3.19), \mathbb{Y}) \\ & \text{s.t.} \quad \Sigma_o\ (3.19) \text{ is } H_2\text{-admissible for } \Sigma(\mathbb{U}_f, \mathbb{Y})\ (3.4), \\ & \quad \sum_{i=1}^{N_y} \operatorname{card}(\|L_i\|) = n_y. \end{aligned} \tag{3.37}$$

These problems are equivalent in the sense that $(C_{yi}, D_{\widetilde{w}yi}, D_{w_y yi}) \in \mathbb{Y}^\star_{n_y}$ if for $L^\star_{N,e}$ we have that $L^\star_i \neq 0$.

In a similar fashion to (3.30), let us also include convex approximations of the cardinality constraint in the cost function to formulate a *sparsity promoting* observer gain design problem as

$$\begin{aligned} \widetilde{L}^\star_{N,e} = \quad \arg \min_{L_N} \ & \gamma_{H_2,e}(\Sigma_o\ (3.19), \mathbb{Y}) + \alpha_y \sum_{i=1}^{N_y} \|L_i\|_F \\ & \text{s.t. } \Sigma_o\ (3.19) \text{ is } H_2\text{-admissible for } \Sigma(\mathbb{U}_f, \mathbb{Y})\ (3.4), \end{aligned} \tag{3.38}$$

with the design parameter $\alpha_y \in \mathbb{R}$ that satisfies $\alpha_y \geq 0$.

Control Relevant Sensor Selection

Finally, we will address the following problem of designing an optimal sensor configuration in Problem 3.1 for a fixed actuator configuration.

Problem 3.5 *For Σ (3.4), let $\mathbb{Y}$ be a set that contains all allowed sensors as defined in (3.3). Furthermore, consider a fixed actuator configuration that is described by $\mathbb{U}_f = \{(B_{uf}, D_{u\tilde{z}f}, D_{uz_uf})\}$ and a number $n_y \in \mathbb{N}$ with $n_y \leq N_y$.*

Then, construct an optimal subset $\mathbb{Y}^\star_{n_y} \subseteq \mathbb{Y}$ of cardinality n_y, which is a solution to

$$\begin{aligned} \mathbb{Y}^\star_{n_y} = \arg \min_{\mathbb{Y}_{n_y} \subseteq \mathbb{Y}} \ \min_{n_c \in \mathbb{N}, \Sigma_{c,n_c}\ (3.5)} \ & \gamma_{H_2}(\Sigma_{c,n_c}\ (3.5), \mathbb{U}_f, \mathbb{Y}_{n_y}) \\ & \text{s.t.} \quad \Sigma_{c,n_c}\ (3.5) \text{ is } H_2\text{-admissible for } \Sigma(\mathbb{U}_f, \mathbb{Y}_{n_y})\ (3.4). \end{aligned}$$

In order to numerically solve this problem with the toolbox by Lin et al. [2014], we will now show that Problem 3.5 can also be transformed into Problem 3.3.

Theorem 3.10 *For Σ (3.4), let $\mathbb{Y}$ be a set that contains all allowed sensors as defined in (3.3), consider a fixed ARE-admissible actuator configuration $\mathbb{U}_f = \{(B_{uf}, D_{u\tilde{z}f}, D_{uz_uf})\}$ and a number $n_y \in \mathbb{N}$ with $n_y \leq N_y$. Furthermore, let the unique stabilising solution $P^+(\Sigma\ (3.4), \mathbb{U}_f) \succeq 0$ to the ARE in (3.25) be used to construct—for any actuator configuration that is described by the set $\mathbb{U}_{n_u}$—the transformed system*

$$\Sigma_P(\mathbb{U}_{n_u}, \mathbb{Y}_{n_y}) =$$

$$\begin{cases} \dot{x}(t) = Ax(t) + \mathrm{row}(\mathbb{U}_{B,n_u})u(t) + \begin{pmatrix} \tilde{B}_w & 0 \end{pmatrix} \begin{pmatrix} \tilde{w}(t) \\ w_y(t) \end{pmatrix} \\ y(t) = \mathrm{col}(\mathbb{Y}_{C,n_y})x(t) + \begin{pmatrix} \mathrm{col}(\mathbb{Y}_{\widetilde{D},n_y}) & \mathrm{diag}(\mathbb{Y}_{D_y,n_y}) \end{pmatrix} \begin{pmatrix} \tilde{w}(t) \\ w_y(t) \end{pmatrix} \\ \begin{pmatrix} \tilde{z}(t) \\ z_u(t) \end{pmatrix} = \begin{pmatrix} (D_{uzf}^\top D_{uzf})^{-\frac{1}{2}}(B_{uf}^\top P^+ + D_{uzf}^\top C_z) \\ 0 \end{pmatrix} x(t) + \begin{pmatrix} \mathrm{row}(\mathbb{U}_{\widetilde{D},n_u}) \\ \mathrm{diag}(\mathbb{U}_{D_u,n_u}) \end{pmatrix} u(t), \end{cases} \tag{3.39}$$

with $C_z = \begin{pmatrix} \widetilde{C}_z \\ 0 \end{pmatrix}$ *and* $D_{uzf} = \begin{pmatrix} D_{u\tilde{z}f} \\ D_{uz_uf} \end{pmatrix}$.

Finally, for Σ (3.4) *let* $\mathbb{Y}^\star_{n_y}$ *be a solution to Problem 3.5 and for* Σ_P (3.39) *let* $\mathbb{Y}^\star_{n_y,e}$ *be a solution to Problem 3.3. Then* $\mathbb{Y}^\star_{n_y} = \mathbb{Y}^\star_{n_y,e}$.

Proof: This theorem is completely dual to Theorem 3.9. □

3.4 Performance Analysis on a Practical Example

3.4.1 Case Study

A Model for Thermal Deformation

As an example, we will aim to solve the control relevant sensor selection problem in Problem 3.5—i.e. with a fixed actuator configuration $\mathbb{U}_f$—for a model that describes the thermally induced deformations of 5 spatially discretised domains. These domains are isolated and attached to an infinitely stiff heat-sink of constant temperature, as shown in figure 3.1.

The first domain—which is depicted in more detail in figure 3.2—is affected by the thermal disturbance $\widetilde{w}_1(t)$, which leads to deformations of the top surface that are described by the control output $\tilde{z}_1(t)$. In order to minimise these deformations, temperature in the domain can be controlled through the control input $u_1(t)$, while there are 64 potential temperature sensor locations within the domain.

Domains 2–5 are directly based in this first domain, in the sense that:

- domain 2 is affected by the thermal disturbance $\widetilde{w}_2(t)$, which leads to the deformations in $\tilde{z}_2(t)$. However, the domain cannot be controlled; i.e. its state is unreachable through $u(t)$.
- domain 3 is affected by the thermal disturbance $\widetilde{w}_3(t)$ and can be controlled through $u_3(t)$. However, the domain does not deform; i.e. its state is unobservable in $\tilde{z}(t)$.
- domain 4 is affected by the thermal disturbance $\widetilde{w}_4(t)$. However, the domain does not deform and cannot be controlled; i.e. its state is unreachable through $u(t)$ and unobservable in $\tilde{z}(t)$.
- domain 5 can be controlled through $u_5(t)$, which leads to the deformations in $\tilde{z}_5(t)$. However, the domain is not affected by the disturbance; i.e. its state is unreachable through $\widetilde{w}(t)$.

The combined model for these 5 domains with the fixed actuator configuration $\mathbb{U}_f$ and any sensor configuration $\mathbb{Y}_{n_y}$ is therefore of the form

$\Sigma_b(\mathbb{U}_f, \mathbb{Y}_{n_y}) =$

$$
\left\{
\begin{aligned}
\begin{pmatrix} \dot{x}_1(t) \\ \dot{x}_2(t) \\ \dot{x}_3(t) \\ \dot{x}_4(t) \\ \dot{x}_5(t) \end{pmatrix} &= \begin{pmatrix} A & 0 & 0 & 0 & 0 \\ 0 & A & 0 & 0 & 0 \\ 0 & 0 & A & 0 & 0 \\ 0 & 0 & 0 & A & 0 \\ 0 & 0 & 0 & 0 & A \end{pmatrix} \begin{pmatrix} x_1(t) \\ x_2(t) \\ x_3(t) \\ x_4(t) \\ x_5(t) \end{pmatrix} + \begin{pmatrix} B_u & 0 & 0 \\ 0 & 0 & 0 \\ 0 & B_u & 0 \\ 0 & 0 & 0 \\ 0 & 0 & B_u \end{pmatrix} \begin{pmatrix} u_1(t) \\ u_3(t) \\ u_5(t) \end{pmatrix} \\
&\quad + \begin{pmatrix} \widetilde{B}_w & 0 & 0 & 0 & 0 \\ 0 & \widetilde{B}_w & 0 & 0 & 0 \\ 0 & 0 & \widetilde{B}_w & 0 & 0 \\ 0 & 0 & 0 & \widetilde{B}_w & 0 \\ 0 & 0 & 0 & 0 & 0 \end{pmatrix} \begin{pmatrix} \widetilde{w}_1(t) \\ \widetilde{w}_2(t) \\ \widetilde{w}_3(t) \\ \widetilde{w}_4(t) \\ w_y(t) \end{pmatrix} \widetilde{w}(t) \\
y(t) &= \operatorname{col}(\mathbb{Y}_{C,n_y}) x(t) + \left(\operatorname{col}(\mathbb{Y}_{\widetilde{D},n_y}) \ \operatorname{diag}(\mathbb{Y}_{D_y,n_y}) \right) \begin{pmatrix} \tilde{w}(t) \\ w_y(t) \end{pmatrix} \\
\begin{pmatrix} \tilde{z}_1(t) \\ \tilde{z}_2(t) \\ \tilde{z}_5(t) \\ z_u(t) \end{pmatrix} &= \begin{pmatrix} \widetilde{C}_z & 0 & 0 & 0 & 0 \\ 0 & \widetilde{C}_z & 0 & 0 & 0 \\ 0 & 0 & 0 & 0 & \widetilde{C}_z \\ 0 & 0 & 0 & 0 & 0 \end{pmatrix} x(t) + \begin{pmatrix} 0 \\ 0 \\ 0 \\ D_{uz_u} \end{pmatrix} u(t),
\end{aligned}
\right. \tag{3.40}
$$

where

$$
\begin{aligned}
x(t) &= \operatorname{col}(\{x_1(t), x_2(t), x_3(t), x_4(t), x_5(t)\}) & u(t) &= \operatorname{col}(\{u_1(t), u_3(t), u_5(t)\}) \\
\widetilde{w}(t) &= \operatorname{col}(\{\widetilde{w}_1(t), \widetilde{w}_2(t), \widetilde{w}_3(t), \widetilde{w}_4(t)\}) & \tilde{z}(t) &= \operatorname{col}(\{\tilde{z}_1(t), \tilde{z}_2(t), \tilde{z}_5(t)\}).
\end{aligned}
$$

For this model,

- the state $x_i(t) \in \mathbb{R}^{100}$ describes the temperature at time t for 100 locations (in a Cartesian grid) in domain i—for $i = 1, \cdots, 5$.
- $A \in \mathbb{R}^{100\times 100}$ describes thermal conduction in each domain.
- $\tilde{B}_w \in \mathbb{R}^{100\times 6}$ describes how 6 independent thermal disturbances in $\widetilde{w}_i(t)$ affect the evolution of domain i through its boundaries—for $i = 1, 2, 3, 4$.
- $\widetilde{C}_z \in \mathbb{R}^{16\times 100}$ describes how temperature variations in domain i lead to deformations (in the x, y-directions) at 8 locations on the top boundary of the domain, which are described by $\tilde{z}_i(t)$—for $i = 1, 2, 5$.
- $B_u \in \mathbb{R}^{100\times 5}$ describes how 5 thermal actuators in $u_i(t)$ can affect the evolution of domain i through its boundaries—for $i = 1, 3, 5$.
- $D_{uz_u} = 0.01 I_{15}$ is used to limit the signal $u(t)$ in magnitude, when an H_2 optimal controller is designed.

Remark 3.5 *In order to avoid any issues with numerical conditioning, the model is created such that input signals $\widetilde{w}(t)$ and $u(t)$ of a given magnitude will lead to trajectories $x(t)$, $y(t)$ and $\tilde{z}(t)$ that are similar in magnitude. In addition, the matrices B_u, $\widetilde{B}_w$, C_{yij} and $\widetilde{C}_z$ are similar in norm.*

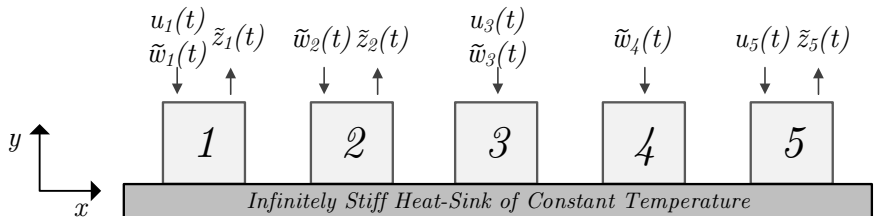

Figure 3.1: A visualisation of Σ_b (3.40).

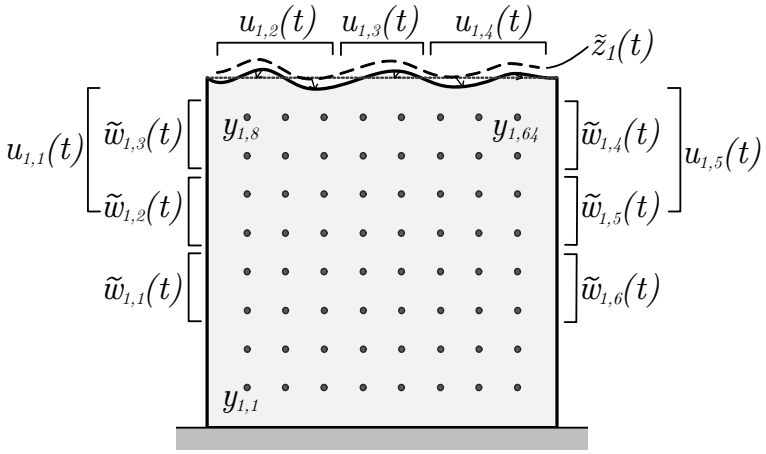

Figure 3.2: A more detailed depiction of domain 1.

Sensor Selection

For Σ_b (3.40), the set of all allowed sensors—as defined in (3.3)—is first decomposed in terms of the individual domains such that

$$\mathbb{Y} = \bigcup_{i=1}^{5} \mathbb{Y}_i = \bigcup_{i=1}^{5} \{y_{i,1}, \cdots, y_{i,64}\},$$

where $\mathbb{Y}_i$ is a set of cardinality 64 that contains all allowed sensors in domain i. Each potential sensor in $\mathbb{Y}_i$ is described by the triple $y_{i,j} = \{(C_{yij},\ 0,\ 0.01)\}$—for $i = 1, \cdots, 5$ and $j = 1, \cdots, 64$—that corresponds to a temperature measurement at a specific location in the domain. The 64 allowed sensors locations in domain 1 are depicted in figure 3.2, while 64 "equivalent" locations are considered within domains 2–5; e.g. the sensors $y_{1,5}$ and $y_{3,5}$ are placed at the same location within the corresponding domain.

Finally, configurations with a varying number of sensors n_y will be created for Σ_b (3.40). These configurations are created by

- solving the modular Gramian optimisation in (3.24) with Algorithm 3.1 for $\alpha_y = \frac{1}{2}$.

- considering the greedy algorithm in Algorithm 3.2, which directly aims to find the subset $\mathbb{Y}_{n_y}$ that minimises $\gamma^\star_{H_2}(\mathbb{U}_f, \mathbb{Y}_{n_y})$ in (3.8).
- the original sparsity promoting method in (3.38)—as implemented by Lin et al. [2014]—that aims to solve the sensor selection problem for estimator design in Problem 3.3.
- the control relevant sparsity promoting method that aims to solve the sensor selection problem for a fixed actuator configuration in Problem 3.5, by utilising the transformed system Σ_P (3.39) for Σ_b (3.40).

An H_2 optimal controller of the form Σ_{c,n_c} (3.5) is then designed for each sensor configuration in order to determine the best achievable closed-loop H_2 performance $\gamma^\star_{H_2}$. This performance measure as a function of the number of sensors n_y is shown in figure 3.3. Furthermore, the selected sensors in domain 1 are depicted in figure 3.4.

3.4.2 Desired Behaviour

Before commenting on the results for this example, let us first establish what should ideally be achieved from the perspective of closed-loop optimal sensor selection with a fixed actuator configuration. I.e. we will first establish what properties are expected for a solution to Problem 3.5.

Firstly, it should *only* be considered to add sensors in domain 1. Namely, domains 2 and 4 are not reachable through $u(t)$, domain 3 is not observable in $\tilde{z}(t)$ and domain 5 is not reachable through $\widetilde{w}(t)$. The placement of sensors in domains 2–5 will therefore not lead to an improvement of the best achievable closed-loop H_2 performance measure $\gamma^\star_{H_2}$.

Secondly, a symmetric sensor configuration is expected in every domain, because the configuration in terms of the external quantities $\widetilde{w}(t)$, $u(t)$ and $\tilde{z}(t)$ is symmetric as well; this can be observed from figure 3.2.

3.4.3 Actual Performance

Modular Gramian Optimisation

The objective function $f_{y,g}$ in (3.23) for the modular Gramian optimisation problem in (3.24) does capture the symmetry in the problem. Therefore a symmetric solution is obtained for an even number of sensors n_y, which can be observed from figure 3.4.

The objective function does, however, allow the placement of sensors in all domains, which is undesired. In order to explain this, let us decompose any sensor configuration with n_y sensors as $\mathbb{Y}_{n_y} = \bigcup_{i=1}^{5} \mathbb{Y}_{i,n_y}$, where $\mathbb{Y}_{i,n_y}$ is a subset that contains all sensors in $\mathbb{Y}_{n_y}$ that correspond to domain i.

Because the domains are isolated, we can also decompose the objective function in (3.24) as $f_{y,g}(\mathbb{Y}_{n_y}, \alpha_y) = \sum_{i=1}^{5} f_i(\mathbb{Y}_{i,n_y}, \alpha_y)$, with

$f_i(\mathbb{Y}_{i,n_y}, \alpha_y) =$

$$\begin{cases} \alpha_y \mathrm{tr}(\widetilde{C}_z \mathcal{Q}(\mathbb{Y}_{i,n_y}, A)\widetilde{C}_z^\top) + (1-\alpha_y)\mathrm{tr}(\widetilde{B}_w^\top \mathcal{Q}(\mathbb{Y}_{i,n_y}, A)\widetilde{B}_w) & \text{for } i = 1,2 \\ (1-\alpha_y)\mathrm{tr}(\widetilde{B}_w^\top \mathcal{Q}(\mathbb{Y}_{i,n_y}, A)\widetilde{B}_w) & \text{for } i = 3,4 \\ \alpha_y \mathrm{tr}(\widetilde{C}_z \mathcal{Q}(\mathbb{Y}_{i,n_y}, A)\widetilde{C}_z^\top) & \text{for } i = 5, \end{cases}$$

where $\mathcal{Q}$ is the observability Gramian as defined in (3.12).

From this decomposition it can be observed that a sensor at location j in domains 1 and 2 is favoured over the "equivalent" sensors at location j in domains 3—5; i.e. $f_i(\{y_{i,k}\}, \alpha_y) \geq f_j(\{y_{j,k}\}, \alpha_y)$ for $j = 1,2$, $j = 3,4,5$ and any k. This does, however, not imply that sensors are never placed in domains 3–5, because $f_1(\{y_{1,j}\}, \alpha_y) \geq f_i(\{y_{i,k}\}, \alpha_y)$, with $i = 3,4,5$, does not necessarily hold for all j, k.

Domain 2, one the other hand, is equivalent to domain 1 in terms of the objective function. Namely, $f_1(\{y_{1,j}\}, \alpha_y) = f_2(\{y_{2,j}\}, \alpha_y)$ for any j, which implies that the placement of a sensor in domain 1 is always accompanied by the placement of a sensor in domain 2. In this example, at least half of the sensors is therefore "wasted" by placement in the domains 2—5. Finally, from figure 3.3 it can be observed that this method performs worst out of all the considered methods.

Closed-Loop Greedy Optimisation

The greedy algorithm places one sensor at a time. After each sensor is placed, however, the improvement in closed-loop performance changes for the remaining sensors and a symmetric sensor configuration is therefore generally speaking not obtained. For this reason, the greedy algorithm might result in an "disorganised" sensor configuration, as is shown in figure 3.4.

Because the closed-loop performance measure is directly taken into consideration, the method recognises that the placement of sensors in domains 2—5 will not improve $\gamma^\star_{H_2}(\mathbb{U}_f, \mathbb{Y}_{n_y})$. This algorithm will, as a direct consequence, only place sensors in domain 1, which is as desired. In terms of closed-loop performance it can be observed that the method performs well in comparison with the modular Gramian optimisation technique.

Furthermore, from this example we can observe the importance of directly considering the closed-loop objective during system design. Namely, the greedy optimisation technique that directly considers the actual objective performs better than modular Gramian optimisation, which considers a different objective in order to provide guarantees on the obtained result. This, again, emphasises the importance of the main research question in section 1.4.

Sparsity Promotion

Finally, the sparsity promoting methods combine the closed-loop performance measure $\gamma^\star_{H_2}$ with a sparsity promoting term. The number of sensors can, however,

not be chosen with these methods; instead, this number must be affected indirectly by changing the parameter α_y—in (3.38)—in magnitude. For this example, the methods create symmetric configurations with an even amount of sensors. Configurations with a small number of sensors can, however, not be obtained—as shown in figure 3.3.

The original sparsity promoting method regards domains 1 and 2 as equivalent, because the control input $u(t)$ is not taken into account. This method therefore "wastes" half of the selected sensors. On the other hand, the control relevant sparsity promoting method will only place sensors in domain 1 and therefore requires half the number of sensors in order to obtain the same performance. Furthermore, the derived configuration with 4 sensors is able to achieve near-optimal performance; that is, the performance when all sensors are selected.

For control relevant sensor selection we can therefore conclude that it is, indeed, important to take the available actuators into account. This, however, also indicates that a substantial improvement could still be obtained by directly considering the combined selection problem in Problem 3.1, when the actuators have to be selected as well.

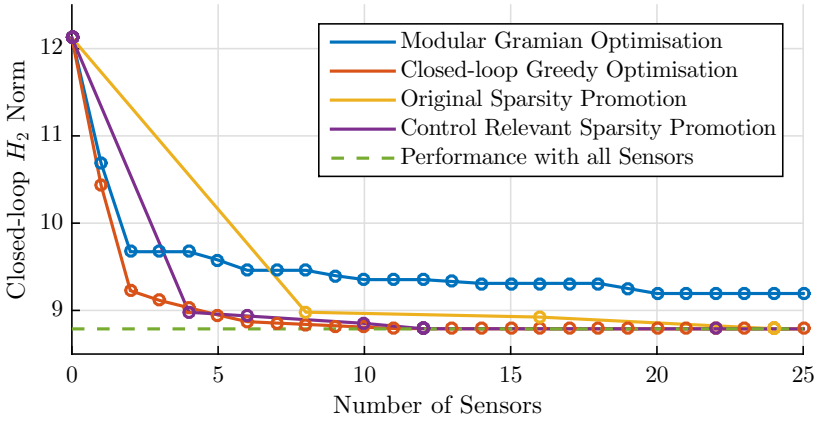

Figure 3.3: The best achievable closed-loop H_2 performance, as a function of the number of sensors, for the sensor configurations that are generated by each algorithm.

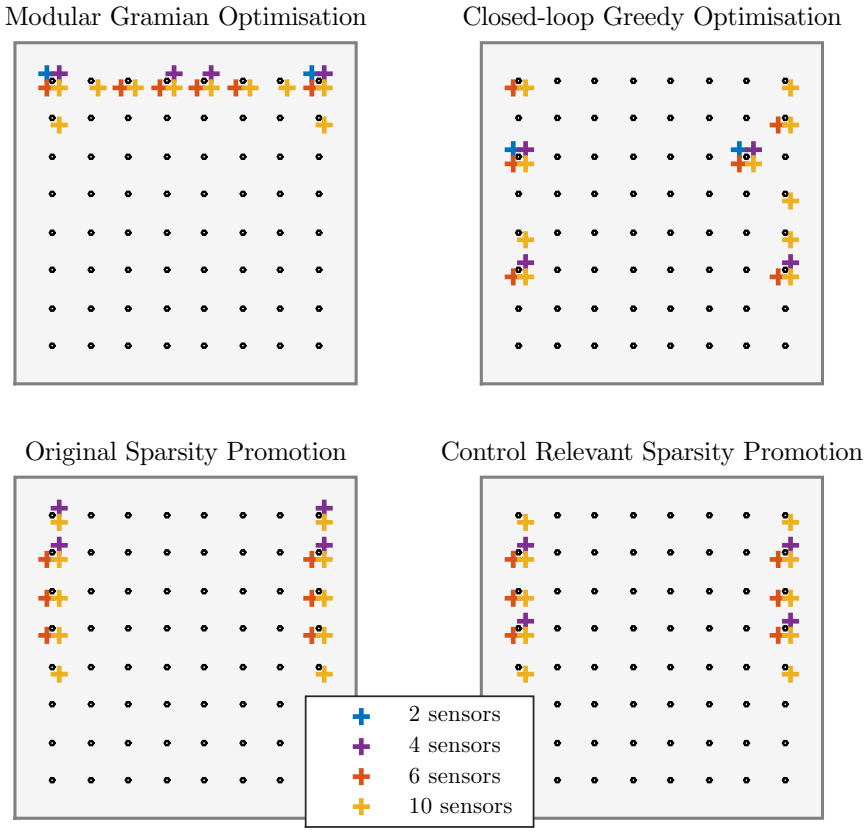

Figure 3.4: The sensor configurations that are generated by each algorithm, which consist of 2, 4, 6 and 10 sensors in domain 1.

Make everything as simple as possible, but not simpler.
Albert Einstein

4

Control Relevant Order Reduction

Over the past decades, a substantial amount of attention has been given to the design of low order controllers that maximise performance for a high order model. Several control relevant order reduction and direct approaches have been developed for this purpose, which should ideally solve the constrained order optimal control problem in Problem 1.3.

In this chapter we will first apply a number of existing order reduction techniques, with the aim of synthesising a low order control that maximises closed-loop H_2 performance for a given high order model. The techniques are: balanced truncation, Linear Quadratic Gaussian balanced truncation and weighted order reduction. It will be demonstrated that none of these methods provide any guarantees on closed-loop H_2 performance; improvements are therefore proposed. This investigation in combination with the results are based on [Merks and Weiland, 2019b].

The chapter is finalised by demonstrating that the best closed-loop performance is obtained by combining these techniques with a fixed order optimisation algorithm.

4.1 Introduction

In a wide range of practical applications, the FEM or FVM is used to create models that accurately describe a given system. For example, this type of model is considered by Thompson and Vogiatzis [2014] for thermal management, by Oyvang et al. [2019] for the control of an air-cooled hydro-generator, by Vermeulen et al. [2005] for groundwater flow modelling, by Jia et al. [2011] for micro-electro-mechanical system (MEMs) design and by Candeo and Dughiero [2009] for hyperthermia treatment of cancer.

It is often desired to utilise such a model for optimal control design. However, this type of model will commonly contain well over $10,000$ states and it is recognised by many authors—e.g. by Adegas et al. [2013], Lordejani et al. [2018], Antoulas [2005] and Benner et al. [2015]—that this will lead to computational issues concerning the synthesis and real-time implementation of an optimal controller.

To be more specific, the synthesis of the controller might become unreliable due to numerical conditioning—or even infeasible due to memory constraints—when the model order is large. In the past, this implied that models with at most $1,000$ states could be used to reliably synthesise an optimal controller. Nowadays there exist several algorithms that can numerically construct an optimal controller for models that contain more than $100,000$ states—as explained by Saak et al. [2019].

In addition, the computational hardware that is considered for the implementation of a controller will directly impose an upper bound on the controller order itself. This, because the hardware must be able to determine the desired control action in real-time. Although the upper bound relies heavily on the type of application and the available computational power, the controller order should typically be well below $1,000$ states.

However, the widely-applied solutions to the H_2 and H_∞ optimal control problems result in a controller that is of the same order as the model for which it is designed. If the model order is large, real-time implementation of these controllers is therefore not possible.

4.1.1 Constrained Order H_2 Optimal Controller Design

In this chapter we will therefore investigate the problem of constructing a constrained order controller that maximises closed-loop H_2 performance for a given model—as defined in Problem 1.3. For this purpose, let us consider an lslsLTI model of the form

$$\Sigma = \begin{cases} \dot{x}(t) = Ax(t) + B_u u(t) + B_w w(t) \\ y(t) = C_y x(t) + D_{wy} w(t) \\ z(t) = C_z x(t) + D_{uz} u(t), \end{cases} \tag{4.1}$$

with vector signals $x(t)$, $u(t)$, $w(t)$, $y(t)$ and $z(t)$ that represent the state, known input, unknown disturbance, measured output and the control output, respectively. These signals assume values in finite-dimensional vector spaces $\mathcal{X} = \mathbb{R}^{n_x}, \mathcal{U} = \mathbb{R}^{n_u}$,

$\mathcal{W} = \mathbb{R}^{n_w}$, $\mathcal{Y} = \mathbb{R}^{n_y}$ and $\mathcal{Z} = \mathbb{R}^{n_z}$, respectively. The dynamical relation between the signals is described by real-valued matrices A, B_u, B_w, C_y, C_z, D_{wy} and D_{uz} of appropriate dimension.

In order to maximise closed-loop H_2 performance, a controller of the form

$$\Sigma_{c,n_c} = \begin{cases} \dot{x}_c(t) &= Jx_c(t) + Ky(t) \\ u(t) &= Mx_c(t) + Ny(t), \end{cases} \tag{4.2}$$

which is of order n_c, will be applied to Σ (4.1).

For the design of such a controller, we will—as mentioned in section 2.4—make the following assumption.

Assumption 4.1 *It is assumed that*
1a) (A, B_u) *is stabilisable.*
1b) (C_y, A) *is detectable.*
2a) $\begin{pmatrix} A - j\omega I_{n_x} & B_u \\ C_z & D_{uz} \end{pmatrix}$ *is full column rank for all* $\omega \in \mathbb{R}$.
2b) $\begin{pmatrix} A - j\omega I_{n_x} & B_w \\ C_y & D_{wy} \end{pmatrix}$ *is full row rank for all* $\omega \in \mathbb{R}$.
3a) D_{uz} *is full column rank.*
3b) D_{wy} *is full row rank.*

Under this assumption, a strictly proper controller must be considered—i.e. $N = 0$. When such a strictly proper controller is applied to Σ (4.1), the closed-loop interconnection is described by

$$\Sigma_{cl,n_c,sp} = \begin{cases} \begin{pmatrix} \dot{x}(t) \\ \dot{x}_c(t) \end{pmatrix} = \begin{pmatrix} A & B_u M \\ KC_y & J \end{pmatrix} \begin{pmatrix} x(t) \\ x_c(t) \end{pmatrix} + \begin{pmatrix} B_w \\ KD_{wy} \end{pmatrix} w(t) \\ z(t) = \begin{pmatrix} C_z & D_{uz}M \end{pmatrix} \begin{pmatrix} x(t) \\ x_c(t) \end{pmatrix}. \end{cases} \tag{4.3}$$

This closed-loop model has an extended state $x^{cl,n_c,sp} = \begin{pmatrix} x(t) \\ x_c(t) \end{pmatrix}$ and extended matrices $A^{cl,n_c,sp}$, $B_w^{cl,n_c,sp}$, $C_z^{cl,n_c,sp}$ and $D_{wz}^{cl,n_c,sp}$. Its extended state-space is characterised by the vector space $\mathcal{X}^{cl,n_c,sp}$ of dimension $n_x + n_c$.

The constrained order H_2 optimal control problem amounts to minimising the norm of this closed-loop model by appropriate construction of an H_2-admissible controller Σ_{c,n_c} (4.2). The problem is formally defined as follows.

Problem 4.1 *Construct an* H_2*-admissible controller* $\Sigma^\star_{c,n_c}$ *of the form* (4.2) *and of order* $n_c \in \mathbb{N}$ *for* Σ (4.1)*, which is a solution to*

$$\begin{aligned} \Sigma^\star_{c,n_c} = \quad & \arg \min_{\Sigma_{c,n_c}\ (4.2)} \ \|\Sigma_{cl,n_c,sp}\ (4.3)\|_{H_2} \\ & \text{s.t.} \qquad \Sigma_{c,n_c}\ (4.2) \text{ is } H_2\text{-admissible for } \Sigma\ (4.1). \end{aligned}$$

The solution to the H_2 optimal control problem as discussed in section 2.4, can be used to solve this problem for all orders $n_c \geq n_x$; for $n_c < n_x$ it remains an open problem. Several approaches that aim at maximising closed-loop H_2 performance with a controller of order $n_c < n_x$ are, however, available. These approaches can be categorised as MOR, COR and direct methods that correspond to paths 1–3 in figure 4.1, respectively. An excellent overview of these approaches is provided by Obinata and Anderson [2001].

With MOR—corresponding to path 1—the high order model Σ (4.1) is first reduced to order $n_r < n_x$, which results in a low order model $\widehat{\Sigma}_{n_r}$. The reduced order model $\widehat{\Sigma}_{n_r}$ is then used for the design of an H_2 optimal controller $\widehat{\Sigma}^{\star}_{c,n_r}$ or order n_r. This approach can be applied to extremely high order models, because the controller itself is designed on the basis of a reduced order model.

On the other hand, with COR—corresponding to path 2—a high order H_2 optimal controller $\Sigma^{\star}_{c,n_x}$ of order n_x is designed directly for the high order model Σ (4.1). An order reduction procedure is then applied to this controller, which results in a reduced order controller $\widehat{\Sigma}^{\star}_{c,n_r}$.

Finally, with the direct methods—corresponding to path 3—the reduced order controller $\widehat{\Sigma}^{\star}_{c,n_r}$ is directly designed for the high order model Σ (4.1).

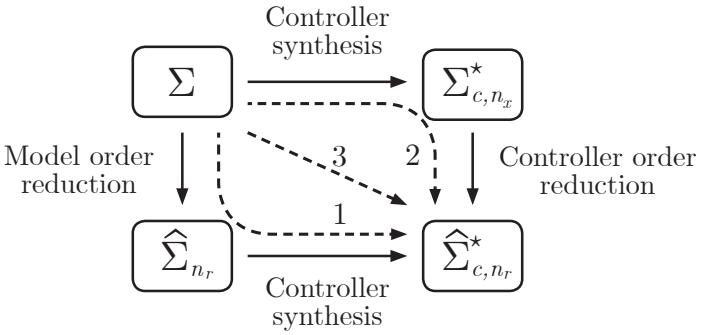

Figure 4.1: The typical constrained order controller design approaches.

4.1.2 Order Reduction for Control

Typical model order reduction techniques aim at creating a reduced order (approximate) model that—in some sense—accurately describes the behaviour of a given high order model; this type of order reduction will be referred to as *open-loop model order reduction*. A large number of open-loop reduction techniques is available, which have been developed for specific types of models and for specific ranges of model orders.

For LTI models as considered in this thesis, model order reduction techniques such as balanced truncation—which is discussed by Gugercin and Antoulas [2004]—and moment matching—which is discussed by Ionescu and Astolfi [2011]—are often

applied. For a more complete overview of all available model order reduction techniques, please consider the work by Antoulas [2005] and by Schilders et al. [2008].

A large number of authors propose to combine these model order reduction techniques with optimal control design in order to construct a constrained order controller that maximises closed-loop performance. To name a few, in recent years it has been considered by Salakij et al. [2016], Picard et al. [2017], Luspay et al. [2018], Yang et al. [2019] and by Banholzer et al. [2019]. However, the combination of a given optimal control design with a model order reduction approach will not result in a controller that provides any guarantees on closed-loop performance.

For example, it is shown in the famous paper by Doyle [1978] that H_2 optimal controllers do not, in general, provide any robustness guarantees. This well-known result has led to the invention of robust and H_∞ optimal control approaches. However, its implications for the combination of open-loop model order reduction with optimal control—as first recognised by Pernebo and Silverman [1982]—are not widely known.

To explain these implications, let $\widehat{\Sigma}_{n_r}$ be an approximation for Σ (4.1), which is of arbitrary accuracy—i.e. the models are almost equal in terms of input to output behaviour. Then, the result by Doyle [1978] states that an H_2 optimal controller, which is designed for $\widehat{\Sigma}_{n_r}$, might not be stabilising when it is applied to the original model Σ (4.1). In other words, an H_2 optimal controller that is designed on the basis of an (arbitrarily) accurate open-loop approximation could destabilise the original model. This observation led to a search for control relevant order reduction techniques, which can be categorised into frequency weighted and closed-loop approaches.

Frequency weighted approaches—as discussed by Obinata and Anderson [2001], Goddard [1995], Varga and Anderson [2001] and by Wortelboer and Bosgra [1992]—are an extension to open-loop model order reduction. These methods utilise a weighting function on the inputs and output of Σ (4.1) to—during model order reduction—emphasise the frequency regions that are important from a control perspective.

It has been shown that these techniques perform well in practice. However, the objectives for the frequency weights are often conflicting, as explained in more detail by Obinata and Anderson [2001, Ch. 3]. For example, a frequency weight that is designed to obtain a stable closed-loop model might severely reduce performance and vice versa. The performance that can be obtained with type of technique is therefore heavily reliant on the type of application and the expertise of an engineer.

Closed-loop approaches, on the other hand, consider the closed-loop interconnection between the model and a controller. Linear Quadratic Gaussian (LQG) balanced truncation, as introduced by Jonckheere and Silverman [1983], was among the first of these methods. This technique considers a full order LQG or H_2 optimal controller connected to a model, in order to determine what states of the model and/or controller are important in the interconnection. This approach has been an inspiration for numerous techniques; see, for example the work by Mustafa [1990], El-Zobaidi and Jaimoukha [1998], Opmeer et al. [2005] and by Choroszucha and Sun [2017].

For several practical examples, it has also been shown that these closed-loop techniques perform relatively well. Furthermore, Wortelboer [1994] created the weighted order reduction approach, which is a combined frequency weighted and closed-loop order reduction technique. Five years later, Wortelboer et al. [1999] demonstrated its potential on an industrial example as well.

4.1.3 Direct Methods

Direct methods aim at avoiding the intermediate model or controller reduction step. Instead, the low order controller is designed directly for a given high order model.

With classical PID controller designs as mentioned in section 1.2.3, the structure of the controller—and therefore the order—is typically fixed. The problem of optimising closed-loop performance with such a controller by appropriate selection of the controller parameters, which is called controller-tuning, can therefore be regarded as a direct method. This problem was first addressed more than 75 years ago by Ziegler et al. [1942]. Nevertheless, it is still relevant today and modern approaches such as the recent work by Grimholt and Skogestad [2018], utilise a numerical optimisation algorithm to select the controller parameters.

These controller-tuning methods are often easy to apply and therefore appealing to industry. However, the underlying theory is developed for SISO systems, which implies that a high order MIMO controller might still be obtained if such a PID tuning technique is applied to all output to input channels of a MIMO system. On the other hand, the performance of such a controller might be severely limited when it is only considered to add a controller between certain inputs and outputs.

A second branch within the controller-tuning methods is called *direct data-driven control design*, which aims at optimising the controller parameters on the basis of data. One of these techniques is called *virtual reference feedback tuning* and was introduced by Campi et al. [2002]. With this approach, the controller parameters are optimised to achieve a given "desired" closed-loop transfer function. The problem of designing an appropriate experiment for this technique has been addressed by Formentin et al. [2012b] and several other extensions, such as the work by Formentin et al. [2012a], have been considered. A similar problem is, however, observed for MIMO systems and it is still unclear how to appropriately select the desired closed-loop transfer function.

The final branch of methods that will be discussed, encompasses the so-called *fixed order optimisation* techniques. These techniques—as discussed in more detail by Hol [2006] and by Hilhorst [2015]—directly formulate Problem 4.1 as a numerical optimisation problem. It is, however, important to note that such an optimisation problem is non-smooth and non-convex in general, which implies that only a locally optimal controller can be found on the basis of some—often randomly chosen—initial controller.

One of these techniques is implemented in the H_∞-H_2 Fixed Order Optimisation HIFOO toolbox, which is developed by Arzelier et al. [2009, 2011]. Currently, this toolbox can be applied to models with more than $1,000$ states. However, the

controller can typically contain at most 20 states when a random initialisation is chosen for the algorithm. It is important to note that recent results by Benner et al. [2018] have reduced the computational time for HIFOO by combining the approach with MOR.

4.1.4 Chapter Outline

In this chapter we will investigate the problem of constructing a constrained order controller that maximises closed-loop H_2 performance for a given LTI model of the form Σ (4.1). For the purpose of designing such a controller, in section 4.2 we will first investigate the following existing control relevant order reduction techniques:

- open-loop balanced truncation (BT) for MOR.
- open-loop balanced truncation for COR.
- Linear Quadratic Gaussian balanced truncation (LQG-BT).
- weighted order reduction (WOR).

Furthermore, the performance of these methods is analysed on a practical example.

This example will demonstrate that the considered open-loop and closed-loop order reduction techniques do not necessarily perform well in situations where a measurement feedback controller with high gain is used. The non-optimality of open-loop order reduction methods in terms of constrained order controller design is therefore directly observed in a practical situation. It is, however, never shown that closed-loop order reduction techniques are non-optimal, which will be established in section 4.3 by means of an example.

A control relevant truncation algorithm is proposed in section 4.4 to improve the existing open-loop and closed-loop order reduction methods. It is, in addition, shown that this new algorithm can be used to significantly improve closed-loop H_2 performance for the practical example. Especially, if it is combined with a fixed order optimisation technique such as HIFOO, which is discussed in section 4.5

The conclusions and future work are discussed in chapter 7.

4.2 Balancing-Based Order Reduction Techniques for Control

All order reduction techniques that are considered in this chapter are balancing-based and consist of two steps. First, a state transformation is applied to the model or controller that—in some sense— orders the model (or controller) states from most important to least important. Then, a model (or controller) of reduced order is obtained by removing the least important states. We will start by discussing how these states are removed.

4.2.1 Truncation and Singular Perturbation

To explain how the states of a model or controller are removed, let us consider a model of the form

$$\Sigma_s = \begin{cases} \dot{x}(t) &= Ax(t) + Bu(t) \\ y(t) &= Cx(t) + Du(t), \end{cases} \tag{4.4}$$

with vector signals $x(t)$, $u(t)$ and $y(t)$ that represent the state, input and output. These signals assume values in finite-dimensional vector spaces $\mathcal{X} = \mathbb{R}^{n_x}$, $\mathcal{U} = \mathbb{R}^{n_u}$ and $\mathcal{Y} = \mathbb{R}^{n_y}$, respectively. The dynamical relation between the signals is described by real-valued matrices A, B, C and D of appropriate dimension.

The states of Σ_s (4.4) are, as explained above, first ordered from most to least important with balancing-based approaches. On the basis of such an ordering, we can partition the states of Σ_s (4.4) as $x(t) = \begin{pmatrix} x_1(t) \\ x_2(t) \end{pmatrix}$, where $x_1(t) \in \mathbb{R}^{n_r}$ contains the n_r most important states and $x_2(t) \in \mathbb{R}^{n_x - n_r}$ the $n_x - n_r$ least important states, to obtain a partitioned model

$$\Sigma_{s,p} = \begin{cases} \begin{pmatrix} \dot{x}_1(t) \\ \dot{x}_2(t) \end{pmatrix} = \begin{pmatrix} A_{11} & A_{12} \\ A_{21} & A_{22} \end{pmatrix} \begin{pmatrix} x_1(t) \\ x_2(t) \end{pmatrix} + \begin{pmatrix} B_1 \\ B_2 \end{pmatrix} u(t) \\ y(t) = \begin{pmatrix} C_1 & C_2 \end{pmatrix} \begin{pmatrix} x_1(t) \\ x_2(t) \end{pmatrix} + Du(t). \end{cases} \tag{4.5}$$

A low order (approximate) model for Σ_s (4.4) is then constructed by removing the states $x_2(t)$. This can, for example, be achieved by imposing the constraint $x_2(t) = 0$, or by imposing the constraint $\dot{x}_2(t) = 0$.

Truncation

The method of imposing $x_2(t) = 0$ to construct a reduced order (approximate) model is called *truncation*. A model of order n_r is obtained with this method, which is described in terms of the original partitioned model as

$$\widehat{\Sigma}_{s,n_r} = \begin{cases} \dot{x}_1(t) &= A_{11}x_1(t) + B_1u(t) \\ y(t) &= C_1x_1(t) + Du(t). \end{cases} \tag{4.6}$$

By utilising truncation, the transfer function of the reduced order model will match the transfer function of the original model at $s = \infty$, which is illustrated in figure 4.2. In other words, let $\Gamma_s(s)$ and $\widehat{\Gamma}_{s,n_r}$ be the transfer functions for Σ_s (4.4) and $\widehat{\Sigma}_{s,n_r}$ (4.6), respectively. We then get that $\Gamma_s(\infty) = \widehat{\Gamma}_{s,n_r}(\infty)$.

Singular Perturbation

The second method of imposing $\dot{x}_2(t) = 0$ to construct a reduced order (approximate) model is called *singular perturbation*. A model of order n_r is—when A_{22} is

nonsingular—described in terms of the original partitioned model as

$$\widehat{\Sigma}_{s,pert,n_r} = \begin{cases} \dot{x}_1(t) = \left(A_{11} - A_{12}A_{22}^{-1}A_{21}\right)x_1(t) + \left(B_1 - A_{12}A_{22}^{-1}B_2\right)u(t) \\ y(t) = \left(C_1 - C_2A_{22}^{-1}A_{21}\right)x_1(t) + \left(D - C_2A_{22}^{-1}B_2\right)u(t). \end{cases} \tag{4.7}$$

The transfer function of this reduced order model will, in contrast with truncation, match the transfer function of the original model at $s = 0$, which is, again, illustrated in figure 4.2. In other words, let $\Gamma_s(s)$ and $\widehat{\Gamma}_{s,pert,n_r}$ be the transfer functions for Σ_s (4.4) and $\widehat{\Sigma}_{s,pert,n_r}$ (4.7), respectively. We then get that $\Gamma_s(0) = \widehat{\Gamma}_{s,pert,n_r}(0)$.

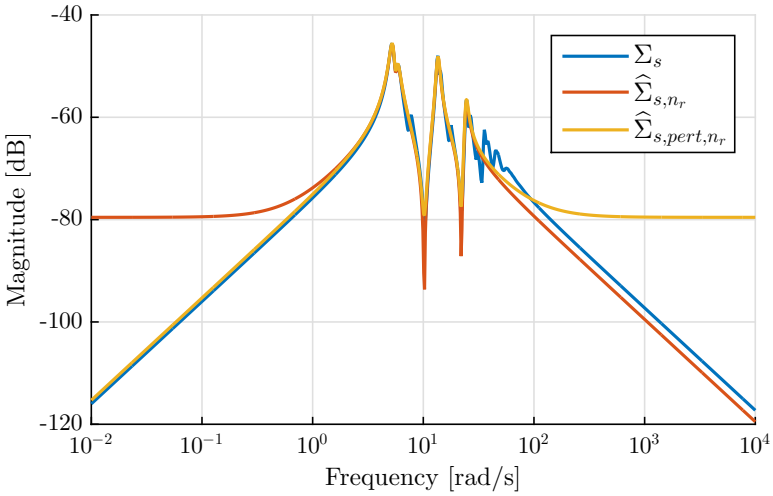

Figure 4.2: The frequency response of a full order model and two reduced order models that are obtained with truncation and singular perturbation.

Truncation for Constrained Order H_2-Admissible Controller Design

Now, let us investigate how these methods can be used to construct a reduced order controller.

With MOR for control—according to path 1 in figure 4.1—the states of a model of the form Σ (4.1) are ordered and partitioned as $x(t) = \begin{pmatrix} x_1(t) \\ x_2(t) \end{pmatrix}$, with $x_1(t) \in \mathbb{R}^{n_r}$ and $x_2(t) \in \mathbb{R}^{n_x - n_r}$. A reduced order (approximate) model of order n_r is therefore in a similar fashion obtained by applying truncation or singular perturbation to this partitioned model.

If truncation is used, the reduced order model is mathematically described as

$$\widehat{\Sigma}_{n_r} = \begin{cases} \dot{x}_1(t) = A_{11}x_1(t) + B_{u1}u(t) + B_{w1}w(t) \\ y(t) = C_{y1}x_1(t) \qquad\qquad + D_{wy}w(t) \\ y(t) = C_{z1}x_1(t) + D_{uz}u(t). \end{cases} \tag{4.8}$$

Furthermore, for singular perturbation the reduced order model is—when A_{22} is nonsingular—of the form

$$\widehat{\Sigma}_{pert,n_r} = \begin{cases} \dot{x}_1(t) = \left(A_{11} - A_{12}A_{22}^{-1}A_{21}\right)x_1(t) + \left(B_{u1} - A_{12}A_{22}^{-1}B_{u2}\right)u(t) \\ \qquad\qquad + \left(B_{w1} - A_{12}A_{22}^{-1}B_{w2}\right)w(t) \\ y(t) = \left(C_{y1} - C_{y2}A_{22}^{-1}A_{21}\right)x_1(t) + \left(-C_{y2}A_{22}^{-1}B_{u2}\right)u(t) \\ \qquad\qquad + \left(D_{wy} - C_{y2}A_{22}^{-1}B_{w2}\right)w(t) \\ z(t) = \left(C_{z1} - C_{z2}A_{22}^{-1}A_{21}\right)x_1(t) + \left(D_{uz} - C_{z2}A_{22}^{-1}B_{u2}\right)u(t) \\ \qquad\qquad + \left(-C_{z2}A_{22}^{-1}B_{w2}\right)w(t). \end{cases} \tag{4.9}$$

However, it can be shown that singular perturbation cannot, in general, be considered for the purpose of designing a reduced order H_2-admissible controller for the original model Σ (4.1).

Lemma 4.1 *Consider a model Σ (4.1) that satisfies assumption 4.1 and which contains a partitioned state $x(t) = \begin{pmatrix} x_1(t) \\ x_2(t) \end{pmatrix}$, with $x_1(t) \in \mathbb{R}^{n_r}$ and $x_2(t) \in \mathbb{R}^{n_x - n_r}$.*

Furthermore, let $\widehat{\Sigma}_{pert,n_r}$ (4.9) be a reduced order (approximate) model for Σ (4.1) that is obtained with singular perturbation.

Then, any H_2-admissible controller for $\widehat{\Sigma}_{pert,n_r}$ (4.9) can only be H_2-admissible for Σ (4.1) if $C_{z2}A_{22}^{-1}B_{w2} = 0$.

Proof: An H_2-admissible controller for Σ (4.1) must, under assumption 4.1, satisfy $N = 0$. It therefore suffices to show that any H_2-admissible controller for $\widehat{\Sigma}_{pert,n_r}$ (4.9) will only satisfy $N = 0$ if $C_{z2}A_{22}^{-1}B_{w2} = 0$, which follows directly from Definition 2.17. □

For COR—according to path 2 in figure 4.1—it is important to note that a controller is essentially a model of the form Σ_s (4.4) with input $y(t)$ and output $u(t)$. The state of the controller Σ_{c,n_c} (4.2) can therefore also be ordered and partitioned as $x_c(t) = \begin{pmatrix} x_{c1}(t) \\ x_{c2}(t) \end{pmatrix}$, with $x_{c1}(t) \in \mathbb{R}^{n_r}$ and $x_{c2}(t) \in \mathbb{R}^{n_c - n_r}$, to obtain a partitioned controller

$$\Sigma_{c,n_c,p} = \begin{cases} \begin{pmatrix} \dot{x}_{c1}(t) \\ \dot{x}_{c2}(t) \end{pmatrix} = \begin{pmatrix} J_{11} & J_{12} \\ J_{21} & J_{22} \end{pmatrix}\begin{pmatrix} x_{c1}(t) \\ x_{c2}(t) \end{pmatrix} + \begin{pmatrix} K_1 \\ K_2 \end{pmatrix} y(t) \\ u(t) = \begin{pmatrix} M_1 & M_2 \end{pmatrix}\begin{pmatrix} x_{c1}(t) \\ x_{c2}(t) \end{pmatrix} + \quad Ny(t). \end{cases} \tag{4.10}$$

If truncation is applied to a controller, the reduced order controller is mathematically described as

$$\widehat{\Sigma}_{c,n_r} = \begin{cases} \dot{x}_{c1}(t) &= J_{11}x_{c1}(t) + K_1 y(t) \\ u(t) &= M_1 x_{c1}(t) + Ny(t). \end{cases} \tag{4.11}$$

Furthermore, for singular perturbation the reduced order controller is—when J_{22} is nonsingular—of the form

$$\widehat{\Sigma}_{c,pert,n_r} = \begin{cases} \dot{x}_{c1}(t) &= \left(J_{11} - J_{12}J_{22}^{-1}J_{21}\right)x_{c1}(t) + \left(K_1 - J_{12}J_{22}^{-1}K_2\right)y(t) \\ u(t) &= \left(M_1 - M_2J_{22}^{-1}J_{21}\right)x_{c1}(t) + \left(N - M_2J_{22}^{-1}K_2\right)y(t). \end{cases} \tag{4.12}$$

In a similar fashion to MOR, it can be shown for COR that singular perturbation cannot, in general, be considered for the purpose of designing a reduced order H_2-admissible controller for the model Σ (4.1).

Lemma 4.2 *Consider an H_2-admissible controller Σ_{c,n_c} (4.2) for the model Σ (4.1) that satisfies assumption 4.1. Let the controller state be partitioned as $x_c(t) = \begin{pmatrix} x_{c1}(t) \\ x_{c2}(t) \end{pmatrix}$, with $x_{c1}(t) \in \mathbb{R}^{n_r}$ and $x_{c2}(t) \in \mathbb{R}^{n_c - n_r}$.*

Furthermore, let $\widehat{\Sigma}_{c,pert,n_r}$ (4.12) be a reduced order controller that is obtained with singular perturbation.

Then, the controller $\widehat{\Sigma}_{c,pert,n_r}$ (4.12) can only be H_2-admissible for Σ (4.1) if $M_2J_{22}^{-1}K_2 = 0$.

Proof: An H_2-admissible controller of the form Σ_{c,n_c} (4.2) for Σ (4.1) must, under assumption 4.1, satisfy $N = 0$. Similarly, $\widehat{\Sigma}_{c,pert,n_r}$ (4.12) can only be H_2 admissible for Σ (4.1) if $N - M_2J_{22}^{-1}K_2 = 0$, which completes the proof. □

Remark 4.1 *For both MOR and COR, we will therefore only consider truncation in this chapter.*

4.2.2 Open-loop Balancing

An introduction to Open-Loop Balancing

Now, let us introduce a state transformation that—in some sense—orders the states of Σ_s (4.4) from most important to least important. With open-loop balancing this ordering is based on the input to output behaviour of the model, which is quantified using the reachability and observability Gramians as introduced in section 2.2.3. For a more complete discussion on balancing, please consider the work by Antoulas [2005, ch. 7]

As explained in chapter 2, the Gramians of an internally stable model Σ (4.1) are the unique positive semidefinite solutions to the following Lyapunov equations:

$$\mathcal{P}(A,B) \succeq 0 \text{ such that } A\mathcal{P} + \mathcal{P}A^\top + BB^\top = 0, \tag{4.13}$$

$$\mathcal{Q}(C,A) \succeq 0 \text{ such that } A^\top\mathcal{Q} + \mathcal{Q}A + C^\top C = 0. \tag{4.14}$$

Furthermore, these Gramians satisfy $\mathcal{P} \succ 0$ and $\mathcal{Q} \succ 0$ if and only if the internally stable model Σ_s (4.4) is reachable and observable, respectively.

Let us now consider a model Σ_s (4.4) that is internally stable, reachable and observable—which therefore is equivalent to assuming that the Gramians are positive definite. Then there exists a state transformation $\bar{x}(t) = T_b x(t)$ that brings Σ_s (4.4) into the so-called balanced form $\bar{\Sigma}_b$, with matrices $\bar{A}_b = T_b A T_b^{-1}$, $\bar{B}_b = T_b B$, $\bar{C}_b = C T_b^{-1}$ and $\bar{D}_b = D$. The Gramians are in this specific form equal, diagonal and the diagonal entries are ordered. I.e. the Gramians of $\bar{\Sigma}_b$ are described by

$$\bar{\mathcal{P}}_b = \bar{\mathcal{Q}}_b = \mathcal{P}(\bar{A}_b, \bar{B}_b) = \mathcal{Q}(\bar{C}_b, \bar{A}_b) = \begin{pmatrix} \sigma_1 \cdots & 0 \\ \vdots \ \ddots & \vdots \\ 0 \ \cdots & \sigma_{n_x} \end{pmatrix},$$

with ordering $\sigma_1 \geq \sigma_2 \geq \cdots \geq \sigma_{n_x} > 0$. This is discussed in more detail by Antoulas [2005, Sec. 7.1].

The values σ_i are called *Hankel singular values*. Each Hankel singular value σ_i is an indication for the relevance of the state $x_i(t)$ in terms of the input to output behaviour of the balanced model $\bar{\Sigma}_b$. This can, for example, be observed from the (squared) H_2 norm:

$$\begin{aligned} \left\|\bar{\Sigma}_b\right\|_{H_2}^2 &= \operatorname{tr}(\bar{C}_b \bar{\mathcal{P}}_b \bar{C}_b^\top) = \sum_{i=1}^{n_x} \sigma_i \left\|\bar{C}_{bi}\right\|_2^2 \\ &= \operatorname{tr}(\bar{B}_b^\top \bar{\mathcal{Q}}_b \bar{B}_b) = \sum_{i=1}^{n_x} \sigma_i \left\|\bar{B}_{bi}^\top\right\|_2^2, \end{aligned}$$

where $\bar{B}_{bi}$ and $\bar{C}_{bi}$ denote the i^{th} row and column of $\bar{B}_b$ and $\bar{C}_b$, respectively.

From this expression we can see that a state, which corresponds to a value σ_i of small magnitude, will have a small contribution towards the H_2 norm of the model.

Furthermore, there exists a well-known error bound when truncation is applied to $\bar{\Sigma}_b$ in order to obtain an (approximate) model $\widehat{\Sigma}_b$ of order n_r. Specifically, the error between $\bar{\Sigma}_b$ and $\widehat{\Sigma}_b$—which is denoted by $\bar{\Sigma}_b - \widehat{\Sigma}_b$—is for distinct Hankel singular values bounded by

$$\left\|\Sigma_s \ (4.4) - \widehat{\Sigma}_b\right\|_{H_\infty} = \left\|\bar{\Sigma}_b - \widehat{\Sigma}_b\right\|_{H_\infty} \leq 2 \sum_{i=r+1}^{n_x} \sigma_i,$$

as explained by Antoulas [2005, Thm. 7.10]. We can therefore observe that the reduced order approximation $\widehat{\Sigma}_b$ will accurately describe the input to output behaviour of Σ_s (4.4) when $\sum_{i=r+1}^{n_x} \sigma_i$ is small in magnitude.

Remark 4.2 *It is important to mention that the norm* $\left\|\bar{\Sigma}_b - \widehat{\Sigma}_b\right\|_{H_\infty}$ *is actually bounded by twice the sum of the (not necessarily smallest) Hankel singular values* σ_i *that correspond to the truncated states—as explained in more detail by Antoulas [2005, Thm. 7.10]. The typical decision to truncate the states corresponding to the smallest values* σ_i *—and to introduce the ordering* $\sigma_1 \geq \sigma_2 \geq \cdots \geq \sigma_{n_x} > 0$*—is therefore a direct result of this bound.*

Open-Loop Balancing of Models that are not Stable, Reachable and Observable

Under assumption 4.1 it is not guaranteed that the model Σ (4.1) or the controller Σ_{c,n_c} (4.2) is internally stable, reachable and observable. For this reason, let us investigate balanced truncation for a model of the form Σ_s (4.4) that is not internally stable, reachable and observable.

Firstly, any state of Σ_s (4.4) that is not reachable or observable will have no contribution toward the input to output behaviour of Σ_s (4.4)—as explained in section 2.2.4. These states can therefore simply be removed from an open-loop model order reduction perspective.

Secondly, the Gramians of the model Σ_s (4.4) are not defined when it is not internally stable. As explained by Chen et al. [2004, sec. 4.2], however, for any unstable model there exists a state transformation $T_{s,u}$ that brings Σ_s (4.4) into the following form:

$$\Sigma_{s,u} = \left\{ \begin{array}{rcl} \begin{pmatrix} \dot{x}_u(t) \\ \dot{x}_s(t) \end{pmatrix} & = & \begin{pmatrix} A_u & 0 \\ 0 & A_s \end{pmatrix} \begin{pmatrix} x_u(t) \\ x_s(t) \end{pmatrix} + \begin{pmatrix} B_u \\ B_s \end{pmatrix} u(t) \\ y(t) & = & \begin{pmatrix} C_u & C_s \end{pmatrix} \begin{pmatrix} x_u(t) \\ x_s(t) \end{pmatrix} + Du(t)\,, \end{array} \right. \tag{4.15}$$

with $\lambda(A_s) \subset \mathbb{C}_-$ and $\lambda(A_u) \cap \mathbb{C}_- = \emptyset$; and with the state partitioning $\mathcal{X} = \mathcal{X}_u \oplus \mathcal{X}_s$ such that $\mathcal{X}_u = \mathbb{R}^{n_{x,u}}$ and $\mathcal{X}_s = \mathbb{R}^{n_{x,s}}$.

Now—provided that A_u has no eigenvalues on the imaginary axis—one can define the (partial) Gramians $\mathcal{P}_u = \mathcal{P}(-A_u, B_u)$ and $\mathcal{Q}_u = \mathcal{Q}(C_u, -A_u)$ as discussed in more detail by Zhou et al. [1999] and by Antoulas [2005, sec.7.6] in order to balance the anti-stable sub-model of $\Sigma_{s,u}$ (4.15)—i.e. the triple (A_u, B_u, C_u). From a control perspective, however, it can be argued that unstable dynamics will always require careful attention and it will therefore not be considered to truncate any state within $x_u(t)$.

In a similar fashion, the (partial) Gramians $\mathcal{P}_s = \mathcal{P}(A_s, B_s)$ and $\mathcal{Q}_s = \mathcal{Q}(C_s, A_s)$ are defined for the stable sub-model of $\Sigma_{s,u}$ (4.15)—i.e. for the triple (A_s, B_s, C_s). Furthermore, the Gramians $\mathcal{P}_s$, $\mathcal{Q}_s$ are positive definite when the unreachable and unobservable states are removed before the construction of $\Sigma_{s,u}$ (4.15); the stable dynamics can therefore be balanced and truncated in order to obtain a low order approximate model.

Open-Loop Balanced Model order Reduction for Control

A controller is essentially a model of the form Σ_s (4.4) with input $y(t)$ and output $u(t)$. For the purpose of open-loop COR, we can therefore directly apply the open-loop balanced truncation method as explained above to a controller of the from Σ_{c,n_c} (4.2). It is, in addition, important to note that the unreachable and unobservable states of a controller will not contribute towards the closed-loop interconnection. These can therefore be removed from the controller without affecting closed-loop performance or stability.

With open-loop MOR for control, the aim is to utilise the balancing approach as described above to construct a reduced order model for Σ (4.1). For this model, the reachability of states is quantified by the Gramians $\mathcal{P}_w = \mathcal{P}(A, B_w)$ and $\mathcal{P}_u = \mathcal{P}(A, B_u)$, while observability is quantified by the Gramians $\mathcal{Q}_y = \mathcal{Q}(C_y, A)$ and $\mathcal{Q}_z = \mathcal{Q}(C_z, A)$.

The model Σ (4.1) is therefore only balanced when all four Gramians are equal and diagonal. It is, however, not guaranteed that such a balanced representation exists. At the same time it is unwise to consider only one reachability and one observability Gramian. For example, a state that is not reachable through $w(t)$ might be reachable through $u(t)$ and therefore important to create an internally stable closed-loop interconnection.

For this reason, let us define the weighted model

$$\Sigma_w = \begin{cases} \dot{x}(t) = Ax(t) + \begin{pmatrix} \alpha_i B_u & (1-\alpha_i)B_w \end{pmatrix} u'(t) \\ y'(t) = \begin{pmatrix} \alpha_o C_y \\ (1-\alpha_o)C_z \end{pmatrix} x(t) + \begin{pmatrix} 0 & (1-\alpha_i)\alpha_o D_{wy} \\ \alpha_i(1-\alpha_o)D_{uz} & \end{pmatrix} u'(t), \end{cases} \tag{4.16}$$

with input weight $0 \leq \alpha_i \leq 1$ and output weight $0 \leq \alpha_o \leq 1$.

Σ_w (4.16) is called a weighted model, because the Gramians are a (quadratically) described in terms of the Gramians of Σ (4.1), which is shown in the following proposition.

Proposition 4.3 *Consider the weights* $0 \leq \alpha_i \leq 1$, $0 \leq \alpha_o \leq 1$ *and the weighted model* Σ_w (4.16).

We then get that:

$$\mathcal{P}\left(A, \begin{pmatrix} \alpha_i B_u & (1-\alpha_i)B_w \end{pmatrix}\right) = \alpha_i^2 \mathcal{P}(A, B_u) + (1-\alpha_i)^2 \mathcal{P}(A, B_w)$$
$$\mathcal{Q}\left(\begin{pmatrix} \alpha_o C_y \\ (1-\alpha_o)C_z \end{pmatrix}, A\right) = \alpha_o^2 \mathcal{P}(C_y, A) + (1-\alpha_o)^2 \mathcal{P}(C_z, A)$$

Proof: This property can directly be observed from the definition of a Gramian. For the reachability Gramian we get that

$$\begin{aligned}\mathcal{P}(A, \begin{pmatrix}\alpha_i B_u & (1-\alpha_i)B_w\end{pmatrix}) &= \int_{t=0}^{\infty} e^{At}(\alpha_i^2 B_u B_u^\top + (1-\alpha_i)^2 B_w B_w^\top)e^{A^\top t}dt \\ &= \alpha_i^2 \int_{t=0}^{\infty} e^{At} B_u B_u^\top e^{A^\top t}dt + (1-\alpha_i)^2 \int_{t=0}^{\infty} e^{At} B_w B_w^\top e^{A^\top t}dt \\ &= \alpha_i^2 \mathcal{P}(A, B_u) + (1-\alpha_i)^2 \mathcal{P}(A, B_w).\end{aligned}$$

This can also be shown for the observability Gramian, when the duality property $\mathcal{Q}(C, A) = \mathcal{P}(A^\top, C^\top)$ is used. □

The reachability and observability properties of this weighted model Σ_w (4.16) can now be used to sort the states of Σ (4.1) from most to least important. In other words, the state transformation that is used to balance Σ_w (4.16)—for some α_i and α_o—is applied to Σ (4.1). Truncation is then applied to this transformed model in order to obtain a reduced model of the from $\widehat{\Sigma}_{n_r}$ (4.8). Finally, a reduced order H_2 optimal controller is designed for $\widehat{\Sigma}_{n_r}$ (4.8), while the weights α_i and α_o can be regarded as tuning parameters for the order reduction procedure.

4.2.3 Linear Quadratic Gaussian Balancing

With LQG-BT as introduced by Jonckheere and Silverman [1983], the closed-loop interconnection between the H_2 optimal controller as derived in section 2.4 and a model of the form Σ (4.1) is considered. This strictly proper controller is described by

$$\Sigma_{c,sp} = \begin{cases}\dot{\tilde{x}}(t) = \Big(A + B_u F + LC_y\Big)\,\tilde{x}(t) - Ly(t) \\ u(t) = F\tilde{x}(t),\end{cases} \tag{4.17}$$

with parameters $F : \mathcal{X} \to \mathcal{U}$ and $L : \mathcal{Y} \to \mathcal{X}$.

Interconnecting Σ (4.1) with $\Sigma_{c,sp}$ (4.17) yields—when a state observation error $e(t) = x(t) - \tilde{x}(t)$ is defined—the closed-loop model

$$\Sigma_{cl,sp} = \left\{\begin{array}{rcl}\begin{pmatrix}\dot{x}(t) \\ \dot{e}(t)\end{pmatrix} &=& \begin{pmatrix}A + B_u F & -B_u F \\ 0 & A + LC_y\end{pmatrix}\begin{pmatrix}x(t) \\ e(t)\end{pmatrix} + \begin{pmatrix}B_w \\ B_w + LD_{wy}\end{pmatrix} w(t) \\ z(t) &=& \Big(C_z + D_{uz}F \quad -D_{uz}F\Big)\begin{pmatrix}x(t) \\ e(t)\end{pmatrix} + \begin{pmatrix}0\end{pmatrix} w(t).\end{array}\right. \tag{4.18}$$

For such a controller, the following solution to the H_2 optimal control problem has been derived in section 2.4.

Corollary 4.4 *Consider a model Σ (4.1) that satisfies assumption 4.1 and let $P^+ \succeq 0$ and $Q^+ \succeq 0$ be the unique stabilising solutions to the following AREs:*

$$A^\top P + PA + C_z^\top C_z - (PB_u + C_z^\top D_{uz})(D_{uz}^\top D_{uz})^{-1}(PB_u + C_z^\top D_{uz})^\top = 0, \tag{4.19}$$

$$AQ + QA^\top + B_w B_w^\top - (QC_y^\top + B_w^\top D_{wy})(D_{wy} D_{wy}^\top)^{-1}(QC_y^\top + B_w^\top D_{wy})^\top = 0. \tag{4.20}$$

Then for all $n_c \geq n_x$, Problem 4.1 is solved by a controller of the form $\Sigma_{c,sp}$ (4.17) if the design parameters are chosen as

$$F = -(D_{uz}^\top D_{uz})^{-1}(B_u^\top P^+ + D_{uz}^\top C_z),$$
$$L = -(Q^+ C_y^\top + B_w^\top D_{wy})(D_{wy} D_{wy}^\top)^{-1}.$$

Proof: The proof can be found in section 2.4. □

Then, let us consider a model Σ (4.1) for which P^+ and Q^+ as defined above are positive definite—i.e. $P^+ \succ 0$ and $Q^+ \succ 0$. Then there exists a state transformation $\bar{x}(t) = T_{H_2,b} x(t)$ that brings Σ (4.1) into the so-called LQG, or H_2, balanced form $\bar{\Sigma}_{H_2,b}$. In this form, the unique stabilising solutions to the AREs in (4.19) and (4.20) are equal, diagonal and the diagonal entries are ordered. I.e. these solutions are for $\bar{\Sigma}_{H_2,b}$ described by

$$\bar{P}_{H_2,b}^+ = \bar{Q}_{H_2,b}^+ = \begin{pmatrix} \mu_1 \cdots & 0 \\ \vdots & \ddots & \vdots \\ 0 & \cdots & \mu_{n_x} \end{pmatrix},$$

with ordering $\mu_1 \geq \mu_2 \geq \cdots \geq \mu_{n_x} > 0$. This is discussed in more detail by Jonckheere and Silverman [1983].

The values μ_i are called *LQG singular values*. Each LQG singular value μ_i is an indication for the relevance of the state $x_i(t)$ in closed-loop, when an H_2 optimal controller is applied to $\bar{\Sigma}_{H_2,b}$. To explain this, let the optimal closed-loop interconnection of the form (4.18) be denoted by $\Sigma_{cl,sp}^\star$.

Then, by observing from section 2.4 that

$$\begin{aligned} \left\| \Sigma_{cl,sp}^\star \right\|_{H_2}^2 &= \operatorname{tr}(B_w^\top P^+ B_w) + \operatorname{tr}(B_u^\top P^+ Q^+ P^+ B_u) \\ &= \operatorname{tr}(C_z Q^+ C_z^\top) + \operatorname{tr}(C_y Q^+ P^+ Q^+ C_y^\top), \end{aligned}$$

we can conclude for an LQG balanced model that

$$\begin{aligned} \left\| \Sigma_{cl,sp}^\star \right\|_{H_2}^2 &= \sum_{i=1}^{n_x} \mu_i \left\| \bar{B}_{wi}^\top \right\|_2^2 + \mu_i^3 \left\| \bar{B}_{ui}^\top \right\|_2^2 \\ &= \sum_{i=1}^{n_x} \mu_i \left\| \bar{C}_{zi} \right\|_2^2 + \mu_i^3 \left\| \bar{C}_{yi} \right\|_2^2, \end{aligned}$$

where $\bar{B}_{ui}$, $\bar{B}_{wi}$ are the i^{th} rows and $\bar{C}_{yi}$, $\bar{C}_{zi}$ the i^{th} columns of $\bar{B}_u = T_{H_2,b} B_u$, $\bar{B}_w = T_{H_2,b} B_w$, $\bar{C}_y = C_y T_{H_2,b}^{-1}$ and $\bar{C}_z = C_z T_{H_2,b}^{-1}$, respectively.

From this expression we can see that the states corresponding to the values μ_i that are small in magnitude, will in general have a small contribution towards the H_2 norm of $\Sigma_{cl,sp}^\star$.

An interesting property for LQG-BT is that paths 1 and 2 in figure 4.1 become commutative. For LQG-BT it is therefore not necessary to distinguish between MOR and COR, because the resulting controllers are equal. This is formally established in the following lemma.

Lemma 4.5 *Consider a model* Σ (4.1) *that satisfies assumption 4.1, with the following partitioned state and stabilising solutions to the AREs in* (4.19) *and* (4.20)*:*

$$x(t) = \begin{pmatrix} x_1(t) \\ x_2(t) \end{pmatrix}, \quad P^+ = \begin{pmatrix} P_1^+ & 0 \\ 0 & P_2^+ \end{pmatrix}, \quad Q^+ = \begin{pmatrix} Q_1^+ & 0 \\ 0 & Q_2^+ \end{pmatrix},$$

for $P_1^+, Q_1^+ \in \mathbb{R}^{n_r \times n_r}$.

Furthermore, let $\Sigma_{c,sp}^\star(\Sigma\ (4.1))$ *and* $\Sigma_{c,sp}^\star(\widehat{\Sigma}_{n_r}\ (4.8))$ *denote the* H_2 *optimal controllers of the form* $\Sigma_{c,sp}$ (4.17) *for* Σ (4.1) *and the truncated model* $\widehat{\Sigma}_{n_r}$ (4.8)*, respectively; and let* $\widehat{\Sigma}_{c,sp}^\star(\Sigma\ (4.1))$ *denote* $\Sigma_{c,sp}^\star(\Sigma\ (4.1))$ *truncated to order* n_r.

Then

$$\Sigma_{c,sp}^\star(\widehat{\Sigma}_{n_r}\ (4.8)) = \widehat{\Sigma}_{c,sp}^\star(\Sigma\ (4.1)).$$

Proof: This is proven in Jonckheere and Silverman [1983, Sec. II]. □

Remark 4.3 *The stabilising solutions to the AREs in* (4.19) *and* (4.20) *are positive definite in most practical applications. Nevertheless, this is in general not guaranteed for a given model* Σ (4.1) *that satisfies assumption 4.1. In order to overcome this problem it can be considered to truncate the states corresponding to the subspace* $\ker(P^+)+\ker(Q^+)$ *before bringing the model to the LQG balanced form. The truncation of these states does, however, not guarantee that an* H_2 *optimal—or an internally stabilising—controller is constructed for the original model.*

4.2.4 Weighted Order Reduction

With WOR as introduced by Wortelboer [1994], the closed-loop interconnection between any internally stabilising controller of the form Σ_{c,n_c} (4.2) and the model Σ (4.1) is considered. For H_2-admissible controller design we—in this chapter—consider a model that satisfies assumption 4.1, which implies that a strictly proper controller must be used and the closed-loop interconnection is therefore described by $\Sigma_{cl,n_c,sp}$ (4.3).

Remark 4.4 *Please note that WOR is a combined frequency weighted and closed-loop order reduction technique. The use of frequency weights will, however, not be considered in this chapter.*

Furthermore, WOR can be used for control relevant MOR and COR corresponding to paths 1 and 2 in figure 4.1, respectively. Both approaches will now be presented. However, we will only investigate the performance WOR, when it is applied for the purpose of COR.

For any H_2-admissible controller, the closed-loop model $\Sigma_{cl,n_c,sp}$ (4.3) admits a pair of closed-loop Gramians

$$\mathcal{P}_{cl} = \mathcal{P}\left(\begin{pmatrix} A & B_u M \\ KC_y & J \end{pmatrix}, \begin{pmatrix} B_w \\ KD_{wy} \end{pmatrix}\right) = \begin{pmatrix} \mathcal{P}_\Sigma & \mathcal{P}_X \\ \mathcal{P}_X^\top & \mathcal{P}_{\Sigma_c} \end{pmatrix}, \tag{4.21}$$

$$\mathcal{Q}_{cl} = \mathcal{Q}\left(\begin{pmatrix} C_z & D_{uz} M \end{pmatrix}, \begin{pmatrix} A & B_u M \\ KC_y & J \end{pmatrix}\right) = \begin{pmatrix} \mathcal{Q}_\Sigma & \mathcal{Q}_X \\ \mathcal{Q}_X^\top & \mathcal{Q}_{\Sigma_c} \end{pmatrix}, \tag{4.22}$$

which are partitioned according to the model and controller states $x(t)$ and $x_c(t)$, respectively. I.e. $\mathcal{P}_\Sigma, \mathcal{Q}_\Sigma \in \mathbb{R}^{n_x \times n_x}$, $\mathcal{P}_X, \mathcal{Q}_X \in \mathbb{R}^{n_x \times n_c}$ and $\mathcal{P}_{\Sigma_c}, \mathcal{Q}_{\Sigma_c} \in \mathbb{R}^{n_c \times n_c}$.

Now, let us consider a closed-loop model for which the closed-loop Gramians $\mathcal{P}_{cl}$ and $\mathcal{Q}_{cl}$ as defined above are positive definite—i.e. $\mathcal{P}_{cl} \succ 0$ and $\mathcal{Q}_{cl} \succ 0$. Then there exists a state transformation that brings $\Sigma_{cl,sp}$ (4.18) into its balanced form—i.e. the closed-loop Gramians are equal, diagonal and the diagonal entries are ordered.

This balancing transformation will, however, "mix" the model and controller states. As a result, the distinction between model and controller states is lost in the balanced representation of the closed-loop model. Such a transformation does therefore not provide specific information about the (independent) relevance of model states or controller states in closed-loop.

For MOR and COR it is, instead, required to consider a state transformation that—in some sense—separately orders the model states and the controller states from most to least important; but this transformation should not "mix" model states with controller states. For this purpose, let us consider a closed-loop state transformation of the form

$$\begin{pmatrix} \bar{x}_{wor}(t) \\ \bar{x}_{c,wor}(t) \end{pmatrix} = \begin{pmatrix} T_\Sigma & 0 \\ 0 & T_{\Sigma_c} \end{pmatrix} \begin{pmatrix} x(t) \\ x_c(t) \end{pmatrix} = T_{wor} \begin{pmatrix} x(t) \\ x_c(t) \end{pmatrix}.$$

Now, if $\mathcal{P}_\Sigma \succ 0$ and $\mathcal{Q}_\Sigma \succ 0$, then there exists a model state transformation $\bar{x}_{wor}(t) = T_\Sigma x(t)$ that brings the partial closed-loop Gramians $\mathcal{P}_\Sigma$ and $\mathcal{Q}_\Sigma$ into a balanced form. Furthermore, if $\mathcal{P}_{\Sigma_c} \succ 0$ and $\mathcal{Q}_{\Sigma_c} \succ 0$, then there exists a controller state transformation $\bar{x}_{c,wor}(t) = T_{\Sigma_c} x_c(t)$ that brings the partial closed-loop Gramians $\mathcal{P}_{\Sigma_c}$ and $\mathcal{Q}_{\Sigma_c}$ into a balanced form.

If we therefore consider a model Σ (4.1) and an internally stabilising controller Σ_{c,n_c} (4.2) for which the closed-loop Gramians $\mathcal{P}_{cl}$ and $\mathcal{Q}_{cl}$ as defined in (4.21) and (4.22), respectively, satisfy $\mathcal{P}_\Sigma \succ 0$, $\mathcal{Q}_\Sigma \succ 0$, $\mathcal{P}_{\Sigma_c} \succ 0$ and $\mathcal{Q}_{\Sigma_c} \succ 0$. Then there exists a state transformation $x^{wor}(t) = T_{wor} x^{cl,n_c,sp}(t)$ that brings $\Sigma_{cl,n_c,sp}$ (4.3) into the so-called WOR-balanced form $\bar{\Sigma}_{cl,wor}$. In this specific form, the closed-loop Gramians $\mathcal{P}_{cl}$ and $\mathcal{Q}_{cl}$ as defined in (4.21) and (4.22), respectively, are described by

$$\bar{\mathcal{P}}_{wor} = \left(\begin{array}{ccc|ccc} \sigma_{cl,1} & \cdots & 0 & \star & \star & \star \\ \vdots & \ddots & \vdots & \star & \star & \star \\ 0 & \cdots & \sigma_{cl,n_x} & \star & \star & \star \\ \hline \star & \star & \star & \sigma_{c,cl,1} & \cdots & 0 \\ \star & \star & \star & \vdots & \ddots & \vdots \\ \star & \star & \star & 0 & \cdots & \sigma_{c,cl,n_c} \end{array}\right),$$

$$\bar{\mathcal{Q}}_{wor} = \left(\begin{array}{ccc|ccc} \sigma_{cl,1} & \cdots & 0 & \star & \star & \star \\ \vdots & \ddots & \vdots & \star & \star & \star \\ 0 & \cdots & \sigma_{cl,n_x} & \star & \star & \star \\ \hline \star & \star & \star & \sigma_{c,cl,1} & \cdots & 0 \\ \star & \star & \star & \vdots & \ddots & \vdots \\ \star & \star & \star & 0 & \cdots & \sigma_{c,cl,n_c} \end{array}\right),$$

with ordering $\sigma_{cl,1} \geq \sigma_{cl,2} \geq \cdots \geq \sigma_{cl,n_x} > 0$ and $\sigma_{c,cl,1} \geq \sigma_{c,cl,2} \geq \cdots \geq \sigma_{c,cl,n_c} > 0$. The values $\sigma_{cl,i}$ and $\sigma_{c,cl,i}$ are called *WOR model and controller singular values*, respectively. This is discussed in more detail by Wortelboer et al. [1999].

Now, we can use the state transformation $\bar{x}_{wor}(t) = T_\Sigma x(t)$ to bring the model Σ (4.1) into the WOR balanced model form $\bar{\Sigma}_{wor}$. Each WOR model singular value $\sigma_{cl,i}$ is—similarly to the other methods—an indication for the relevance of the model state $\bar{x}_{wor,i}(t)$ in terms of the input to output behaviour of the WOR balanced closed-loop model $\bar{\Sigma}_{cl,wor}$. It is therefore proposed to truncate the model states of $\bar{\Sigma}_{wor}$ that correspond to the WOR singular values $\sigma_{cl,i}$ that are small in magnitude.

Similarly, we can use the state transformation $\bar{x}_{c,wor}(t) = T_{\Sigma_c} x_c(t)$ to bring the controller Σ_{c,n_c} (4.2) into the WOR balanced controller form $\bar{\Sigma}_{c,n_c,wor}$. Each WOR controller singular value $\sigma_{c,cl,i}$ is, again, an indication for the relevance of the controller state $\bar{x}_{c,wor,i}(t)$ in terms of the input to output behaviour of the WOR balanced closed-loop model $\bar{\Sigma}_{cl,wor}$. It is therefore proposed to truncate the controller states of $\bar{\Sigma}_{c,n_c,wor}$ that correspond to the WOR singular values $\sigma_{c,cl,i}$ that are small in magnitude.

Remark 4.5 *For MOR it is required that the (partial) closed-loop Gramians $\mathcal{P}_\Sigma$ and $\mathcal{Q}_\Sigma$ as defined in* (4.21) *and* (4.22)*, respectively, are positive definite; this holds for most practical applications. Nevertheless, it is in general not guaranteed for an arbitrary closed-loop interconnection of a model Σ* (4.1) *with an H_2-admissible controller Σ_{c,n_c}* (4.2)*. In order to overcome this problem, it can be considered to truncate the model states corresponding to the subspace $\ker(\mathcal{P}_\Sigma) + \ker(\mathcal{Q}_\Sigma)$ before bringing the model to the WOR balanced form.*

Similarly, for COR it is required that the (partial) closed-loop Gramians $\mathcal{P}_{\Sigma_c}$ and $\mathcal{Q}_{\Sigma_c}$ as defined in (4.21) *and* (4.22)*, respectively, are positive definite. This is, again, in general not guaranteed for an arbitrary closed-loop interconnection of a model Σ* (4.1) *with an H_2-admissible controller Σ_{c,n_c}* (4.2)*. In order to overcome this problem, it can therefore be considered to truncate the controller states corresponding to the subspace $\ker(\mathcal{P}_{\Sigma_c}) + \ker(\mathcal{Q}_{\Sigma_c})$ before bringing the controller to the WOR balanced form.*

It must, however, be observed that $\ker(\mathcal{P}_{\Sigma_c}) \nsubseteq \ker(\mathcal{P}_{cl})$) and $\ker(\mathcal{Q}_{\Sigma_c}) \nsubseteq \ker(\mathcal{Q}_{cl})$), which implies that the truncation of these controller states may directly impact closed-loop stability and H_2 performance.

4.2.5 Performance Analysis on a Practical Example

Let us now investigate how well these four methods perform for the purpose of designing a constrained order H_2-admissible controller.

Case Study

As an example, a model for thermal conduction of a spatially discretised one dimensional bar that is attached to a heat-sink of constant temperature—as depicted in figure 4.3—will be considered. This system is modelled as

$$\Sigma_1 = \begin{cases} \dot{x}(t) = Ax(t) + \rho B_u u(t) + \begin{pmatrix} \widetilde{B}_w & 0 \end{pmatrix} w(t) \\ y(t) = \rho C_y x(t) + \begin{pmatrix} 0 & I_{n_y} \end{pmatrix} w(t) \\ z(t) = \begin{pmatrix} \widetilde{C}_z \\ 0 \end{pmatrix} x(t) + \begin{pmatrix} 0 \\ I_{n_u} \end{pmatrix} u(t) \end{cases} \tag{4.23}$$

and satisfies assumption 4.1 for $\rho \neq 0$.

Σ_1 (4.23) contains 200 states which represent temperatures at given locations on the bar. The matrix A is a tri-diagonal matrix that contains values -2.5 on the main diagonal and values 1 on the first diagonals above and below the main diagonal, which represent thermal conductivity and heat capacity parameters.

The control input $u(t)$ represents actuators that are capable of heating and cooling groups of 5 elements at a time. The model contains 39 control inputs, where column i of B_u is given by $B_{ui} = e_{n_x}(5i-2, 5i+2)$. Please note that $e_{n_x}(i,j)$ is an indicator vector as introduced in section 2.1.

The state disturbances act on a single state at a time. The model contains 99 state disturbances, where column i of $\widetilde{B}_w$ is given by $\widetilde{B}_{wi} = e_{n_x}(2i, 2i)$. Similarly, the model contains 61 measurements where row i of C_y is given by $C_{yi} = e_{n_x}^\top(7+3i, 7+3i)$. The matrix $\widetilde{C}_z$ contains 130 rows of uniformly distributed random numbers in the interval $[-0.01, 0.01]$. The matrices D_{wy} and D_{uz} are identity matrices.

Finally, observe that the matrices B_u and C_y are multiplied by a value ρ, which can be regarded as a tuning parameter that affects the gain of an H_2 optimal controller. For example, a small value of ρ will result in a conservative "low gain" controller, while a large value of ρ will result in a more aggressive "high gain" controller.

A low order controller of the form Σ_{c,n_c} (4.2) will be designed for Σ_1 (4.23) by utilising open-loop BT for MOR with $\alpha_i = \alpha_o = \frac{1}{2}$, open-loop BT for COR, LQG-BT and WOR. For each method, truncation will be based on the magnitude of the corresponding singular values. Furthermore, each low order controller is applied to the full order model Σ_1 (4.23) to determine its performance, which is measured in the H_2 norm of the closed-loop interconnection.

The performance for each method as a function of the controller order is shown in figure 4.5 at the end of this chapter for a low gain situation with $\rho = 10$, a moderate gain situation with $\rho = 50$, a high gain situation with $\rho = 200$ and an

extremely high gain situation with $\rho = 3000$. Please note that a star is used in the figure to indicate that the closed-loop interconnection of the low order controller with Σ_1 (4.23) is not internally stable.

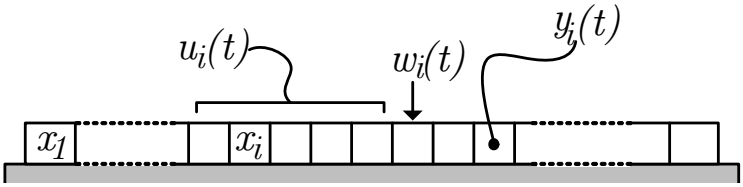

Figure 4.3: A visualisation of Σ_1 (4.23).

Desired Behaviour

Before commenting on the results for this example, let us first establish what should ideally be achieved from the perspective of constrained order H_2 optimal controller design. I.e. we will first establish what properties are expected for a solution to Problem 4.1.

Firstly, it is known that H_2 optimal performance is obtained when a full order controller—i.e. with $n_c = 200$— is considered. Secondly, the open-loop H_2 norm of Σ_1 (4.23) is obtained for $n_c = 0$, because a strictly proper controller of order zero is simply a zero gain; i.e. $u(t) = 0$.

Furthermore, the closed-loop H_2 norm should ideally be non-increasing when n_c increases. In other words, an *optimal* constrained order controller cannot contain states that reduce performance. Truncation of additional controller states should therefore not lead to an improvement in closed-loop performance.

Finally, an increase in ρ indicates from a control perspective, that the control inputs $u(t)$ can become larger in magnitude and that the signal to noise ratio for the measured outputs $y(t)$ is reduced in magnitude. An increase in ρ should therefore not reduce closed-loop performance when the controller order n_c is fixed.

Actual Performance

For the low gain situation with $\rho = 10$ it is observed that open-loop BT for COR and WOR both show the desired behaviour; it is, however, important to emphasise that optimality is not implied by this observation. LQG-BT shows the desired behaviour as well, but with a slight reduction in closed-loop performance. Finally, BT for MOR only shows the desired behaviour for low controller orders $n_c \leq 35$ and performs worst on average.

For the moderate gain situation with $\rho = 50$ it is observed that only open-loop BT for COR shows the desired behaviour. WOR does show the desired behaviour for $n_c \geq 75$, but does not result in an internally stable closed-loop interconnection for

lower orders. LQG-BT shows again a lower performance than these methods, while BT for MOR only shows the desired behaviour for low controller orders $n_c \leq 35$.

Finally, the desired behaviour is not observed with any method for the (extremely) high gain situations with $\rho = 200$ and $\rho = 3000$. In particular, the low order controllers will—for most orders—actually perform worse than the open-loop situation without controller. BT for MOR does, however, show the desired behaviour for low controller orders $n_c \leq 35$.

In can therefore be concluded that existing (control relevant) MOR and COR methods will only result in a reasonable closed-loop H_2 performance for relatively low gain situations. For high gain situations—where optimal control will actually be able to show its potential—none of the presented methods is able to consistently perform better than not utilising any control. The importance of the main research question in Chapter 1 is therefore directly observed in this example.

4.3 The Non-Optimality of Closed-Loop Order Reduction for Constrained Order Control

In section 4.2.5 it has been shown that the considered open-loop and closed-loop order reduction techniques do not necessarily perform well in high gain situations. The non-optimality of open-loop order reduction methods for constrained order controller design—as explained in section 4.1.2—is therefore directly observed from a relatively simple example. In fact, these methods may provide controllers that perform worse than the open-loop behaviour of the model.

It is, however, never established that the use of closed-loop order reduction for constrained order controller design is non-optimal. This non-optimality will now be demonstrated on the following model:

$$\Sigma_{ex} = \left\{ \begin{array}{rcl} \begin{pmatrix} \dot{x}_1(t) \\ \dot{x}_2(t) \end{pmatrix} = \begin{pmatrix} -0.1 & 0 \\ 0 & -0.5 \end{pmatrix} \begin{pmatrix} x_1(t) \\ x_2(t) \end{pmatrix} + \begin{pmatrix} \rho & 0 \\ 0 & 0.05 \end{pmatrix} u(t) + \begin{pmatrix} 1 & 0 & 0 & 0 \\ 0 & 1 & 0 & 0 \end{pmatrix} w(t) \\ y(t) = \begin{pmatrix} \rho & 0 \\ 0 & 0.05 \end{pmatrix} \begin{pmatrix} x_1(t) \\ x_2(t) \end{pmatrix} + \begin{pmatrix} 0 & 0 & 1 & 0 \\ 0 & 0 & 0 & 1 \end{pmatrix} w(t) \\ z(t) = \begin{pmatrix} 1 & 0 \\ 0 & 1 \\ 0 & 0 \\ 0 & 0 \end{pmatrix} \begin{pmatrix} x_1(t) \\ x_2(t) \end{pmatrix} + \begin{pmatrix} 0 & 0 \\ 0 & 0 \\ 1 & 0 \\ 0 & 1 \end{pmatrix} u(t), \end{array} \right. \tag{4.24}$$

which satisfies assumption 4.1 for $\rho \neq 0$.

It must be noted that Σ_{ex} (4.24) consists of two decoupled single-state models in parallel; i.e. each state has its own inputs, outputs and the states do not interact. An H_2 (or H_∞) optimal controller for Σ_{ex} (4.24) can therefore be described by two decoupled controllers in parallel as well. The removal of a state from such

a controller is, as a consequence, equivalent to leaving the corresponding state of Σ_{ex} (4.24) uncontrolled.

Figure 4.4 shows the closed-loop H_2 performance as function of ρ, if

- a full order H_2 optimal controller is used.
- the state $x_1(t)$ is controlled—i.e. $\tilde{x}_2(t)$ is truncated from the controller.
- the state $x_2(t)$ is controlled—i.e. $\tilde{x}_1(t)$ is truncated from the controller.
- truncation is based on the LQG singular values.
- truncation is based on the WOR singular values.

From this figure it can be observed that the optimal closed-loop performance is almost completely achieved by only controlling state $x_1(t)$. This is according to intuition, because the state $x_1(t)$ is much easier to control through $u(t)$ and easier to observe in $y(t)$ than the state $x_2(t)$ for $\rho \gg 0.05$.

Viewed as function of ρ, the closed-loop H_2 performance for a controller that is designed with LQG-BT and WOR is shown as the red and blue lines in figure 4.4. From this figure, it can be observed that the former only achieves near optimal performance for $\rho \leq 0.9$, while the latter achieves near optimal performance for $\rho \leq 202$. Therefore, the example clearly shows that both methods become non-optimal when ρ is sufficiently large in magnitude.

The non-optimality of LQG-BT can directly be observed from the stabilising solutions to the AREs, which are described by

$$P^+ = Q^+ = \begin{pmatrix} \frac{1-\sqrt{100\rho^2+1}}{10\rho^2} & 0 \\ 0 & 0.998 \end{pmatrix}.$$

Thus, Σ_{ex} (4.24) is an LQG balanced model, provided that the states are ordered according to the magnitude of the diagonal entries within P^+ and Q^+. Now it is easy to see that $\frac{1-\sqrt{100\rho^2+1}}{10\rho^2} < 0.998$ for $\rho > 0.9$, which implies that $x_1(t)$ is truncated rather than $x_2(t)$.

For WOR it can, in a similar fashion, be observed that $x_1(t)$ is truncated for $\rho > 202$ when the Gramians of the closed-loop interconnection are expressed as a function of ρ. Therefore, the magnitude of both the LQG and WOR singular values does not—in terms of maximising closed-loop performance—determine the relevance of states.

This example has implications that go beyond these two closed-loop order reduction techniques. Namely, an H_2 (or H_∞) optimal controller will, for increasing values of ρ, mainly aim at reducing the relevance of the state $x_1(t)$ in closed-loop. Any closed-loop order reduction technique will therefore truncate the state $x_1(t)$ when ρ becomes sufficiently large, while near optimal closed-loop performance can only be achieved by controlling this state.

We can therefore conclude that the relevance of a state *in closed-loop* does not determine how important the state is *for control*. When constrained order controller design is considered, closed-loop order reduction techniques will therefore be non-optimal in general.

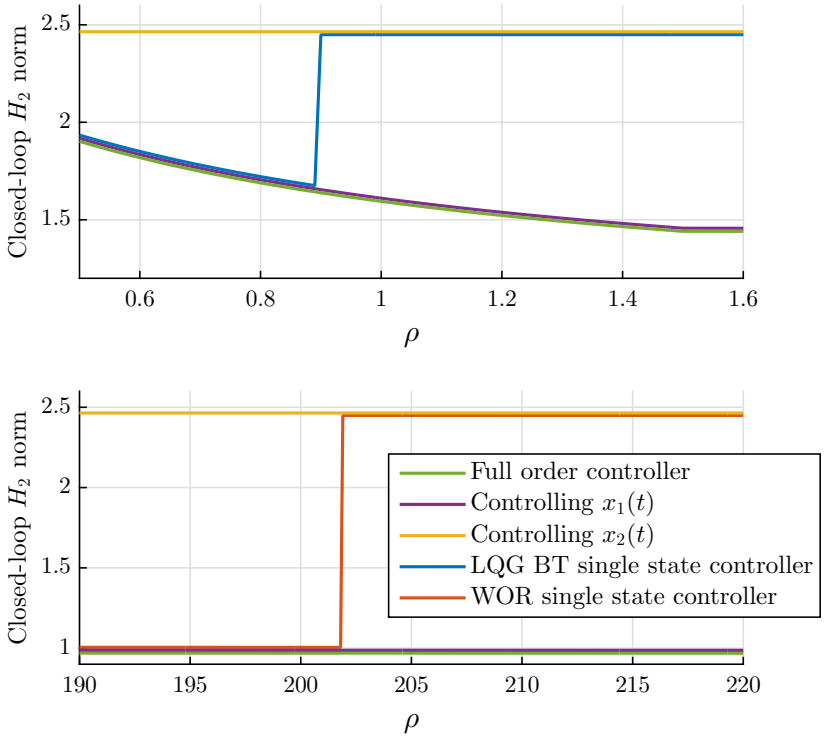

Figure 4.4: The H_2 performance of several controllers for Σ_{ex} (4.24) as a function of ρ.

4.4 Proposed Improvements

It is now established that neither the relevance of a state in open-loop, nor in closed-loop determines the closed-loop performance loss if such a state is truncated. In order to overcome this problem, let us define a measure for this performance loss.

Definition 4.6 *Consider an H_2-admissible controller Σ_{c,n_c} (4.2) for Σ (4.1), let $\mathbb{X}_c$ denote a subset of controller states—e.g. $\mathbb{X}_c = \{x_{c1}, x_{c3}, \cdots, x_{c9}\}$—and let $\Sigma_{c,n_c}^{\mathbb{X}_c}$ denote Σ_{c,n_c} (4.2) for which the states $\mathbb{X}_c$ are truncated. Furthermore, let $\Sigma_{cl,n_c,sp}$ (4.3) and $\Sigma_{cl,n_c,sp}^{\mathbb{X}_c}$ denote the closed-loop models that are obtained by applying Σ_{c,n_c} (4.2) and $\Sigma_{c,n_c}^{\mathbb{X}_c}$ to Σ (4.1), respectively.*

Then the "H_2 performance loss" due to truncation of the states $\mathbb{X}_c$ from Σ_{c,n_c} (4.2)

is defined as

$$\delta_{H_2}(\Sigma\ (4.1),\ \Sigma_{c,n_c}\ (4.2), \mathbb{X}_c) = \begin{cases} \left\| \Sigma^{\mathbb{X}_c}_{cl,n_c,sp} \right\|_{H_2} - \left\| \Sigma_{cl,n_c,sp}\ (4.3) \right\|_{H_2} & \text{if } \Sigma^{\mathbb{X}_c}_{c,n_c} \text{ is } H_2\text{-admissible for } \Sigma\ (4.1) \\ \infty & \text{otherwise.} \end{cases}$$

To maximise the closed-loop H_2 performance for a given controller order, it is desired to minimise δ_{H_2} over all subsets $\mathbb{X}_c$ of a given cardinality, which is a combinatorial optimisation problem. In section 3.2 it is explained that a greedy search algorithm can, under certain conditions, be used to efficiently find an approximate solution to this type of problem. Specifically, there is an upper-bound on the degree of non-optimality for a solution that is obtained with a greedy search, if the function is monotone decreasing and supermodular. In the following theorem it is shown that δ_{H_2} does not, in general, have these properties.

Theorem 4.7 *Consider an H_2-admissible controller Σ_{c,n_c} (4.2) for Σ (4.1) and let $\mathbb{X}_{ci}$, $\mathbb{X}_{cj}$ be non-empty subsets of controller states. Then*

(a) $\mathbb{X}_{ci} \cap \mathbb{X}_{cj} = \emptyset \nRightarrow \delta_{H_2}(\Sigma\ (4.1),\ \Sigma_{c,n_c}\ (4.2), \mathbb{X}_{ci}) + \delta_{H_2}(\Sigma\ (4.1),\ \Sigma_{c,n_c}\ (4.2), \mathbb{X}_{cj}) \leq \delta_{H_2}(\Sigma\ (4.1),\ \Sigma_{c,n_c}\ (4.2), \mathbb{X}_{ci} \cup \mathbb{X}_{cj})$,
$\nRightarrow \delta_{H_2}(\Sigma\ (4.1),\ \Sigma_{c,n_c}\ (4.2), \mathbb{X}_{ci}) + \delta_{H_2}(\Sigma\ (4.1),\ \Sigma_{c,n_c}\ (4.2), \mathbb{X}_{cj}) \geq \delta_{H_2}(\Sigma\ (4.1),\ \Sigma_{c,n_c}\ (4.2), \mathbb{X}_{ci} \cup \mathbb{X}_{cj})$.

(b) $\mathbb{X}_{ci} \subset \mathbb{X}_{cj} \nRightarrow \delta_{H_2}(\Sigma\ (4.1),\ \Sigma_{c,n_c}\ (4.2), \mathbb{X}_{ci})) \leq \delta_{H_2}(\Sigma\ (4.1),\ \Sigma_{c,n_c}\ (4.2), \mathbb{X}_{cj})$.

Proof: The proof will use Σ_1 (4.23) as discussed above as a counter example.

(a) Consider—for Σ_1 (4.23) with $\rho = 200$—open-loop BT for COR and consider the subsets of controller states $\{x_{c,i}\}$, $\{x_{c,i+1}, \cdots, x_{c,200}\}$. Then, the first inequality is observed by analysing δ_{H_2} for these subsets with $i = 82$ and the second with $i = 81$.

(ii) For Σ_1 (4.23) it can also be observed that truncation of an additional state could improve performance with all approaches. □

The loss of closed-loop H_2 performance can therefore only be minimised by considering all possible subsets $\mathbb{X}_c$ of a given cardinality, which is computationally infeasible for high order models. To avoid solving this computationally expensive problem, a new truncation algorithm as described in Algorithm 4.1 is proposed. It is, however, important to emphasise that this algorithm utilises a greedy search and therefore does not provide explicit guarantees on optimality.

In the first phase of Algorithm 4.1, the truncation procedure as described in section 4.2 is considered. The aim of this phase is to remove states without substantially affecting closed-loop performance—i.e. δ_{H_2} should be below a given threshold ϵ_i. Please note that for $\epsilon_i = 0$, there will be no performance loss as a result of this phase.

The second phase of the algorithm utilises a greedy search to reduce the performance loss as a result of truncation. In each step of this search, the loss of H_2

performance δ_i is calculated for each controller state $\{x_{ci}\}$ and the state corresponding to the smallest loss of performance is truncated. A controller of the desired order is therefore obtained by subsequently applying these steps.

Remark 4.6 *Please note that Algorithm 4.1 is applicable to any balancing-based order reduction technique. It is therefore assumed that all frequency weighted extensions to the considered order reduction methods can benefit from this algorithm.*

Algorithm 4.1 Greedy Cost Minimisation

procedure GREEDYMIN($\Sigma, \Sigma_{c,n_c}, n_r, \epsilon_i$)
  Perform a line search to find a smallest value k such that
  $\delta(\Sigma, \Sigma_{c,n_c}, \mathbb{X}_{c0}) \leq \epsilon_i$ for $\mathbb{X}_{c0} = \{x_{ck}, x_{ck+1}, \cdots, x_{n_c}\}$
  $\Sigma_{c,n_c,1} = \Sigma_{c,n_c}^{\mathbb{X}_{c0}}$
  for $i = 1, 2, \cdots, n_p - k - n_r$ **do**
    Set n_i as the order of $\Sigma_{c,n_c,i}$
    for $j = 1, 2, \cdots, n_i$ **do**
      $\delta_j = \delta_{H_2}(\Sigma, \Sigma_{c,n_c,i}, \{x_{cj}\})$
    end for
    $\mathbb{X}_c = \{x_{ck}\}$, with k such that $\delta_k \leq \delta_l$ for all $l \neq k$
    $\Sigma_{c,n_c,i+1} = \Sigma_{c,n_c,i}^{\mathbb{X}_c}$
  end for
  return $\widehat{\Sigma}_{c,n_r} = \Sigma_{c,n_c,i+1}$
end procedure

4.4.1 Improvements for the Practical Example

Let us now investigate what improvements can be achieved with the greedy truncation algorithm by applying it to the case study in section 4.2.5. First, the value $\epsilon_i = 0$ is considered to determine the best achievable closed-loop H_2 performance of the algorithm in combination with open-loop BT for COR, LQG-BT and WOR; the results are shown in figure 4.6 at the end of this chapter. It is important to note that open-loop BT for MOR is not considered; the reason for this will be explained below.

Figure 4.6 shows that an improvement is achieved for all methods in the low, moderate and (extremely) high gain situations. The greedy algorithm can for the (extremely) high gain situations be used to obtain a stabilising controller of order $n_c < 100$ that improves the H_2 performance in closed-loop, which is a substantial improvement. Furthermore, the combined greedy algorithm with WOR show the desired behaviour for the low, moderate and high gain situations.

This improvement in performance comes, however, at an increase in computational time. To put this into perspective, the original truncation methods will produce a controller of order 1 within one second, while the greedy algorithm requires approximately 12 minutes[1] of computational time.

[1] On a computer with an Intel® Xeon® E5-2630 v3 (8 cores at 2.40 GHz) processor.

It is important to note that the three investigated greedy COR algorithms require the construction of only one H_2 optimal controller. The use of such a greedy truncation algorithm for MOR approaches, however, requires the construction an H_2 optimal controller for every evaluation of the H_2 performance loss δ_{H_2}, which severely reduces scalability. To provide a comparison, BT for MOR requires approximately 2 hours to construct a controller of order 1 for this case study.

Finally, let us verify whether the computational time of 12 minutes can be reduced by tuning ϵ_i. For this purpose, let us consider the relative loss of performance

$$\epsilon_i = \epsilon_{i,r}(\gamma_{ol} - \gamma_{cl}),$$

where γ_{ol} and γ_{cl} are the H_2 norm in open-loop and the optimal closed-loop H_2 norm, respectively.

Then, for $\epsilon_{i,r} = 0.05$ a substantial reduction in computational time can be achieved without significantly affecting closed-loop performance—which can be observed from figure 4.7 at the end of the chapter. This reduction in computational time is shown in table 4.1. Furthermore, it is important to observe that the largest reduction is achieved when the original truncation procedure performs well for relatively low controller orders; i.e. in the low and moderate gain situations.

	$\rho = 10$	$\rho = 50$	$\rho = 200$	$\rho = 3000$
Open-loop BT for COR	18.9 sec.	91.6 sec.	202.0 sec.	165.0 sec.
LQG-BT	312.1 sec.	584.4 sec.	675.4 sec.	705.6 sec.
WOR	15.7 sec.	67.2 sec.	221.3 sec.	393.2 sec.

Table 4.1: The computational time of the greedy truncation algorithm in Algorithm 4.1, when a controller of order 1 is constructed with $\epsilon_{i,r} = 0.05$. Please note that the average computational time with $\epsilon_{i,r} = 0$ is 720 seconds. Furthermore, these numbers are generated on a computer with an Intel® Xeon® E5-2630 v3 (8 cores at 2.40 GHz) processor.

4.5 Fixed Order Optimisation

To finalise this chapter, it will be investigated how these order reduction techniques perform in comparison with the existing fixed order optimisation method called HIFOO, which is developed by Arzelier et al. [2009, 2011].

Fixed order optimisation techniques aim at directly solving the optimisation problem in Problem 4.1 for a given controller order n_c. It is, however, explained by Benner et al. [2018] that such an optimisation problem is non-smooth and non-convex for all controller orders (including $n_c = n_x$). Existing methods such as the HIFOO algorithm therefore iteratively optimise the matrices of some initial controller, which implies that only a locally optimal controller can be found. For example, if no initial controller is provided, the HIFOO algorithm will construct one locally optimal constrained order controller on the bases of three random initial controllers

Figure 4.8, at the end of this chapter, shows the performance of several controllers that are created with the HIFOO algorithm. The algorithm is used five times per controller order, such that the average performance with random initial controllers can be determined. From the figure it can be observed that the HIFOO algorithm performs similarly to the greedy algorithms for $n_c \leq 9$ in the low gain situation with $\rho = 10$, while for higher orders it is not able to construct a stabilising controller. In the moderate to extremely high gain situations with $\rho \geq 50$, however, the algorithm is only able to consistently construct a controller that performs better than the open-loop situation for $n_c \leq 5$. We can therefore observe that—if no initial controller is provided—the HIFOO algorithm does not perform better than the greedy COR techniques that have been developed in this chapter.

The investigated MOR and COR approaches can also be used to provide an initial controller for the HIFOO algorithm. It is now considered to use the greedy search in combination with WOR to provide such an initial controller. The closed-loop H_2 performance that is obtained with this combined method is presented in figure 4.7 at the end of this chapter, which shows that the desired behaviour is now even obtained in the extremely high feedback situation with $\rho = 3000$. This improvement in performance comes, again, with an increase in computational time that becomes larger as the controller order increases; this is shown in table 4.2

It can therefore be concluded that the best closed-loop H_2 performance is obtained by combining the greedy search with WOR; and to provide the resulting controller as an initial controller for the HIFOO algorithm. The performance of these combined algorithms does show the desired behaviour for all situations in the case study (including the extremely high gain situation). It must, however, be emphasised that closed-loop stability—or optimality of the controller—is still not guaranteed in general.

	$n_c = 150$	$n_c = 100$	$n_c = 50$	$n_c = 20$	$n_c = 10$
HIFOO	22.1 min.	12.7 min.	9.2 min.	4.5 min.	1.8 min.

Table 4.2: The computational time of the HIFOO algorithm, when an initial controller of order n_c is optimised. Please note that these numbers are generated on a computer with an Intel® Xeon® E5-2630 v3 (8 cores at 2.40 GHz) processor.

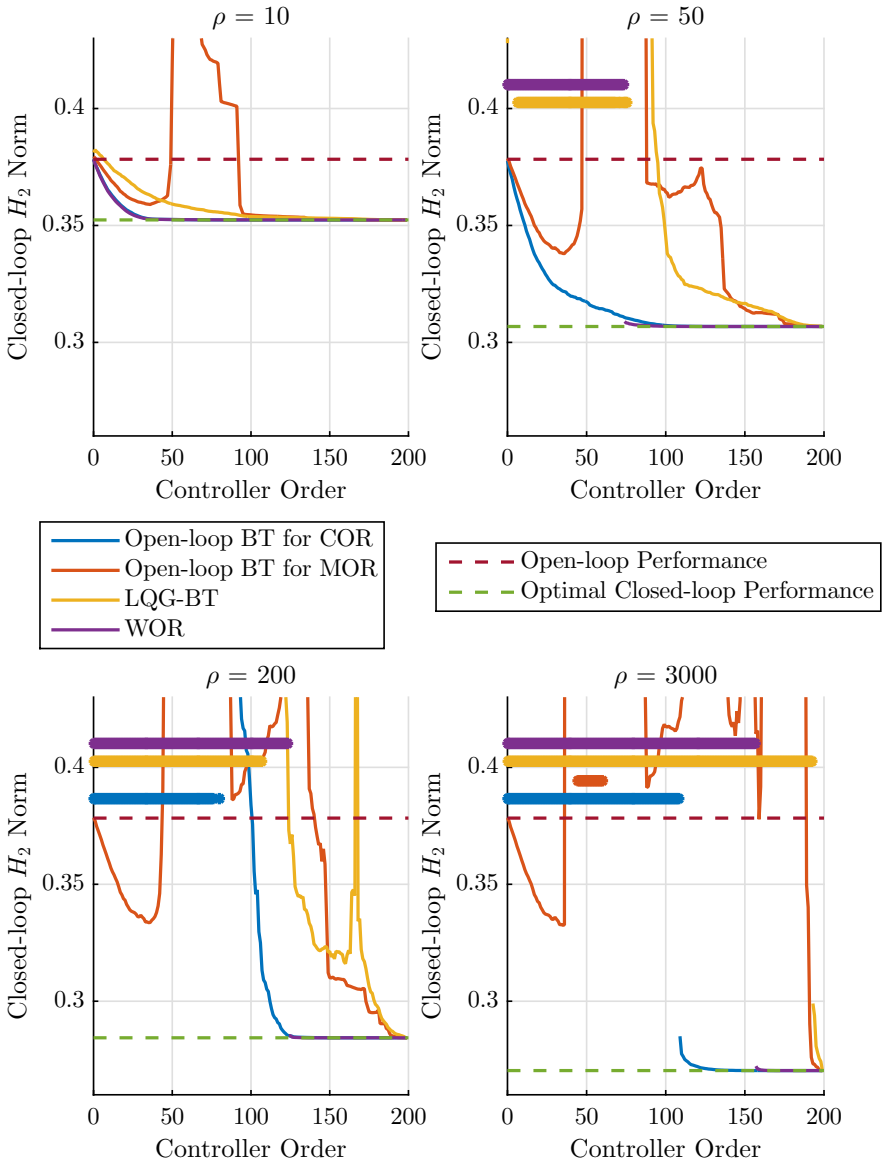

Figure 4.5: The H_2 performance of low order controllers that are designed with several MOR and COR methods for a low gain situation with $\rho = 10$, a moderate gain situation with $\rho = 50$, a high gain situation with $\rho = 200$ and an extremely high gain situation with $\rho = 3000$. A star is used to indicate that the low order controller does not result in an internally stable closed-loop interconnection.

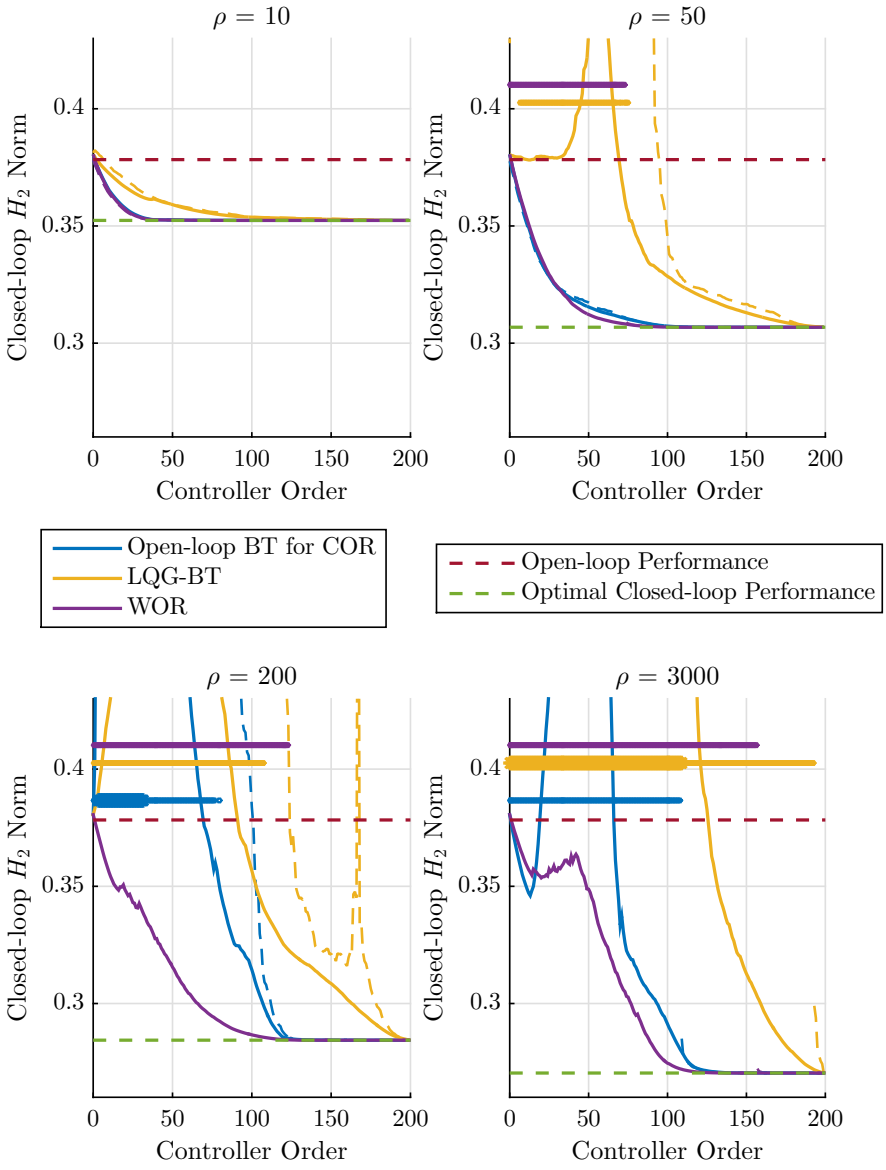

Figure 4.6: The H_2 performance of low order controllers that are designed by using a greedy search with $\epsilon_i = 0$ for several MOR and COR methods in a low gain situation with $\rho = 10$, a moderate gain situation with $\rho = 50$, a high gain situation with $\rho = 200$ and an extremely high gain situation with $\rho = 3000$. A star is used to indicate that the low order controller does not result in an internally stable closed-loop interconnection. To provide a comparison: the performance of the original truncation methods as depicted in figure 4.5 is included as a dashed line and instability is denoted by a small circle.

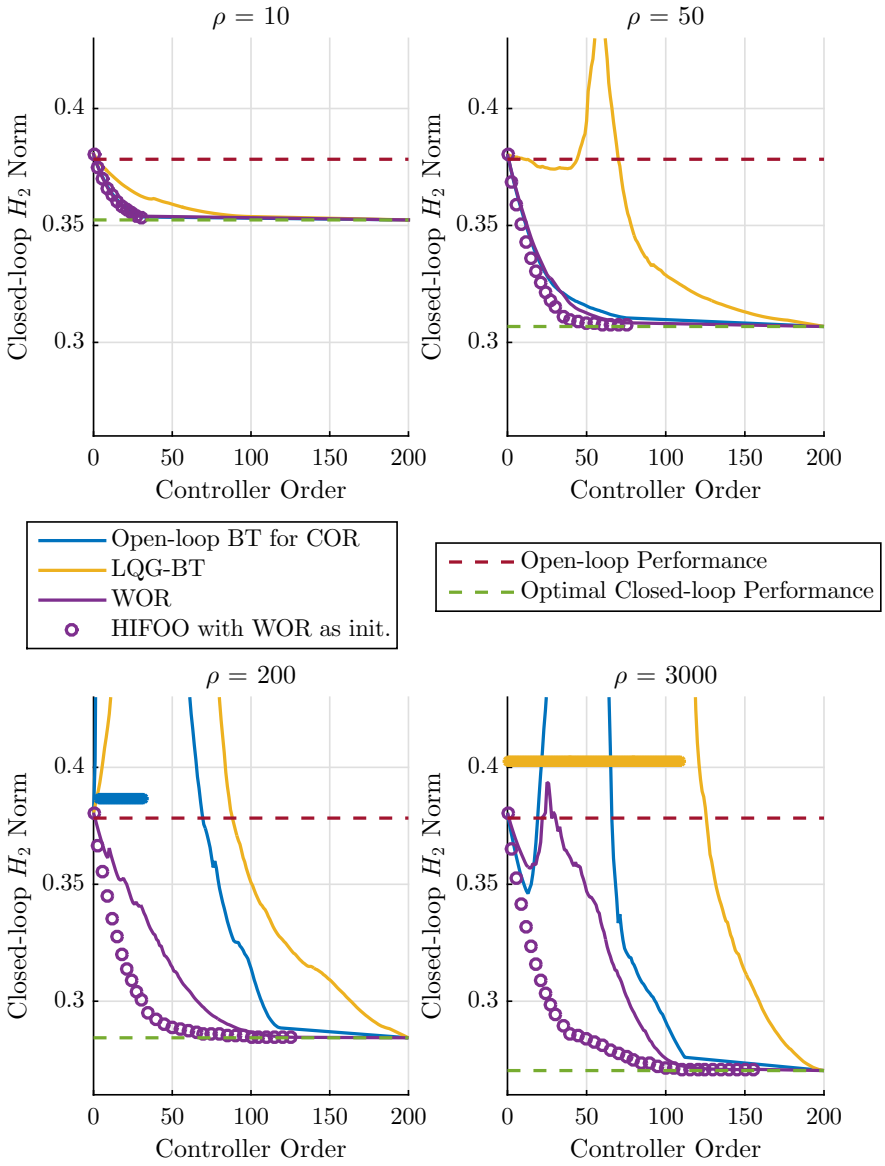

Figure 4.7: The H_2 performance of low order controllers that are designed by using a greedy search with $\epsilon_{i,r} = 0.05$ for several MOR and COR methods in a low gain situation with $\rho = 10$, a moderate gain situation with $\rho = 50$, a high gain situation with $\rho = 200$ and an extremely high gain situation with $\rho = 3000$. In addition, the greedy search combined with WOR is used to provide an initial controller to the HIFOO algorithm.

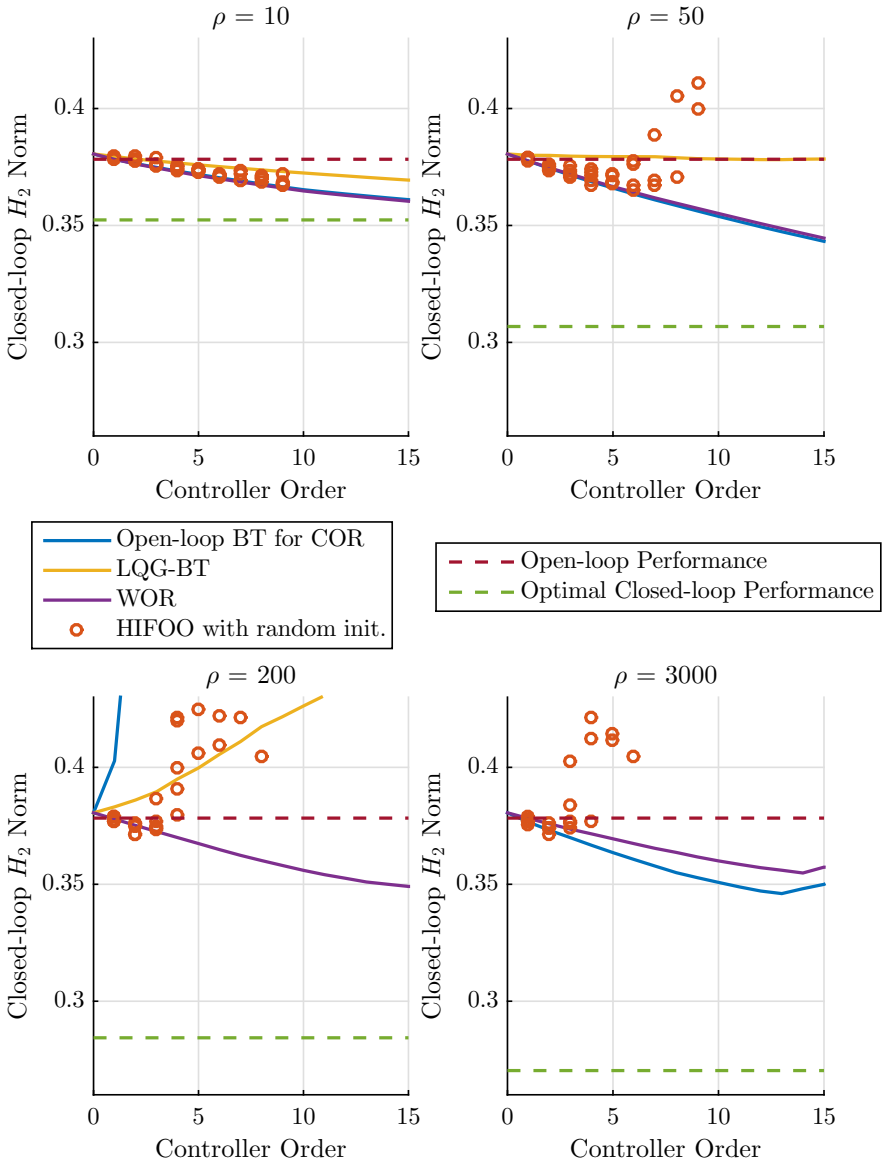

Figure 4.8: The H_2 performance of low order controllers that are constructed with the HIFOO algorithm on the basis of three random initial controllers in a low gain situation with $\rho = 10$, a moderate gain situation with $\rho = 50$, a high gain situation with $\rho = 200$ and an extremely high gain situation with $\rho = 3000$. The results for the greedy truncation methods as depicted in figure 4.6 are included to provide a comparison.

There is nothing more practical than a good theory.
Kurt Lewin

5

Minimal Order Optimal Estimation and Control

In this chapter, we aim at characterising all controller orders for which the H_2 optimal control problem—as described in section 2.4—can be solved. Such a characterisation can be used to solve the minimal order optimal control problem in Problem 1.4 and, in addition, to partially solve the constrained order optimal control problem in Problem 1.3.

For this purpose, the design of constrained order controllers (and estimators) is first investigated for disturbance decoupling problems; the results of this investigation are novel and are based on [Merks et al., 2019] and [Merks and Weiland, 2019a]. Then, by utilising the well-known relation between optimal control problems and disturbance decoupling problems, a first step is taken towards numerically characterising these orders and, in addition, to synthesise the corresponding constrained order H_2 optimal controller.

The approach that is considered in this chapter, essentially exploits the non-uniqueness in the design of optimal controllers for the purpose of constrained order controller synthesis. Such an approach is fundamentally different from chapter 4, where the control design is considered to be fixed.

5.1 Introduction

The optimal control problem in Problem 1.1 has—as mentioned in section 1.2.4—received a considerable amount of attention over the past decades. Today, its solution is well-known for several norms. For example, the design procedure for H_2 and H_∞ optimal controllers is known to most control engineers. The resulting optimal controllers are, however, of the same order as the model that is used in its design. The synthesis and real-time implementation of these controllers may therefore be hampered when a model or large order is used—as discussed in section 4.1—and for these models it is more appropriate to consider the constrained order optimal control problem in Problem 1.3 instead.

In chapter 4 it is shown that the problem of designing constrained order H_2 optimal controllers is not solved with existing MOR or COR techniques. This implies that an order reduction approach does not generally provide a solution to Problem 1.3 and instead of solving this problem, improvements to existing techniques are proposed. Simulation results demonstrate that these improved techniques perform well in most practical situations, although this cannot be guaranteed.

By investigating the design of constrained order controllers from a control perspective, a fundamentally different approach can be considered. Namely, the non-uniqueness in the design of optimal controllers can be exploited for the purpose of constrained order controller design, while the control design is considered to be fixed with order reduction. Furthermore, Saberi et al. [1995a, Sec. 9.4] did show that a reduced order H_2 optimal controller—i.e. with $n_c < n_x$—can be considered for the so-called singular H_2 optimal control problem. This result can, however, not be used for the "regular" H_2 optimal control problem—that is, under assumption 2.1—as discussed in this thesis.

To explain this, it must first be mentioned that the singular H_2 optimal control problem allows the existence of "noise-free measurements"—i.e. the disturbance $w(t)$ does not have to affect all measured outputs $y(t)$ through the mapping D_{wy}. These measurement will therefore provide *direct* information about certain states of the system. And for this reason we can remove up to $n_y - \dim(\mathrm{im}(D_{wy}))$ controller states without affecting the performance of the internal state observer. However, under assumption 2.1 it is required that $\dim(\mathrm{im}(D_{wy})) = n_y$ and therefore no states can be removed with this method.

In this chapter, we aim at characterising all controller orders for which the "regular" H_2 optimal control problem can be solved. For this purpose, the non-uniqueness in the design of optimal controllers is exploited. Such a characterisation can potentially provide a solution to the minimal order optimal control problem in Problem 1.4. Furthermore, it is important to note that the solution to this minimal order problem is a solution to the constrained order control problem in Problem 1.3 for all orders $n_r \geq n_r^\star$.

5.1.1 Exploiting the Non-Uniqueness in the Design of Optimal Controllers

The H_2 optimal control problem is solved in section 2.4 by utilising the unique stabilising solutions to AREs. It is, however, observed by Iwasaki and Skelton [1994] and by Saberi et al. [1996] that the solution to this optimal control problem is non-unique in general.

To provide some intuition as to why this solution is non-unique, let us consider the design of an H_2 optimal state feedback $u(t) = F^\star x(t)$ as an example. In section 2.4 we saw under assumptions 2.1 and 2.2, that the H_2 optimal feedback $u(t) = -B_u^\top P^+ x(t)$ achieves H_2 optimal performance. This unique and optimal feedback is created completely independent of the mapping B_w, which implies that it must be optimal for *any* mapping B_w. Uniqueness of the solution is a result of this specific property, while optimal performance can be obtained with a larger class of feedbacks when a specific mapping B_w is considered.

In other words, the unique solution $u(t) = -B_u^\top P^+ x(t)$ is optimal for all mappings B_w, while for a given mapping B_w it is, in general, possible to construct a different state feedback $u(t) = F^\star x(t)$ that achieves H_2 optimal performance as well. Non-uniqueness can, in a similar fashion, be observed for the problem of designing H_2 optimal measurement feedback controllers (or estimators).

5.1.2 Minimal Order Optimal Controller Synthesis by using Disturbance Decoupling

It is, however, not directly obvious how this non-uniqueness can be exploited for constrained order controller design. In this chapter we will utilise the close relation between the H_2 optimal control problem and disturbance decoupling problems—as discussed in great detail by Saberi et al. [1995a], Stoorvogel [2000] and Trentelman et al. [2001]—for this purpose.

This close relation can be observed from Theorem 2.33, which states that any H_2 optimal controller $\Sigma^\star_{c,n_c}$ for the system Σ (2.14) essentially renders the H_2 norm of the interconnection between Σ_{PQ} (2.36) and $\Sigma^\star_{c,n_c}$ equal to 0; this is equivalent to achieving disturbance decoupling.

It was first observed by Schumacher [1980, Thm. 3.1] that it is possible to determine the *minimal* required controller order for disturbance decoupling problems without stability requirements. This observation was repeated by Stoorvogel and van der Woude [1991], while mentioning that a similar result is not known when stability requirements are included. The problem did receive some attention thereafter from Basile and Marro [1992], Mutsaers and Weiland [2011] and Mutsaers [2012]; however, a complete solution has never been found.

From a constrained order optimal control perspective, it is therefore directly relevant to consider the design of constrained order controllers for disturbance decoupling problems. Namely, the solution to these disturbance decoupling problems can be used to characterise the controller orders for which H_2 optimal performance

can be achieved and, in addition, to synthesise the corresponding constrained order controller.

5.1.3 Chapter Outline

In this chapter we will consider, again, an LTI system of the form

$$\Sigma = \begin{cases} \dot{x}(t) = Ax(t) + B_u u(t) + B_w w(t) \\ y(t) = C_y x(t) + D_{wy} w(t) \\ z(t) = C_z x(t) + D_{uz} u(t), \end{cases} \tag{5.1}$$

with vector signals $x(t)$, $u(t)$, $w(t)$, $y(t)$ and $z(t)$ that represent the state, known input, unknown disturbance, measured output and the control output, respectively. These signals assume values in finite-dimensional vector spaces $\mathcal{X} = \mathbb{R}^{n_x}$, $\mathcal{U} = \mathbb{R}^{n_u}$, $\mathcal{W} = \mathbb{R}^{n_w}$, $\mathcal{Y} = \mathbb{R}^{n_y}$ and $\mathcal{Z} = \mathbb{R}^{n_z}$, respectively. The dynamical relation between the signals is described by real-valued matrices A, B_u, B_w, C_y, C_z, D_{wy} and D_{uz} of appropriate dimension.

For control problems it is often desired to achieve closed-loop stability; we will therefore utilise the stability domain $\mathbb{C}_g$—as introduced in section 2.1.1 —in this chapter. Furthermore, we say that the system Σ (5.1) is $\mathbb{C}_g$-stabilisable if the pair (A, B_u) is $\mathbb{C}_g$-stabilisable, while we say that the system Σ (5.1) is $\mathbb{C}_g$-detectable if the pair (C_y, A) is $\mathbb{C}_g$-detectable.

In section 5.2 we will first consider the problem of constructing an estimator with a constrained order that decouples the output estimation errors from the disturbances that are acting on the system, while stabilising the underlying error dynamics. In addition, it is investigated under what conditions, for which orders and how this problem can numerically be solved.

Then, in section 5.3 the results from section 5.2 are extended in order to address the problem of constructing a measurement feedback controller with a constrained order. This controller aims at decoupling the control outputs from the disturbances that are acting in the system, while simultaneously rendering the closed-loop system internally stable. Furthermore, it is, again, investigated under what conditions, for which orders and how this problem can numerically be solved.

Finally, in section 5.4 we will discuss the problem of designing H_2 optimal measurement feedback controllers and estimators. These problems are solved by utilising the relation between disturbance decoupling problems and optimal control problems to directly apply the results from sections 5.3 and 5.2. In addition, an equivalence is established between several properties of the optimal control problems—for example, the separation principle—and their corresponding disturbance decoupling problem.

The conclusions and future work are discussed in chapter 7.

5.2 The Disturbance Decoupled Estimation Problem with a Constrained Order Estimator[1]

5.2.1 Problem Definition and Section Outline

In section 5.2, let us consider the design of an estimator

$$\Sigma_{e,n_e} = \begin{cases} \dot{x}_e(t) &= Jx_e(t) + Ky(t) + K_u u(t) \\ \tilde{z}(t) &= Mx_e(t) + Ny(t) + N_u u(t) \end{cases} \tag{5.2}$$

that produces an estimated output $\tilde{z}(t)$ for the "to-be-estimated output" $z(t)$ of the system Σ (5.1). Any estimation problem consists of appropriately selecting the mappings J, K, K_u, M, N and N_u of Σ_{e,n_e} (5.2). Such a problem is—as explained in section 2.4—often formulated by defining the output estimation error $\epsilon_z(t) = z(t) - \tilde{z}(t)$ in order to obtain the error system $\Sigma_{\epsilon,n_e} =$

$$\begin{cases} \begin{pmatrix} \dot{x}(t) \\ \dot{x}_e(t) \end{pmatrix} = \begin{pmatrix} A & 0 \\ KC_y & J \end{pmatrix} \begin{pmatrix} x(t) \\ x_e(t) \end{pmatrix} + \begin{pmatrix} B_u \\ K_u \end{pmatrix} u(t) + \begin{pmatrix} B_w \\ KD_{wy} \end{pmatrix} w(t) \\ \epsilon_z(t) = \begin{pmatrix} C_z - NC_y & -M \end{pmatrix} \begin{pmatrix} x(t) \\ x_e(t) \end{pmatrix} + \begin{pmatrix} D_{uz} - N_u \end{pmatrix} u(t) + \begin{pmatrix} -ND_{wy} \end{pmatrix} w(t). \end{cases} \tag{5.3}$$

This error system has an extended state $x^{\epsilon,n_e}(t) = \begin{pmatrix} x(t) \\ x_e(t) \end{pmatrix}$ and extended system matrices A^{ϵ,n_e}, B_u^{ϵ,n_e}, B_w^{ϵ,n_e}, C_z^{ϵ,n_e}, D_{uz}^{ϵ,n_e} and D_{wz}^{ϵ,n_e}. Its extended state-space is characterised by the vector space $\mathcal{X}^{\epsilon,n_e}$.

In section 5.2 we will address the problem of constructing (if it exists) an estimator Σ_{e,n_e} (5.2) with a constrained order that decouples the output estimation error $\epsilon_z(t)$ of Σ_{ϵ,n_e} (5.3) from the input signals $u(t)$ and $w(t)$. These signals are, from an estimation perspective, both viewed as disturbances and a distinction is made by assuming that the signal $u(t)$ is known, while $w(t)$ is unknown.

It is important to note that unobservable or unreachable states do not contribute towards the input to output behaviour of Σ (5.1). These states can therefore be disregarded when an estimation problem is considered and the following assumption is made throughout section 5.2.

Assumption 5.1 *It is assumed in section 5.2 that any state of* Σ (5.1) *can be reached through the pair* $(u(t), w(t))$ *and observed in the pair* $(y(t), z(t))$.

The main problem that will be addressed in section 5.2 is the *disturbance decoupled estimation problem with stability using a constrained order estimator* (DDEPS-CO). The DDEPS-CO cannot, in general, be solved for all systems and estimator orders. We will therefore also investigate under which conditions the DDEPS-CO can be solved.

[1] Section 5.2 is based on the journal article: R. W. H. Merks, E. M. M. Kivits and S. Weiland. Constrained Order Observer Design for Disturbance Decoupled Output Estimation. *IEEE Control Systems Letters*, 3(1):49-54, 2019. ISSN 2475-1456. doi: 10.1109/LCSYS.2018.2851539

Definition 5.1 *Consider a stability domain $\mathbb{C}_g$, a number $n_e \in \mathbb{N}$ and let $\mathcal{N} \subseteq \mathcal{X}^{\epsilon,n_e}$ denote the unobservable subspace of Σ_{ϵ,n_e} (5.3) for a given estimator Σ_{e,n_e} (5.2).*

Then Σ_{e,n_e} (5.2) of order n_e "solves" the DDEPS-CO for (Σ (5.1), n_e, $\mathbb{C}_g$) if the output estimation error $\epsilon_z(t) = z(t) - \hat{z}(t)$ of Σ_{ϵ,n_e} (5.3) is independent of input $u(t)$ and disturbance $w(t)$, while $\lambda(A^{\epsilon,n_e}|(\mathcal{X}^{\epsilon,n_e} \bmod \mathcal{N})) \subseteq \mathbb{C}_g$.

We say that the DDEPS-CO "can be solved" for (Σ (5.1), n_e, $\mathbb{C}_g$) if such an estimator exists.

Remark 5.1 *For estimation problems, stability is included to impose that $\lim_{t\to\infty} \epsilon_z(t) = 0$ for any initial condition. For this reason it is only required that the observable dynamics of Σ_{ϵ,n_e} (5.3) are stable.*

Furthermore, it is important to note that $\lambda(A^{\epsilon,n_e}|(\mathcal{X}^{\epsilon,n_e} \bmod \mathcal{N}))$ is well-defined, because the unobservable subspace $\mathcal{N}$ satisfies $A^{\epsilon,n_e}\mathcal{N} \subseteq \mathcal{N}$.

In section 5.2.2 we will first discuss the known solution to the disturbance decoupled estimation problem with stability (DDEPS). Furthermore, an extension is added in order to characterise *all* estimators Σ_{e,n_e} (5.2) that can solve the problem.

This characterisation is used in section 5.2.3 to solve the DDEPS-CO. Conditions on the estimator order are presented in section 5.2.4 and a numerical procedure to explicitly construct a constrained order estimator is given in section 5.2.5. Finally, an illustrative example is presented in section 5.2.6.

5.2.2 The Disturbance Decoupled Estimation Problem with Stability

For any stability domain $\mathbb{C}_g$, let $\mathcal{S}_g$ be an input-containing $\mathbb{C}_g$-detectability subspace and $\mathcal{S}_g^\star$ the $\mathbb{C}_g$-detectable strongly reachable subspace as defined in Lemma 2.42 and Theorem 2.43, respectively.

A specific type of estimator is the so-called Luenberger state observer with estimated output

$$\Sigma_o = \begin{cases} \dot{\tilde{x}}(t) = \left(A + LC_y\right)\tilde{x}(t) - Ly(t) + B_u u(t) \\ \tilde{z}(t) = M\tilde{x}(t) + Ny(t) + D_{uz}u(t) \end{cases} \tag{5.4}$$

of order n_x and with design parameters $L : \mathcal{Y} \to \mathcal{X}$, $M : \mathcal{X} \to \mathcal{Z}$ and $N : \mathcal{Y} \to \mathcal{Z}$. Consider Σ (5.1) connected to Σ_o (5.4), the output estimation error $\epsilon_z(t) = z(t) - \tilde{z}(t)$ and define a state observation error $e(t) = x(t) - \tilde{x}(t)$ to obtain the error system

$$\Sigma_\epsilon = \left\{ \begin{array}{l} \begin{pmatrix} \dot{x}(t) \\ \dot{e}(t) \end{pmatrix} = \begin{pmatrix} A & 0 \\ 0 & A + LC_y \end{pmatrix} \begin{pmatrix} x(t) \\ e(t) \end{pmatrix} + \begin{pmatrix} B_u \\ 0 \end{pmatrix} u(t) + \begin{pmatrix} B_w \\ B_w + LD_{wy} \end{pmatrix} w(t) \\ \epsilon_z(t) = \begin{pmatrix} C_z - NC_y - M & M \end{pmatrix} \begin{pmatrix} x(t) \\ e(t) \end{pmatrix} + \left(-ND_{wy}\right) w(t). \end{array} \right. \tag{5.5}$$

This system has an extended state $x^\epsilon(t) = \begin{pmatrix} x(t) \\ e(t) \end{pmatrix}$ and extended system matrices A^ϵ, B_u^ϵ, B_w^ϵ, C_z^ϵ and D_{uz}^ϵ. Its extended state-space is characterised by the vector space $\mathcal{X}^\epsilon$.

With the following proposition we will establish when Σ_ϵ (5.5) can be disturbance decoupled and that it is non-restrictive to consider Σ_o (5.4).

Proposition 5.2 *Consider a stability domain $\mathbb{C}_g$, the subspace $\mathcal{S}_g^\star \subseteq \mathcal{X}$ as defined in Theorem 2.43 and let $\mathcal{N} \subseteq \mathcal{X}^{\epsilon,n_e}$ denote the unobservable subspace of Σ_{ϵ,n_e} (5.3) for a given estimator Σ_{e,n_e} (5.2).*

Then there exists an estimator Σ_{e,n_e} (5.2) for Σ (5.1) such that the output estimation error $\epsilon_z(t) = z(t) - \hat{z}(t)$ of Σ_{ϵ,n_e} (5.3) is independent of input $u(t)$ and disturbance $w(t)$, while $\lambda(A^{\epsilon,n_e}|(\mathcal{X}^{\epsilon,n_e} \bmod \mathcal{N})) \subseteq \mathbb{C}_g$ if and only if

$$\mathcal{S}_g^\star \cap C_y^{-1}\mathrm{im}(D_{wy}) \subseteq \ker(C_z).$$

When this condition is satisfied, an observer of the form Σ_o (5.4) can be considered for this purpose.

Proof: The proof can be found in appendix A.3. □

The DDEPS therefore consists of finding the mappings L, M and N for Σ_o (5.4) such that $\epsilon(z)$ of Σ_ϵ (5.5) is independent of $u(t)$ and $w(t)$; whether this can be achieved is strongly related to the subspace $\mathcal{S}_g^\star$. This subspace has, as a result, been thoroughly investigated in geometric control theory—for example, by Wonham [1985], Basile and Marro [1992] and Trentelman et al. [2001]. Furthermore, Marro [2018] and Chen [2018] developed several algorithms that can construct a numerical representation for this subspace.

We will, however, see in section 5.2.3 that the dimension of certain input-containing $\mathbb{C}_g$-detectability subspaces $\mathcal{S}_g$ determines the orders for which the DDEPS-CO can be solved. To characterise these orders, let us therefore consider the set

$$\begin{aligned} \mathbb{S}_g(\Sigma) = \{\ \mathcal{S}_g \subseteq \mathcal{X} \quad | \quad & \mathcal{S}_g \text{ is as defined in Lemma 2.42,} \\ & \mathcal{S}_g \cap C_y^{-1}\mathrm{im}(D_{wy}) \subseteq \ker(C_z)\}\,, \end{aligned} \tag{5.6}$$

for which the functional dependency on Σ is omitted when it is clear what system is implied.

First, we will relate Proposition 5.2 to the set $\mathbb{S}_g$.

Lemma 5.3 *Consider a stability domain $\mathbb{C}_g$ and let $\mathcal{N} \subseteq \mathcal{X}_\epsilon$ denote the unobservable subspace of Σ_ϵ (5.5) for a given observer Σ_o (5.4).*

Then there exist mappings $L : \mathcal{Y} \to \mathcal{X}$, $M : \mathcal{X} \to \mathcal{Z}$ and $N : \mathcal{Y} \to \mathcal{Z}$ such that the output estimation error $\epsilon_z(t) = z(t) - \hat{z}(t)$ of Σ_ϵ (5.5) is independent of input $u(t)$ and disturbance $w(t)$, while $\lambda(A^\epsilon|(\mathcal{X}^\epsilon \bmod \mathcal{N})) \subseteq \mathbb{C}_g$ if and only if $\mathbb{S}_g(\Sigma\ (5.1)) \neq \emptyset$.

Proof: ($\Rightarrow$) In Proposition 5.2 it is established that these mappings exist if $\mathcal{S}_g^\star \cap C_y^{-1}\text{im}(D_{wy}) \subseteq \ker(C_z)$, which implies that $\mathcal{S}_g^\star \in \mathbb{S}_g$ and therefore $\mathbb{S}_g \neq \emptyset$.

($\Leftarrow$) If $\mathbb{S}_g \neq \emptyset$, then there exists a subspace $\mathcal{S}_g \in \mathbb{S}_g$. By definition we have that $\mathcal{S}_g^\star \subseteq \mathcal{S}_g$, which implies that $\mathcal{S}_g^\star \in \mathbb{S}_g$ as well. This subspace will therefore satisfy the condition in Proposition 5.2, which completes the proof. □

Lemma 5.3 actually states that $\mathbb{S}_g$ is non-empty if and only if $\mathcal{S}_g^\star \in \mathbb{S}_g$. Σ_ϵ (5.5) can therefore be disturbance decoupled if and only if $\mathbb{S}_g$ is non-empty. We will now relate the DDEPS to the entire set $\mathbb{S}_g$, since such a relation is used in section 5.2.3 to characterise all orders for which the DDEPS-CO can be solved. For this purpose, let us consider the following formal definition for the DDEPS.

Definition 5.4 *Consider a stability domain $\mathbb{C}_g$ and let $\mathcal{N} \subseteq \mathcal{X}^\epsilon$ denote the unobservable subspace of Σ_ϵ (5.5) for a given observer Σ_o (5.4).*

Then Σ_o (5.4) "solves" the DDEPS for (Σ (5.1), $\mathcal{S}_g$, $\mathbb{C}_g$) if the output estimation error $\epsilon_z(t) = z(t) - \hat{z}(t)$ of Σ_ϵ (5.5) is independent of input $u(t)$ and disturbance $w(t)$, while $\lambda(A^\epsilon|(\mathcal{X}^\epsilon \bmod \mathcal{N})) \subseteq \mathbb{C}_g$. Furthermore, for Σ_ϵ (5.5) it holds that $e(t) \in \mathcal{S}_g$ for all $t \geq 0$ and for any triple $(x(t), u(t), w(t))$, provided that $e(0) = e_0 \in \mathcal{S}_g$.

We say that the DDEPS "can be solved" for (Σ (5.1), $\mathcal{S}_g$, $\mathbb{C}_g$) if such an observer exists.

An observer can be designed for Σ (5.1) on the basis of any system that is equivalent in terms of input to output behaviour. Let us now define a specific representation of Σ (5.1) in order to provide an intuitive interpretation for the solution to the DDEPS.

With a subspace $\mathcal{S}_g \in \mathbb{S}_g$, the state-space $\mathcal{X}$ of Σ (5.1) can be decomposed as

$$\mathcal{X} = \mathcal{S}_g \oplus \mathcal{S}_{g,c}, \tag{5.7}$$

where $\mathcal{S}_{g,c}$ is a complement of $\mathcal{S}_g$.

For a given subspace $\mathcal{S}_g \in \mathbb{S}_g$, let $T_{e,g}$ be a state transformation that transforms Σ (5.1) into the system

$$\Sigma^{T_{e,g}} = \left\{ \begin{array}{rcl} \begin{pmatrix} \dot{x}_1(t) \\ \dot{x}_2(t) \end{pmatrix} & = & \begin{pmatrix} A_{11} & A_{12} \\ A_{21} & A_{22} \end{pmatrix} \begin{pmatrix} x_1(t) \\ x_2(t) \end{pmatrix} + \begin{pmatrix} B_{u1} \\ B_{u2} \end{pmatrix} u(t) + \begin{pmatrix} B_{w1} \\ B_{w2} \end{pmatrix} w(t) \\ y(t) & = & \begin{pmatrix} C_{y1} & C_{y2} \end{pmatrix} x(t) + D_{wy} w(t) \\ z(t) & = & \begin{pmatrix} C_{z1} & C_{z2} \end{pmatrix} x(t) + D_{uz} u(t), \end{array} \right. \tag{5.8}$$

which is compatible to the decomposition in (5.7). In other words, the state-space $\mathcal{X} = \mathcal{X}_1 \oplus \mathcal{X}_2$ of $\Sigma^{T_{e,g}}$ (5.8) is partitioned in such a way that $\mathcal{X}_1 = T_{e,g}\mathcal{S}_g$ and $\mathcal{X}_2 = T_{e,g}\mathcal{S}_{g,c}$.

By applying to $\Sigma^{T_{e,g}}$ (5.8), the observer Σ_o (5.4) with an identical state partitioning, the following error system is obtained:

$$\Sigma_\epsilon^{T_{e,g}} = \left\{ \begin{array}{l} \left(\begin{array}{c} \dot{x}_1(t) \\ \dot{x}_2(t) \\ \hline \dot{e}_1(t) \\ \dot{e}_2(t) \end{array}\right) = \left(\begin{array}{cc|cc} A_{11} & A_{12} & 0 & 0 \\ A_{21} & A_{22} & 0 & 0 \\ \hline 0 & 0 & A_{11}+L_1C_{y1} & A_{12}+L_1C_{y2} \\ 0 & 0 & \mathbf{A_{21}+L_2C_{y1}} & A_{22}+L_2C_{y2} \end{array}\right) \left(\begin{array}{c} x_1(t) \\ x_2(t) \\ \hline e_1(t) \\ e_2(t) \end{array}\right) \\ \qquad\qquad + \left(\begin{array}{c} B_{u1} \\ B_{u2} \\ \hline 0 \\ 0 \end{array}\right) u(t) + \left(\begin{array}{c} B_{w1} \\ B_{w2} \\ \hline B_{w1}+L_1D_{wy} \\ \mathbf{B_{w2}+L_2D_{wy}} \end{array}\right) w(t) \\ \epsilon_z(t) \;= \Big(\mathbf{C_{z1}-NC_{y1}-M_1} \quad \mathbf{C_{z2}-NC_{y2}-M_2} \;\Big|\; \mathbf{M_1} \quad M_2\Big) \left(\begin{array}{c} x(t) \\ \hline e(t) \end{array}\right) \\ \qquad\qquad - \Big(\mathbf{ND_{wy}}\Big)\, w(t). \end{array} \right. \tag{5.9}$$

In the following theorem we will see how the DDEPS is solved for (Σ (5.1), $\mathcal{S}_g$, $\mathbb{C}_g$) by an observer Σ_o (5.4). The mappings L, M and N of this observer are—for $\Sigma^{T_{e,g}}$ (5.8)—essentially chosen such that all bold-font mappings in $\Sigma_\epsilon^{T_{e,g}}$ (5.9) vanish and such that $\lambda(A_{22}+L_2C_{y2}) \subseteq \mathbb{C}_g$. This representation is therefore convenient for numerical implementation, while additionally providing an intuitive interpretation for the solution to the problem.

Theorem 5.5 *Consider a stability domain $\mathbb{C}_g$ and a subspace $\mathcal{S}_g \in \mathbb{S}_g$.*

Then Σ_o (5.4) "solves" the DDEPS for (Σ (5.1), $\mathcal{S}_g$, $\mathbb{C}_g$) if and only if the mappings $L : \mathcal{Y} \to \mathcal{X}$, $M : \mathcal{X} \to \mathcal{Z}$ and $N : \mathcal{Y} \to \mathcal{Z}$ satisfy

$$\begin{array}{l} (A+LC_y)\mathcal{S}_g \subseteq \mathcal{S}_g, \quad \mathrm{im}(B_w+LD_{wy}) \subseteq \mathcal{S}_g, \\ C_z - NC_y - M = 0, \quad M\mathcal{S}_g = 0, \quad ND_{wy} = 0, \\ \lambda((A+LC_y)|(\mathcal{X} \bmod \mathcal{S}_g)) \subseteq \mathbb{C}_g. \end{array} \tag{5.10}$$

Proof: The proof can be found in appendix A.3. □

Finally, in the following corollary we will show that the solution to the DDEPS is indeed linked to the entire set $\mathbb{S}_g$ by considering Definition 5.4.

Corollary 5.6 *Consider a stability domain $\mathbb{C}_g$.*

Then the DDEPS "can be solved" for (Σ (5.1), $\mathcal{S}_g$, $\mathbb{C}_g$) if and only if $\mathcal{S}_g \in \mathbb{S}_g$.

Proof: The proof can be found in appendix A.3. □

5.2.3 The Disturbance Decoupled Estimation Problem with Stability using a Constrained Order Estimator

In Corollary 5.6 it is established that the solution to the DDEPS is related to the subspaces $\mathcal{S}_g \in \mathbb{S}_g$. To solve the problem for a given subspace, it is shown in Theorem 5.5 that the mappings of the observer Σ_o (5.4) should satisfy $(A + LC_y)\mathcal{S}_g \subseteq \mathcal{S}_g$ and $M\mathcal{S}_g = 0$. These two conditions actually imply that the observer states $\tilde{x} \in \mathcal{S}_g$ are unobservable in the observer output $\tilde{z}(t)$, which tells us that these estimator states can be removed.

In view of the state decomposition in (5.7), consider $\Pi_c = \Pi(\mathcal{S}_{g,c}, \mathcal{S}_g)$ to define

$$\hat{J} = (\Pi_c A + L_c C_y)|\mathcal{S}_{g,c}, \quad \hat{K} = -L_c \text{ and } \hat{K}_u = \Pi_c B_u,$$

which depend on the mapping $L_c : \mathcal{Y} \to \mathcal{S}_{g,c}$.

We now claim that the reduced order observer

$$\widehat{\Sigma}_o = \begin{cases} \dot{\tilde{x}}_o(t) = \hat{J}\tilde{x}_o(t) + \hat{K}y(t) + \hat{K}_u u(t) \\ \tilde{z}(t) = \hat{M}\tilde{x}_o(t) + Ny(t) + D_{uz}u(t). \end{cases} \tag{5.11}$$

of order $n_e = \dim(\mathcal{X}) - \dim(\mathcal{S}_g)$ will be able to solve the DDEPS-CO for appropriate mappings $L_c : \mathcal{Y} \to \mathcal{S}_{g,c}$, $\hat{M} : \mathcal{S}_{g,c} \to \mathcal{Z}$ and $N : \mathcal{Y} \to \mathcal{Z}$; this will be established in Theorem 5.8.

Proposition 5.7 *Consider a stability domain $\mathbb{C}_g$ and a number $n_e \in \mathbb{N}$.*

Then the DDEPS-CO "can be solved" for (Σ (5.1), n_e, $\mathbb{C}_g$) if there exists a subspace $\mathcal{S}_g \in \mathbb{S}_g$ with $\dim(\mathcal{X}) - \dim(\mathcal{S}_g) = n_e$.

Proof: In Theorem 5.8 below it will be shown for a given subspace $\mathcal{S}_g \in \mathbb{S}_g$ that the reduced order observer $\widehat{\Sigma}_o$ (5.11) can solve this problem. □

Remark 5.2 *It is important to note that an "only if" statement does not, in general, hold for Proposition 5.7. Namely, we know that $0 \leq \dim(\mathcal{S}_g)$ and such a statement would therefore imply that an estimator of dimension $n_e > n_x$ cannot solve the DDEPS-CO. This, while any number of states that do not affect $\tilde{z}(t)$ can be added to an estimator without affecting the input to output behaviour of the corresponding error system.*

Proposition 5.7 states that the orders n_e for which the DDEPS-CO can be solved are related to the dimension of subspaces $\mathcal{S}_g \in \mathbb{S}_g$. By considering the subspace $\mathcal{S}_g^\star \in \mathbb{S}_g$—which by definition satisfies $\dim(\mathcal{S}_g^\star) \subseteq \dim(\mathcal{S}_g)$—an "unnecessarily large" estimator could therefore be created, while it is often desired to create an estimator of minimal order. For this specific reason, the solution to the DDEPS was related to the entire set $\mathbb{S}_g$ in section 5.2.2.

Before formally solving the DDEPS-CO, consider again the equivalent system $\Sigma^{T_{e,g}}$ (5.8) that is created for a given subspace $\mathcal{S}_g \in \mathbb{S}_g$ by utilising the decomposition in (5.7). The reduced order observer $\widehat{\Sigma}_o$ (5.11) is for $\Sigma^{T_{e,g}}$ (5.8) explicitly described as

$$\widehat{\Sigma}_o^{T_{e,g}} = \begin{cases} \dot{\tilde{x}}_2(t) = \left(A_{22} + L_2 C_{y2}\right) \tilde{x}_2(t) - L_2 y(t) + B_{u2} u(t) \\ \tilde{z}(t) = M_2 \;\; \tilde{x}_2(t) + N y(t) + D_{uz} u(t), \end{cases} \tag{5.12}$$

where $\tilde{x}_o(t)$ and L_c of $\widehat{\Sigma}_o$ (5.11) are described by $\tilde{x}_2(t)$ and L_2 in $\widehat{\Sigma}_o^{T_{e,g}}$ (5.12), respectively. Applying $\widehat{\Sigma}_o^{T_{e,g}}$ (5.12) to $\Sigma^{T_{e,g}}$ (5.8) results in the error system

$$\widehat{\Sigma}_\epsilon^{T_{e,g}} = \begin{cases} \left(\begin{array}{c} \dot{x}_1(t) \\ \dot{x}_2(t) \\ \hline \dot{e}_2(t) \end{array}\right) = \left(\begin{array}{cc|c} A_{11} & A_{12} & 0 \\ A_{21} & A_{22} & 0 \\ \hline \mathbf{A_{21} + L_2 C_{y1}} & 0 & A_{22} + L_2 C_{y2} \end{array}\right) \left(\begin{array}{c} x_1(t) \\ x_2(t) \\ \hline e_2(t) \end{array}\right) \\ \qquad\qquad + \left(\begin{array}{c} B_{u1} \\ B_{u2} \\ \hline 0 \end{array}\right) u(t) + \left(\begin{array}{c} B_{w1} \\ B_{w2} \\ \hline \mathbf{B_{w2} + L_2 D_{wy}} \end{array}\right) w(t) \\ \epsilon_z(t) = \left(\mathbf{C_{z1} - N C_{y1}} \quad \mathbf{C_{z2} - N C_{y2} - M_2} \;\middle|\; M_2\right) \left(\begin{array}{c} x(t) \\ \hline e(t) \end{array}\right) \\ \qquad\qquad - \left(\mathbf{N D_{wy}}\right) w(t), \end{cases} \tag{5.13}$$

for which, again, a bold font is used when mappings can vanish by construction.

In the following theorem we will see how the DDEPS-CO is solved by an observer $\widehat{\Sigma}_o$ (5.11). The observer mappings are, for $\Sigma^{T_{e,g}}$ (5.8), again chosen such that all bold-font mappings in $\widehat{\Sigma}_\epsilon^{T_{e,g}}$ (5.13) vanish.

Theorem 5.8 *Consider a stability domain $\mathbb{C}_g$, a subspace $\mathcal{S}_g \in \mathbb{S}_g$ with $\dim(\mathcal{S}_g) = \dim(\mathcal{X}) - n_e$, the decomposition in (5.7) and define $\Pi_c = \Pi(\mathcal{S}_{g,c}, \mathcal{S}_g)$.*

Then $\widehat{\Sigma}_o$ (5.11) "solves" the DDEPS-CO for (Σ (5.1), n_e, $\mathbb{C}_g$) if the mappings $L_c : \mathcal{Y} \to \mathcal{S}_{g,c}$, $\hat{M} : \mathcal{S}_{g,c} \to \mathcal{Z}$ and $N : \mathcal{Y} \to \mathcal{Z}$ satisfy

$$\begin{array}{ll} (\Pi_c A + L_c C_y)|\mathcal{S}_g = 0, & \Pi_c B_w + L_c D_{wy} = 0, \\ (C_z - N C_y)|\mathcal{S}_g = 0, & (C_z - N C_y)|\mathcal{S}_{g,c} - \hat{M} = 0, \\ N D_{wy} = 0, & \lambda((\Pi_c A + L_c C_y)|\mathcal{S}_{g,c}) \subseteq \mathbb{C}_g. \end{array} \tag{5.14}$$

Proof: The proof can be found in appendix A.3. □

5.2.4 Conditions on the Estimator Order

It is shown in Proposition 5.7 that the dimension of the subspaces $\mathcal{S}_g \in \mathbb{S}_g$ is related to the values n_e for which the DDEPS-CO can be solved. Now let us characterise the *minimal* estimator order n_e^-. In addition, we will see that the observer based architecture $\widehat{\Sigma}_o$ (5.11) is not restrictive in terms of minimising this order.

Theorem 5.9 *Consider a stability domain $\mathbb{C}_g$.*

Then for a given system Σ (5.1), the minimal order for which the DDEPS-CO can be solved is given by

$$n_e^- = \min_{\mathcal{S}_g \in \mathbb{S}_g} \dim(\mathcal{X}) - \dim(\mathcal{S}_g).$$

The reduced order observer $\widehat{\Sigma}_o$ (5.11) can be used to solve the DDEPS-CO for (Σ (5.1), n_e^-, $\mathbb{C}_g$).

Proof: The proof can be found in appendix A.3. □

We can therefore conclude that the minimal estimator order n_e^- is directly determined by the largest dimension of any subspace $\mathcal{S}_g \in \mathbb{S}_g$. However, it is still unclear how small the magnitude of n_e^- can theoretically become.

Theorem 5.10 *For any stability domain $\mathbb{C}_g$ we have that $n_e^- \geq \dim(\mathrm{im}(C_z)) - \dim(\mathrm{im}(C_y))$.*

Proof: A subspace $\mathcal{S}_g \in \mathbb{S}_g$ must satisfy $\dim(\mathcal{S}_g) - \dim(\mathrm{im}(C_y)) \leq \dim(\mathcal{S}_g \cap \ker(C_y)) \leq \dim(\mathcal{S}_g \cap C_y^{-1}\mathrm{im}(D_{wy})) \leq \dim(\ker(C_z)) = \dim(\mathcal{X}) - \dim(\mathrm{im}(C_z))$. This imposes an upper bound $\dim(\mathcal{S}_g) \leq \dim(\mathcal{X}) - \dim(\mathrm{im}(C_z)) + \dim(\mathrm{im}(C_y))$, which combined with $n_e = \dim(\mathcal{X}) - \dim(\mathcal{S}_g)$ implies that $n_e^- \geq \dim(\mathrm{im}(C_z)) - \dim(\mathrm{im}(C_y))$. □

5.2.5 Numerical Construction of the Estimator

In section 2.1 it is explained that a matrix $R \in \mathbb{R}^{n_x \times n_r}$ satisfying $\mathrm{im}(R) = \mathcal{R}$ is a (minimal) numerical representation for the subspace $\mathcal{R}$ of dimension n_r. Furthermore, for this type of representation there exist numerical implementations of all subspace operations.

A numerical procedure to solve the DDEPS(-CO) consists of the following steps:

1. determine a numerical representation for a subspace $\mathcal{S}_g \in \mathbb{S}_g$.
2. a state transformation $T_{e,g}$ is constructed on the basis of this subspace, which transforms the system Σ (5.1) into an equivalent system $\Sigma^{T_{e,g}}$ (5.8).
3. the system $\Sigma^{T_{e,g}}$ (5.8) is used to solve the DDEPS or the DDEPS-CO by construction of the appropriate observer mappings.

The toolboxes that are developed by Marro [2018] and Chen [2018] can be used to create a matrix $S_g^\star$, which numerically represents the subspace $\mathcal{S}_g^\star$. Furthermore, by utilising subspace operations it is possible to numerically verified whether $\mathcal{S}_g^\star \in \mathbb{S}_g$. A numerical procedure to construct a representation for larger dimensional subspaces $\mathcal{S}_g \in \mathbb{S}_g$—or to find a largest one—does, however, not exist. For this reason it is assumed that a minimal representation S_g for some subspace $\mathcal{S}_g \in \mathbb{S}_g$ is constructed.

The states of $\Sigma^{T_{e,g}}$ (5.8) are compatible to the state decomposition in (5.7). By utilising the subspace $\mathcal{S}_g \in \mathbb{S}_g$, it is possible to define the subspace $\mathcal{S}_{g,c}$ such that

$\mathcal{S}_g \oplus \mathcal{S}_{g,c} = \mathcal{X}$; for example, we can consider $\mathcal{S}_{g,c} = \mathcal{S}_g^\perp$. Minimal representations for these subspaces can directly be used to transform Σ (5.1) into $\Sigma^{T_{e,g}}$ (5.8) by applying the state transformation

$$T_{e,g} = \begin{pmatrix} \Pi_s(\mathcal{S}_g, \mathcal{S}_{g,c}) \\ \Pi_s(\mathcal{S}_{g,c}, \mathcal{S}_g) \end{pmatrix}. \tag{5.15}$$

Solving the DDEPS(-CO)

As mentioned before, an observer can be designed for Σ (5.1) by using any equivalent system; a representation of the form $\Sigma^{T_{e,g}}$ (5.8) can therefore be considered. This representation is—based on a subspace $\mathcal{S}_g \in \mathbb{S}_g$—created using the state transformation $T_{e,g}$ as defined in (5.15). The observer Σ_o (5.4) is for $\Sigma^{T_{e,g}}$ (5.8) characterised in the mappings $L = \begin{pmatrix} L_1 \\ L_2 \end{pmatrix}$, $M = \begin{pmatrix} M_1 & M_2 \end{pmatrix}$ and N.

For a given subspace $\mathcal{S}_g \in \mathbb{S}_g$, it is established in Theorem 5.5 that the solution to the DDEPS is characterised by the mappings L, M and N that satisfy (5.10). For $\Sigma^{T_{e,g}}$ (5.8) it has been shown that the first four requirements in (5.10) are equivalent to vanishing of the bold-font mappings in $\Sigma_\epsilon^{T_{e,g}}$ (5.9), which makes this system representation convenient from a numerical perspective.

The requirements in (5.10) imply for $\Sigma^{T_{e,g}}$ (5.8) that the mappings M_1, M_2 and N should satisfy

$$C_{z1} - NC_{y1} = 0, \quad ND_{wy} = 0, \quad M_2 = C_{z2} - NC_{y2}, \quad M_1 = 0. \tag{5.16}$$

The mappings L_1 and L_2 should satisfy

$$A_{21} + L_2 C_{y1} = 0, \quad B_{w2} + L_2 D_{wy} = 0, \quad \lambda(A_{22} + L_2 C_{y2}) \subseteq \mathbb{C}_g, \quad L_1 : \mathcal{Y} \to \mathcal{X}_1.$$

The mappings M and N are therefore constructed by numerically solving a set of linear equations. It is, however, not directly clear how to numerically construct the mapping L_2, because it should satisfy a stability requirement.

It is explained in section 2.3 that—for stability domain $\mathbb{C}_g = \mathbb{C}_-$—all mappings L_2 which achieve $\lambda(A_{22} + L_2 C_{y2}) \subset \mathbb{C}_-$ can be characterised by an LMI; such an LMI can numerically be solved. In this way, all stabilising mappings $L_2 = Z_2^{-1} J_2$ are described by the matrices J_2 and $Z_2 \succ 0$ that satisfy $A_{22}^\top Z_2 + Z_2 A_{22} + C_{y2}^\top J_2^\top + J_2 C_{y2} \prec 0$.

By expressing all conditions on L_2 in terms of these matrices, we can obtain the following equality constrained LMI:

$$Z_2 \succ 0, \quad Z_2 \begin{pmatrix} A_{21} & B_{w2} \end{pmatrix} + J_2 \begin{pmatrix} C_{y1} & D_{wy} \end{pmatrix} = 0, \quad A_{22}^\top Z_2 + Z_2 A_{22} + C_{y2}^\top J_2^\top + J_2 C_{y2} \prec 0. \tag{5.17}$$

Σ_o (5.4)—which is defined using $\Sigma^{T_{e,g}}$ (5.8)—therefore solves the DDEPS for ($\Sigma^{T_{e,g}}$ (5.8), $\mathcal{X}_1$, $\mathbb{C}_-$), when the mappings M_1, M_2 and N are a solution to (5.16), when any solution to (5.17) is used to define $L_2 = Z_2^{-1} J_2$; and when a mapping

L_1 of appropriate dimensions is considered. Because Σ (5.1) and $\Sigma^{T_{e,g}}$ (5.8) are equivalent in terms of input to output behaviour—and because $\mathcal{X}_1 = T_{e,g}\mathcal{S}_g$—it can be concluded that this observer will solve the DDEPS for (Σ (5.1), $\mathcal{S}_g$, $\mathbb{C}_-$) as well.

Finally, let the considered subspace $\mathcal{S}_g \in \mathbb{S}_g$ satisfy $\dim(\mathcal{S}_g) = \dim(\mathcal{X}) - n_e$. Then $\widehat{\Sigma}_o^{T_{e,g}}$ (5.12) solves the DDEPS-CO for ($\Sigma^{T_{e,g}}$ (5.8), n_e, $\mathbb{C}_-$)—and again (Σ (5.1), n_e, $\mathbb{C}_-$)—when the mappings M_2 and N are a solution to (5.16) and any solution to (5.17) is used to define $L_2 = Z_2^{-1}J_2$.

It is important to note for the DDEPS-CO, that the estimator order n_e is directly determined by the dimension of the subspace $\mathcal{S}_g \in \mathbb{S}_g$ that is considered in its design. The mappings L_c, $\hat{M}$ and N, on the other hand, determine the mappings of this constrained order estimator.

5.2.6 An Illustrative Example

An example is now presented to illustrate the design of a constrained order estimator. In addition, the example is used to demonstrate that an unnecessarily large estimator can indeed be created by utilising the subspace $\mathcal{S}_g^\star \in \mathbb{S}_g$.

Consider a system that is similar to $\Sigma^{T_{e,g}}$ (5.8), as described by

$$\Sigma_{ex,e} = \left\{ \begin{array}{rcl} \begin{pmatrix} \dot{x}_1(t) \\ \dot{x}_2(t) \\ \dot{x}_3(t) \\ \dot{x}_4(t) \end{pmatrix} & = & \begin{pmatrix} -1 & 0 & 0 & 1 \\ 0.1 & -2 & 0 & 1 \\ 0 & -0.5 & -0.4 & 0 \\ 0 & 0.2 & 0.2 & -2 \end{pmatrix} \begin{pmatrix} x_1(t) \\ x_2(t) \\ x_3(t) \\ x_4(t) \end{pmatrix} + \begin{pmatrix} 1 & 0 \\ 0 & 2 \\ 0 & 0 \\ 0 & 0 \end{pmatrix} w(t) \\ y(t) & = & \begin{pmatrix} 0 & 1 & 0 & 0 \\ 0 & 0 & 1 & 0 \end{pmatrix} x(t) \\ z(t) & = & \begin{pmatrix} 0 & 1 & 1 & 2 \end{pmatrix} x(t). \end{array} \right. \tag{5.18}$$

For stability domain $\mathbb{C}_g = \mathbb{C}_-$ we have that $\mathcal{S}_g^\star = \mathcal{X}_1 \oplus \mathcal{X}_2 \in \mathbb{S}_g$ and $\mathcal{S}_g = \mathcal{X}_1 \oplus \mathcal{X}_2 \oplus \mathcal{X}_3 \in \mathbb{S}_g$.

A reduced order observer $\widehat{\Sigma}_o$ (5.11) of order 2 is constructed for $\Sigma_{ex,e}$ (5.18), when the subspace $\mathcal{S}_g^\star$ is used in its design. Let us consider the state decomposition $\mathcal{X} = \mathcal{S}_g^\star \oplus \mathcal{S}_g^{\star\perp}$ in (5.7)—i.e. with $\mathcal{S}_g^{\star\perp} = \mathcal{X}_3 \oplus \mathcal{X}_4$—to create the reduced order observer

$$\widehat{\Sigma}_{ex,e,o2} = \left\{ \begin{array}{rcl} \begin{pmatrix} \dot{\tilde{x}}_3(t) \\ \dot{\tilde{x}}_4(t) \end{pmatrix} & = & \begin{pmatrix} L_{212} - 0.4 & 0 \\ L_{222} + 0.2 & -2 \end{pmatrix} \begin{pmatrix} \tilde{x}_3(t) \\ \tilde{x}_4(t) \end{pmatrix} - \begin{pmatrix} L_{211} & L_{212} \\ L_{221} & L_{222} \end{pmatrix} y(t) \\ \tilde{z}(t) & = & \begin{pmatrix} M_{21} & M_{22} \end{pmatrix} \begin{pmatrix} \tilde{x}_3(t) \\ \tilde{x}_4(t) \end{pmatrix} + \begin{pmatrix} N_1 & N_2 \end{pmatrix} y(t). \end{array} \right. \tag{5.19}$$

In order to solve—with this observer—the DDEPS-CO for ($\Sigma_{ex,e}$ (5.18), 2, $\mathbb{C}_-$), we can consider $N = \begin{pmatrix} 1 & 0 \end{pmatrix}$, $M_2 = \begin{pmatrix} 1 & 2 \end{pmatrix}$ as established in (5.16) and the LMI in (5.17) can be used to construct $L_2 = \begin{pmatrix} 0.5 & 0 \\ -0.2 & 0 \end{pmatrix}$.

However, a reduced order observer $\widehat{\Sigma}_o$ (5.11) of order 1 is constructed when the larger subspace $\mathcal{S}_g = \mathcal{X}_1 \oplus \mathcal{X}_2 \oplus \mathcal{X}_3$ is considered instead. In a similar fashion, by utilising $\mathcal{S}_{g,c} = \mathcal{S}_g^{\perp}$ it can be shown that the observer

$$\widehat{\Sigma}_{ex,e,o1} = \begin{cases} \dot{\tilde{x}}_4(t) = -2\tilde{x}_4(t) + \begin{pmatrix} 0.2 & 0.2 \end{pmatrix} y(t) \\ \tilde{z}(t) = 2\tilde{x}_4(t) + \begin{pmatrix} 1 & 1 \end{pmatrix} y(t), \end{cases} \tag{5.20}$$

solves the DDEPS-CO for ($\Sigma_{ex,e}$ (5.18), 1, $\mathbb{C}_-$).

Let us finalise this example with a simulation for the interconnection of $\Sigma_{ex,e}$ (5.18) with $\widehat{\Sigma}_{ex,e,o1}$ (5.20), in order to demonstrate that $\epsilon_z(t)$ is indeed not affected by $w(t)$ and, for some initial condition, that it will converge to 0 as time progresses.

For this simulation, let the disturbances be of the form $w_i(t) = c_{i0} + c_{i1}\sin(\omega_i t) + c_{i2}\eta(t)$, where $\eta(t)$ is unitary white noise; and with $c_{10} = -c_{20} = 50$, $c_{11} = c_{21} = 20$, $\omega_1 = 1$, $\omega_2 = 3$ and $c_{12} = c_{22} = 1$. Then figure 5.1 shows the response of this interconnection with initial states $x(0) = \begin{pmatrix} 10 & 10 & 10 & 10 \end{pmatrix}^\top$ and $\hat{x}_4(0) = -30$.

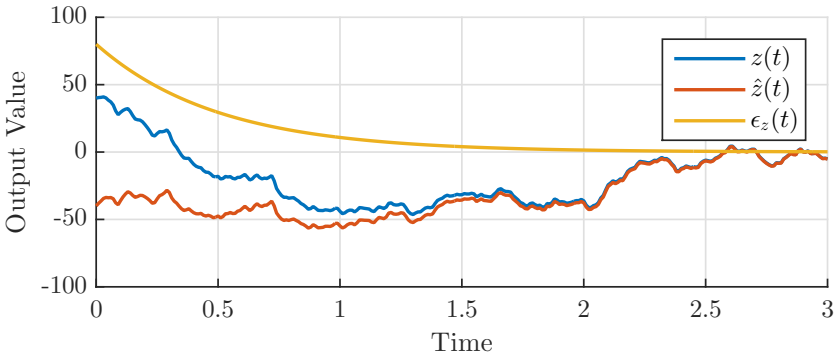

Figure 5.1: A time response for the interconnection of $\Sigma_{ex,e}$ (5.18) with $\widehat{\Sigma}_{ex,e,o1}$ (5.20).

5.3 The Disturbance Decoupling Problem with Measurement Feedback using a Constrained Order Controller[1]

5.3.1 Problem Definition and Section Outline

In section 5.3 we will consider the design of a measurement feedback controller

$$\Sigma_{c,n_c} = \begin{cases} \dot{x}_c(t) = Jx_c(t) + Ky(t) \\ u(t) = Mx_c(t) + Ny(t) \end{cases} \tag{5.21}$$

that, based on the measured output $y(t)$, produces a control input $u(t)$ for the system Σ (5.1). Any control problem consists of appropriately selecting the mappings J, K, M and N of Σ_{c,n_c} (5.21) in order to achieve a given objective in closed-loop. The closed-loop interconnection between Σ (5.1) and Σ_{c,n_c} (5.21) is mathematically described by

$$\Sigma_{cl,n_c} = \left\{ \begin{array}{rl} \begin{pmatrix} \dot{x}(t) \\ \dot{x}_c(t) \end{pmatrix} = & \begin{pmatrix} A + B_u N C_y & B_u M \\ KC_y & J \end{pmatrix} \begin{pmatrix} x(t) \\ x_c(t) \end{pmatrix} + \begin{pmatrix} B_w + B_u N D_{wy} \\ KD_{wy} \end{pmatrix} w(t) \\ z(t) = & \begin{pmatrix} C_z + D_{uz} N C_y & D_{uz} M \end{pmatrix} \begin{pmatrix} x(t) \\ x_c(t) \end{pmatrix} + \begin{pmatrix} D_{uz} N D_{wy} \end{pmatrix} w(t). \end{array} \right. \tag{5.22}$$

This closed-loop system has an extended state $x^{cl,n_c} = \begin{pmatrix} x(t) \\ x_c(t) \end{pmatrix}$ and extended system matrices A^{cl,n_c}, B_w^{cl,n_c}, C_z^{cl,n_c} and D_{wz}^{cl,n_c}. Its extended state-space is characterised by the vector space $\mathcal{X}^{cl,n_c}$.

In section 5.3 we will address the problem of constructing a controller Σ_{c,n_c} (5.21) with a constrained order n_c that decouples the control output $z(t)$ of Σ_{cl,n_c} (5.22) from the disturbance $w(t)$, while internally stabilising Σ_{cl,n_c} (5.22). This problem is called the *disturbance decoupling problem with measurement feedback and stability using a constrained order controller* (DDPMS-CO). The DDPMS-CO can, in general, not be solved for all systems and all controller orders. We will therefore also investigate under which conditions the problem can be solved.

Definition 5.11 *Consider a stability domain $\mathbb{C}_g$ and a number $n_c \in \mathbb{N}$.*

Then Σ_{c,n_c} (5.21) of order n_c "solves" the DDPMS-CO for (Σ (5.1), n_c, $\mathbb{C}_g$) if the control output $z(t)$ of Σ_{cl,n_c} (5.22) is independent of the disturbance $w(t)$, while $\lambda(A^{cl,n_c}) \subseteq \mathbb{C}_g$.

We say that the DDPMS-CO "can be solved" for (Σ (5.1), n_c, $\mathbb{C}_g$) if such a controller exists.

The problem is called the DDPM-CO when the stability domain $\mathbb{C}_g = \mathbb{C}$ is considered.

[1] Section 5.3 is based on the (submitted) journal article: R. W. H. Merks and S. Weiland. Constrained Order Controller Design for the Disturbance Decoupling Problem with Dynamic Measurement Feedback and Stability. Submitted to *IEEE Transactions on Automatic Control*.

The known solution to the disturbance decoupling problem with measurement feedback and stability (DDPMS) consists of separately solving a state feedback design problem and an estimator design problem. To solve this problem, we will consider the same procedure as presented in section 5.2.

In section 5.3.2 we will therefore discuss the known solution to the disturbance decoupling problem with state feedback and stability (DDPS). This solution is then combined with the solution to the DDEPS in order to solve the DDPMS in section 5.3.3. In addition, an extension is added to this solution in order to characterise *all* controllers Σ_{c,n_c} (5.21) that can solve the problem.

This characterisation is used in section 5.3.4 to solve the DDPM-CO—i.e. without a closed-loop stability requirement; a solution to the DDPMS-CO is presented thereafter in section 5.3.5. Conditions on the controller order are presented in section 5.3.6 and a numerical procedure to explicitly construct a constrained order controller is given in section 5.3.7. Finally, an illustrative example is presented in section 5.3.8.

5.3.2 The Disturbance Decoupling Problem with State Feedback and Stability

For any stability domain $\mathbb{C}_g$, let $\mathcal{V}_g$ be an output-nulling $\mathbb{C}_g$-stabilisability subspace and $\mathcal{V}_g^\star$ the $\mathbb{C}_g$-stabilisable weakly unobservable subspace as defined in Lemma 2.39 and Theorem 2.40, respectively.

We will now consider the design of a state feedback $u(t) = Fx(t)$; applying this feedback to Σ (5.1) results in the closed-loop system

$$\Sigma_{cl,F} = \begin{cases} \dot{x}(t) = \Big(A + B_u F\Big) x(t) + B_w w(t) \\ z(t) = \Big(C_z + D_{uz} F\Big) x(t). \end{cases} \tag{5.23}$$

With the following proposition we will establish when $\Sigma_{cl,F}$ (5.23) can be disturbance decoupled.

Proposition 5.12 *Consider a stability domain $\mathbb{C}_g$ and the subspace $\mathcal{V}_g^\star \subseteq \mathcal{X}$ as defined in Theorem 2.40.*

Then there exists a state feedback $u(t) = Fx(t)$ for Σ (5.1) such that the control output $z(t)$ of $\Sigma_{cl,F}$ (5.23) is independent of the disturbance $w(t)$, while $\lambda(A + B_u F) \subseteq \mathbb{C}_g$ if and only if Σ (5.1) is $\mathbb{C}_g$-stabilisable and

$$\operatorname{im}(B_w) \subseteq \mathcal{V}_g^\star + B_u \ker(D_{uz}).$$

Proof: The proof can be found in appendix A.3. □

Whether the DDPS can be solved is strongly related to the subspace $\mathcal{V}_g^\star$. This subspace therefore has, in a similar fashion to $\mathcal{S}_g^\star$, been thoroughly investigated in

geometric control theory and there exist algorithms that can construct a numerical representation for this subspace. To characterise all feedbacks that can solve the DDPS, let us consider the set

$$\mathbb{V}_g(\Sigma) = \{\ \mathcal{V}_g \subseteq \mathcal{X} \quad | \quad \begin{array}{l} \mathcal{V}_g \text{ is as defined in Lemma 2.39,} \\ \operatorname{im}(B_w) \subseteq \mathcal{V}_g + B_u \ker(D_{uz})\}\,, \end{array} \tag{5.24}$$

for which the functional dependency on Σ is omitted when it is clear what system is implied.

This set is similar to $\mathbb{S}_g$, in the sense that $\mathbb{V}_g \neq \emptyset$ if and only if $\mathcal{V}_g^\star \in \mathbb{V}_g$. It is therefore also desired to relate the DDPS to the entire set $\mathbb{V}_g$. For this purpose, let us consider the following formal definition for the DDPS.

Definition 5.13 *Consider a stability domain $\mathbb{C}_g$.*

Then a state feedback $u(t) = Fx(t)$ "solves" the DDPS for (Σ (5.1), $\mathcal{V}_g$, $\mathbb{C}_g$) if the the control output $z(t)$ of $\Sigma_{cl,F}$ (5.23) is independent of the disturbance $w(t)$, while $\lambda(A + B_uF) \subseteq \mathbb{C}_g$. Furthermore, for $\Sigma_{cl,F}$ (5.23) it holds that $x(t) \in \mathcal{V}_g$ for all $t \geq 0$ and for any disturbance $w(t)$, provided that $x(0) = x_0 \in \mathcal{V}_g$.

We say that the DDPS "can be solved" for (Σ (5.1), $\mathcal{V}_g$, $\mathbb{C}_g$) if such a state feedback exists.

Remark 5.3 *Similarly to the DDEPS, it can be shown that the DDPS can be solved for (Σ (5.1), $\mathcal{V}_g$, $\mathbb{C}_g$) if and only if Σ (5.1) is $\mathbb{C}_g$-stabilisable and $\mathcal{V}_g \in \mathbb{V}_g$. Furthermore, the state feedback $u(t) = Fx(t)$ solves the DDPS for (Σ (5.1), $\mathcal{V}_g$, $\mathbb{C}_g$) if and only if $(A + B_uF)\mathcal{V}_g \subseteq \mathcal{V}_g$, $(C_z + D_{uz}F)\mathcal{V}_g = 0$ and $\lambda(A + B_uF) \subseteq \mathbb{C}_g$.*

We do, however, not require a thorough discussion on these results in order to solve the DDPMS below.

5.3.3 The Disturbance Decoupling Problem with Measurement Feedback and Stability

For any stability domain $\mathbb{C}_g$, let $\mathcal{S}_g$ be an input-containing $\mathbb{C}_g$-detectability subspace and $\mathcal{S}_g^\star$ the $\mathbb{C}_g$-detectable strongly reachable subspace as defined in Lemma 2.42 and Theorem 2.43, respectively. Furthermore, let $\mathcal{V}_g$ be an output-nulling $\mathbb{C}_g$-stabilisability subspace and $\mathcal{V}_g^\star$ the $\mathbb{C}_g$-stabilisable weakly unobservable subspace as defined in Lemma 2.39 and Theorem 2.40, respectively.

An observer-based control architecture will considered, which is described by

$$\Sigma_c = \begin{cases} \dot{\tilde{x}}(t) &= \Big(A + B_uF + LC_y\Big)\,\tilde{x}(t) + \Big(B_uN - L\Big)\,y(t) \\ u(t) &= \qquad\qquad F\ \tilde{x}(t) + \qquad\quad N\ y(t), \end{cases} \tag{5.25}$$

of order n_x and with design parameters $L : \mathcal{Y} \to \mathcal{X}$, $F : \mathcal{X} \to \mathcal{U}$ and $N : \mathcal{Y} \to \mathcal{U}$.

When Σ_c (5.25) is applied to Σ (5.1)—and by considering the state observation error $e(t) = x(t) - \tilde{x}(t)$—we obtain the closed-loop system $\Sigma_{cl} =$

$$\left\{\begin{array}{l} \left(\begin{array}{c}\dot{x}(t)\\ \dot{e}(t)\end{array}\right) = \left(\begin{array}{c|c} A + B_u(F + NC_y) & -B_uF \\ \hline 0 & A + LC_y \end{array}\right)\left(\begin{array}{c}x(t)\\ e(t)\end{array}\right) + \left(\begin{array}{c} B_w + B_uND_{wy} \\ \hline B_w + LD_{wy}\end{array}\right) w(t) \\ z(t) \;\; = \left(\begin{array}{c|c} C_z + D_{uz}(F + NC_y) & -D_{uz}F \end{array}\right)\left(\begin{array}{c}x(t)\\ e(t)\end{array}\right) + \left(\begin{array}{c} D_{uz}ND_{wy}\end{array}\right) w(t), \end{array}\right. \tag{5.26}$$

which has a closed-loop state $x^{cl}(t) = \begin{pmatrix} x(t) \\ e(t) \end{pmatrix}$ and system matrices A^{cl}, B_w^{cl}, C_z^{cl} and D_{wz}^{cl}. The closed-loop state-space is characterised by the vector space $\mathcal{X}^{cl}$.

With the following proposition we will establish when Σ_{cl} (5.26) can be disturbance decoupled and that it is non-restrictive to consider the controller Σ_c (5.25).

Proposition 5.14 *Consider a stability domain $\mathbb{C}_g$ and the subspaces $\mathcal{V}_g^\star \subseteq \mathcal{X}$, $\mathcal{S}_g^\star \subseteq \mathcal{X}$ as defined in Theorem 2.40 and 2.43, respectively.*

Then there exists a controller Σ_{c,n_c} (5.21) for Σ (5.1) such that the control output $z(t)$ of Σ_{cl} (5.26) is independent of the disturbance $w(t)$, while $\lambda(A^{cl}) \subseteq \mathbb{C}_g$ if and only Σ (5.1) is $\mathbb{C}_g$-stabilisable, $\mathbb{C}_g$-detectable and

(a) $\mathrm{im}(B_w) \subseteq \mathcal{V}_g^\star + B_u \ker(D_{uz})$.
(b) $\mathcal{S}_g^\star \cap (C_y^{-1}\mathrm{im}(D_{wy}) \subseteq \ker(C_z)$.
(c) $\mathcal{S}_g^\star \subseteq \mathcal{V}_g^\star$.

When this condition is satisfied, a controller of the form Σ_c (5.25) can be considered for this purpose.

Proof: The proof is given by by Stoorvogel and van der Woude [1991, Thm. 2.2, Cor. 2.3]. □

The DDPMS therefore consists of finding the mappings L, F and N for Σ_{c,n_c} (5.21) such that $z(t)$ of Σ_{cl} (5.26) is independent of $w(t)$; whether this can be achieved is—similarly to the DDPS and the DDEPS—strongly related to the subspaces $\mathcal{S}_g^\star$ and $\mathcal{V}_g^\star$. We will consider the same procedure as for the DDEPS to solve the DDPMS. Let us therefore start by defining the set

$$\mathbb{T}_g(\Sigma) = \{\ (\mathcal{S}_g, \mathcal{V}_g) \mid \mathcal{S}_g \in \mathbb{S}_g(\Sigma),\ \ \mathcal{V}_g \in \mathbb{V}_g(\Sigma),\ \ \mathcal{S}_g \subseteq \mathcal{V}_g\} \tag{5.27}$$

with $\mathbb{S}_g$ and $\mathbb{V}_g$ as defined in (5.6) and (5.24) , respectively. Again, the functional dependency on Σ is omitted when it is clear what system is implied.

First, Proposition 5.14 is related to the set $\mathbb{T}_g$.

Lemma 5.15 *Consider a stability domain $\mathbb{C}_g$.*

Then there exist mappings $L : \mathcal{Y} \to \mathcal{X}$, $F : \mathcal{X} \to \mathcal{U}$ and $N : \mathcal{Y} \to \mathcal{U}$ such that the control output $z(t)$ of Σ_{cl} (5.26) is independent of the disturbance $w(t)$, while $\lambda(A^{cl}) \subseteq \mathbb{C}_g$ if and only Σ (5.1) is $\mathbb{C}_g$-stabilisable, $\mathbb{C}_g$-detectable and $\mathbb{T}_g(\Sigma\ (5.1)) \neq \emptyset$.

Proof: ($\Rightarrow$) In Proposition 5.14 it is established that these mappings exist if and only if Σ (5.1) is $\mathbb{C}_g$-stabilisable, $\mathbb{C}_g$-detectable and the subspaces $\mathcal{S}_g^\star$ and $\mathcal{V}_g^\star$ satisfy conditions (a)-(c). This implies that $(\mathcal{S}_g^\star, \mathcal{V}_g^\star) \in \mathbb{T}_g$ and therefore that $\mathbb{T}_g \neq \emptyset$.

($\Leftarrow$) If $\mathbb{T}_g \neq \emptyset$, then there exists a pair of subspaces $(\mathcal{S}_g, \mathcal{V}_g) \in \mathbb{T}_g$. By definition, we have that $\mathcal{S}_g^\star \subseteq \mathcal{S}_g$ and $\mathcal{V}_g \subseteq \mathcal{V}_g^\star$, which implies that $(\mathcal{S}_g^\star, \mathcal{V}_g^\star) \in \mathbb{T}_g$ as well. These subspaces will therefore satisfy conditions (a)-(c) in Proposition 5.14, which combined with the fact that Σ (5.1) is $\mathbb{C}_g$-stabilisable and $\mathbb{C}_g$-detectable completes the proof. □

Lemma 5.15 actually states that $\mathbb{T}_g$ is non-empty if and only if $(\mathcal{S}_g^\star, \mathcal{V}_g^\star) \in \mathbb{T}_g$. Σ_{cl} (5.26) can therefore be disturbance decoupled if and only if $\mathbb{T}_g$ is non-empty. Closed-loop stability requires that Σ (5.1) is $\mathbb{C}_g$-stabilisable and $\mathbb{C}_g$-detectable as well. We will now relate the DDPMS to the entire set $\mathbb{T}_g$, which will be utilised in sections 5.3.4 ands 5.3.5 to characterise all orders for which the problems can be solved. For this purpose, let us consider the following formal definition for the DDPMS.

Definition 5.16 *Consider a stability domain $\mathbb{C}_g$.*

Then Σ_c (5.25) "solves" the DDPMS for (Σ (5.1), $\mathcal{S}_g$, $\mathcal{V}_g$, $\mathbb{C}_g$) if the control output $z(t)$ of Σ_{cl} (5.26) is independent of the disturbance $w(t)$, while $\lambda(A^{cl}) \subseteq \mathbb{C}_g$. Furthermore, for Σ_{cl} (5.26) it holds for any disturbance $w(t)$ that

(a) $e(t) \in \mathcal{S}_g$ for all $t \geq 0$, provided that $e(0) = e_0 \in \mathcal{S}_g$ and $x(0) = x_0 \in \mathcal{X}$.

(b) $x(t) \in \mathcal{V}_g$ for all $t \geq 0$, provided that $e(0) = e_0 \in \mathcal{S}_g$ and $x(0) = x_0 \in \mathcal{V}_g$.

We say that the DDPMS "can be solved" for (Σ (5.1), $\mathcal{S}_g$, $\mathcal{V}_g$, $\mathbb{C}_g$) if such a controller exists.

The problem is called the DDPM when the stability domain $\mathbb{C}_g = \mathbb{C}$ is considered.

We can, similarly to an estimator, design a controller Σ_c (5.25) for Σ (5.1) by using any equivalent system. Let us now define a specific representation of Σ (5.1) in order to provide an intuitive interpretation for the solution to the DDPMS.

With a pair of subspaces $(\mathcal{S}_g, \mathcal{V}_g) \in \mathbb{T}_g$—which by definition satisfy $\mathcal{S}_g \subseteq \mathcal{V}_g$—the state-space $\mathcal{X}$ of Σ (5.1) can be decomposed as

$$\mathcal{X} = \mathcal{S}_g \oplus \mathcal{X}_m \oplus \mathcal{V}_{g,c}, \tag{5.28}$$

with $\mathcal{V}_{g,c}$ such that $\mathcal{V}_g \oplus \mathcal{V}_{g,c} = \mathcal{X}$ and $\mathcal{X}_m$ such that $\mathcal{S}_g \oplus \mathcal{X}_m = \mathcal{V}_g$.

For a given pair of subspaces $(\mathcal{S}_g, \mathcal{V}_g) \in \mathbb{T}_g$, let T_c be a state transformation that transforms Σ (5.1) into the system

$$\Sigma^{T_c} = \left\{ \begin{array}{rcl} \begin{pmatrix} \dot{x}_1(t) \\ \dot{x}_2(t) \\ \dot{x}_3(t) \end{pmatrix} & = & \begin{pmatrix} A_{11} & A_{12} & A_{13} \\ A_{21} & A_{22} & A_{23} \\ A_{31} & A_{32} & A_{33} \end{pmatrix} \begin{pmatrix} x_1(t) \\ x_2(t) \\ x_3(t) \end{pmatrix} + \begin{pmatrix} B_{u1} \\ B_{u2} \\ B_{u3} \end{pmatrix} u(t) + \begin{pmatrix} B_{w1} \\ B_{w2} \\ B_{w3} \end{pmatrix} w(t) \\ y(t) & = & \begin{pmatrix} C_{y1} & C_{y2} & C_{y3} \end{pmatrix} x(t) + D_{wy} w(t) \\ z(t) & = & \begin{pmatrix} C_{z1} & C_{z2} & C_{z3} \end{pmatrix} x(t) + D_{uz} u(t), \end{array} \right. \tag{5.29}$$

which is compatible to the decomposition in (5.28). In other words, the state-space $\mathcal{X} = \mathcal{X}_1 \oplus \mathcal{X}_2 \oplus \mathcal{X}_3$ of Σ^{T_c} (5.29) is partitioned in such a way that $\mathcal{X}_1 = T_c\mathcal{S}_g$, $\mathcal{X}_2 = T_c\mathcal{X}_m$ and $\mathcal{X}_3 = T_c\mathcal{V}_{g,c}$.

By applying to Σ^{T_c} (5.29), the controller Σ_c (5.25) with an identical state partitioning, the closed-loop system $\Sigma_{cl}^{T_c}$ (B.1) is obtained. Please note that the mathematical description for this closed-loop system is added to appendix B.

In the following theorem we will see how the DDPMS is solved for (Σ (5.1), $\mathcal{S}_g$, $\mathcal{V}_g$, $\mathbb{C}_g$). The mappings L, F and N of this controller are, for Σ^{T_c} (5.29), essentially chosen such that all bold-font mappings in $\Sigma_{cl}^{T_c}$ (B.1) vanish and such that closed-loop stability is achieved. This representation is therefore convenient for numerical implementation, while additionally providing an intuitive interpretation for the solution to the problem.

Theorem 5.17 *Consider a stability domain $\mathbb{C}_g$ and the subspaces $(\mathcal{S}_g, \mathcal{V}_g) \in \mathbb{T}_g$.*

Then Σ_c (5.25) "solves" the DDPMS for (Σ (5.1), $\mathcal{S}_g$, $\mathcal{V}_g$, $\mathbb{C}_g$) if and only if the mappings $L : \mathcal{Y} \to \mathcal{X}$, $F : \mathcal{X} \to \mathcal{U}$ and $N : \mathcal{Y} \to \mathcal{U}$, which uniquely define $\tilde{F} = F + NC_y$, satisfy

$$\begin{aligned}
&(A + LC_y)\mathcal{S}_g \subseteq \mathcal{S}_g, && \operatorname{im}(B_w + LD_{wy}) \subseteq \mathcal{S}_g,\\
&(A + B_u\tilde{F})\mathcal{V}_g \subseteq \mathcal{V}_g, && (C_z + D_{uz}\tilde{F})\mathcal{V}_g = 0,\\
&\operatorname{im}(B_w + B_uND_{wy}) \subseteq \mathcal{V}_g, && D_{uz}ND_{wy} = 0,\\
&(A + B_uNC_y)\mathcal{S}_g \subseteq \mathcal{V}_g, && (C_z + D_{uz}NC_y)\mathcal{S}_g = 0,\\
&\lambda(A^{cl}) \subseteq \mathbb{C}_g \text{ for } \Sigma_{cl} \text{ (5.26)}.
\end{aligned} \tag{5.30}$$

Proof: The proof can be found in appendix A.3. □

Finally, in the following corollary we will show that the solution to the DDPMS is indeed linked to the entire set $\mathbb{T}_g$ by considering Definition 5.16.

Corollary 5.18 *Consider a stability domain $\mathbb{C}_g$.*

Then the DDPMS "can be solved" for (Σ (5.1), $\mathcal{S}_g$, $\mathcal{V}_g$,$\mathbb{C}_g$) if and only if Σ (5.1) is $\mathbb{C}_g$-stabilisable, $\mathbb{C}_g$-detectable and $(\mathcal{S}_g, \mathcal{V}_g) \in \mathbb{T}_g$.

Proof: The proof can be found in appendix A.3. □

5.3.4 The Disturbance Decoupling Problem with Measurement Feedback using a Constrained Order Controller

From Corollary 5.18 we can conclude that the solution to the DDPMS is related to pairs of subspaces $(\mathcal{S}_g, \mathcal{V}_g) \in \mathbb{T}_g$. Theorem 5.17 establishes conditions on the mappings L, F and N, which will solve the problem for a given pair $(\mathcal{S}_g, \mathcal{V}_g) \in \mathbb{T}_g$.

These conditions imply—similarly to the DDEPS—that the controller states $\tilde{x} \in \mathcal{S}_g$ are unobservable in the output $z(t)$, while the states $\tilde{x} \in \mathcal{V}_{g,c}$ are not reachable through $w(t)$. This tells us that a controller of order $n_c = \dim(\mathcal{X}_m) = \dim(\mathcal{V}_g) - \dim(\mathcal{S}_g)$ can achieve disturbance decoupling in closed-loop.

It is, however, stated by Stoorvogel and van der Woude [1991] that a controller of this order might not be able to achieve closed-loop stability as well. We will therefore solve the DDPM-CO first; the subscript g is omitted for notational clarity.

In view of the state decomposition in (5.28), consider $\Pi_m = \Pi(\mathcal{X}_m, \mathcal{S} \oplus \mathcal{V}_c)$ to define

$$\hat{J} = \Pi_m(A|\mathcal{X}_m + B_u F_m) + L_m C_y|\mathcal{X}_m, \quad \hat{K} = \Pi_m B_u N - L_m, \quad \hat{M} = F_m,$$

which depend on the mappings $L_m : \mathcal{Y} \to \mathcal{X}_m$, $F_m : \mathcal{X}_m \to \mathcal{U}$ and $N : \mathcal{Y} \to \mathcal{U}$.

We now claim that the reduced order controller

$$\widehat{\Sigma}_c = \begin{cases} \dot{\tilde{x}}_m(t) = \hat{J}\tilde{x}_m(t) + \hat{K}y(t) \\ u(t) = \hat{M}\tilde{x}_m(t) + Ny(t). \end{cases} \tag{5.31}$$

of order $n_c = \dim(\mathcal{V}) - \dim(\mathcal{S})$ will be able to solve the DDPM-CO for appropriate mappings $L_m : \mathcal{Y} \to \mathcal{X}_m$, $F_m : \mathcal{X}_m \to \mathcal{U}$ and $N : \mathcal{Y} \to \mathcal{U}$; this will be established in Theorem 5.20.

Proposition 5.19 *Consider a number $n_c \in \mathbb{N}$.*

Then the DDPM-CO "can be solved" for (Σ (5.1), n_c) if there exists subspaces $(\mathcal{S}, \mathcal{V}) \in \mathbb{T}$ with $\dim(\mathcal{V}) - \dim(\mathcal{S}) = n_c$.

Proof: In Theorem 5.20 below it will be shown for a given pair of subspaces $(\mathcal{S}, \mathcal{V}) \in \mathbb{T}$ that the reduced order controller $\widehat{\Sigma}_c$ (5.31) can solve this problem. □

In a similar fashion to Remark 5.2, it can be noted that an "only if" statement does not hold in general for Proposition 5.19. Furthermore, by definition we get that $\dim(\mathcal{V}^\star) \geq \dim(\mathcal{V})$ and that $\dim(\mathcal{S}^\star) \leq \dim(\mathcal{S})$ for any pair $(\mathcal{S}, \mathcal{V}) \in \mathbb{T}$. Therefore, by considering $(\mathcal{S}^\star, \mathcal{V}^\star) \in \mathbb{T}$ an "unnecessarily large" controller could be created, while it is often desired to minimise this order. This is, again, the reason why the solution to the DDPMS was related to the entire set $\mathbb{T}_g$ in section 5.3.3.

Before formally solving the DDPM-CO, let us consider the equivalent system Σ^{T_c} (5.29) that is created for a given pair $(\mathcal{S}, \mathcal{V}) \in \mathbb{T}$ by utilising the decomposition in (5.28). The reduced order controller $\widehat{\Sigma}_c$ (5.31) is for Σ^{T_c} (5.29) explicitly described as

$$\widehat{\Sigma}_c^{T_c} = \begin{cases} \dot{\tilde{x}}_2(t) = \Big(A_{22} + B_{u2}F_2 + L_2C_{y2}\Big)\,\tilde{x}_2(t) + \Big(B_{u2}N - L_2\Big)\,y(t) \\ u(t) = \qquad\qquad F_2\;\tilde{x}_2(t) + \qquad\qquad N\;y(t), \end{cases} \tag{5.32}$$

where $\tilde{x}_m(t)$, L_m and F_m of $\widehat{\Sigma}_c$ (5.31) are described by $\tilde{x}_2(t)$, L_2 and F_2 in $\widehat{\Sigma}_c^{T_c}$ (5.32), respectively. Applying $\widehat{\Sigma}_c^{T_c}$ (5.32) to Σ^{T_c} (5.29) results in the closed-loop

system $\widehat{\Sigma}_{cl}^{T_c}$ (B.2)—for which the mathematical description is added to appendix B. A bold font is, again, used for mappings that can vanish by construction.

In the following theorem we will see how the DDPM-CO is solved by a controller $\widehat{\Sigma}_c$ (5.31). The controller mappings are, for Σ^{T_c} (5.29), essentially chosen such that all bold-font mappings in $\widehat{\Sigma}_{cl}^{T_c}$ (B.2) vanish.

Theorem 5.20 *Consider a pair of subspaces* $(\mathcal{S}, \mathcal{V}) \in \mathbb{T}$ *with* $n_c = \dim(\mathcal{V}) - \dim(\mathcal{S})$*, the decomposition in* (5.28) *and define* $\Pi_m = \Pi(\mathcal{X}_m, \mathcal{S} \oplus \mathcal{V}_c)$ *and* $\Pi_{\mathcal{V}} = \Pi(\mathcal{V}_c, \mathcal{V})$*.*

Then $\widehat{\Sigma}_c$ (5.31) *"solves" the DDPM-CO for (*Σ (5.1)*,* n_c*) if the mappings* $L_m : \mathcal{Y} \to \mathcal{X}_m$*,* $F_m : \mathcal{X}_m \to \mathcal{U}$ *and* $N : \mathcal{Y} \to \mathcal{U}$*, which uniquely define* $\tilde{F}_m = F_m + NC_y|\mathcal{X}_m$*, satisfy*

$$\begin{aligned} &(\Pi_m A + L_m C_y)|\mathcal{S} = 0, && \Pi_m B_w + L_m D_{wy} = 0, \\ &\Pi_{\mathcal{V}}(A|\mathcal{X}_m + B_u \tilde{F}_m) = 0, && C_z|\mathcal{X}_m + D_{uz}\tilde{F}_m = 0, \\ &\Pi_{\mathcal{V}}(B_w + B_u N D_{wy}) = 0, && D_{uz} N D_{wy} = 0, \\ &\Pi_{\mathcal{V}}(A + B_u N C_y)|\mathcal{S} = 0, && (C_z + D_{uz} N C_y)|\mathcal{S} = 0. \end{aligned} \tag{5.33}$$

Proof: The proof can be found in appendix A.3. □

5.3.5 The Disturbance Decoupling Problem with Measurement Feedback and Stability using a Constrained Order Controller

Stability of a closed-loop system is required in most, if not all, control problems that are considered in practice. We should therefore consider the DDPMS-CO in order to make this theoretical investigation relevant.

In Theorem 5.20 it is shown for the system Σ^{T_c} (5.29) that the controller mappings L_1, L_3, F_1 and F_3 are not required to solve the DDPM-CO. It is, however, not sufficient to only consider conditions on the mappings L_2, F_2 and N in order to guarantee that both disturbance decoupling and stability can be achieved in closed-loop by replacing $\mathbb{T}$ with $\mathbb{T}_g$.

In order to overcome this problem, let us first characterise all controllers Σ_c (5.25) that solve the DDPMS for given subspaces $(\mathcal{S}_g, \mathcal{V}_g) \in \mathbb{T}_g$ in terms of the mappings L, F and N by defining

$$\underline{M}_g(\mathcal{S}_g, \mathcal{V}_g) = \{(L, F, N) \mid \Sigma_c \text{ (5.25) solves the DDPMS for } (\Sigma \text{ (5.1)}, \mathcal{S}_g, \mathcal{V}_g, \mathbb{C}_g) \text{ with mappings } L : \mathcal{Y} \to \mathcal{X},\ F : \mathcal{X} \to \mathcal{U},\ N : \mathcal{Y} \to \mathcal{U}\}.$$

The notation $F \in \underline{M}_g(\mathcal{S}_g, \mathcal{V}_g)$, $(F, N) \in \underline{M}_g(\mathcal{S}_g, \mathcal{V}_g)$ or $L \in \underline{M}_g(\mathcal{S}_g, \mathcal{V}_g)$ is used when not all mappings are of interest.

The set $\underline{M}_g$ has some interesting properties, which will now be proven.

Lemma 5.21 *$\underline{M}_g(\mathcal{S}_g, \mathcal{V}_g)$ has the following properties:*

(a) $\underline{M}_g(\mathcal{S}_g, \mathcal{V}_g) = \emptyset$ if and only if $(\mathcal{S}_g, \mathcal{V}_g) \notin \mathbb{T}_g$.

(b) $(L_1, F_1, N_1), (L_2, F_2, N_2) \in \underline{M}_g(\mathcal{S}_g, \mathcal{V}_g)$ implies that $(L_1, F_2, N_2) \in \underline{M}_g(\mathcal{S}_g, \mathcal{V}_g)$ and that $(L_2, F_1, N_1) \in \underline{M}_g(\mathcal{S}_g, \mathcal{V}_g)$.

Proof: (a) follows directly from Corollary 5.18.

(b) states that the mappings $L \in \underline{M}_g(\mathcal{S}_g, \mathcal{V}_g)$ are independent of the mappings F and N. This follows directly from Theorem 5.17, where no requirement on L depends on F or N. □

This second property implies that the design requirements on the mapping L are independent from the design requirements on the mappings F and N. This "separation property" holds for the solution to the DDPMS as well as the DDPM-CO.

Now, in order to provide a solution to the DDPMS-CO we can consider making the design of L depend on the choice of F (and N). More specifically, we will provide a solution to the DDPMS-CO by constructing an appropriate mapping L on the basis of a given mapping $F \in \underline{M}_g(\mathcal{S}_g, \mathcal{V}_g)$. Let us define the following two subspaces—which are used to construct an extension to $\mathcal{X}_m$—for this purpose.

Definition 5.22 *Consider a stability domain $\mathbb{C}_g$, the subspaces $(\mathcal{S}_g, \mathcal{V}_g) \in \mathbb{T}_g$, the decomposition in* (5.28) *and a mapping $F \in \underline{M}_g(\mathcal{S}_g, \mathcal{V}_g)$. Furthermore, let us define $A_{\mathcal{S}} = \Pi(\mathcal{S}_g, \mathcal{S}_{g,c})A|\mathcal{S}_g$, $C_{y,\mathcal{S}} = C_y|\mathcal{S}_g$ and $F_{\mathcal{S}} = F|\mathcal{S}_g$.*

Then the subspaces $\mathcal{S}_1$ and $\mathcal{S}_3$ of vector space $\mathcal{X}$ are defined as follows:

$\mathcal{S}_1$ (Σ (5.1), $\mathcal{S}_g$, $\mathcal{S}_{g,c}$, F) is a subspace $\mathcal{S}_1 \subseteq \mathcal{S}_g \subseteq \mathcal{X}$ for which there exists a mapping $L_1 : \mathcal{Y} \to \mathcal{S}_g$ such that $(A_{\mathcal{S}} + L_1 C_{y,\mathcal{S}})\mathcal{S}_1 \subseteq \mathcal{S}_1$, $\lambda((A_{\mathcal{S}} + L_1 C_{y,\mathcal{S}})|(\mathcal{S}_g \bmod \mathcal{S}_1)) \subseteq \mathbb{C}_g$ and $\mathcal{S}_1 \subseteq \ker(F_{\mathcal{S}})$.

$\mathcal{S}_3$ (Σ (5.1), $\mathcal{S}_g$, $\mathcal{V}_{g,c}$, F) is a subspace $\mathcal{S}_3 \subseteq \mathcal{X}$ for which there exists a mapping $L_3 : \mathcal{Y} \to \mathcal{X}$ such that $(A + L_3 C_y)(\mathcal{S}_g \oplus \mathcal{S}_3) \subseteq \mathcal{S}_g \oplus \mathcal{S}_3$, $\mathrm{im}(B_w + L_3 D_{wy}) \subseteq \mathcal{S}_g \oplus \mathcal{S}_3$, $\lambda((A + L_3 C_y)|(\mathcal{X} \bmod (\mathcal{S}_g \oplus \mathcal{S}_3))) \subseteq \mathbb{C}_g$ and $\mathcal{S}_3 \subseteq \ker(F|\mathcal{V}_{g,c}) \subseteq \mathcal{S}_g \oplus \mathcal{V}_{g,c}$.

The subspace $\mathcal{S}_1$ is used to partition the subspace $\mathcal{S}_g$ as $\mathcal{S}_g = \mathcal{S}_1 \oplus \mathcal{S}_{1,c}$; the subspace $\mathcal{S}_3$ is used to partition the subspace $\mathcal{V}_{g,c}$ as $\mathcal{V}_{g,c} = \mathcal{S}_3 \oplus \mathcal{S}_{3,c}$. In this way, the state-space $\mathcal{X}$ of Σ (5.1) is decomposed as

$$\mathcal{X} = \mathcal{S}_1 \oplus \mathcal{S}_{1,c} \oplus \mathcal{X}_m \oplus \mathcal{S}_{3,c} \oplus \mathcal{S}_3. \tag{5.34}$$

Furthermore, let us define $\mathcal{X}_{m,g} = \mathcal{S}_{1,c} \oplus \mathcal{X}_m \oplus \mathcal{S}_{3,c}$ and the complement $\mathcal{X}_{m,g,c} = \mathcal{S}_1 \oplus \mathcal{S}_3$. For clarity, an overview of all considered subspaces is depicted in figure 5.2.

Now, let $T_{c,g}$ be a state transformation that transforms Σ (5.1) into $\Sigma^{T_{c,g}}$ (B.3), which is compatible to the decomposition in (5.34). In other words, the state-space of $\Sigma^{T_{c,g}}$ (B.3) is partitioned in such a way that $\mathcal{X}_1 = T_{c,g}\mathcal{S}_1$, $\mathcal{X}_2 = T_{c,g}\mathcal{S}_{1,c}$, $\mathcal{X}_3 = T_{c,g}\mathcal{X}_m$, $\mathcal{X}_4 = T_{c,g}\mathcal{S}_{3,c}$ and $\mathcal{X}_5 = T_{c,g}\mathcal{S}_3$. Please note that the mathematical description for this system is added to appendix B.

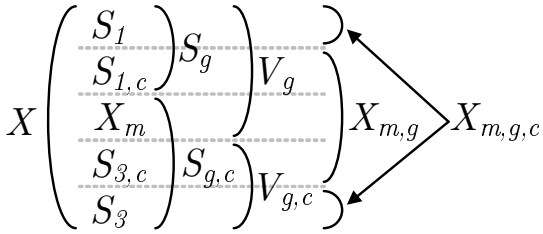

Figure 5.2: An overview of the subspaces that have been defined for Σ (5.1).

In view of the state decomposition in (5.34) and the derived subspaces as depicted in fig. 5.2, consider $\Pi_{m,g} = \Pi(\mathcal{X}_{m,g}, \mathcal{X}_{m,g,c})$ to define

$$\hat{J}_g = \Pi_{m,g}(A|\mathcal{X}_{m,g} + B_u F_{m,g}) + L_{m,g} C_y|\mathcal{X}_{m,g},$$
$$\hat{K}_g = \Pi_{m,g} B_u N - L_{m,g}, \qquad \hat{M}_g = F_{m,g},$$

which depend on the mappings $L_{m,g} : \mathcal{Y} \to \mathcal{X}_{m,g}$, $F_{m,g} : \mathcal{X}_{m,g} \to \mathcal{U}$ and $N : \mathcal{Y} \to \mathcal{U}$. We now claim that the reduced order controller

$$\widehat{\Sigma}_{c,g} = \begin{cases} \dot{\tilde{x}}_{m,g}(t) = \hat{J}_g \tilde{x}_{m,g}(t) + \hat{K}_g y(t) \\ u(t) = \hat{M}_g \tilde{x}_{m,g}(t) + N y(t). \end{cases} \tag{5.35}$$

of order $n_c = \dim(\mathcal{X}) - \dim(\mathcal{S}_1) - \dim(\mathcal{S}_3)$ will be able to solve the DDPMS-CO for appropriate mappings $L_{m,g} : \mathcal{Y} \to \mathcal{X}_{m,g}$, $F_{m,g} : \mathcal{X}_{m,g} \to \mathcal{U}$ and $N : \mathcal{Y} \to \mathcal{U}$; this will be established in Theorem 5.24.

Proposition 5.23 *Consider a stability domain $\mathbb{C}_g$ and a number $n_c \in \mathbb{N}$.*

Then the DDPMS-CO "can be solved" for (Σ (5.1), n_c, $\mathbb{C}_g$) if Σ (5.1) is $\mathbb{C}_g$-stabilisable, $\mathbb{C}_g$-detectable and for some pair of subspaces $(\mathcal{S}_g, \mathcal{V}_g) \in \mathbb{T}_g$ and a mapping $F \in \underline{M}_g(\mathcal{S}_g, \mathcal{V}_g)$ there exist subspaces $\mathcal{S}_1$ and $\mathcal{S}_3$—corresponding to Definition 5.22—that satisfy $n_c = \dim(\mathcal{X}) - \dim(\mathcal{S}_1) - \dim(\mathcal{S}_3)$.

Proof: In Theorem 5.24 below it will be shown for a given pair of subspaces $\mathcal{S}_1$, $\mathcal{S}_3$ that the reduced order controller $\widehat{\Sigma}_{c,g}$ (5.35) can solve this problem. □

From Proposition 5.23 we can, again, observe that the orders n_c for which the DDPMS-CO can be solved are related to the dimension of subspaces $\mathcal{S}_1$, $\mathcal{S}_3$. In order to construct a controller of small order, it is therefore desired to find subspaces $\mathcal{S}_1$, $\mathcal{S}_3$ that are large in dimension.

Before formally solving the DDPMS-CO, let us consider again the equivalent system $\Sigma^{T_{c,g}}$ (B.3). The reduced order controller $\widehat{\Sigma}_{c,g}$ (5.35) is for $\Sigma^{T_{c,g}}$ (B.3) explicitly described as $\widehat{\Sigma}_{c,g}^{T_{c,g}}$ (B.4). The controller state $\tilde{x}_{m,g}(t)$ and the mappings $L_{m,g}$ and $F_{m,g}$ of $\widehat{\Sigma}_{c,g}$ (5.35) are described by $\begin{pmatrix} \tilde{x}_{12}(t) \\ \tilde{x}_2(t) \\ \tilde{x}_{31}(t) \end{pmatrix}$, $\begin{pmatrix} L_{12} \\ L_2 \\ L_{31} \end{pmatrix}$ and $\begin{pmatrix} F_{12} & F_2 & F_{31} \end{pmatrix}$ in

$\widehat{\Sigma}_{c,g}^{T_{c,g}}$ (B.4), respectively. Applying $\widehat{\Sigma}_{c,g}^{T_{c,g}}$ (B.4) to $\Sigma^{T_{c,g}}$ (B.3) results in the closed-loop system $\widehat{\Sigma}_{cl,g}^{T_{c,g}}$ (B.5), for which a bold font is used when mappings can vanish by construction.

The subspaces $\mathcal{S}_1$ and $\mathcal{S}_3$ are created such that $F|\mathcal{X}_{m,g,c} = 0$ for a given $F \in \underline{M}_g(\mathcal{S}_g, \mathcal{V}_g)$. This implies for $\Sigma^{T_{c,g}}$ (B.3) that there exists a mapping $F = \begin{pmatrix} 0 & F_{12} & F_2 & F_{31} & 0 \end{pmatrix} \in \underline{M}_g(\mathcal{X}_{11} \oplus \mathcal{X}_{12}, \mathcal{X}_{11} \oplus \mathcal{X}_{12} \oplus \mathcal{X}_2)$.

In the following theorem we will see how the DDPMS-CO is solved by a controller $\widehat{\Sigma}_{c,g}$ (5.35). The controller mappings are, for $\Sigma^{T_{c,g}}$ (B.3), essentially chosen such that all bold-font mappings in $\widehat{\Sigma}_{cl,g}^{T_{c,g}}$ (B.5) vanish.

Theorem 5.24 *Consider a stability domain $\mathbb{C}_g$, the subspaces $(\mathcal{S}_g, \mathcal{V}_g) \in \mathbb{T}_g$ and mappings $(F, N) \in \underline{M}_g(\mathcal{S}_g, \mathcal{V}_g)$. Furthermore, consider a pair of subspaces $\mathcal{S}_1$, $\mathcal{S}_3$—corresponding to Definition 5.22—with $n_c = \dim(\mathcal{X}) - \dim(\mathcal{S}_1) - \dim(\mathcal{S}_3)$ and the derived subspaces as depicted in figure 5.2.*

Finally, define $\Pi_{m,g} = \Pi(\mathcal{X}_{m,g}, \mathcal{X}_{m,g,c})$ and $\Pi_{m,3} = \Pi(\mathcal{X}_m \oplus \mathcal{S}_{3,c}, \mathcal{S}_{1,c})$.

Then $\widehat{\Sigma}_{c,g}$ (5.35) solves the DDPMS-CO for (Σ (5.1), n_c, $\mathbb{C}_g$) if $F_{m,g} = F|\mathcal{X}_{m,g}$ and the mapping $L_{m,g} : \mathcal{Y} \to \mathcal{X}_{m,g}$ satisfies

$$\begin{aligned} &(\Pi_{m,g}A + L_{m,g}C_y)|\mathcal{S}_1 = 0, && \Pi_{m,3}(\Pi_{m,g}A + L_{m,g}C_y)|(\mathcal{S}_3 \oplus \mathcal{S}_{1,c}) = 0, \\ &\Pi_{m,3}(\Pi_{m,g}B_w + L_{m,g}D_{wy}) = 0, && \lambda((\Pi_{m,g}A + L_{m,g}C_y)|\mathcal{X}_{m,g}) \subseteq \mathbb{C}_g. \end{aligned} \tag{5.36}$$

Proof: The proof can be found in appendix A.3. □

5.3.6 Conditions on the Controller Order

It is shown in Proposition 5.19 that the dimensions of subspaces $(\mathcal{S}, \mathcal{V}) \in \mathbb{T}$ determine the values n_c for which the DDPM-CO can be solved. Now let us characterise the *minimal* controller order n_c^- for which the DDPM-CO can be solved. In addition, we will see that the controller architecture $\widehat{\Sigma}_c$ (5.31) is not restrictive in terms of minimising the controller order.

Theorem 5.25 *For a given system Σ (5.1), the minimal order for which the DDPM-CO can be solved is given by*

$$n_c^- = \min_{(\mathcal{S},\mathcal{V})\in\mathbb{T}} \dim(\mathcal{V}) - \dim(\mathcal{S}).$$

The reduced order controller $\widehat{\Sigma}_c$ (5.31) can be used to solve the DDPM-CO for (Σ (5.1), n_c^-).

Proof: Stoorvogel and van der Woude [1991] state that the controller order for this control problem is characterised in terms of subspaces $(\mathcal{S}, \mathcal{V}) \in \mathbb{T}$. Therefore, according to Schumacher [1980, Thm. 3.1] we get that

$$n_c^- = \min_{(\mathcal{S},\mathcal{V})\in\mathbb{T}} \dim(\mathcal{V}) - \dim(\mathcal{S}),$$

which completes the first part of the proof.

Finally, in Theorem 5.20 it is demonstrated that a controller of order n_c^- can be created for a given pair $(\mathcal{S}, \mathcal{V}) \in \mathbb{T}$ with $n_c^- = \dim(\mathcal{V}) - \dim(\mathcal{S})$, □

It is shown in Proposition 5.23 that the dimensions of subspaces $\mathcal{S}_1$ and $\mathcal{S}_3$ determine the values n_c for which the DDPMS-CO can be solved. These dimensions are dependent on the choice of $\mathcal{S}_g$, $\mathcal{V}_g$ and on F. For this approach to the problem, let us characterise the minimal order at which the DDPMS-CO can be solved.

Lemma 5.26 *Consider a stability domain $\mathbb{C}_g$ and the subspaces $\mathcal{S}_1$ and $\mathcal{S}_3$—corresponding to Definition 5.22—which are constructed on the basis of a pair $(\mathcal{S}_g, \mathcal{V}_g) \in \mathbb{T}_g$ and a mapping $F \in \underline{M}_g(\mathcal{S}_g, \mathcal{V}_g)$.*

Then for a given system Σ (5.1), the minimal order for which the DDPMS-CO can be solved with $\widehat{\Sigma}_{c,g}^{T_{c,g}}$ (B.4) is given by

$$n_{c,g}^- = \min_{(\mathcal{S}_g,\mathcal{V}_g)\in\mathbb{T}_g} \min_{F\in\underline{M}_g(\mathcal{S}_g,\mathcal{V}_g)} \min_{\mathcal{S}_1,\ \mathcal{S}_3} \dim(\mathcal{X}) - \dim(\mathcal{S}_1) - \dim(\mathcal{S}_3).$$

Proof: In Theorem 5.24 it is demonstrated that a controller of order $n_{c,g}^-$ can be created for a given pair of subspaces $\mathcal{S}_1$ and $\mathcal{S}_3$ with $n_c^- = \dim(\mathcal{X}) - \dim(\mathcal{S}_1) - \dim(\mathcal{S}_3)$. □

In this lemma, the minimal order at which the DDPMS-CO can be solved by utilising the controller $\widehat{\Sigma}_{c,g}^{T_{c,g}}$ (B.4) is presented. The example in section 5.3.8 will, however, show that the presented solution to the DDPMS-CO is restrictive in terms of minimising $n_{c,g}^-$. This implies that $n_{c,g}^-$ is not necessarily the minimal order for which the DDPMS-CO can be solved; we do know that this minimal order is bounded from below by n_c^-.

In some situations, however, the minimal controller order can be characterised for the DDPMS-CO as well. For optimal control problems it is often assumed that the mapping D_{wy} is full row rank and that the mapping D_{uz} is full column rank. Under these conditions, it can be shown that a controller of the form $\widehat{\Sigma}_c$ (5.31) can be used to solve the DDPMS-CO and that the solution is not restrictive in terms of minimising the controller order.

Theorem 5.27 *Consider a stability domain $\mathbb{C}_g$ and a system Σ (5.1) for which the mapping D_{wy} is full row rank and the mapping D_{uz} is full column rank.*

Then, for Σ (5.1), the minimal order for which the DDPMS-CO can be solved is given by

$$n_c^- = \min_{(\mathcal{S}_g,\mathcal{V}_g)\in\mathbb{T}_g} \dim(\mathcal{V}_g) - \dim(\mathcal{S}_g).$$

The reduced order controller $\widehat{\Sigma}_c$ (5.31) *can be used to solve the DDPMS-CO for* (Σ (5.1), n_c^-, $\mathbb{C}_g$).

Proof: The proof can be found in appendix A.3. □

5.3.7 Numerical Construction of the Controller

For the construction of a constrained order controller, we will again consider numerical representations for subspaces and utilise numerical implementations of all the subspace operations—as is described in more detail in section 2.1.

A numerical procedure to solve the DDPMS-CO consists of the following steps:

1. determine numerical representations for the subspaces $(\mathcal{S}_g, \mathcal{V}_g) \in \mathbb{T}_g$.
2. a state transformation T_c is—if $\mathbb{T}_g \neq \emptyset$—constructed on the basis of these subspaces, which transforms the system Σ (5.1) into an equivalent system Σ^{T_c} (5.29).
3. the system Σ^{T_c} (5.29) is used to solve the DDPM, DDPMS or DDPM-CO by construction of the appropriate controller mappings.
4. for some $(F, N) \in \underline{M}_g(\mathcal{S}_g, \mathcal{V}_g)$, numerical representations for the subspaces $\mathcal{S}_1$, $\mathcal{S}_3$—corresponding to Definition 5.22—are determined.
5. a state transformation T_g is constructed on the basis of these subspaces, which transforms the system Σ^{T_c} (5.29) into an equivalent system $\Sigma^{T_{c,g}}$ (B.3).
6. the system $\Sigma^{T_{c,g}}$ (B.3) is used to solve the DDPMS-CO by construction of the appropriate controller mappings.

Steps 1 and 2

As explained before, the toolboxes that are developed by Marro [2018] and Chen [2018] can be used to create numerical representations for the subspaces $\mathcal{S}_g^\star$ and $\mathcal{V}_g^\star$. In addition, by utilising subspace operations it is possible to numerically verify whether $(\mathcal{S}_g^\star, \mathcal{V}_g^\star) \in \mathbb{T}_g$. A numerical procedure to construct a representation for other subspaces in $\mathbb{T}_g$ does, however, not exist. For this reason it is assumed that a minimal representation for these subspaces is constructed.

Let us define the state transformations T_c that transforms Σ (5.1) into Σ^{T_c} (5.29). The states of Σ^{T_c} (5.29) are compatible to the state decomposition in (5.28). By utilising the subspaces $\mathcal{S}_g$ and $\mathcal{V}_g$—which satisfy $\mathcal{S}_g \subseteq \mathcal{V}_g$—it is possible to define the subspaces $\mathcal{X}_m$ and $\mathcal{V}_{g,c}$ such that $\mathcal{S}_g \oplus \mathcal{X}_m = \mathcal{V}_g$ and $\mathcal{V}_g \oplus \mathcal{V}_{g,c} = \mathcal{X}$. For example, we can consider $\mathcal{X}_m = \mathcal{S}_g^\perp \cap \mathcal{V}_g$ and $\mathcal{V}_{g,c} = \mathcal{V}_g^\perp$. Minimal representations for these subspaces can directly be used to transform Σ (5.1) into Σ^{T_c} (5.29) by applying the state transformation

$$T_c = \begin{pmatrix} \Pi_s(\mathcal{S}_g, \mathcal{X}_m \oplus \mathcal{V}_{g,c}) \\ \Pi_s(\mathcal{X}_m, \mathcal{S}_g \oplus \mathcal{V}_{g,c}) \\ \Pi_s(\mathcal{V}_{g,c}, \mathcal{S}_g \oplus \mathcal{X}_m) \end{pmatrix}. \tag{5.37}$$

Step 3

Solving the DDPM(-CO): A representation of the form Σ^{T_c} (5.29) is considered for these problems, which is created using a state transformation T_c (5.37) that is based on a pair $(\mathcal{S}, \mathcal{V}) \in \mathbb{T}$. The controller Σ_c (5.25) is for Σ^{T_c} (5.29) characterised in the mappings $L = \begin{pmatrix} L_1 \\ L_2 \\ L_3 \end{pmatrix}$, $F = \begin{pmatrix} F_1 & F_2 & F_3 \end{pmatrix}$ and N, which uniquely define the mapping $\tilde{F} = \begin{pmatrix} \tilde{F}_1 & \tilde{F}_2 & \tilde{F}_3 \end{pmatrix} = F + NC_y$.

For a given pair of subspaces $(\mathcal{S}, \mathcal{V}) \in \mathbb{T}$, it is established in Theorem 5.17 that the solution to the DDPM is characterised in therms of the mappings L, $\tilde{F}$ and N that satisfy (5.30) for $\mathbb{C}_g = \mathbb{C}$. For Σ^{T_c} (5.29) it has been shown that these requirements are equivalent to vanishing of the bold-font mappings in $\Sigma_{cl}^{T_c}$ (B.1), which makes this system representation convenient from a numerical perspective.

The requirements in (5.30) imply for Σ^{T_c} (5.29) that these mappings should satisfy

$$\begin{aligned} &A_{21} + L_2 C_{y1} = 0, \quad A_{31} + L_3 C_{y1} = 0, \\ &B_{w2} + L_2 D_{wy} = 0, \quad B_{w3} + L_3 D_{wy} = 0, \\ &L_1 : \mathcal{Y} \to \mathcal{X}_1, \end{aligned} \tag{5.38}$$

$$\begin{aligned} &A_{31} + B_{u3}\tilde{F}_1 = 0, \quad A_{32} + B_{u3}\tilde{F}_2 = 0, \\ &C_{z1} + D_{uz}\tilde{F}_1 = 0, \quad C_{z2} + D_{uz}\tilde{F}_2 = 0, \\ &\tilde{F}_3 : \mathcal{X}_3 \to \mathcal{U}, \end{aligned} \tag{5.39}$$

$$\begin{aligned} &B_{w3} + B_{u3} N D_{wy} = 0, \quad D_{uz} N D_{wy} = 0, \\ &A_{31} + B_{u3} N C_{y1} = 0, \quad C_{z1} + D_{uz} N C_{y1} = 0. \end{aligned} \tag{5.40}$$

The mappings L, $\tilde{F}$ and N are therefore constructed by numerically solving a set of linear equations.

Σ_c (5.25)—which is designed using Σ^{T_c} (5.29)—therefore solves the DDPM for (Σ^{T_c} (5.29), $\mathcal{X}_1$, $\mathcal{X}_1 \oplus \mathcal{X}_2$) when the mapping L satisfies (5.38), the mapping N satisfies (5.40); and when the mapping $F = \tilde{F} - NC_y$ is constructed with this specific N in combination with the mapping $\tilde{F}$ satisfying (5.39). Because Σ (5.1) and Σ^{T_c} (5.29) are equivalent in terms of input to output behaviour—and because $\mathcal{X}_1 = T_c\mathcal{S}$ and $\mathcal{X}_1 \oplus \mathcal{X}_2 = T_c\mathcal{V}$—it can be concluded that this controller will solve the DDPM for (Σ (5.1), $\mathcal{S}$, $\mathcal{V}$) as well.

Finally, let the considered subspaces $(\mathcal{S}, \mathcal{V}) \in \mathbb{T}$ satisfy $\dim(\mathcal{V}) - \dim(\mathcal{S}) = n_c$. Then $\widehat{\Sigma}_c^{T_c}$ (5.32) solves the DDPM-CO for (Σ^{T_c} (5.29), n_c) and for (Σ (5.1), n_c), when the mappings L_2, $F_2 = \tilde{F}_2 - NC_{y2}$ and N satisfy (5.38)–(5.40).

It is important to note for the DDPM-CO, that the controller order n_c is directly determined by dimension of the subspaces $(\mathcal{S}, \mathcal{V}) \in \mathbb{T}$. The mappings L, F and N, on the other hand, determine the mappings of this constrained order controller.

Solving the DDPMS: A representation of the form Σ^{T_c} (5.29) is also considered for the DDPMS, which is created using a state transformation T_c (5.37) that is now based on the different pair $(\mathcal{S}_g, \mathcal{V}_g) \in \mathbb{T}_g$.

For a given pair of subspaces $(\mathcal{S}_g, \mathcal{V}_g) \in \mathbb{T}_g$, it is established in Theorem 5.17 that the solution to the DDPMS is characterised in therms of the mappings L, $\tilde{F}$ and N that satisfy (5.30). The requirements in (5.30) imply for Σ^{T_c} (5.29), that the mappings L_1, L_2 and L_3 should satisfy (5.38) and, in addition, should achieve

$$\lambda\left(A_{11} + L_1 C_{y1}\right) \subseteq \mathbb{C}_g, \quad \begin{pmatrix} A_{22} + L_2 C_{y2} & A_{23} + L_2 C_{y3} \\ A_{32} + L_3 C_{y2} & A_{33} + L_3 C_{y3} \end{pmatrix} \subseteq \mathbb{C}_g.$$

For stability domain $\mathbb{C}_-$, it has been shown in section 2.3 that any mapping L_1 that achieves $\lambda\left(A_{11} + L_1 C_{y1}\right) \subset \mathbb{C}_-$ can be characterised by an LMI. In this way, all stabilising mappings $L_1 = Z_1^{-1} J_1$ are described by solutions to

$$Z_1 \succ 0, \quad A_{11}^\top Z_1 + Z_1 A_{11} + C_{y1}^\top J_1^\top + J_1 C_{y1} \prec 0. \tag{5.41}$$

Like the solution to the DDEPS in section 5.2.5, it is easy to show that the conditions on $\begin{pmatrix} L_2 \\ L_3 \end{pmatrix} = \begin{pmatrix} Z_{22} & Z_{23} \\ Z_{23}^\top & Z_{33} \end{pmatrix}^{-1} \begin{pmatrix} J_2 \\ J_3 \end{pmatrix}$ are described by solutions to

$$\begin{aligned} &\begin{pmatrix} Z_{22} & Z_{23} \\ Z_{23}^\top & Z_{33} \end{pmatrix} \succ 0, \quad \begin{pmatrix} A_{21}^\top & A_{31}^\top \\ B_{w2}^\top & B_{w3}^\top \end{pmatrix} \begin{pmatrix} Z_{22} & Z_{23} \\ Z_{32} & Z_{33} \end{pmatrix} + \begin{pmatrix} C_{y1}^\top \\ D_{wy}^\top \end{pmatrix} \begin{pmatrix} J_2^\top & J_3^\top \end{pmatrix} = 0, \\ &\begin{pmatrix} A_{22}^\top & A_{32}^\top \\ A_{23}^\top & A_{33}^\top \end{pmatrix} \begin{pmatrix} Z_{22} & Z_{23} \\ Z_{23}^\top & Z_{33} \end{pmatrix} + \begin{pmatrix} Z_{22} & Z_{23} \\ Z_{23}^\top & Z_{33} \end{pmatrix} \begin{pmatrix} A_{22} & A_{23} \\ A_{32} & A_{33} \end{pmatrix} \\ &\qquad + \begin{pmatrix} J_2 C_{y2} & J_2 C_{y3} \\ J_3 C_{y2} & J_3 C_{y3} \end{pmatrix} + \begin{pmatrix} J_2 C_{y2} & J_2 C_{y3} \\ J_3 C_{y2} & J_3 C_{y3} \end{pmatrix}^\top \prec 0. \end{aligned} \tag{5.42}$$

The design of a state feedback $\tilde{F}$ is dual to the design of an observer gain L. The requirements in (5.30) imply, in a similar manner, that the mappings $\tilde{F}_1$, $\tilde{F}_2$ and $\tilde{F}_3$ should satisfy (5.39) and, in addition, should achieve

$$\lambda\left(A_{33} + B_{u3}\tilde{F}_3\right) \subseteq \mathbb{C}_g, \quad \begin{pmatrix} A_{11} + B_{u1}\tilde{F}_1 & A_{12} + B_{u1}\tilde{F}_2 \\ A_{21} + B_{u2}\tilde{F}_1 & A_{22} + B_{u2}\tilde{F}_2 \end{pmatrix} \subseteq \mathbb{C}_g.$$

All stabilising mappings $\tilde{F}_3 = K_3 Y_3^{-1}$ are therefore—for stability domain $\mathbb{C}_-$—described by solutions to

$$Y_3 \succ 0, \quad Y_3 A_{33}^\top + A_{33} Y_3 + K_3^\top B_{u3}^\top + B_{u3} K_3 \prec 0. \tag{5.43}$$

The conditions on $\begin{pmatrix} \tilde{F}_1 & \tilde{F}_2 \end{pmatrix} = \begin{pmatrix} K_1 & K_2 \end{pmatrix} \begin{pmatrix} Y_{11} & Y_{12} \\ Y_{12}^\top & Y_{22} \end{pmatrix}^{-1}$ are described by solutions to

$$\begin{aligned} &Y = \begin{pmatrix} Y_{11} & Y_{12} \\ Y_{12}^\top & Y_{22} \end{pmatrix} \succ 0, \quad \begin{pmatrix} A_{31} & A_{32} \\ C_{z1} & C_{z1} \end{pmatrix} \begin{pmatrix} Y_{11} & Y_{12} \\ Y_{12}^\top & Y_{22} \end{pmatrix} + \begin{pmatrix} B_{u3} \\ D_{uz} \end{pmatrix} \begin{pmatrix} K_1 & K_2 \end{pmatrix} = 0, \\ &\begin{pmatrix} Y_{11} & Y_{12} \\ Y_{12}^\top & Y_{22} \end{pmatrix} \begin{pmatrix} A_{11}^\top & A_{12}^\top \\ A_{21}^\top & A_{22}^\top \end{pmatrix} + \begin{pmatrix} A_{11} & A_{12} \\ A_{21} & A_{22} \end{pmatrix} \begin{pmatrix} Y_{11} & Y_{12} \\ Y_{12}^\top & Y_{22} \end{pmatrix} \\ &\qquad + \begin{pmatrix} B_{u1} K_1 & B_{u1} K_2 \\ B_{u2} K_1 & B_{u2} K_2 \end{pmatrix} + \begin{pmatrix} B_{u1} K_1 & B_{u1} K_2 \\ B_{u2} K_1 & B_{u2} K_2 \end{pmatrix}^\top \prec 0. \end{aligned} \tag{5.44}$$

Σ_c (5.25)—which is designed using Σ^{T_c} (5.29)—therefore solves the DDPMS for (Σ^{T_c} (5.29), $\mathcal{X}_1$, $\mathcal{X}_1 \oplus \mathcal{X}_2$, $\mathbb{C}_-$) when the mapping L satisfies (5.41),(5.42); the mapping N satisfies (5.40); and when the mapping $F = \tilde{F} - NC_y$ is constructed with this specific N in combination with the mapping $\tilde{F}$ satisfying (5.43),(5.44). Because Σ (5.1) and Σ^{T_c} (5.29) are equivalent in terms of input to output behaviour—and because $\mathcal{X}_1 = T_c\mathcal{S}_g$ and $\mathcal{X}_1 \oplus \mathcal{X}_2 = T_c\mathcal{V}_g$—it can again be concluded that this controller will solve the DDPMS for (Σ (5.1), $\mathcal{S}$, $\mathcal{V}$, $\mathbb{C}_-$) as well.

Steps 4 and 5

Similarly to step 1, it is assumed that a minimal representation is constructed for the subspaces $\mathcal{S}_1$, $\mathcal{S}_3$—corresponding to Definition 5.22.

Then, let us define the state transformation $T_{c,g}$ that transforms Σ (5.1) into $\Sigma^{T_{c,g}}$ (B.3). The states of $\Sigma^{T_{c,g}}$ (B.3) are compatible to the state decomposition in (5.34). By utilising the subspaces $\mathcal{S}_1$ and $\mathcal{S}_3$—in combination with $\mathcal{S}_g$ and $\mathcal{V}_{g,c}$ as described in step 2—it is possible to define the subspaces $\mathcal{S}_{1,c}$ and $\mathcal{S}_{3,c}$ such that $\mathcal{S}_1 \oplus \mathcal{S}_{1,c} = \mathcal{S}_g$ and $\mathcal{S}_3 \oplus \mathcal{S}_{3,c} = \mathcal{V}_{g,c}$. For example, we can consider $\mathcal{S}_{1,c} = \mathcal{S}_1^{\perp} \cap \mathcal{S}_g$ and $\mathcal{S}_{3,c} = \mathcal{S}_3^{\perp} \cap \mathcal{V}_{g,c}$.

Minimal representation for these subspaces can be used to transform Σ^{T_c} (5.29)—as constructed in step 2—into $\Sigma^{T_{c,g}}$ (B.3). The structure of Σ^{T_c} (5.29), actually implies that the minimal representations for the subspaces $\mathcal{S}_1$, $\mathcal{S}_{1,c}$, $\mathcal{S}_3$ and $\mathcal{S}_{3,c}$ are of the form

$$S_1 = \begin{pmatrix} \bar{S}_1 \\ 0 \\ 0 \end{pmatrix}, \quad S_{1,c} = \begin{pmatrix} \bar{S}_{1,c} \\ 0 \\ 0 \end{pmatrix}, \quad S_3 = \begin{pmatrix} 0 \\ 0 \\ \bar{S}_3 \end{pmatrix}, \quad S_{3,c} = \begin{pmatrix} 0 \\ 0 \\ \bar{S}_{3,c} \end{pmatrix}.$$

In other words, $\bar{S}_1$ and $\bar{S}_{1,c}$ are minimal representations for subspaces $\bar{\mathcal{S}}_1$ and $\bar{\mathcal{S}}_{1,c}$ of vector space $\mathcal{X}_1$. Similarly, $\bar{S}_3$ and $\bar{S}_{3,c}$ are minimal representations for subspaces $\bar{\mathcal{S}}_3$ and $\bar{\mathcal{S}}_{3,c}$ of vector space $\mathcal{X}_3$. The system Σ^{T_c} (5.29) can therefore be transformed into $\Sigma^{T_{c,g}}$ (B.3) by utilising the state transformation

$$T_g = \begin{pmatrix} \Pi_s(\bar{\mathcal{S}}_1, \bar{\mathcal{S}}_{1,c}) & 0 & 0 \\ \Pi_s(\bar{\mathcal{S}}_{1,c}, \bar{\mathcal{S}}_1) & 0 & 0 \\ 0 & \mathbb{I}_{\dim(\mathcal{X}_2)} & 0 \\ 0 & 0 & \Pi_s(\bar{\mathcal{S}}_{3,c}, \bar{\mathcal{S}}_3) \\ 0 & 0 & \Pi_s(\bar{\mathcal{S}}_3, \bar{\mathcal{S}}_{3,c}) \end{pmatrix}. \tag{5.45}$$

The state transformation that transforms Σ (5.1) directly into $\Sigma^{T_{c,g}}$ (B.3) is now given by $T_{c,g} = T_g T_c$.

Step 6

For the DDPMS-CO we will consider a representation of the form Σ^{T_c} (5.29), which is created with a state transformation T_c (5.37) that is based on a pair $(\mathcal{S}_g, \mathcal{V}_g) \in \mathbb{T}_g$. In addition, a pair $(F_g, N_g) \in \underline{M}_g(\mathcal{S}_g, \mathcal{V}_g)$ is constructed; for stability domain $\mathbb{C}_g = \mathbb{C}_-$ we have shown that N_g is a solution to (5.40) and that the solutions to (5.43),(5.44) can be used to obtain $F_g = \tilde{F} - N_g C_y$.

With these mappings it is possible to construct a pair of subspaces $\mathcal{S}_1$ and $\mathcal{S}_3$—corresponding to Definition 5.22. These subspaces are used to create the system representation $\Sigma^{T_{c,g}}$ (B.3) by applying a state transformation T_g as defined in (5.45) to Σ^{T_c} (5.29). The constrained order controller $\widehat{\Sigma}_{c,g}^{T_{c,g}}$ (B.4) is for $\Sigma^{T_{c,g}}$ (B.3) characterised in the mappings
$\begin{pmatrix} L_{12} \\ L_2 \\ L_{31} \end{pmatrix}$, $\begin{pmatrix} F_{12} & F_2 & F_{31} \end{pmatrix}$ and N.

In Theorem 5.24 it is established that the mappings $\begin{pmatrix} F_{12} & F_2 & F_{31} \end{pmatrix}$ and N of this controller can directly be derived from F_g and N_g. Similar to the DDPMS, it is easy to show for stability domain $\mathbb{C}_-$ that $L_{12} = V_{12}^{-1} H_{12}$ is described by solutions to

$$\begin{aligned} V_{12} \succ 0, \quad A_{1211}^\top V_{12} + C_{y11} H_{12} = 0, \\ A_{1212}^\top V_{12} + V_{12} A_{1212} + C_{y12}^\top H_{12}^\top + H_{12} C_{y12} \prec 0. \end{aligned} \tag{5.46}$$

And that the conditions on $\begin{pmatrix} L_2 \\ L_{31} \end{pmatrix} = \begin{pmatrix} V_{22} & V_{231} \\ V_{231}^\top & V_{3131} \end{pmatrix}^{-1} \begin{pmatrix} H_2 \\ H_{31} \end{pmatrix}$ are described by solutions to

$$\begin{aligned} &\begin{pmatrix} V_{22} & V_{231} \\ V_{231}^\top & V_{3131} \end{pmatrix} \succ 0, \quad \begin{pmatrix} A_{211}^\top & A_{3111}^\top \\ A_{212}^\top & A_{3112}^\top \\ A_{232}^\top & A_{3132}^\top \\ B_{w2}^\top & B_{w31}^\top \end{pmatrix} \begin{pmatrix} V_{22} & V_{231} \\ V_{231}^\top & V_{3131} \end{pmatrix} + \begin{pmatrix} C_{y11}^\top \\ C_{y12}^\top \\ C_{y32}^\top \\ D_{wy}^\top \end{pmatrix} \begin{pmatrix} H_2^\top & H_{31}^\top \end{pmatrix} = 0, \\ &\begin{pmatrix} A_{22}^\top & A_{312}^\top \\ A_{231}^\top & A_{3131}^\top \end{pmatrix} \begin{pmatrix} V_{22} & V_{231} \\ V_{231}^\top & V_{3131} \end{pmatrix} + \begin{pmatrix} V_{22} & V_{231} \\ V_{231}^\top & V_{3131} \end{pmatrix} \begin{pmatrix} A_{22} & A_{231} \\ A_{312} & A_{3131} \end{pmatrix} \\ &\qquad + \begin{pmatrix} H_2 C_{y2} & H_2 C_{y31} \\ H_{31} C_{y2} & H_{31} C_{y31} \end{pmatrix} + \begin{pmatrix} H_2 C_{y2} & H_2 C_{y31} \\ H_{31} C_{y2} & H_{31} C_{y31} \end{pmatrix}^\top \prec 0. \end{aligned} \tag{5.47}$$

Finally, let the subspaces $\mathcal{S}_1$ and $\mathcal{S}_3$ satisfy $\dim(\mathcal{S}_1) + \dim(\mathcal{S}_3) = \dim(\mathcal{X}) - n_c$. Then $\widehat{\Sigma}_{c,g}^{T_{c,g}}$ (B.4) solves the DDPMS-CO for ($\Sigma^{T_{c,g}}$ (B.3), $\mathbb{C}_-$, n_c), (Σ^{T_c} (5.29), $\mathbb{C}_-$, n_c) and (Σ (5.1), $\mathbb{C}_-$, n_c) when the mappings N_g and F_g as defined above are used to design the controller mappings $N = N_g$ and $\begin{pmatrix} 0 & F_{12} & F_2 & F_{31} & 0 \end{pmatrix} = T_g F_g$; and when the mapping $\begin{pmatrix} L_{12} \\ L_2 \\ L_{31} \end{pmatrix}$ satisfies (5.46),(5.47).

Similarly to the DDPM-CO, it is important to note for the DDPMS-CO, that the controller order n_c is directly determined by the dimension of the subspaces $\mathcal{S}_1$ and $\mathcal{S}_3$. The mappings $L_{m,g}$, $F_{m,g}$ and N, on the other hand, determine the mappings of this constrained order controller.

5.3.8 An Illustrative Example

An example is now presented to illustrate the design of a constrained order controller. In addition, the example is used to demonstrate that the solution to the

DDPMS-CO—as presented in section 5.3.5—is restrictive in terms of minimising the controller order.

In this example, a system of the form $\Sigma^{T_{c,g}}$ (B.3)—with $\dim(\mathcal{X}_{12}) = 0$—is considered. The system is described by $\Sigma_{ex,c} =$

$$\left\{\begin{array}{rcl} \begin{pmatrix}\dot{x}_{11}(t)\\ \dot{x}_2(t)\\ \dot{x}_{31}(t)\\ \dot{x}_{32}(t)\end{pmatrix} &=& \begin{pmatrix}-10 & -2 & 1 & -2\\ -1 & -12 & 3 & 5\\ 0 & -6 & 1 & -1\\ 0 & 2 & 0 & -1\end{pmatrix}\begin{pmatrix}x_{11}(t)\\ x_2(t)\\ x_{31}(t)\\ x_{32}(t)\end{pmatrix} + \begin{pmatrix}0 & 0\\ 0 & 0\\ 1 & 0\\ 0 & 1\end{pmatrix}u(t) + \begin{pmatrix}1 & 5\\ 4 & 2\\ 0 & 0\\ 0 & 0\end{pmatrix}w(t)\\ y(t) &=& \begin{pmatrix}1 & 0 & 0 & 0\\ 0 & 0 & 0 & 8\end{pmatrix}x(t) + \begin{pmatrix}-4 & -2\\ 0 & 0\end{pmatrix}w(t)\\ z(t) &=& \begin{pmatrix}0 & -8 & 6 & 4\\ 0 & -4 & 7 & 3\end{pmatrix}x(t) + \begin{pmatrix}1 & -1\\ 1 & 1\end{pmatrix}u(t). \end{array}\right. \tag{5.48}$$

Note that the system representation is of the form Σ^{T_c} (5.29) as well, by defining $x_1(t) = x_{11}(t)$ and $x_3(t) = \begin{pmatrix}x_{31}(t)\\ x_{32}(t)\end{pmatrix}$.

Solving the DDPM-CO

A controller $\widehat{\Sigma}_c^{T_c}$ (5.32) of order $\dim(\mathcal{X}_2) = 1$ can be used to solve the DDPM-CO for $\Sigma_{ex,c}$ (5.48), as explained in section 5.3.4. Applying this controller—with $N = 0$ as will be explained below—to $\Sigma_{ex,c}$ (5.48) will result in a closed-loop system of the form $\widehat{\Sigma}_{cl}^{T_c}$ (B.2), which is described by $\widehat{\Sigma}_{ex,c,cl} =$

$$\left\{\begin{array}{rcl} \begin{pmatrix}\dot{x}_{11}(t)\\ \dot{x}_2(t)\\ \dot{x}_{31}(t)\\ \dot{x}_{32}(t)\\ \hline \dot{e}_2(t)\end{pmatrix} &=& \left(\begin{array}{cccc|c} -10 & -2 & 1 & -2 & 0\\ -1 & -12 & 3 & 5 & 0\\ 0 & \boldsymbol{F_{21}-6} & 1 & -1 & -F_{21}\\ 0 & \boldsymbol{F_{22}+2} & 0 & -1 & -F_{22}\\ \hline \boldsymbol{L_{21}-1} & 0 & 3 & 8L_{22}+5 & -12 \end{array}\right)\begin{pmatrix}x_{11}(t)\\ x_2(t)\\ x_{31}(t)\\ x_{32}(t)\\ \hline e_2(t)\end{pmatrix}\\ &&+\left(\begin{array}{cc} 1 & 5\\ 2 & 4\\ 0 & 0\\ 0 & 0\\ \hline \boldsymbol{4-4L_{21}} & \boldsymbol{2-L_{21}}\end{array}\right)w(t)\\ z(t) &=& \left(\begin{array}{cccc|c} 0 & \boldsymbol{F_{21}-F_{22}-8} & 6 & 4 & F_{22}-F_{21}\\ 0 & \boldsymbol{F_{21}+F_{22}-4} & 7 & 3 & -F_{21}-F_{22}\end{array}\right)\begin{pmatrix}x(t)\\ \hline e_2(t)\end{pmatrix} \end{array}\right. \tag{5.49}$$

In section 5.3.7 it is explained that the reduced order controller should satisfy the conditions on L_2, F_2 and N in (5.38)-(5.40). These conditions imply that $\widehat{\Sigma}_c^{T_c}$ (5.32) solves the DDPM-CO for ($\Sigma_{ex,c}$ (5.48), 1) if we consider $N = 0$, $F_2 = \begin{pmatrix}6\\ -2\end{pmatrix}$ and $L_{21} = 1$, while L_{22} is completely free.

Solving the DDPMS-CO

For this specific example we can observe that by choosing $L_{22} = -1$, the controller $\widehat{\Sigma}_c^{T_c}$ (5.32) as described above will solve the DDPMS-CO for ($\Sigma_{ex,c}$ (5.48), $\mathbb{C}_-$, 1) as well. It is, however, in general not guaranteed that a controller wich is designed in this way will be able to solve the DDPMS-CO.

Therefore, let us solve the DDPMS-CO for stability domain $\mathbb{C}_g = \mathbb{C}_-$, by utilising the method as described in section 5.3.5 instead. With this method, an extension is essentially added to $\widehat{\Sigma}_c^{T_c}$ (5.32) as constructed above. In order to determine this extension, it is required to first find a mapping $F \in \underline{M}_g(\mathcal{X}_{11}, \mathcal{X}_{11} \oplus \mathcal{X}_2)$ in order to determine the subspaces $\mathcal{S}_1$ and $\mathcal{S}_3$—corresponding to Definition 5.22. These subspaces are then used to construct a system of the form $\Sigma^{T_{c,g}}$ (B.3).

We can consider $F = \begin{pmatrix} 0 & 6 & -2 & 0 \\ 0 & -2 & 0 & 0 \end{pmatrix} \in \underline{M}_g(\mathcal{X}_{11}, \mathcal{X}_{11} \oplus \mathcal{X}_2)$, $\mathcal{S}_1 = \mathcal{X}_{11}$ and $\mathcal{S}_3 = \mathcal{X}_{32}$ to conclude that $\Sigma_{ex,c}$ (5.48) is indeed of the form $\Sigma^{T_{c,g}}$ (B.3). The controller $\widehat{\Sigma}_{c,g}^{T_{c,g}}$ (B.4) of order $\dim(\mathcal{X}_2) + \dim(\mathcal{X}_{31}) = 2$ can then be designed according to section 5.3.7.

In section 5.3.7, it is established for $\widehat{\Sigma}_{c,g}^{T_{c,g}}$ (B.4) that $N = 0$, $F_2 = \begin{pmatrix} 6 & -2 \end{pmatrix}^\top$ and $F_{31} = \begin{pmatrix} -2 & 0 \end{pmatrix}^\top$ can be used. The mappings L_2 and L_{31} are characterised by solutions to (5.47) and it can easily be verified that this uniquely defines $L_2 = \begin{pmatrix} 1 & -\frac{5}{8} \end{pmatrix}$ and $L_{31} = \begin{pmatrix} 0 & \frac{1}{8} \end{pmatrix}$.

Applying this controller of order 2 to $\Sigma_{ex,c}$ (5.48), results in a stable disturbance decoupled closed-loop system, which is described by

$$\widehat{\Sigma}_{ex,c,cl,g} = \left\{ \begin{array}{rcl} \begin{pmatrix} \dot{x}_{11}(t) \\ \dot{x}_2(t) \\ \dot{x}_{31}(t) \\ \dot{x}_{32}(t) \\ \hline \dot{e}_2(t) \\ \dot{e}_{31}(t) \end{pmatrix} & = & \left(\begin{array}{cccc|cc} -10 & -2 & 1 & -2 & 0 & 0 \\ -1 & -12 & 3 & 5 & 0 & 0 \\ 0 & 0 & -1 & -1 & -6 & 2 \\ 0 & 0 & 0 & -1 & 2 & 0 \\ \hline 0 & 0 & 0 & 0 & -12 & 3 \\ 0 & 0 & 0 & 0 & -6 & 1 \end{array}\right) \begin{pmatrix} x_{11}(t) \\ x_2(t) \\ x_{31}(t) \\ x_{32}(t) \\ \hline e_2(t) \\ e_{31}(t) \end{pmatrix} + \begin{pmatrix} 1 & 5 \\ 2 & 4 \\ 0 & 0 \\ 0 & 0 \\ \hline 0 & 0 \\ 0 & 0 \end{pmatrix} w(t) \\ z(t) & = & \left(\begin{array}{cccc|cc} 0 & 0 & 4 & 4 & -8 & 2 \\ 0 & 0 & 5 & 3 & -4 & 2 \end{array}\right) \left(\begin{array}{c} x(t) \\ \hline e(t) \end{array}\right). \end{array} \right. \tag{5.50}$$

Remark 5.4 *The solution to the DDPMS-CO—as described in section 5.3.5—utilises a stabilising mapping $F \in \underline{M}_g(\mathcal{S}_g, \mathcal{V}_g)$ to construct the constrained order controller $\widehat{\Sigma}_{c,g}^{T_{c,g}}$ (B.4). In this example, such an approach will always result in a controller of at least order 2. It has, however, been shown that a controller $\widehat{\Sigma}_c^{T_c}$ (5.32) of order 1 can solve the DDPMS-CO as well. Therefore, we can conclude that the solution to the DDPMS-CO as described in section 5.3.5 is restrictive in terms of minimising the controller order.*

5.4 H_2 Optimal Estimation and Control with a Constrained Order

5.4.1 Problem Definition and Section Outline

In this section, the results from sections 5.2 and 5.3—that were obtained for disturbance decoupling problems—are applied to the more practical H_2 optimal control problem. Namely, we will aim to characterise all controller orders $n_c^\star$—and to construct the corresponding constrained order controller—for which the following H_2 optimal control problem can be solved:

Problem 5.1 *Construct an H_2-admissible controller $\Sigma_{c,n_c}^\star$ of the form (5.21) and of order $n_c^\star \in \mathbb{N}$ for Σ (5.1), which is a solution to*

$$(\Sigma_{c,n_c}^\star, n_c^\star) = \arg \min_{\Sigma_{c,n_c},\ n_c \in \mathbb{N}} \|\Sigma_{cl,n_c}\ (5.22)\|_{H_2} \quad \text{s.t.} \quad \Sigma_{c,n_c}\ (5.21) \text{ is } H_2\text{-admissible for } \Sigma\ (5.1).$$

A solution to the minimal order optimal control problem in Problem 1.4 can be obtained for the H_2 norm by characterising all orders $n_c^\star$ that can be used to achieve H_2 optimal performance in closed-loop. In addition, an answer is provided to the corresponding research questions, while the resulting constrained order controllers provide a solution to Problem 1.3 for these orders.

The well-known solution to the H_2 optimal control problem in Problem 5.1—that utilises a controller of order $n_c = n_x$—is derived in section 2.4. We will, again, make the following assumption for the design of such a controller.

Assumption 5.2 *It is assumed that*

1a) (A, B_u) *is* $\mathbb{C}_-$*-stabilisable.*
1b) (C_y, A) *is* $\mathbb{C}_-$*-detectable.*
2a) $\begin{pmatrix} A - j\omega I_{n_x} & B_u \\ C_z & D_{uz} \end{pmatrix}$ *is full column rank for all* $\omega \in \mathbb{R}$.
2b) $\begin{pmatrix} A - j\omega I_{n_x} & B_w \\ C_y & D_{wy} \end{pmatrix}$ *is full row rank for all* $\omega \in \mathbb{R}$.
3a) D_{uz} *is full column rank.*
3b) D_{wy} *is full row rank.*

The following solution to the H_2 optimal control problem is obtained under this assumption:

Corollary 5.28 *Consider a system Σ (5.1) that satisfies assumption 5.2 and let $P^+ \succeq 0$ and $Q^+ \succeq 0$ be the unique stabilising solutions to the following AREs:*

$$A^\top P + PA + C_z^\top C_z - (PB_u + C_z^\top D_{uz})(D_{uz}^\top D_{uz})^{-1}(PB_u + C_z^\top D_{uz})^\top = 0, \tag{5.51}$$

$$AQ + QA^\top + B_w B_w^\top - (QC_y^\top + B_w^\top D_{wy})(D_{wy} D_{wy}^\top)^{-1}(QC_y^\top + B_w^\top D_{wy})^\top = 0. \tag{5.52}$$

These positive semidefinite solutions satisfy $P^+ \succeq P$ and $Q^+ \succeq Q$, for any real and symmetric solution P and Q to the AREs in (5.51) *and* (5.52)*, respectively.*

Then Problem 5.1 "can be solved" by using a controller of the form Σ_c (5.25)*—which is of order n_x—with design parameters $L : \mathcal{Y} \to \mathcal{X}$, $F : \mathcal{X} \to \mathcal{U}$ and $N : \mathcal{Y} \to \mathcal{U}$.*

Furthermore, the controller Σ_c (5.25) *"solves" Problem 5.1 with*

$$\begin{aligned} L &= -(Q^+ C_y^\top + B_w^\top D_{wy})(D_{wy} D_{wy}^\top)^{-1}, \\ F &= -(D_{uz}^\top D_{uz})^{-1}(B_u^\top P^+ + D_{uz}^\top C_z), \\ N &= 0. \end{aligned}$$

Proof: The proof can be found in section 2.4. □

This solution to the H_2 optimal control problem consists of separately solving a state feedback design problem and an estimator design problem. We will therefore first investigate the design of H_2 optimal state feedbacks in section 5.4.2 and the design of H_2 optimal estimators with a constrained order in section 5.4.3. Then, the results for these problems are combined in section 5.4.4 in order to characterise all controller orders $n_c^\star$ that solve Problem 5.1.

For each of these problems, its well-known solution in section 2.4 is related to the concepts from geometric control theory as discussed in sections 5.2 and 5.3.

5.4.2 State Feedback Design

For H_2 optimal state feedback design, the stability domain $\mathbb{C}_g = \mathbb{C}_-$ is considered. With this stability domain, let $\mathcal{V}_-$ be an output-nulling $\mathbb{C}_-$-stabilisability subspace and $\mathcal{V}_-^\star$ the $\mathbb{C}_-$-stabilisable weakly unobservable subspace as defined in Lemma 2.39 and Theorem 2.40, respectively; and let $\mathbb{V}_-(\Sigma)$ denote the set as defined in (5.24).

We will now discuss the design of an H_2 optimal state feedback $u(t) = Fx(t)$ for the system Σ (5.1). Such a feedback essentially minimises, in the H_2 norm, the effect of $w(t)$ onto $z(t)$ for $\Sigma_{cl,F}$ (5.23); the measured output $y(t)$ of Σ (5.1) can be disregarded for this type of control problem. For the design of an H_2 optimal feedback, the following definitions from section 2.4 are utilised.

Definition 5.29 *Consider a state feedback $u(t) = Fx(t)$ applied to the system Σ* (5.1)*, which results in the closed-loop system $\Sigma_{cl,F}$* (5.23)*.*

Then we say that $u(t) = Fx(t)$ is H_2-admissible for Σ (5.1) *if for $\Sigma_{cl,F}$* (5.23) *we have that $\lambda(A + B_u F) \subset \mathbb{C}_-$.*

The performance of an H_2-admissible state feedback is defined as

$$\gamma_{H_2,F}(\Sigma \text{ (5.1)}, F) = \|\Sigma_{cl,F} \text{ (5.23)}\|_{H_2}^2 .$$

We say that a state feedback is H_2 optimal for Σ (5.1) if it is a solution to

$$F = \begin{array}{ll} \arg\min\limits_{\tilde{F}} & \gamma_{H_2,F}(\Sigma\ (5.1), \tilde{F}) \\ \text{s.t.} & u(t) = \tilde{F}x(t) \text{ is } H_2\text{-admissible for } \Sigma\ (5.1). \end{array}$$

The H_2 performance of an H_2 optimal state feedback $u(t) = F^\star x(t)$ for Σ (5.1) is denoted by

$$\gamma^\star_{H_2,F}(\Sigma\ (5.1)) = \gamma_{H_2,F}(\Sigma\ (5.1), F^\star).$$

In addition, let us recite the typical solution to the H_2 optimal state feedback design problem as derived in section 2.4.

Corollary 5.30 *Consider a system Σ (5.1) that satisfies items 1a, 2a and 3a in assumption 5.2 and let $P^+ \succeq 0$ be the unique stabilising solution to the ARE in (5.51). Furthermore, let Σ' denote Σ (5.1) for which the mapping $B_w : \mathcal{W} \to \mathcal{X}$ is replaced with any mapping $B'_w : \mathcal{W}' \to \mathcal{X}$. Finally, let us consider the mapping $F^\star := -(D_{uz}^\top D_{uz})^{-1}(B_u^\top P^+ + D_{uz}^\top C_z)$.*

Then the state feedback $u(t) = F^\star x(t)$ is H_2 optimal for Σ (5.1).

Furthermore, the following statements are equivalent:

(i) $u(t) = F^\star x(t)$ is H_2 optimal for Σ (5.1).

(ii) $u(t) = F^\star x(t)$ is H_2 optimal for Σ'.

Proof: A proof for the first statement is provided in section 2.4.

To prove the second statement, it suffices to observe that P^+ and the state feedback $u(t) = F^\star x(t)$ are, for both systems, created independently of B_w and B'_w. Therefore the same H_2 optimal feedback is obtained for each system. □

For a system Σ (5.1) that satisfies the assumptions in Corollary 5.30, we can—by utilising the unique stabilising solution P^+—define the transformed system

$$\Sigma_P = \begin{cases} \dot{x}(t) = Ax(t) + B_u u(t) + B_w w(t) \\ y(t) = C_y x(t) + D_{wy} w(t) \\ z(t) = (D_{uz}^\top D_{uz})^{-\frac{1}{2}}(B_u^\top P^+ + D_{uz}^\top C_z)x(t) + (D_{uz}^\top D_{uz})^{\frac{1}{2}} u(t). \end{cases} \tag{5.53}$$

This transformed system will be used to transform the H_2 optimal state feedback design problem into a DDPS as discussed in section 5.3.2. For this purpose, let us first derive some useful properties for the system Σ_P (5.53).

Lemma 5.31 *Consider a system Σ (5.1) that satisfies items 1a, 2a and 3a in assumption 5.2 and let $P^+ \succeq 0$ be the unique stabilising solution to the ARE in (5.51).*

Then the transformed system Σ_P (5.53) has the following properties:

(a) $\mathbb{V}_-(\Sigma_P\ (5.53)) = \{\ \mathcal{V}_- \subseteq \mathcal{X}$ | *$\mathcal{V}_-$ is as defined in Lemma 2.39 for stability domain $\mathbb{C}_g = \mathbb{C}_-$,* $\operatorname{im}(B_w) \subseteq \mathcal{V}_-\}$.

(b) $\mathcal{V}_-^\star = \mathcal{X}$.
(c) the DDPS "can be solved" for Σ_P (5.53).

Proof: (a) follows directly from the definition in (5.24), when it is observed that $\ker((D_{uz}^\top D_{uz})^{\frac{1}{2}}) = 0$.

(b) In Theorem 2.40 it is established that $\mathcal{V}_- \subseteq \mathcal{V}_-^\star$, for any subspace $\mathcal{V}_-$ for which there exists a mapping $F : \mathcal{X} \to \mathcal{U}$ such that $(A+B_uF)\mathcal{V}_- \subseteq \mathcal{V}_-$, $(C_z+D_{uz}F)\mathcal{V}_- = 0$ and $\lambda((A+B_uF)|\mathcal{V}_-) \subset \mathbb{C}_-$. By utilising $F = -(D_{uz}^\top D_{uz})^{-1}(B_u^\top P^+ + D_{uz}^\top C_z)$, it can be observed that $\mathcal{V}_-^\star = \mathcal{X}$ is indeed the largest subspace that satisfies these requirements.

(c) The inclusion $\mathrm{im}(B_w) \subseteq \mathcal{X}$ holds by definition, which implies that $\mathcal{V}_-^\star \in \mathbb{V}_-(\Sigma_P \text{ (5.53)})$ and therefore the DDPS can be solved. □

Now it will be shown that Σ_P (5.53) can indeed be used to directly transform the H_2 optimal state feedback design problem into a disturbance decoupling problem.

Theorem 5.32 *Consider a system* Σ (5.1) *that satisfies items 1a, 2a and 3a in assumption 5.2, let* $P^+ \succeq 0$ *be the unique stabilising solution to the ARE in* (5.51) *and consider the transformed system* Σ_P (5.53). *Furthermore, let* $\Sigma_{cl,P,F}$ *denote the closed-loop interconnection of a state feedback* $u(t) = Fx(t)$ *with* Σ_P (5.53).

Then a state feedback $u(t) = Fx(t)$ *is* H_2 *optimal for* Σ (5.1) *if and only if the state feedback* $u(t) = Fx(t)$ *is* H_2*-admissible for* Σ_P (5.53) *and the control output* $z(t)$ *of* $\Sigma_{cl,P,F}$ *is independent of the disturbance* $w(t)$.

Proof: The proof can be found in appendix A.3. □

A state feedback $u(t) = Fx(t)$ is therefore H_2 optimal for Σ (5.1) when it solves the DDPS for the transformed system Σ_P (5.53). Now it is interesting to establish how the unique H_2 optimal state feedback from Corollary 5.30 is characterised in terms of the solutions to the DDPS for Σ_P (5.53).

Proposition 5.33 *Consider a system* Σ (5.1) *that satisfies items 1a, 2a and 3a in assumption 5.2, let* $P^+ \succeq 0$ *be the unique stabilising solution to the ARE in* (5.51) *and consider the transformed system* Σ_P (5.53). *Furthermore, let* Σ' *denote* Σ (5.1) *for which the mapping* $B_w : \mathcal{W} \to \mathcal{X}$ *is replaced with any mapping* $B'_w : \mathcal{W}' \to \mathcal{X}$ *and let* Σ'_P *be the corresponding transformed system.*

Then the following statements are equivalent for a state feedback:
(i) $u(t) = Fx(t)$ *solves the DDPS for (*Σ_P (5.53), $\mathcal{V}_-^\star$, $\mathbb{C}_-$*), with* $\mathcal{V}_-^\star \in \mathbb{V}_-(\Sigma_P \text{ (5.53)})$.
(ii) $u(t) = Fx(t)$ *solves the DDPS for (*Σ'_P, $\mathcal{V}_-^\star$, $\mathbb{C}_-$*), with* $\mathcal{V}_-^\star \in \mathbb{V}_-(\Sigma'_P)$.
(iii) $F = -(D_{uz}^\top D_{uz})^{-1}(B_u^\top P^+ + D_{uz}^\top C_z)$.

Proof: The proof can be found in appendix A.3. □

It can therefore be concluded that the unique H_2 optimal state feedback from corollary 5.30 is the unique state feedback that solves the DDPS for Σ_P (5.53) by

utilising the subspace $\mathcal{V}_-^\star$. The additional property that this feedback solves both problems for any mapping B_w, is obtained because $\mathcal{V}_-^\star = \mathcal{X}$ for Σ_P (5.53).

By utilising the equivalence between H_2 optimality and disturbance decoupling, all H_2 optimal state feedbacks for Σ (5.1) are essentially paired with subspaces $\mathcal{V}_- \in \mathbb{V}_-(\Sigma_P$ (5.53)). It is, however, important to note that this pairing is not "one to one" in general. For example, multiple subspaces could be paired with a given H_2 optimal feedback.

Such a pairing is not directly interesting for state feedback design. However, it has been shown in section 5.3 that the controller order for the DDPMS-CO is (partially) determined by $\dim(\mathcal{V}_-)$. A relation between the H_2 optimal state feedbacks $u(t) = Fx(t)$ and "potential controller orders" has therefore been established, which is exactly what we require to characterise the controller orders that can be considered for the H_2 optimal control problem.

5.4.3 Estimator Design

For H_2 optimal estimator design, again the stability domain $\mathbb{C}_g = \mathbb{C}_-$ is considered. With this stability domain, let $\mathcal{S}_-$ be an input-containing $\mathbb{C}_-$-detectability subspace and $\mathcal{S}_-^\star$ the $\mathbb{C}_-$-detectable strongly reachable subspace as defined in Lemma 2.42 and Theorem 2.43, respectively; and let $\mathbb{S}_-(\Sigma)$ denote the set as defined in (5.6).

It is important to note that unobservable or unreachable states do not contribute towards the input to output behaviour of Σ (5.1). These states can therefore be disregarded when an estimation problem is considered and the following assumption is made.

Assumption 5.3 *For H_2 optimal estimator design it is assumed that any state of Σ (5.1) can be reached through the pair $(u(t), w(t))$ and observed in the pair $(y(t), z(t))$.*

We will now discuss the design of an H_2 optimal estimator Σ_{e,n_e} (5.2) for the system Σ (5.1). Such an estimator minimises, in the H_2 norm, the effect of $w(t)$ and $u(t)$ onto $\epsilon_z(t)$ for Σ_{ϵ,n_e} (5.3). The following definitions from section 2.4 are utilised.

Definition 5.34 *Consider an estimator Σ_{e,n_e} (5.2) applied to the system Σ (5.1), which results in the error system Σ_{ϵ,n_e} (5.3). Furthermore, let $\mathcal{N} \subseteq \mathcal{X}^{\epsilon,n_e}$ denote the unobservable subspace of Σ_{ϵ,n_e} (5.3).*

Then we say that Σ_{e,n_e} (5.2) is H_2-admissible for Σ (5.1) if for Σ_{ϵ,n_e} (5.3) we have that $D_{uz}^{\epsilon,n_e} = 0$, $D_{wz}^{\epsilon,n_e} = 0$ and $\lambda(A^{\epsilon,n_e}|(\mathcal{X}^{\epsilon,n_e} \bmod \mathcal{N})) \subset \mathbb{C}_-$.

The performance of an H_2-admissible estimator for Σ (5.1) is defined as

$$\gamma_{H_2,e}(\Sigma \text{ (5.1)}, \Sigma_{e,n_e} \text{ (5.2)}) = \|\Sigma_{\epsilon,n_e} \text{ (5.3)}\|_{H_2}^2 .$$

We say that an estimator is H_2 optimal for Σ (5.1) if it is a solution to

$$\begin{aligned}\Sigma_{e,n_e} = \arg \min_{\widetilde{\Sigma}_{e,n_e},\ n_e\in\mathbb{N}} & \gamma_{H_2,e}(\Sigma\ (5.1), \widetilde{\Sigma}_{e,n_e}) \\ \text{s.t.} \quad & \widetilde{\Sigma}_{e,n_e} \text{ is } H_2\text{-admissible for } \Sigma\ (5.1).\end{aligned}$$

The H_2 performance of an H_2 optimal estimator $\Sigma^\star_{e,n_e}$ for Σ (5.1) is denoted by

$$\gamma^\star_{H_2,e}(\Sigma\ (5.1)) = \gamma_{H_2,e}(\Sigma\ (5.1), \Sigma^\star_{e,n_e}).$$

It is important to note that the norm $\|\Sigma_{\epsilon,n_e}\ (5.3)\|^2_{H_2}$ describes the effect of both inputs $w(t)$ and $u(t)$ on the output $\epsilon_z(t)$ of Σ_{ϵ,n_e} (5.3). Furthermore, the spectrum $\lambda(A^{\epsilon,n_e}|(\mathcal{X}^{\epsilon,n_e} \bmod \mathcal{N}))$ is well-defined, because the unobservable subspace $\mathcal{N}$ satisfies $A^{\epsilon,n_e}\mathcal{N} \subseteq \mathcal{N}$.

Let us recite the typical solution to the H_2 optimal estimator design problem as derived in section 2.4.

Corollary 5.35 *Consider a system Σ (5.1) that satisfies items 1b, 2b and 3b in assumption 5.2 and let $Q^+ \succeq 0$ be the unique stabilising solutions to the ARE in (5.52). Furthermore, let Σ' denote Σ (5.1) for which the mappings $C_z : \mathcal{X} \to \mathcal{Z}$ and $D_{uz} : \mathcal{U} \to \mathcal{Z}$ are replaced with any pair of mappings $C'_z : \mathcal{X} \to \mathcal{Z}'$ and $D'_{uz} : \mathcal{U} \to \mathcal{Z}'$, respectively. Finally, let us consider the mapping $L^\star := -(Q^+C_y^\top + B_w^\top D_{wy})(D_{wy}D_{wy}^\top)^{-1}$.*

Then the H_2 optimal estimation problem "can be solved" by using an observer of the form

$$\Sigma_o = \begin{cases} \dot{\tilde{x}}(t) = \Big(A + LC_y\Big)\tilde{x}(t) - Ly(t) + B_u u(t) \\ \tilde{z}(t) = M\tilde{x}(t) + Ny(t) + N_u u(t), \end{cases} \tag{5.54}$$

with design parameters $L : \mathcal{Y} \to \mathcal{X}$, $M : \mathcal{X} \to \mathcal{Z}$, $N : \mathcal{R} \to \mathcal{Z}$ and $N_u : \mathcal{U} \to \mathcal{Z}$.

The observer Σ_o (5.54) is H_2 optimal for Σ (5.1) when the mappings $L = L^\star$, $M = C_z$, $N = 0$ and $N_u = D_{uz}$ are considered.

Furthermore, the following statements are equivalent when the mapping $L = L^\star$ is considered:

(i) Σ_o (5.54) with mappings $M = C_z$, $N = 0$ and $N_u = D_{uz}$ is H_2 optimal for Σ (5.1).

(ii) Σ_o (5.54) with mappings $M = C'_z$, $N = 0$ and $N_u = D'_{uz}$ is H_2 optimal for Σ'.

Proof: A proof for the first two statements is provided in section 2.4.

To prove the third statement, it suffices to note that Q^+ and $L^\star$ are, for both systems, created independently of C_z, D_{uz}, C'_z and D'_{uz}. Therefore the same H_2 optimal observer gain L is obtained for each system. □

This corollary contains two important results. Firstly, the H_2 optimal *output estimation* problem can be transformed into an H_2 optimal *state observation* problem.

Secondly, there exists a unique observer gain L which is optimal for any "to be estimated" output $z(t)$—that is, for any pair of mappings C_z and D_{uz}.

For a system Σ (5.1) that satisfies the assumptions in Corollary 5.35, we can—by utilising the unique stabilising solution Q^+—define the transformed system

$$\Sigma_Q = \begin{cases} \dot{x}(t) = Ax(t) + B_u u(t) + (Q^+ C_y^\top + B_w D_{wy}^\top)(D_{wy} D_{wy}^\top)^{-\frac{1}{2}} w(t) \\ y(t) = C_y x(t) + (D_{wy} D_{wy}^\top)^{\frac{1}{2}} w(t) \\ z(t) = C_z x(t) + D_{uz} u(t). \end{cases} \tag{5.55}$$

This transformed system will—similarly to Σ_P (5.53)—be used to transform the H_2 optimal estimation problem into a DDEPS as discussed in section 5.2. Again, let us first derive some useful properties for the system Σ_Q (5.55).

Lemma 5.36 *Consider a system Σ (5.1) that satisfies items 1b, 2b and 3b in assumption 5.2 and let $Q^+ \succeq 0$ be the unique stabilising solution to the ARE in (5.52).*

Then the transformed system Σ_Q (5.55) has the following properties:

(a) $\mathbb{S}_-(\Sigma_Q \text{ (5.55)}) = \{ \mathcal{S}_- \subseteq \mathcal{X} \mid \mathcal{S}_-$ *is as defined in Lemma 2.42 for stability domain* $\mathbb{C}_g = \mathbb{C}_-,\ \mathcal{S}_- \subseteq \ker(C_z) \}$.

(b) $\mathcal{S}_-^\star = 0$.

(c) the DDEPS "can be solved" for Σ_Q (5.55).

Proof: (a) follows directly from the definition in (5.6), when it is observed that $\mathrm{im}((D_{wy} D_{wy}^\top)^{\frac{1}{2}}) = \mathcal{Y}$ and therefore that $C_y^{-1}\mathrm{im}((D_{wy} D_{wy}^\top)^{\frac{1}{2}}) = \mathcal{X}$.

(b) In Theorem 2.43 it is established that $\mathcal{S}_-^\star \subseteq \mathcal{S}_-$, for any subspace $\mathcal{S}_-$ for which there exists a mapping $L : \mathcal{Y} \to \mathcal{X}$ such that $(A + LC_y)\mathcal{S}_- \subseteq \mathcal{S}_-$, $\mathrm{im}((Q^+ C_y^\top + B_w D_{wy}^\top)(D_{wy} D_{wy}^\top)^{-\frac{1}{2}} + L(D_{wy} D_{wy}^\top)^{\frac{1}{2}}) \subseteq \mathcal{S}_-$ and $\lambda((A+LC_y)|(\mathcal{X} \bmod \mathcal{S}_-)) \subset \mathbb{C}_-$. By utilising $L = -(Q^+ C_y^\top + B_w^\top D_{wy})(D_{wy} D_{wy}^\top)^{-1}$, it can be observed that $\mathcal{S}_-^\star = 0$ is indeed the smallest subspace that satisfies these requirements.

(c) The inclusion $0 \subseteq \ker(C_z)$ holds by definition, which implies that $\mathcal{S}_-^\star \in \mathbb{S}_-(\Sigma_Q \text{ (5.55)})$ and therefore the DDEPS can be solved. □

Now it will be shown that Σ_Q (5.55) can indeed be used to directly transform the H_2 optimal estimation problem into a disturbance decoupling problem.

Theorem 5.37 *Consider a system Σ (5.1) that satisfies items 1b, 2b and 3b in assumption 5.2, let $Q^+ \succeq 0$ be the unique stabilising solution to the ARE in (5.52) and consider the transformed system Σ_Q (5.55). Furthermore, let $\Sigma_{\epsilon,n_e,Q}$ denote the error system when an estimator Σ_{e,n_e} (5.2) is applied to Σ_Q (5.55).*

Then an estimator Σ_{e,n_e} (5.2) is H_2 optimal for Σ (5.1) if and only if the estimator Σ_{e,n_e} (5.2) is H_2-admissible for Σ_Q (5.55) and the output estimation error $\epsilon_z(t)$ of $\Sigma_{\epsilon,n_e,Q}$ is independent of input $u(t)$ and disturbance $w(t)$.

Proof: The proof can be found in appendix A.3. □

An estimator Σ_{e,n_e} (5.2) is therefore H_2 optimal for Σ (5.1) when it solves the DDEPS(-CO) for the transformed system Σ_Q (5.55). In a similar fashion to state feedback design, let us establish how the unique H_2 optimal observer Σ_o (5.54) from Corollary 5.35 is characterised in terms of the solutions to the DDEPS for Σ_Q (5.55).

Proposition 5.38 *Consider a system Σ (5.1) that satisfies items 1b, 2b and 3b in assumption 5.2, let $Q^+ \succeq 0$ be the unique stabilising solution to the ARE in (5.52) and consider the transformed system Σ_Q (5.55). Furthermore, let Σ' denote Σ (5.1) for which the mappings $C_z : \mathcal{X} \to \mathcal{Z}$ and $D_{uz} : \mathcal{U} \to \mathcal{Z}$ are replaced with $C'_z : \mathcal{X} \to \mathcal{Z}'$ and $D'_{uz} : \mathcal{U} \to \mathcal{Z}'$, respectively; and let Σ'_Q be the corresponding transformed system.*

Then the following statements are equivalent for an observer:

(i) Σ_o (5.54) *solves the DDEPS for* (Σ_Q (5.55), $\mathcal{S}^\star_-$, $\mathbb{C}_-$), *with* $\mathcal{S}^\star_- \in \mathbb{S}_-(\Sigma_Q$ (5.55)), $M = C_z$, $N = 0$ *and* $N_u = D_{uz}$.

(ii) Σ_o (5.54) *solves the DDEPS for* (Σ'_Q, $\mathcal{S}^\star_-$, $\mathbb{C}_-$), *with* $\mathcal{S}^\star_- \in \mathbb{S}_-(\Sigma'_Q)$, $M = C'_z$, $N = 0$ *and* $N_u = D'_{uz}$.

(iii) $L = -(Q^+ C_y^\top + B_w^\top D_{wy})(D_{wy} D_{wy}^\top)^{-1}$.

Proof: The proof can be found in appendix A.3. □

It can therefore be concluded that the unique H_2 optimal observer Σ_o (5.54) from corollary 5.35 is the unique observer that solves the DDEPS for Σ_Q (5.55) by utilising the subspace $\mathcal{S}^\star_-$. The additional property that this specific observer solves both problems for any pair of mappings C_z and D_{uz} is obtained because $\mathcal{S}^\star_- = 0$ for Σ_Q (5.55).

By utilising the equivalence between H_2 optimality and disturbance decoupling, all H_2 optimal estimators Σ_{e,n_e} (5.2) for Σ (5.1) are paired with subspaces $\mathcal{S}_- \in \mathbb{S}_-(\Sigma_Q$ (5.55)). It is, again, important to note that this pairing is not "one to one" in general. For example, multiple subspaces could be paired with a given H_2 optimal estimator.

This pairing can *directly* be used to characterise all estimator orders for the H_2 optimal estimation problem, since in section 5.2 it is established that these orders are—for the DDEPS-CO—directly determined by $\dim(\mathcal{S}_-)$.

Therefore, one of the main results in this chapter is obtained by transforming the H_2 optimal estimation problem into the DDEPS-CO.

Theorem 5.39 *Consider a system Σ (5.1) that satisfies items 1b, 2b and 3b in assumption 5.2, let $Q^+ \succeq 0$ be the unique stabilising solution to the ARE in (5.52) and consider the transformed system Σ_Q (5.55).*

Then there exists an estimator Σ_{e,n_e} (5.2) of order $n_e \in \mathbb{N}$ that is H_2 optimal for Σ (5.1) if, for Σ_Q (5.55), there exists a subspace $\mathcal{S}_- \in \mathbb{S}_-(\Sigma_Q$ (5.55)) with $\dim(\mathcal{X}) - \dim(\mathcal{S}_-) = n_e$.

A reduced order observer of the form $\widehat{\Sigma}_o$ (5.11) *and of order* n_e *can be used to solve the* H_2 *optimal estimation problem.*

Proof: In Corollary 2.30 it is shown for any H_2-admissible estimator Σ_{e,n_e} (5.2) that $\gamma_{H_2,e}(\Sigma\ (5.1), \Sigma_{e,n_e}\ (5.2)) = \operatorname{tr}\left(C_z Q^+ C_z^\top\right) + \gamma_{H_2,e}(\Sigma_Q\ (5.55), \Sigma_{e,n_e}\ (5.2))$. Furthermore, an H_2 optimal estimator achieves $\gamma^\star_{H_2,e}(\Sigma\ (5.1)) = \operatorname{tr}\left(C_z Q^+ C_z^\top\right)$ in combination with the stability requirement.

Therefore, there exists an H_2 optimal estimator of order n_e if the DDEPS-CO can be solved for (Σ_Q (5.55), n_e, $\mathbb{C}_-$). The proof is concluded by applying Proposition 5.7 and Theorem 5.8 to Σ_Q (5.55). □

Now, it is important to note that the inclusion $\mathcal{S}_- \subseteq \ker(C_y)$—with $\mathcal{S}_- \in \mathbb{S}(\Sigma_Q\ (5.55))$—is not by definition satisfied for a subspace $\mathcal{S}_- \neq \mathcal{S}^\star_-$. A reduced order observer that is not based on $\mathcal{S}^\star_-$ will therefore not be H_2 optimal for all "to be estimated" outputs $z(t)$—that is, for any pair of mappings C_z and D_{uz}. Instead, the observer will be H_2 optimal for a given output $z(t)$. This implies that the H_2 optimal estimation problem with an estimator of order $n_e < n_x$ is, in general, not a "pure" state observation problem.

In view of the minimal order optimal control problem in Problem 1.4, it is also desired to characterise the minimal order n_e^- for any H_2 optimal estimator Σ_{e,n_e} (5.2).

Theorem 5.40 *Consider a system* Σ (5.1) *that satisfies items 1b, 2b and 3b in assumption 5.2, let* $Q^+ \succeq 0$ *be the unique stabilising solution to the ARE in* (5.52) *and consider the transformed system* Σ_Q (5.55).

Then for a given system Σ (5.1), *the minimal order* $n_e^- \in \mathbb{N}$ *for an estimator* Σ_{e,n_e} (5.2) *that solves the* H_2 *optimal estimation problem is*

$$n_e^- = \min_{\mathcal{S}_- \in \mathbb{S}_-(\Sigma_Q\ (5.55))} \dim(\mathcal{X}) - \dim(\mathcal{S}_-).$$

A reduced order observer of the form $\widehat{\Sigma}_o$ (5.11) *and of order* n_e^- *can be used to solve the* H_2 *optimal estimation problem.*

Proof: This is Theorem 5.39 combined with Theorem 5.9. □

To conclude, it has been shown that there exist estimators of a reduced order—i.e. with $n_e < n_x$—that can solve the H_2 optimal estimation problem. In addition, the minimal estimator order n_e^- has been characterised and it shown that a reduced order observer of the form $\widehat{\Sigma}_o$ (5.11) can be considered for this purpose. Finally, in section 5.2.5 a numerical design procedure has been developed for these reduced order observers.

The minimal order H_2 optimal estimation problem—which is similar to the minimal order optimal control problem in Problem 1.4—is therefore solved on a theoretical level. However, an algorithm to construct numerical representations for subspaces $\mathcal{S}_- \in \mathbb{S}_-(\Sigma_Q\ (5.55))$ that are large in dimension does not exist, which implies that the problem cannot be solved numerically yet.

Remark 5.5 *The unique H_2 optimal observer Σ_o (5.54) from Corollary 5.35 is, as explained in Proposition 5.38, related to the subspace $\mathcal{S}_-^\star \in \mathbb{S}_-(\Sigma_Q\ (5.55))$. Because this subspace satisfies $\dim(\mathcal{S}_-^\star) = 0$, an estimator of order $n_e = n_x$ must indeed be considered.*

It can happen that this observer coincidentally solves the DDEPS for some other subspace $\mathcal{S}_- \in \mathbb{S}_-(\Sigma_Q\ (5.55))$ as well. In such a situation, the observer mappings will satisfy $(A+LC_y)\mathcal{S}_- \subseteq \mathcal{S}_-$ and $M\mathcal{S}_- = 0$, which implies that the observer states $\tilde{x} \in \mathbb{S}_-$ are unobservable in $\tilde{z}(t)$. Any MOR procedure can, when applied to this specific observer, therefore be used to design a reduced order H_2 optimal estimator. This situation will, however, not happen in general and does not guarantee that an H_2 optimal estimator of minimal order is obtained.

5.4.4 Measurement Feedback Controller Design

The results for H_2 optimal state feedback and estimator design can now be combined for the purpose of H_2 optimal measurement feedback controller design; let us consider again the stability domain $\mathbb{C}_g = \mathbb{C}_-$. With this stability domain, let $\mathcal{S}_-$ be an input-containing $\mathbb{C}_-$-detectability subspace and $\mathcal{S}_-^\star$ the $\mathbb{C}_-$-detectable strongly reachable subspace as defined in Lemma 2.42 and Theorem 2.43, respectively; and let $\mathbb{S}_-(\Sigma)$ denote the set as defined in (5.6). In addition, let $\mathcal{V}_-$ be an output-nulling $\mathbb{C}_-$-stabilisability subspace and $\mathcal{V}_-^\star$ the $\mathbb{C}_-$-stabilisable weakly unobservable subspace as defined in Lemma 2.39 and Theorem 2.40, respectively; and let $\mathbb{V}_-(\Sigma)$ denote the set as defined in (5.24).

We will now discuss the design of an H_2 optimal controller Σ_{c,n_c} (5.21) for the system Σ (5.1). Such a controller minimises, in the H_2 norm, the effect of $w(t)$ onto $z(t)$ for Σ_{cl,n_c} (5.22), while internally stabilising the closed-loop system. For this type of optimal control problems, the following definitions from section 2.4 are utilised.

Definition 5.41 *Consider a controller Σ_{c,n_c} (5.21) applied to the system Σ (5.1), which results in the closed-loop system Σ_{cl,n_c} (5.22).*

Then we say that Σ_{c,n_c} (5.21) is H_2-admissible for Σ (5.1) if for Σ_{cl,n_c} (5.22) we have that $D_{wz}^{cl,n_c} = 0$ and $\lambda(A^{cl,n_c}) \subset \mathbb{C}_-$.

The performance of an H_2-admissible controller for Σ (5.1) is defined as

$$\gamma_{H_2}(\Sigma\ (5.1), \Sigma_{c,n_c}\ (5.21)) = \|\Sigma_{cl,n_c}\ (5.22)\|_{H_2}^2 .$$

We say that a controller is H_2 optimal for Σ (5.1) if it is a solution to

$$\begin{aligned} \Sigma_{c,n_c} = \ \arg \min_{\widetilde{\Sigma}_{c,n_c},\ n_c \in \mathbb{N}} \ & \gamma_{H_2}(\Sigma\ (5.1), \widetilde{\Sigma}_{c,n_c}) \\ \text{s.t.} \quad & \widetilde{\Sigma}_{c,n_c} \text{ is } H_2\text{-admissible for } \Sigma\ (5.1). \end{aligned}$$

The H_2 performance of an H_2 optimal controller $\Sigma_{c,n_c}^\star$ for Σ (5.1) is denoted by

$$\gamma_{H_2}^\star(\Sigma\ (5.1)) = \gamma_{H_2,e}(\Sigma\ (5.1), \Sigma_{c,n_c}^\star).$$

The solution to the H_2 optimal control problem is typically described by a controller of the form Σ_c (5.25)—as is shown in Corollary 5.28. In this way, the H_2 optimal observer from Corollary 5.35 is essentially combined with the H_2 optimal state feedback from Corollary 5.30. The fact that an H_2 optimal controller can, under assumption 5.2, be obtained by separately solving an estimator and a state feedback design problems, is called the *separation principle*.

Now let us consider the unique stabilising solutions P^+ and Q^+ to the AREs in (5.51) and (5.52), respectively. By utilising these solutions for a system Σ (5.1), it is possible to define the transformed system

$$\Sigma_{PQ} = \left\{ \begin{array}{rcl} \dot{x}(t) &=& Ax(t) + B_u u(t) + \tilde{B}_w w(t) \\ y(t) &=& C_y x(t) + (D_{wy} D_{wy}^\top)^{\frac{1}{2}} w(t) \\ z(t) &=& \tilde{C}_z x(t) + (D_{uz}^\top D_{uz})^{\frac{1}{2}} u(t), \end{array} \right. \tag{5.56}$$

with $\tilde{C}_z = (D_{uz}^\top D_{uz})^{-\frac{1}{2}}(B_u^\top P^+ + D_{uz}^\top C_z)$ and $\tilde{B}_w = (Q^+ C_y^\top + B_w D_{wy}^\top)(D_{wy} D_{wy}^\top)^{-\frac{1}{2}}$.

This system can, again, be used to transform the H_2 optimal control problem into a DDPMS as discussed in section 5.3. First, let us derive some useful properties for Σ_{PQ} (5.56).

Lemma 5.42 *Consider a system Σ (5.1) that satisfies assumption 5.2 and let $P^+ \succeq 0$ and $Q^+ \succeq 0$ be the unique stabilising solutions to the AREs in (5.51) and (5.52), respectively.*

Then the transformed system Σ_{PQ} (5.56) has the following properties:

(a) $\mathbb{T}_-(\Sigma_{PQ}\ (5.56)) =$
$$\left\{ (\mathcal{S}_-, \mathcal{V}_-) \subseteq \mathcal{X} \;\middle|\; \begin{array}{l} \mathcal{S}_- \text{ and } \mathcal{V}_- \text{ are as defined in Lemmas 2.42 and 2.39,} \\ \text{respectively, for stability domain } \mathbb{C}_g = \mathbb{C}_-, \\ \mathcal{S}_- \subseteq \ker(\tilde{C}_z),\ \operatorname{im}(\tilde{B}_w) \subseteq \mathcal{V}_-,\ A\mathcal{S}_- \subseteq \mathcal{V}_- \end{array} \right\}.$$
(b) $(\mathcal{S}_-^\star, \mathcal{V}_-^\star) = (0, \mathcal{X})$.
(c) the DDPMS "can be solved" for Σ_{PQ} (5.56).
(d) $\mathcal{S}_- \subseteq \mathcal{V}_-$ *for any pair of subspaces* $(\mathcal{S}_-, \mathcal{V}_-) \in \mathbb{T}_-(\Sigma_{PQ}\ (5.56))$.

Proof: The proof can be found in appendix A.3. □

It will now be shown that Σ_{PQ} (5.56) can indeed be used to transform the H_2 optimal control problem into a disturbance decoupling problem.

Theorem 5.43 *Consider a system Σ (5.1) that satisfies assumption 5.2, let $P^+ \succeq 0$ and $Q^+ \succeq 0$ be the unique stabilising solutions to the AREs in (5.51) and (5.52), respectively; and consider the transformed system Σ_{PQ} (5.56). Furthermore, let $\Sigma_{cl,PQ}$ denote the closed-loop interconnection of a controller Σ_{c,n_c} (5.21) with Σ_{PQ} (5.56).*

Then a controller Σ_{c,n_c} (5.21) is H_2 optimal for Σ (5.1) if and only if the controller Σ_{c,n_c} (5.21) is H_2-admissible for Σ_{PQ} (5.56) and the control output $z(t)$ of $\Sigma_{cl,PQ}$ is independent of the disturbance $w(t)$.

Proof: The proof can be found in appendix A.3. □

A controller Σ_{c,n_c} (5.21) is therefore H_2 optimal for Σ (5.1) when it solves the DDPMS(-CO) for the transformed system Σ_{PQ} (5.56). In a similar fashion to the other problems, let us now establish how the unique H_2 optimal controller Σ_c (5.25) from Corollary 5.28 is characterised in terms of the solutions to the DDPMS for Σ_{PQ} (5.56).

Proposition 5.44 *Consider a system* Σ (5.1) *that satisfies assumption 5.2, let* $P^+ \succeq 0$ *and* $Q^+ \succeq 0$ *be the unique stabilising solutions to the AREs in* (5.51) *and* (5.52)*, respectively; and consider the transformed system* Σ_{PQ} (5.56)*.*

Then the following statements are equivalent for a controller:

(i) Σ_c (5.25) *solves the DDPMS for (*Σ_{PQ} (5.56)*,* $\mathcal{S}_-^\star$*,* $\mathcal{V}_-^\star$*,* $\mathbb{C}_-$*), with* $(\mathcal{S}_-^\star, \mathcal{V}_-^\star) \in \mathbb{V}_-(\Sigma_{PQ}$ (5.56)*).*

(ii) $L = -(Q^+C_y^\top + B_w^\top D_{wy})(D_{wy}D_{wy}^\top)^{-1}$*,* $F = -(D_{uz}^\top D_{uz})^{-1}(B_u^\top P^+ + D_{uz}^\top C_z)$ *and* $N = 0$*.*

Proof: (i) ⇒ (ii): By observing that $\mathcal{S}_-^\star = 0$ and $\mathcal{V}_-^\star = \mathcal{X}$, the requirements in (5.30) on the mappings L, F and N to solve the DDPMS for (Σ_Q (5.55), $\mathcal{S}_-^\star$, $\mathbb{C}_-$) are—among others—$\operatorname{im}((Q^+C_y^\top + B_w D_{wy}^\top)(D_{wy}D_{wy}^\top)^{-\frac{1}{2}} + L(D_{wy}D_{wy}^\top)^{\frac{1}{2}}) \subseteq 0$, $((D_{uz}^\top D_{uz})^{-\frac{1}{2}}(B_u^\top P^+ + D_{uz}^\top C_z) + (D_{uz}^\top D_{uz})^{\frac{1}{2}}F)\mathcal{X} = 0$ and $(D_{uz}^\top D_{uz})^{\frac{1}{2}} N (D_{wy}D_{wy}^\top)^{\frac{1}{2}} = 0$. These conditions uniquely define the mappings in (ii), while the other requirements are satisfied as well.

(ii) ⇒ (i): By observing that $\mathcal{S}_-^\star = 0$ and $\mathcal{V}_-^\star = \mathcal{X}$, it is easy to show for the given mappings that the requirements in (5.30) are satisfied, which completes the proof. □

It can therefore be concluded that the unique H_2 optimal controller Σ_c (5.25) from corollary 5.28 is the unique controller that solves the DDPMS for Σ_{PQ} (5.56) by utilising the subspaces $\mathcal{S}_-^\star$ and $\mathcal{V}_-^\star$.

The design of the mappings L and F is directly related to the subspaces $\mathcal{S}_-$ and $\mathcal{V}_-$, respectively. The additional property that these mappings can be designed independently—which is called the separation principle—is obtained because $\mathcal{S}_-^\star = 0$ and $\mathcal{V}_-^\star = \mathcal{X}$ for Σ_{PQ} (5.56). The inclusion $A\mathcal{S}_-^\star \subseteq \mathcal{V}_-^\star$, which imposes a relation between these subspaces, is therefore by definition satisfied.

All H_2 optimal controllers Σ_c (5.25) for Σ (5.1) are therefore paired with subspaces $(\mathcal{S}_-, \mathcal{V}_-) \in \mathbb{T}_-(\Sigma_{PQ}$ (5.56)); it is, again, important to note that this pairing is not "one to one" in general. Similarly to the estimation problem, this pairing can *directly* be used to characterise all controller orders for the H_2 optimal control problem.

This will now be used to solve one of the main problems that is addressed in this chapter.

Theorem 5.45 *Consider a system* Σ (5.1) *that satisfies assumption 5.2, let* $P^+ \succeq 0$ *and* $Q^+ \succeq 0$ *be the unique stabilising solutions to the AREs in* (5.51) *and* (5.52)*, respectively; and consider the transformed system* Σ_{PQ} (5.56)*.*

Then there exists a controller Σ_{c,n_c} (5.21) *of order* $n_c \in \mathbb{N}$ *that is* H_2 *optimal for* Σ (5.1) *if, for* Σ_{PQ} (5.56)*, there exist subspaces* $(\mathcal{S}_-, \mathcal{V}_-) \in \mathbb{T}_-(\Sigma_{PQ}$ (5.56)*) with* $\dim(\mathcal{V}_-) - \dim(\mathcal{S}_-) = n_c$*.*

A reduced order controller of the form $\widehat{\Sigma}_c$ (5.31) *and of order* n_c *can be used to solve the* H_2 *optimal control problem.*

Proof: In Corollary 2.34 it is shown for any H_2-admissible controller Σ_{c,n_c} (5.21) that $\gamma_{H_2}(\Sigma\ (5.1), \Sigma_{c,n_c}\ (5.21)) = \operatorname{tr}(B_w^\top P_r^+ B_w) + \operatorname{tr}(B_u^\top P_r^+ Q_r^+ P_r^+ B_u) + \gamma_{H_2}(\Sigma_{PQ}\ (5.56), \Sigma_{c,n_c}\ (5.21))$.
Furthermore, an H_2 optimal controller achieves closed-loop stability in combination with $\gamma^\star_{H_2}(\Sigma\ (5.1)) = \operatorname{tr}(B_w^\top P_r^+ B_w) + \operatorname{tr}(B_u^\top P_r^+ Q_r^+ P_r^+ B_u)$.

Therefore, there exists an H_2 optimal controller of order n_e if the DDPMS-CO can be solved for (Σ_{PQ} (5.56), n_e, $\mathbb{C}_-$). The proof is concluded by applying Proposition 5.19 to Σ_{PQ} (5.56) and by considering the extension as introduced in Theorem 5.27. □

The design of the mappings L_m and F_m of the reduced order controller $\widehat{\Sigma}_c$ (5.31) is directly related to the subspaces $\mathcal{S}_-$ and $\mathcal{V}_-$, respectively. Now it is important to note that the inclusion $A\mathcal{S}_- \subseteq \mathcal{V}_-$ is not by definition satisfied for the subspaces $\mathcal{S}_- \neq \mathcal{S}_-^\star$ and $\mathcal{V}_- \neq \mathcal{V}_-^\star$—with $(\mathcal{S}_-, \mathcal{V}_-) \in \mathbb{T}_-(\Sigma_{PQ}$ (5.56)). These mappings can therefore not be designed independently, which implies that the separation principle does, in general, not hold for the H_2 optimal control problem with a controller of order $n_c < n_x$.

Finally, in view of the minimal order optimal control problem in Problem 1.4, it is also desired to characterise the minimal order n_c^- for any H_2 optimal controller Σ_{c,n_c} (5.21).

Theorem 5.46 *Consider a system* Σ (5.1) *that satisfies assumption 5.2, let* $P^+ \succeq 0$ *and* $Q^+ \succeq 0$ *be the unique stabilising solutions to the AREs in* (5.51) *and* (5.52)*, respectively; and consider the transformed system* Σ_{PQ} (5.56)*.*

Then for a given system Σ (5.1)*, the minimal order* $n_c^- \in \mathbb{N}$ *for a controller* Σ_{c,n_c} (5.21) *that solves the* H_2 *optimal control problem is*

$$n_c^- = \min_{(\mathcal{S}_-, \mathcal{V}_-) \in \mathbb{T}_-(\Sigma_{PQ}\ (5.56))} \dim(\mathcal{V}_-) - \dim(\mathcal{S}_-).$$

A reduced order controller of the form $\widehat{\Sigma}_c$ (5.31) *and of order* n_c^- *can be used to solve the* H_2 *optimal control problem.*

Proof: This is Theorem 5.45 combined with Theorem 5.27. □

To conclude the main contribution of this section: It has been shown that there exist controllers of a reduced order—i.e. with $n_c < n_x$—that can solve the H_2 optimal control problem. In addition, the minimal controller order n_c^- has been characterised and it shown that a reduced order controller $\widehat{\Sigma}_c$ (5.31) can be considered for this purpose. Finally, in section 5.3.7 a numerical design procedure has been developed for these reduced order controllers.

The minimal order H_2 optimal control problem in Problem 1.4 is therefore solved on a theoretical level. However, an algorithm to construct numerical representations for subspaces $(\mathcal{S}_-, \mathcal{V}_-) \in \mathbb{T}_-(\Sigma_{PQ}\ (5.56))$ that result in a controller of low order does not exist, which implies that the problem cannot be solved numerically yet.

Remark 5.6 *Similarly to the estimation problem, the unique H_2 optimal controller Σ_c (5.25) from Corollary 5.28 is, as explained in Proposition 5.44, related to the subspace $(\mathcal{S}_-^\star, \mathcal{V}_-^\star) \in \mathbb{T}_-(\Sigma_{PQ}\ (5.56))$. Because these subspaces satisfy $\dim(\mathcal{V}_-^\star) - \dim(\mathcal{S}_-^\star) = n_x$, a controller of order $n_c = n_x$ must indeed be considered.*

It can happen that this controller coincidentally solves the DDPMS for some other subspaces $(\mathcal{S}_-, \mathcal{V}_-) \in \mathbb{T}_-(\Sigma_{PQ}\ (5.56))$ as well. In that situation it can be shown—by interpreting the controller as a system with input $y(t)$ and output $u(t)$—that the controller states $\tilde{x} \in \mathbb{S}_-$ are unobservable in $u(t)$. Any MOR procedure can, when applied to this specific controller, therefore be used to design a reduced order H_2 optimal controller. This situation will, however, not happen in general and it is not observed that the subspace $\mathcal{V}_-$ implies that additional controller states can be removed. Therefore, it is not guaranteed that an H_2 optimal controller of minimal order is obtained.

Results from industry are often normalised for reasons of confidentiality. Mathematicians, on the other hand, normalise for convenience.

Hans Zwart

6

Results for a Thermal Control Application

In this chapter we investigate the potential of coordinating the system design, the modelling procedure and controller synthesis on a practical example. For this purpose, we will consider a number of improvements for the application as described in section 1.2.1. A numerical model is first introduced in section 6.1, for which the design of a classical controller and an H_2 optimal controller is described in section 6.2.

In section 6.3 it will be shown that a substantial improvement in performance can be achieved if H_2 optimal control is considered in combination with multiple improvements to the system. Finally, the design of a constrained order controller is discussed in section 6.4.

6.1 The Control of Thermally Induced Deformations

6.1.1 A Model for the Thermally Induced Deformations of a Wafer

In this chapter we will utilise a FEM model that describes the thermally induced deformation of a wafer surface. The model is graphically depicted in figure 6.1 and consists of the following three components:

- A thermally isolated and infinitely stiff domain—i.e. it does not affect thermal aspects in the other domains and does not deform—which is used to infer boundary conditions within the model.
- A wafer table consisting of the material SiSiC, which contains a cooling channel. This table is mechanically connected to the stiff domain with a "thin elastic layer". This layer essentially consists of an infinite number of springs with a combined spring constant per unit area of $3 \cdot 10^{10}\ \frac{\mathrm{N}}{\mathrm{m}^3}$ in the x, y-directions and $2.5 \cdot 10^{11}\ \frac{\mathrm{N}}{\mathrm{m}^3}$ in the z-direction. The cooling channel is modelled as a heat flux to constant (room) temperature, with a heat transfer coefficient of $1 \cdot 10^4\ \frac{\mathrm{W}}{\mathrm{Km}^2}$.
- A silicon wafer that is clamped onto the wafer table. This clamping is mechanically described by a thin elastic layer with $1.8 \cdot 10^{12}\ \frac{\mathrm{N}}{\mathrm{m}^3}$ in the x, y, z-direction and thermally by a resistive layer with a heat transfer coefficient of $2500\ \frac{\mathrm{W}}{\mathrm{Km}^2}$.

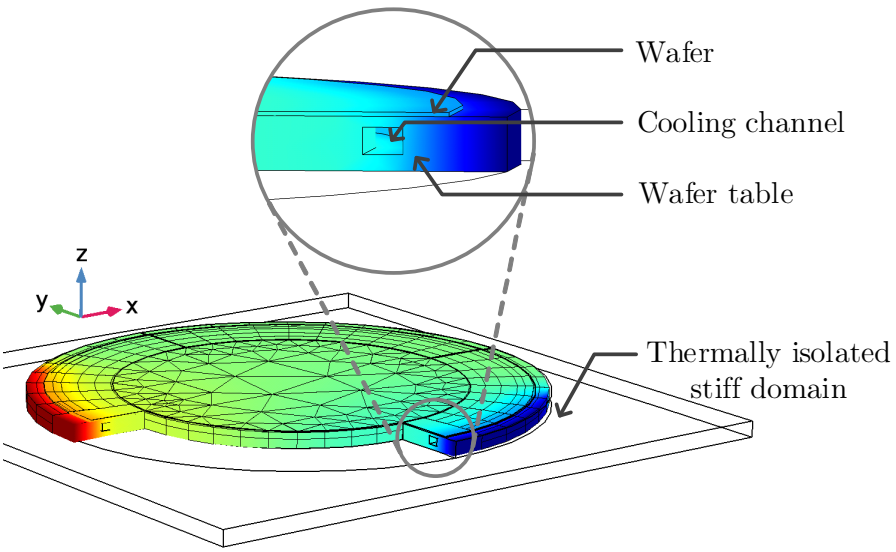

Figure 6.1: A graphical depiction of the FEM model that is used to describe the thermally induced deformation of the wafer surface.

The system is affected by a disturbance that supplies heat to and removes heat from the wafer table through the outer (cylindrical) surface. This disturbance is modelled as 40 individual disturbance signals in $\widetilde{w}(t)$ that are equally distributed over this outer surface. I.e. each disturbance has a "surface" that covers a fraction of $\frac{1}{40}$ of the wafer table perimeter, as shown in figure 6.2.

To compensate for this disturbance, 10 heaters that can generate 0–6 W are attached to the same surface. In a similar fashion to the disturbance, these heaters are modelled as 10 individual control input signals in $u(t)$ that are equally distributed over the outer (cylindrical) surface of the wafer table. I.e. each heater has a "surface" that covers a fraction of $\frac{1}{10}$ of the wafer table perimeter.

An equal number of temperature sensors is collocated with the heaters. These are located at the bottom surface of the wafer table and are modelled as 10 measured outputs in $y(t)$. Finally, the deformation of any location on the wafer surface is described by a displacement vector with three components; i.e. in the x, y, z-directions. In this example we will, however, ignore the displacements in the z-direction. The planar deformations (in the x, y-directions) at 756 locations on the wafer surface are therefore modelled as 1512 control outputs in $\tilde{z}(t)$.

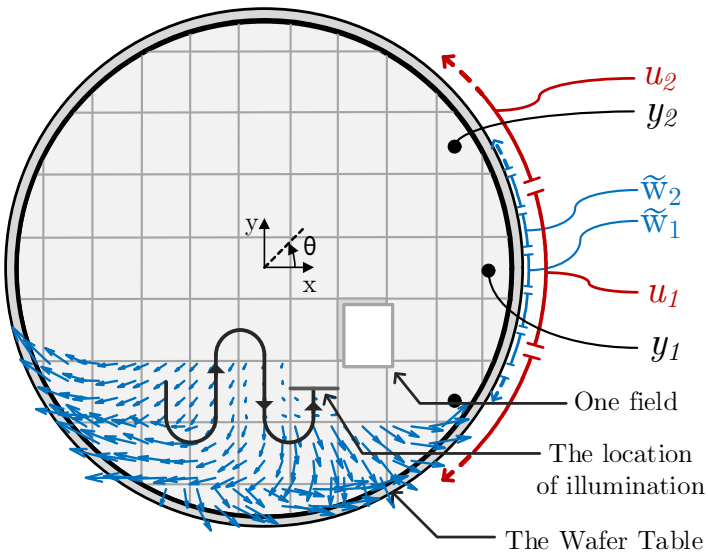

Figure 6.2: A top view of the wafer (and wafer table), in combination with the signals of interest and the overlay errors that are caused by wafer surface deformations.

By constructing a FEM model with COMSOL Multiphysics [2019], we obtain a state-space model of the form

$$\Sigma_{wt,ol} = \begin{cases} \dot{x}(t) = Ax(t) + B_u u(t) + \widetilde{B}_w \widetilde{w}(t) \\ y(t) = C_y x(t) \\ \tilde{z}(t) = \widetilde{C}_z x(t), \end{cases} \tag{6.1}$$

which refers to the open-loop wafer table model and where

- the state $x(t) \in \mathbb{R}^{1940}$ describes the temperature variation (with respect to room temperature) at time t for specific locations in the wafer and the wafer table.
- $A \in \mathbb{R}^{1940\times 1940}$—with $\lambda(A) \subseteq \mathbb{C}_-$—describes thermal conduction in the wafer and the wafer table.
- $B_u \in \mathbb{R}^{1940\times 10}$ describes how 10 heaters in $u(t)$ affect the evolution of temperature in the wafer and wafer table through the outer (cylindrical) surface of the wafer table.
- $\widetilde{B}_w \in \mathbb{R}^{1940\times 40}$ describes how 40 independent thermal disturbances in $\widetilde{w}(t)$ affect the evolution of temperature in the wafer and wafer table through the outer (cylindrical) surface of the wafer table.
- $C_y \in \mathbb{R}^{10\times 1940}$ represents the mapping from temperature (with respect to room temperature) to the 10 measured outputs in $y(t)$.
- $\widetilde{C}_z \in \mathbb{R}^{1512\times 1940}$ describes how temperature variations (with respect to room temperature) lead to planar wafer surface deformations; i.e. in the x, y-directions. It is therefore assumed that the system is without deformations, if it is at (uniform) room temperature. The deformations at 756 locations on the wafer surface are modelled as 1512 control outputs in $\tilde{z}(t)$. E.g. for location i on this surface, the displacement in the x-direction is described by $\tilde{z}_i(t)$ and the displacement in the y-direction by $\tilde{z}_{i+756}(t)$.

6.1.2 Overlay Errors

The deformation of a wafer surface is, as explained in section 1.2.1, closely related to undesired imaging errors. To explain this relation, it must first be observed from figure 6.2 that the so-called fields on the wafer surface are—with a scanning motion—illuminated by a thin slit of light. Imaging errors are therefore caused by the deformations at a given location on the wafer surface, when this specific location is illuminated. The deformations at any location on the wafer surface are essentially "sampled" by this spatially varying location of illumination. The blue arrows in figure 6.2 indicate the direction and the magnitude of these sampled deformations, when they are projected in the x, y-directions.

In order to minimise overlay errors—as introduced in section 1.1.4—at all locations on the wafer surface, it is therefore desired to reduce these sampled deformations in magnitude. For reasons of simplicity, we will consider sampled deformations as actual overlay errors in this chapter.

6.1.3 The Thermal Disturbance

Inside the BES—as introduced in section 1.2.1—a disturbance is created due to the evaporation of water, which can be regarded as a constant cooling load. However, if during operation the location of illumination is sufficiently close to the edge of the wafer, water that is warmer than the wafer table will enter this BES. The thermal disturbance therefore becomes a heating load at specific time instances and locations around the wafer edge.

To simulate the overlay errors as a result of this disturbance, a relatively simple model is created for this disturbance. The model describes a cooling load of constant magnitude that, if the location of illumination is within 5 cm of the disturbance location as shown in figure 6.2, becomes a heating load of equal magnitude. These disturbance signals are mathematically described as

$$\widetilde{w}_i(t) = \begin{cases} c_i & \text{for all } t \geq 0 \text{ at which the location of illumination} \\ & \text{is within 5 cm of "the location" of disturbance } \widetilde{w}_i \\ -c_i & \text{otherwise,} \end{cases} \tag{6.2}$$

where $c_i \geq 0$ is the magnitude of the disturbance in Watt. Please note that a positive value for $\widetilde{w}(t)$ corresponds to a heating load, while a negative value corresponds to cooling. Finally, to create variation among the different disturbance signals, the magnitude is given by a function of the form

$$c_i = 0.28 + 0.08 \sin\left(\frac{(i-1)\pi}{10}\right) \qquad \text{for } i = 1, \cdots, 40. \tag{6.3}$$

6.1.4 Performance Measures

We will aim to reduce the overlay errors as a result of this disturbance, by investigating several system configurations and controller designs. The performance of these solutions is quantified with two measures.

The H_2 optimal control problem has extensively been investigated throughout this thesis. The first performance measure is therefore the H_2 norm—between the signals $\widetilde{w}(t)$ and $\tilde{z}(t)$—for the closed-loop interconnection of $\Sigma_{wt,ol}$ (6.1) and several types of controllers that are specified below.

The second performance measure is the worst-case overlay error—which closely relates to actual machine performance—that is described by the largest *length* of any arrow in figure 6.2. In order to determine this error, a "simulation experiment" is performed with the disturbance $\widetilde{w}$ as described by (6.2) and (6.3), while the input signal $u(t)$ is generated by a given controller.

This simulation study is first initialised with the constant cooling disturbance $\widetilde{w}(t)$ as described by (6.2) and (6.3), such that the model is close to an equilibrium state at $t = 0$—i.e. $\dot{x}(0) \approx 0$. A specific illumination trajectory is then applied, which affects the disturbance signal $\widetilde{w}(t)$ and which is used to determine the sampled overlay errors. Finally, the worst-case overlay error is given by the sampled deformation of largest magnitude.

6.2 Controller Design

If no controller is applied to $\Sigma_{wt,ol}$ (6.1)—i.e. for $u(t) = 0$—a worst-case overlay error of 11.38 nm and an H_2 norm of 73.33 is obtained. In section 1.2.5 it is explained that this worst-case overlay error should, in the future, be reduced to a value below 1 nm. For this reason, we will now consider the design of classical controllers and H_2 optimal controllers for $\Sigma_{wt,ol}$ (6.1). The closed-loop performance for these controllers is compared at the end of this section.

6.2.1 Classical Control

First, let us consider the design of a classical controller that aims to minimise the magnitude of the measured temperature variations $y(t)$ (with respect to room temperature) by generating an appropriate input signal $u(t)$. With this type of control, the construction of a MIMO controller is often replaced by the design of multiple SISO controllers that independently determine each input signal.

To be more specific, a classical controller is synthesised under the assumption that the input $u_i(t)$ does not (significantly) affect the measured outputs $y_j(t)$, for $i \neq j$. This means that 10 collocated SISO controllers are developed, which control $u_i(t)$ on the basis of $y_i(t)$, for $i = 1, \cdots, 10$.

For this application, let us consider the design of a relatively simple PI-controller for each heater-sensor pair. Specifically, the i^{th} measured output $y_i(t)$ determines the input $u_i(t)$ with the following SISO controller:

$$\Sigma_{ci,PI} = \left\{ \begin{array}{rcl} \dot{x}_{ci}(t) &=& 0x_{ci}(t) + 1y_i(t) \\ u_i(t) &=& K_I x_{ci}(t) + K_P y_i(t). \end{array} \right.$$

The integral term $K_I \in \mathbb{R}$ of this controller is used to ensure that the measured output $y(t)$ converges to zero for any constant (cooling) disturbance. The proportional term $K_P \in \mathbb{R}$, on the other hand, is used to compensate for variations in the disturbance signal.

Next, let us apply these 10 SISO controllers to $\Sigma_{wt,ol}$ (6.1) with the aim of finding the parameters K_I and K_P that minimise the worst-case overlay error in the simulation experiment as described in section 6.1.4. The values $K_i = 5$ and $K_P = 20$ are obtained after a number of iterations, which result in a worst-case overlay error of 1.82 nm and a closed-loop H_2 norm of 57.44.

It is important to emphasise that a relatively simple controller is used and that not much effort is made to optimise the parameters of this controller. Nevertheless, the worst-case overlay error is reduced in magnitude by more than a factor of 5.

6.2.2 H_2 Optimal State Feedback

Secondly, let us construct an H_2 optimal state feedback of the form $u(t) = Fx(t)$ that determines the control input $u(t)$ on the basis of the system state $x(t)$. The

method as described in section 2.4 cannot be used to design such a state feedback for $\Sigma_{wt,ol}$ (6.1), because the system does not contain a positive definite mapping D_{uz}. In most practical situations, however, the mapping D_{uz} does not relate to the physical behaviour of a system. Instead, it is introduced as a tuning parameter that limits the magnitude of the control input $u(t)$.

An H_2 optimal state feedback is therefore designed for the system

$$\Sigma_{wt,F} = \begin{cases} \dot{x}(t) = Ax(t) + B_u u(t) + \begin{pmatrix} \widetilde{B}_w & 0 \end{pmatrix} w(t) \\ z(t) = \begin{pmatrix} \widetilde{C}_z \\ 0 \end{pmatrix} x(t) + \begin{pmatrix} 0 \\ \rho_u I_{10} \end{pmatrix} u(t), \end{cases} \tag{6.4}$$

with parameter $\rho_u \in \mathbb{R}$.

The value of ρ_u is optimised in an iterative fashion, with the aim of minimising the worst-case overlay error for the original system $\Sigma_{wt,ol}$ (6.1)[1], in the simulation experiment as described in section 6.1.4. After a number of iterations we obtain the value $\rho_u = 1$, which results in a worst-case overlay error of 1.72 nm and a closed-loop H_2 norm of 21.32.

6.2.3 H_2 Optimal Control

Finally, let us construct an H_2 optimal controller according to the method as described in section 2.4. The design of such a controller does—similarly to H_2 optimal state feedback design—require the introduction of two positive definite mappings D_{wy} and D_{uz}, which are regarded as tuning parameters for the controller.

For the design of an H_2 optimal controller, let us consider the system

$$\Sigma_{wt} = \begin{cases} \dot{x}(t) = Ax(t) + B_u u(t) + \begin{pmatrix} \widetilde{B}_w & 0 \end{pmatrix} w(t) \\ y(t) = C_y x(t) + \begin{pmatrix} 0 & \rho_y I_{10} \end{pmatrix} w(t) \\ z(t) = \begin{pmatrix} \widetilde{C}_z \\ 0 \end{pmatrix} x(t) + \begin{pmatrix} 0 \\ \rho_u I_{10} \end{pmatrix} u(t), \end{cases} \tag{6.5}$$

with parameters $\rho_u, \rho_y \in \mathbb{R}$.

An H_2 optimal controller is essentially an H_2 optimal observer that can be tuned with the parameter ρ_y, which is combined with an H_2 optimal state feedback that can be tuned with the parameter ρ_u. The value $\rho_u = 1$ that is obtained for the H_2 optimal state feedback design problem as described above, will therefore be used.

To determine the parameter ρ_y, we will consider the design of an H_2 optimal controller $\Sigma_c^\star$—of the form 2.18—on the basis of Σ_{wt} (6.5) with $\rho_u = 1$. The value of ρ_y is also optimised in an iterative fashion, with the aim of minimising the worst-case overlay error for $\Sigma_{wt,ol}$ (6.1) in the same simulation experiment. The value $\rho_y = 0.1$ is obtained in an iterative fashion, which results in a worst-case overlay error of 5.06 nm and a closed-loop H_2 norm of 54.74.

[1] It is important to note that the optimal control action is therefore designed for a similar, yet different, system.

6.2.4 Closed-Loop Performance

The closed-loop performance measures as introduced in section 6.1.4 are presented in table 6.1, for each type of controller as described above. The performance without control—i.e. for $u(t) = 0$—is included as a reference.

If compared to a situation without control, the classical controller is able to slightly reduce the H_2 norm from a value of 77.33 to 57.44. A much larger improvement is observed for the worst-case overlay error, which is reduced in magnitude from 11.38 nm to 1.82 nm. In terms of the overlay we can therefore observe that a significant improvement is achieved with a relatively simple type of controller.

An H_2 optimal state feedback is—in comparison with the classical controller—able to significantly improve H_2 performance, while only a marginal improvement is achieved in terms of overlay. This type of controller does, however, require exact state knowledge and can therefore not be applied in practice.

When an H_2 optimal measurement feed controller is considered, a slight improvement in H_2 performance is achieved in comparison with the classical controller. If the worst-case overlay error is considered, it must be concluded that the classical controller performs significantly better.

This large difference in overlay performance—as depicted in figure 6.3—is a result of the considered disturbance signal. Namely, the H_2 optimal controller minimises deformations for an impulse on the disturbance $\widetilde{w}(t)$, while a step input is a better description for the disturbance signal in (6.2) and (6.3). The controller—which essentially contains an observer—is therefore not able to accurately observe the system state, which significantly reduces the performance in terms of overlay.

	H_2 norm	Worst-case overlay error
No controller	73.33	11.38 nm
Classical Control	57.44	1.82 nm
H_2 optimal state feedback	21.32	1.72 nm
H_2 optimal control	54.74	5.06 nm

Table 6.1: The performance that is obtained for $\Sigma_{wt,ol}$ (6.1) with each type of controller.

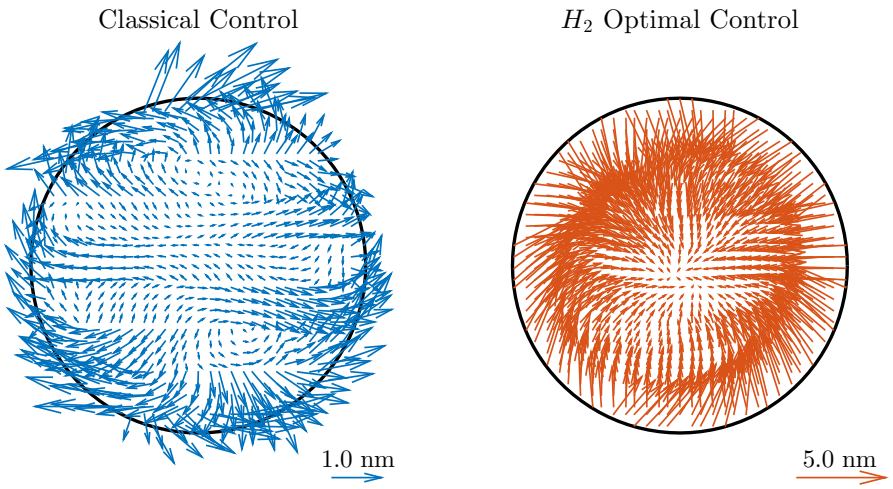

Figure 6.3: A graphical depiction of the overlay errors that are obtained with classical control and H_2 optimal control.

6.3 Improved System Design

It is observed in section 6.2.3 that the introduction of H_2 optimal state feedback and H_2 optimal control does not result in a significant reduction of the worst-case overlay error. We will now consider several system improvements to overcome this problem. The closed-loop performance for several closed-loop configurations—with and without an improved system design—are presented at the end of this section.

6.3.1 Utilising the Wafer Positioning System

First, let us introduce the positioning system that is used to correctly align the wafer surface with respect to the location of illumination. This system essentially aims to follow a given reference on the position (x, y) and orientation θ of the wafer—as depicted with the black meandering pattern in figure 6.2.

With this system, we can compensate for the effect that wafer surface deformations have on wafer alignment. For example, a deformation in the positive x-direction implies that an alignment correction should be applied in the negative x-direction.

Wafer alignment cannot be included in the design of a classical controller, because temperature is controlled instead of the actual deformations. With H_2 optimal state feedback and control, on the other hand, it is possible to include the heaters as well as alignment. This, because the controller aims to directly minimise the deformations.

For this reason, let us add the wafer alignment set-points in the x, y, θ-directions to $\Sigma_{wt,ol}$ (6.1) in order to obtain a system of the form

$$\Sigma_{wt,ps,ol} = \left\{ \begin{array}{rcl} \dot{x}(t) &=& Ax(t) + \begin{pmatrix} B_u & 0 \end{pmatrix} \begin{pmatrix} u(t) \\ u_{ps}(t) \end{pmatrix} + \widetilde{B}_w \widetilde{w}(t) \\ y(t) &=& C_y x(t) \\ \tilde{z}_e(t) &=& \widetilde{C}_z x(t) + \begin{pmatrix} 0 & \widetilde{D}_{uz} \end{pmatrix} \begin{pmatrix} u(t) \\ u_{ps}(t) \end{pmatrix}, \end{array} \right. \tag{6.6}$$

where the set-points for wafer alignment are given by $u_{ps}(t) \in \mathbb{R}^3$. The matrix $\widetilde{D}_{uz} \in \mathbb{R}^{1512 \times 3}$ describes how these set-points influence the wafer surface positioning. I.e. the position error of the wafer surface $\tilde{z}_e(t)$—with respect to the location of illumination—is determined by the *combined effect* of the thermally induced deformations and the adjustments in alignment.

It could now be considered to design a controller for $\Sigma_{wt,ps,ol}$ (6.6) that aims to minimise the average position error $\tilde{z}_e(t)$, which relates to the entire wafer surface. In order to reduce overlay errors, however, we should align the wafer such that the position error is specifically reduced *at the location of illumination.*

Remark 6.1 *It is important to note that this type of "moving objective" will require the design of a time-varying controller. The design of such a controller is beyond the scope of this thesis and will therefore not directly be considered.*

Instead, the location of illumination is (indirectly) taken into account by assuming that the 81 fields in figure 6.2 can be aligned independently. In other words, two "virtual" translational control inputs corresponding to the x, y-directions and one "virtual" rotational input that corresponds to the θ-direction are added for each field. For example, the three virtual control inputs for the "highlighted" field in figure 6.2 are visualised in figure 6.4.

For the design of an H_2 optimal controller, we will therefore consider a system of the form

$$\Sigma_{wt,ps,v} = \left\{ \begin{array}{rcl} \dot{x}(t) &=& Ax(t) + \begin{pmatrix} B_u & 0 \end{pmatrix} \begin{pmatrix} u(t) \\ u_{ps,v}(t) \end{pmatrix} + \begin{pmatrix} \widetilde{B}_w & 0 \end{pmatrix} w(t) \\ y(t) &=& C_y x(t) + \begin{pmatrix} 0 & \rho_y I_{10} \end{pmatrix} w(t) \\ z(t) &=& \begin{pmatrix} \widetilde{C}_z \\ 0 \\ 0 \end{pmatrix} x(t) + \begin{pmatrix} 0 & \widetilde{D}_{uz,v} \\ \rho_u I_{10} & 0 \\ 0 & \rho_{u_{ps}} I_{243} \end{pmatrix} \begin{pmatrix} u(t) \\ u_{ps,v}(t) \end{pmatrix}, \end{array} \right. \tag{6.7}$$

with parameters $\rho_u, \rho_{ps,v}, \rho_y \in \mathbb{R}$ that are used as tuning parameters for the H_2 optimal controller. The virtual set-points for wafer alignment are given by $u_{ps,v}(t) \in \mathbb{R}^{243}$, while the matrix $\widetilde{D}_{uz,v} \in \mathbb{R}^{1512 \times 243}$ describes how these virtual set-points influence the virtual position error of the wafer surface.

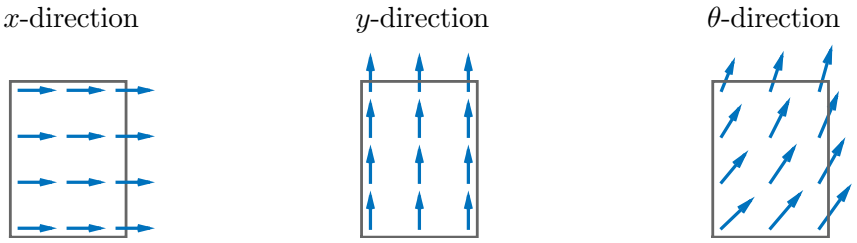

Figure 6.4: A graphical depiction of the alignment directions that, for the highlighted field in figure 6.2, correspond to the three virtual set-points of the positioning system.

An H_2 optimal controller for $\Sigma_{wt,ps,v}$ (6.7) will generate the 10 optimal heater control inputs $u(t)$ in combination with the 243 virtual set-points $u_{ps,v}(t)$. To apply these inputs to $\Sigma_{wt,ps,ol}$ (6.6), we will utilise an input selector function

$$u_{ps} = S(t)u_{ps,v} \in \mathbb{R}^3$$

that selects—from the 243 virtual set-points—the 3 set-points corresponding to the field that is actively illuminated at a given moment in time. This input selector function is essentially a time-varying matrix multiplication.

A time-varying controller is therefore applied to $\Sigma_{wt,ps,ol}$ (6.6), which implies that the closed-loop interconnection is not described by an LTI system; formally speaking the H_2 norm is therefore not defined for this interconnection. As a consequence, we will only quantify closed-loop performance using the worst-case overlay error as a result of the wafer surface position error $\tilde{z}_e(t)$.

To be more specific, the time-varying controller in combination with wafer alignment is used in the simulation study as described in section 6.1.4, in order to calculate the sampled wafer positioning errors that determine the worst-case overlay error.

In a similar fashion to section 6.2, we will first optimise the parameters ρ_u and $\rho_{ps,v}$ by designing an H_2 optimal state feedback

$$\begin{pmatrix} u(t) \\ u_{ps,v}(t) \end{pmatrix} = \begin{pmatrix} F \\ F_{ps,v} \end{pmatrix} x(t)$$

on the basis of $\Sigma_{wt,ps,v}$ (6.7). The optimal value for these parameters should minimise the worst-case overlay error for $\Sigma_{wt,ps,ol}$ (6.6), when the time-varying state feedback

$$\begin{pmatrix} u(t) \\ u_{ps}(t) \end{pmatrix} = \begin{pmatrix} I_{10} & 0 \\ 0 & S(t) \end{pmatrix} \begin{pmatrix} F \\ F_{ps,v} \end{pmatrix} x(t)$$

is used. After a number of iterations we obtain the values $\rho_u = \sqrt{0.3}$ and $\rho_{ps,v} = \sqrt{0.1}$, which results in a worst-case overlay error of 0.42 nm.

To determine the parameter ρ_y, we then consider the design of an H_2 optimal controller $\Sigma_c^\star$—of the form 2.18—for $\Sigma_{wt,ps,v}$ (6.7). This controller should, again, minimise the worst-case overlay error for $\Sigma_{wt,ps,ol}$ (6.6) when the input selector function

is applied to this controller; i.e. we introduce the function $u_{ps}(t) = S(t)u_{ps,v}(t)$ in order to obtain a time-varying controller. The value $\rho_y = 0.1$ is obtained in an iterative fashion, which results in a worst-case overlay error of 3.45 nm for $\Sigma_{wt,ps,ol}$ (6.6).

In terms of overlay, it must therefore still be concluded that the relatively simple classical controller performs significantly better than an H_2 optimal controller.

6.3.2 Optimising the Sensor Configuration

Next, let us optimise the sensor configuration of $\Sigma_{wt,ps,v}$ (6.7) by following the sensor selection procedure in chapter 3. The mesh-nodes of the FEM model—i.e. the intersections as depicted in figure 6.1—at the bottom surface of the wafer table will be used as "allowed sensor locations". In other words, the set that contains all allowed sensors as defined in (3.3) is of the form

$$\mathbb{Y} = \{y_1, \cdots, y_{351}\},$$

where each potential sensor in $\mathbb{Y}$ is described by the triple $y_i = \{(C_{yi},\ 0,\ 0.01)\}$—for $i = 1, \cdots, 351$—that corresponds to a temperature measurement at a specific location on the bottom surface of the wafer table. These locations are depicted in figure 6.5.

For the optimal selection of sensors, we will consider the actuator configuration as described in section 6.3.1 to be fixed. It is therefore desired to numerically solve the closed-loop H_2 optimal sensor selection problem for a fixed actuator configuration in Problem 3.5.

In section 3.3.3 it is explained how this problem can numerically be solved with the toolbox by Lin et al. [2014], which treats it as a sparsity promoting observer design problem. To provide a comparison, the problem is numerically solved with the greedy optimisation algorithm in Algorithm 3.2 as well. The resulting configurations for $n_y = 40$—i.e. we utilise 40 sensors—are depicted in figure 6.5.

Both algorithms place the 40 sensors around the outer (cylindrical) surface of the wafer table, which is where heat is exchanged by the thermal disturbances and (heater) control inputs. It is important to note that the sparsity promoting method places all sensors as close as possible to this outer surface, while the greedy search algorithm places some sensors slightly inwards.

To compare the closed-loop performance that can be achieved with these sensor configurations, let us now design an H_2 optimal controller $\Sigma_c^\star$ of the form 2.18. This controller is, again, constructed on the basis of $\Sigma_{wt,ps,v}$ (6.7); for which the sensors are now replaced by the new sensor configurations as depicted in figure 6.5.

With the approach as explained in section 6.3.1, we optimise the parameters $\rho_u, \rho_{ps,v}$ and ρ_y such that the worst-case overlay error is minimised for both sensor configurations. The values $\rho_u = \sqrt{0.3}$, $\rho_{ps,v} = \sqrt{0.1}$ and $\rho_y = 0.01$ are obtained in an iterative fashion, which result in a worst-case overlay error of 0.4 nm for the sparsity promoting method and a worst-case overlay error of 0.85 nm for the greedy search algorithm.

For this example, it can therefore be concluded that the sparsity promoting method performs significantly better than the greedy search algorithm. In addition, by comparing the sensor locations in figure 6.5, it must be emphasised that the worst-case overlay error is severely affected by only slight changes in the placement of sensors. This demonstrates how important it is to correctly place the temperature sensors in this type of application.

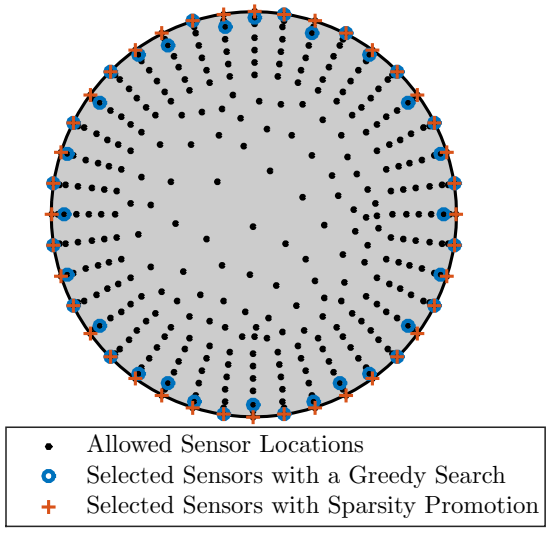

Figure 6.5: A graphical depiction of the allowed sensor locations at the bottom of the wafer table, in combination with 40 sensors that—for a fixed actuator configuration—are selected by the greedy search algorithm and the sparsity promoting method.

6.3.3 Closed-Loop Performance

To conclude this section, let us compare the worst-case overlay error as introduced in section 6.1.4 for several closed-loop configurations. An overview of these errors is provided in table 6.2.

If compared to a situation without control, we have seen that a classical controller is able to reduce the worst-case overlay error from 11.38 nm to 1.82 nm in magnitude. A significant improvement in closed-loop performance can therefore be achieved with a relatively simple controller and without adjusting the system design.

To further improve this performance, a configuration with 40 heaters and 40 collocated temperature sensors can be considered in combination with classical control design. The introduction of these heaters and sensors does, however, not significantly reduce the overlay errors—as is shown in figure 6.6. Namely, the worst-case overlay error is only reduced to 1.77 nm, which indicates that the addition of

heaters and temperature sensors does not significantly improve closed-loop performance when classical control is considered.

Because the addition of sensors and actuators does not significantly improve closed-loop performance with classical control, it can be considered to optimise the controller instead. As explained above, the worst-case overlay error is not reduced with either H_2 optimal state feedback or H_2 optimal controller design if the system design is not adjusted. It has, however, been shown that the worst-case overlay error can (significantly) be reduced when improvements to the system and the controller are introduced *together*.

Namely, the worst-case overlay error is reduced to a value of 0.4 nm by H_2 optimal control, if the set-points for the positioning system are utilised and the sensor configuration is optimised—the resulting overlay errors are depicted in figure 6.6. Furthermore, it can be observed from table 6.2 that *both* changes must be made to the system design in order to achieve this improvement.

From this example, we can therefore conclude that a significant improvement in closed-loop is not achieved by separately optimising the controller or the system design. Instead, a significant improvement in closed-loop performance is only obtained by a joint optimisation of both aspects. This conclusion therefore emphasises the importance coordinating the system design and controller synthesis in industrial applications, which directly relates to the main research question in chapter 1.

	Worst-case overlay error
No control	11.38 nm
Classical Control without alignment, with 10 sensors and 10 actuators	1.82 nm
Classical Control without alignment, with 40 sensors and 40 actuators	1.77 nm
H_2 optimal state feedback without alignment and with 10 actuators	1.72 nm
H_2 optimal state feedback with alignment and 10 actuators	0.42 nm
H_2 optimal control without alignment, with 10 sensors and 10 actuators	5.06 nm
H_2 optimal control without alignment, with 40 sensors and 10 actuators	1.67 nm
H_2 optimal control with alignment, 10 sensors and 10 actuators	3.45 nm
H_2 optimal control with alignment, 40 sensors and 10 actuators	0.40 nm

Table 6.2: The performance that is obtained for several closed-loop configurations.

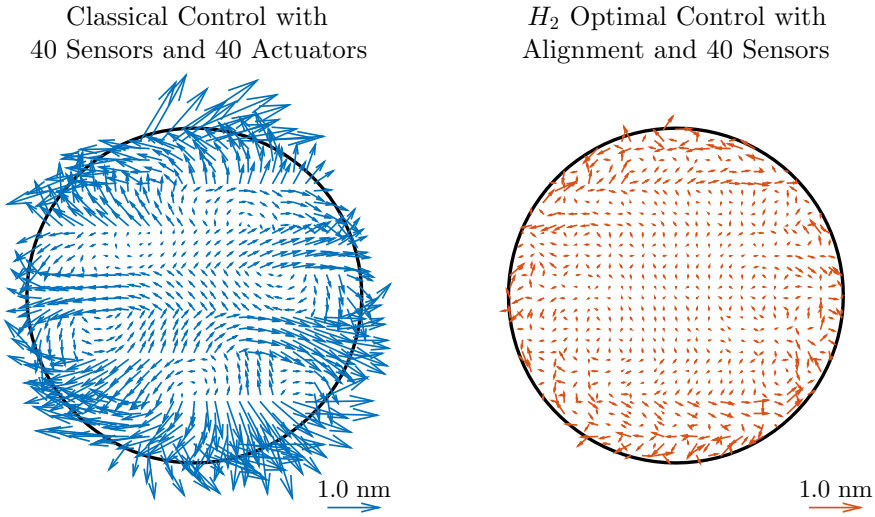

Figure 6.6: A graphical depiction of the overlay errors that are obtained if additional actuators and sensors are combined with classical control and H_2 optimal control.

6.4 Constrained Order Controller Design

In section 6.3 it has been shown that a full order H_2 optimal controller—i.e. with 1940 states—can significantly reduce the worst-case overlay error in this example, when the set-points for the positioning system are utilised and the sensor configuration of the system is optimised. For real-time implementation in practice, however, such a high order controller cannot be used due to computational limitations.

To finalise this chapter, we therefore consider the design of a constrained order controller for the system with alignment, 40 temperature sensors and 10 heaters. In chapter 4 it is demonstrated that existing order reduction techniques can perform well in most practical situations; although this is not guaranteed in general. For this reason, we will only use the proposed improvements from section 4.4, if the original techniques result in a significant loss of closed-loop performance.

First, we utilise open-loop BT for COR as discussed in section 4.2.2. To be more specific, a full order H_2 optimal controller $\Sigma_c^\star$ is designed on the basis of $\Sigma_{wt,ps,v}$ (6.7). Open-loop BT is then applied to this controller, which results in a low order controller $\widehat{\Sigma}_c^\star$.

The low order controller $\widehat{\Sigma}_c^\star$ is connected with $\Sigma_{wt,ps,v}$ (6.7) in order to quantify closed-loop H_2 performance. In addition, the low order controller $\widehat{\Sigma}_c^\star$ is—by taking into account the time-varying aspect as described in section 6.3.1—connected to $\Sigma_{wt,ps,ol}$ (6.6) in order to quantify closed-loop performance in terms of the worst-case overlay error.

Both performance measures as a function of the controller order, are shown in figure 6.7. From this figure it can be observed that a controller with 50 states is almost completely able to achieve optimal closed-loop H_2 performance. Furthermore, only 20 states are required to achieve optimal performance in terms of overlay. For the considered model we can therefore utilise a controller of order 20, which is designed by applying BT for COR to a full order H_2 optimal controller; that is, without considering the proposed improvement in section 4.4.

Finally, it is important to note that the considered model is only of order 1940, while models that contain over $50,000$ states are no exception in practice. To design a controller of sufficiently low order for those models, it might be necessary to consider the proposed improvements from section 4.4.

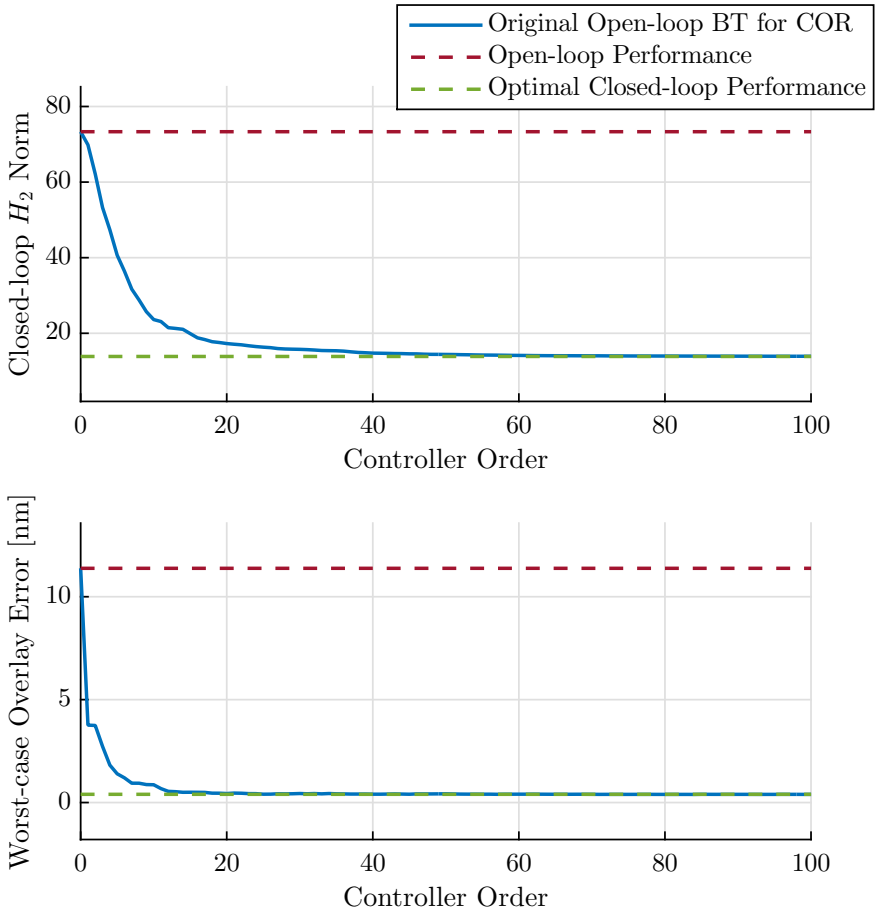

Figure 6.7: The closed-loop H_2 performance of low order controllers that are constructed for $\Sigma_{wt,ps,v}$ (6.7), with open-loop BT for COR.

To succeed, jump as quickly at opportunities as you do at conclusions.

Benjamin Franklin

7

To Conclude this Thesis

In chapter 1 it is hypothesised that potential closed-loop performance is compromised by separating the system design, modelling procedure and controller synthesis. This hypothesis led to the main research question of how to coordinate these three aspects, with the aim of meeting a set of closed-loop performance requirements.

In order to address this question, it is proposed to investigate three problems for the purpose of acquiring a better understanding of the relation between these aspects. Each problem is paired with a set of research questions that are investigated in chapters 3–5. The results for these problems are illustrated on a practical example in chapter 6.

We will now present the conclusions and future work for each problem. These conclusions are, in addition, related to the main research question and a set of future research directions is proposed. The chapter is finalised by presenting the implications of this thesis for industry and academia.

7.1 Conclusions and Future Work

7.1.1 Closed-loop Optimal Actuator and Sensor Selection

The closed-loop optimal actuator and sensor selection problem in Problem 1.2 is—together with the corresponding set of research questions—investigated in chapter 3. This problem amounts to maximising closed-loop performance by selection of a limited number of actuators and a limited number of sensors.

In the past, a considerable amount of attention has been given to a variety of actuator and sensor selection problems. These problems are often formulated as a combinatorial optimisation problem, which can be solved by evaluating all possible subsets of actuators and sensors of a given cardinality. Such a brute force approach will quickly become computationally infeasible when large sets of allowed actuators and sensors are provided.

Several set functions that relate to open-loop system properties, such as the trace of the reachability and observability Gramians, are monotone increasing and (sub)-modular in the sets of allowed actuators and sensors. Recently, it has been shown that a modular or greedy search algorithm can be used to efficiently solve actuator and sensor selection problems with an upper bound on the degree of non-optimality, if this type of objective function is considered.

It is shown in chapter 3 that the selection of actuators and sensors, which is based on the trace of the reachability and observability Gramians, does not provide any guarantees with regards to the closed-loop performance measure $\gamma^\star_{H_2}$ as defined in (3.8). Furthermore, it is proven that the function $\gamma^\star_{H_2}$ is not supermodular and not submodular in general, which implies that a greedy search algorithm cannot be used to optimise this objective function with a bounded degree of non-optimality. The results that were obtained for several open-loop system measures do therefore not carry over to the considered closed-loop performance measure, which implies that a different solution must be considered.

In recent years, much attention has been given to sparsity promoting controller design methods, which can be used in solving closed-loop optimal actuator and sensor selection problems. To consider this type of solution for large sets of allowed actuators and sensors, it is proposed by Dhingra et al. [2014] to separately solve an actuator selection problem that does not depend on the selected sensors; and a sensor selection problem that does not depend on the selected actuators.

For the example system $\Sigma_{ce,3}$ (3.31) it is, however, shown that the optimal selection of actuators is dependent on the available sensors. Furthermore, because the actuator selection and sensor selection problems are—in a well-defined sense—dual, it can be concluded that the optimal selection of sensors depends on the available actuators as well. To optimise the best achievable H_2 (squared) performance $\gamma^\star_{H_2}$, these problems can therefore not be viewed as independent. For this reason, an extension is proposed that considers the optimal selection of actuators for a fixed sensor configuration. In addition, the dual problem of designing an optimal sensor configuration for a fixed actuator configuration is discussed.

Finally, the importance of directly optimising the closed-loop performance measure $\gamma^\star_{H_2}$ is observed for the example system Σ_b that is discussed in section 3.4. Namely, it is shown that the best closed-loop performance is achieved with the closed-loop greedy search algorithm and the improved sparsity promoting method that selects the sensors for a fixed actuator configuration. It is, however, important to emphasise that these methods do not provide explicit guarantees on optimality of the obtained result.

From the perspective of the main research question we can conclude that the best performance is indeed obtained, if the optimal closed-loop performance measure $\gamma^\star_{H_2}$—and therefore also the use of an H_2 optimal controller—is explicitly taken into consideration with the selection of actuators and sensors. It should, however, be acknowledged that a further investigation into closed-loop optimal selection of actuators and sensors is still required. In terms of future work, the following research directions are proposed:

- We derived conclusions on closed-loop optimal selection of actuators for a fixed sensor configuration and on closed-loop optimal selection of sensors for a fixed actuator configuration. The combined optimal sensor and actuator selection problem is, however, largely open and is left for future research.
- Several methods for the closed-loop optimal selection of actuators and sensors have been developed. To further improve these methods, it is proposed to first acquire a better understanding of what type and combination of actuators and sensors will lead to the best closed-loop performance. A fundamental investigation into the *design* of actuators and sensors is therefore regarded as particularly useful.

7.1.2 Constrained Order Controller Design

The constrained order optimal control problem in Problem 1.3 is—together with the corresponding set of research questions—investigated in chapter 4. This problem amounts to maximising closed-loop performance with a controller of fixed order. Such a problem is often replaced in practice by combining full order optimal control design with model order reduction (MOR) and controller order reduction (COR) approaches.

It is known that explicit guarantees on stability and closed-loop performance cannot be obtained with (frequency weighted) open-loop order reduction techniques. In chapter 4 it is shown—by utilising the example model Σ_{ex} (4.24)—that the (closed-loop) Linear Quadratic Gaussian (LQG) balanced reduction and Weighted Order Reduction (WOR) techniques do not provide any explicit guarantees on stability and closed-loop performance either. We can therefore conclude, on a theoretical level, that the open-loop, LQG and WOR balanced reduction techniques do not provide a solution to Problem 1.3. These methods might, however, still perform well in practice.

For the example model Σ_1 (4.23) it is shown that the open-loop, LQG and WOR balanced reduction techniques perform well when a "low gain" controller is considered. For a "high gain" controller, on the other hand, it is shown that all of

the considered reduction techniques might result in a constrained order controller, which performs worse than not utilising any control at all. In addition, for each technique it is observed that

- a high gain controller can, after reduction, perform worse than a low gain controller that is reduced to the same order.
- for a given constrained order controller, truncation of additional states might lead to an improved closed-loop H_2 performance.

Furthermore, it is shown that the magnitude of the Hankel, LQG and WOR singular values—which are related to each type of balancing—does not determine the loss of closed-loop H_2 performance as a result of truncating the corresponding (controller) state. Closed-loop H_2 performance is therefore not optimised by truncating states that coincide with singular values of small magnitude.

For this reason, minimisation of the closed-loop performance loss as a result of truncating controller states must be regarded as a combinatorial optimisation problem. Such a problem can, as explained above, be solved by evaluating all possible subsets of controller states $\mathbb{X}_c$ that are of a given cardinality. This brute force approach will, however, be computationally infeasible for models of high order.

To improve closed-loop performance, while simultaneously taking computational feasibility into account, we propose to utilise a greedy search algorithm instead. It is important to emphasise that such an algorithm does not provide explicit guarantees on stability and closed-loop performance. Nevertheless, a significant improvement in closed-loop H_2 performance is achieved in comparison with several techniques that have been advocated in literature.

Finally, fixed order optimisation techniques such as H_∞-H_2 Fixed Order Optimisation (HIFOO) have received a considerable amount of attention in recent years. For the example model Σ_1 (4.23) it is shown that HIFOO does—by itself—not perform better than the investigated order reduction techniques. The performance of HIFOO can, however, be improved significantly by providing a suitable initial controller to the algorithm. The best closed-loop performance is, as a consequence, achieved when the (improved) order reduction techniques are used for the purpose of providing an initial controller to HIFOO.

In terms of the main research question, an important conclusion can be drawn if the results from chapter 4 are combined with chapter 5. Namely, it is shown in section 5.4.4 that a constraint on the controller order must explicitly be taken into account *during* the design of an H_2 optimal controller. A solution to the constrained order control problem is therefore not obtained by successively—and independently—solving a full order controller design problem and an order reduction problem.

Nevertheless, it is shown in chapters 4 and 6 that an order reduction approach will typically perform well in practical situations, which implies that these methods still deserve a further investigation. In terms of future work, the following research directions can be considered:

- We have mainly focussed on improving closed-loop H_2 performance by the design of an appropriate constrained order controller. Conclusions that have been drawn for this norm, do not immediately carry over to other performance

measures. An investigation on the use of MOR and COR approaches with the aim of improving closed-loop H_∞ performance is considered to be particularly relevant.

- It has been shown that the open-loop, LQG and WOR balanced reduction techniques do not—in terms of constrained order controller design—provide explicit guarantees on stability and closed-loop performance. These techniques are all based on projections of the state variable to lower dimensional manifolds (through truncation). It is an interesting research direction to investigate whether different reduction techniques and different system representations exist that will provide explicit guarantees with regards to constrained order controller design.

7.1.3 Minimal Order Optimal Control

The minimal order optimal control problem in Problem 1.4 is—together with the corresponding set of research questions—investigated in chapter 5. This problem amounts to constructing an optimal controller of minimal order.

It was first observed by Schumacher [1980, Thm. 3.1] that all required controller orders can be characterised for disturbance decoupling problems without stability requirements. In chapter 5, a characterisation for these orders has been derived for disturbance decoupling problems with stability requirements. In addition, a geometrical characterisation of the *minimal* required controller order is derived for a system of the form Σ (5.1), if the mapping D_{wy} is full row rank and the mapping D_{uz} is full column rank.

We have considered an entirely geometric approach in the characterisation of this minimal required controller order. Namely, it has been shown that specific pairs of subspaces $(\mathcal{S}_g, \mathcal{V}_g) \in \mathbb{T}_g$—as defined in (5.27)—play a crucial role in understanding the relation between disturbance decoupling and the minimal required controller order.

There exists an elegant relation between disturbance decoupling problems with stability requirements and H_2 optimal control. By utilising this relation, a characterisation of the minimal required controller order n_c^- has been derived for the H_2 optimal control problem.

Specifically, it is known that—under assumption 5.2—a controller is H_2 optimal for a system if and only if it solves a disturbance decoupling problem (with internal stability) for the transformed system Σ_{PQ} (5.56). As a consequence, the H_2 optimal controller of minimal order is characterised by the minimal order controller that achieves disturbance decoupling for this transformed system. This leads to one of the main conclusions: H_2 optimal controllers may have a lower order than the system they control; i.e. the inequality $n_c^- < n_x$ can, in general, be satisfied.

In addition, a geometrical characterisation of the *minimal* required estimator order is derived for the disturbance decoupled estimation problem with stability. For this problem, it has been shown that the subspaces $\mathcal{S}_g \in \mathbb{S}_g$—as defined in (5.6)—can be used to establish a direct relation between disturbance decoupling and the minimal

required estimator order. There also exists a relation between disturbance decoupled estimation problems with stability requirements and H_2 optimal estimation. By utilising this relation, a characterisation of the minimal required estimator order n_e^- has been derived for the H_2 optimal estimation problem. An H_2 optimal estimator may therefore also have a lower order than the system for which it is designed; i.e. the inequality $n_e^- < n_x$ can, in general, be satisfied.

The proposed minimal order controller design approach essentially combines controller design with a modelling point of view. To be more specific, the optimal controller is designed such that certain states of the closed-loop system become unreachable or unobservable. Several controller states can, as a consequence, be truncated without affecting closed-loop performance. We can therefore conclude that it is, indeed, relevant to coordinate modelling with controller design, which emphasises the importance of the main research question.

In terms of future work, the following research directions can be considered:

- It has been shown that the subspaces $(\mathcal{S}_g, \mathcal{V}_g) \in \mathbb{T}_g$ play a crucial role in the construction of a minimal order H_2 optimal controller. The development of an algorithm, which can numerically construct a pair of subspaces $(\mathcal{S}_g, \mathcal{V}_g) \in \mathbb{T}_g$ that result in a controller of small—or potentially even minimal—order, should therefore be considered for future research.
- The relation between H_2 optimal controllers and controllers that achieve disturbance decoupling with internal stability has been used to solve the minimal order H_2 optimal control problem. An interesting generalisation can be achieved by utilising the known relation between H_∞ optimal control problems and (almost) disturbance decoupling problems with internal stability. In doing so, the geometric results as described above would enable a characterisation of the minimal required controller order for H_∞ optimal control.
- A solution to the minimal order optimal control problem can essentially be viewed as a partial solution to the constrained order control problem in Problem 1.3. I.e. a solution to the former problem can be used to synthesise constrained order *optimal* controllers that are of order n_c^- or larger. A complete geometrical characterisation for the (more general) constrained order optimal control problem is left for future research.

7.1.4 Future Research Directions

The three problems that are discussed above, have been investigated with the aim of coordinating the system design, modelling procedure and controller synthesis. Aside from these three problems, a wide range of potential future research directions can be considered from the perspective of this larger objective. Let us now discuss a number of directions that are worth investigating.

Firstly, it would be interesting to combine the problems in this thesis. For example, Problem 1.2 can be combined with Problem 1.3 in order to maximise closed-loop performance with a constrained order controller, by selection of a limited number of actuators and a limited number of sensors.

Secondly, the methods as described in chapters 3 and 4 resulted in the formulation of combinatorial optimisation problems, for which no computationally efficient solution that provides guarantees on the obtained result has been found yet. A further investigation into the field of combinatorial optimisation can therefore be of benefit to the main research question.

Furthermore, from the perspective of improving the system design, it would be especially interesting to research the effect (or sensitivity) of physical system parameters on the best achievable closed-loop performance. From a modelling point of view, the problem of estimating these parameters can be cast in the context of closed-loop performance; rather than the more common open-loop performance measures.

Finally, we have assumed throughout this entire thesis that high order linear and time-invariant models are able to accurately describe a given system. This assumption does not hold in most practical situations, which implies that model errors should be taken into account as well. Incorporating robustness in the design of constrained order controllers, or in the selection of actuators and sensors, is a completely open—and absolutely important—problem that is left for future research.

7.2 Implications for Industry and Academia

The example in chapter 6 provides convincing evidence for our claim that the system design, modelling procedure and controller synthesis should be coordinated in order to maximise closed-loop performance in industrial applications. This thesis does, however, not present a case closed; nor was it ever intended to. Instead, it will hopefully become a starting point for a number of research projects that will be of benefit to both industry and academia.

7.2.1 Industry

The complexity of industrial high-tech systems, the corresponding models and the considered control approaches is progressively increasing over time, in order to meet the ever-increasing requirements on performance. Large-scale experiments and investigations on actuator and sensor placement are typically performed to optimise the system design, while model order reduction is, for example, investigated to handle model complexity. To maximise performance, the results from these investigations are then combined with (model based) control design.

To optimise closed-loop performance in these applications, improvements are therefore successively—and iteratively—made to each aspect of the control system. The disadvantage of regarding these aspects as independent is clearly illustrated in this thesis; even for methods that have been geared towards solving control-relevant order reduction or actuator and sensor selection problems.

For example, in chapter 6 it is observed that a significant improvement in performance can only be achieved if additional actuators, sensors and H_2 optimal

control are introduced *together*. This, while an increase in the number of actuators and sensors does—when classical control is considered—not result in a significant improvement in closed-loop performance. Similarly, an improvement cannot be obtained when H_2 optimal control is considered without the introduction of additional actuators and sensors.

Regarding the design of a control system, the implications of this thesis are therefore as much for the technical aspects of the design as for the decision making process. Namely, the best achievable closed-loop performance may never be observed if these three aspects are individually, and extensively, investigated in an iterative fashion. The design choices during any step of development should therefore be coordinated and geared towards improvement of a given (collective) closed-loop performance measure.

7.2.2 Academia

Over the past decades, a significant amount of effort has been made in academia to optimise the (aforementioned) individual aspects of a control system. For example, several optimal control designs and modelling approaches have been developed. A number of examples is presented in this thesis, which demonstrate that these techniques do not necessarily perform well in terms of a *combined* closed-loop performance measure.

For example, much attention is given to the design of an accurate low order approximate model for a given high order system. It is, however, observed that a controller might not stabilise the system if it is based on an approximate model of arbitrary accuracy. Closed-loop stability can therefore not be guaranteed when model order reduction is used during control design; no matter how accurate the model becomes.

In this thesis, it has therefore been demonstrated that the (individual) optimisation of each aspect in a control system may, in the long run, not lead to substantial improvements for industrial applications. The coordination of these aspects does therefore provide academia with a number of interesting, and relevant, problems for the future.

The modern king has become a vermiform appendix: useless when quiet; when obtrusive, in danger of removal.

Austin O'Malley

A

Mathematical Proofs

A.1 Proofs for Chapter 2

Proof for Proposition 2.9:

The structure of Σ_k (2.5) implies—if we, for now, do not consider internal stability—that its Gramians are of the form

$$\mathcal{P}_k = \begin{pmatrix} P_{11,k} & P_{12,k} & 0 & 0 \\ P_{21,k} & P_{22,k} & 0 & 0 \\ 0 & 0 & 0 & 0 \\ 0 & 0 & 0 & 0 \end{pmatrix}, \qquad \mathcal{Q}_k = \begin{pmatrix} 0 & 0 & 0 & 0 \\ 0 & Q_{22,k} & 0 & Q_{24,k} \\ 0 & 0 & 0 & 0 \\ 0 & Q_{42,k} & 0 & Q_{44,k} \end{pmatrix}.$$

Furthermore, this structure implies that the norm of Σ_k (2.5) is described by $\|\Sigma_k \text{ (2.5)}\|_{H_2}^2 = \text{tr}(C_2 \mathcal{P}_{k,22} C_2^\top) = \text{tr}(B_2^\top \mathcal{Q}_{k,22} B_2)$.

The complete Gramians are, however, only defined for internally stable systems. In order to complete this proof, we must therefore show that the partial Gramians $\mathcal{P}_{k,22}$ and $\mathcal{Q}_{k,22}$ are indeed defined when Σ_s (2.3) is BIBO stable.

The structure of Σ_k (2.5) also implies that $\mathcal{P}_{22,k}$ and $\mathcal{Q}_{22,k}$ are *only* determined by the matrix partitions (A_{22}, B_2) and (C_2, A_{22}), respectively. These (partial) Gramians are therefore defined when the system

$$\Sigma_{2,2} = \begin{cases} \dot{x}_2(t) &= A_{22} x(t) + B_2 u(t) \\ y(t) &= C_2 x_2(t) \end{cases}$$

is internally stable, which requires that $\lambda(A_{22}) \subseteq \mathbb{C}_-$. This is indeed guaranteed, because Σ_s (2.3) is BIBO stable. □

Proof for Lemma 2.18:

The procedure as discussed in this proof is visualised in figure A.1. In this figure, $\Sigma_{c,n_c,f}$ denotes the controller for Σ_f (2.11), which can directly be derived from the controller $\Sigma_{c,n_c,sp}$ that is designed for Σ_{new} as defined below.

H_2-admissibility requires that there exists a controller Σ_{c,n_c} (2.12) such that the closed-loop system Σ_{f,cl,n_c} (2.13) is internally stable, well-posed and such that $D_{cl} = 0$. The existence a mapping N such that $D_{wz} + D_{uz}(I_{n_u} - N D_{uy})^{-1} N D_{wy} = 0$ does only not imply that internal stability can be achieved. This condition will therefore be sufficient and necessary if it is shown that internal stability can, by definition, be achieved independent of the mapping N.

In order to prove this, consider the mapping $\tilde{N} = -(I_{n_u} - N D_{uy})^{-1} N$, which depends on the mapping N as defined above. It is easy to show that $(I_{n_u} - N D_{uy})^{-1} = (I_{n_u} - \tilde{N} D_{uy})$, which implies that $(I_{n_u} - \tilde{N} D_{uy})$ is non-singular and that $N = -(I_{n_u} - \tilde{N} D_{uy})^{-1} \tilde{N}$.

By utilising this mapping, it is possible to consider a new input signal $u(t) = -(I_{n_u} - \tilde{N} D_{uy})^{-1} \tilde{N} y(t) + (I_{n_u} - \tilde{N} D_{uy})^{-1} u_{new}(t)$ and a new output signal $y_{new}(t) =$

$(I_{n_y} - D_{uy}\tilde{N})^{-1}y(t) - (I_{n_y} - D_{uy}\tilde{N})^{-1}D_{uy}u_{new}(t)$ in order to obtain the system

$$\Sigma_{new} = \begin{cases} \dot{x}(t) = \left(A - B_u\tilde{N}C_y\right)x(t) + B_u u_{new}(t) + \left(B_w - B_u\tilde{N}D_{wy}\right)w(t) \\ y_{new}(t) = C_y x(t) + D_{wy}w(t) \\ z(t) = \left(C_z - D_{uz}\tilde{N}C_y\right)x(t) + D_{uz}u_{new}(t), \end{cases}$$

which is similar in form to Σ (2.14); furthermore, it is easy to show that it satisfies assumption 2.1 as well. Because this system has no direct mapping from $w(t)$ to $z(t)$, a strictly proper controller must under assumption 2.1 indeed be considered for Σ_{new}.

Finally, assumption 2.1 implies for Σ_{new} that there exist mappings F and L such that $\left(A + B_u(F - \tilde{N}C_y)\right) \subseteq \mathbb{C}_-$ and $(A + (L - B_u\tilde{N})C_y) \subseteq \mathbb{C}_-$. This implies that the controller $\Sigma_{c,n_c,sp}$ can achieve internal stability for Σ_{new} and indeed that this is independent of the mapping N. □

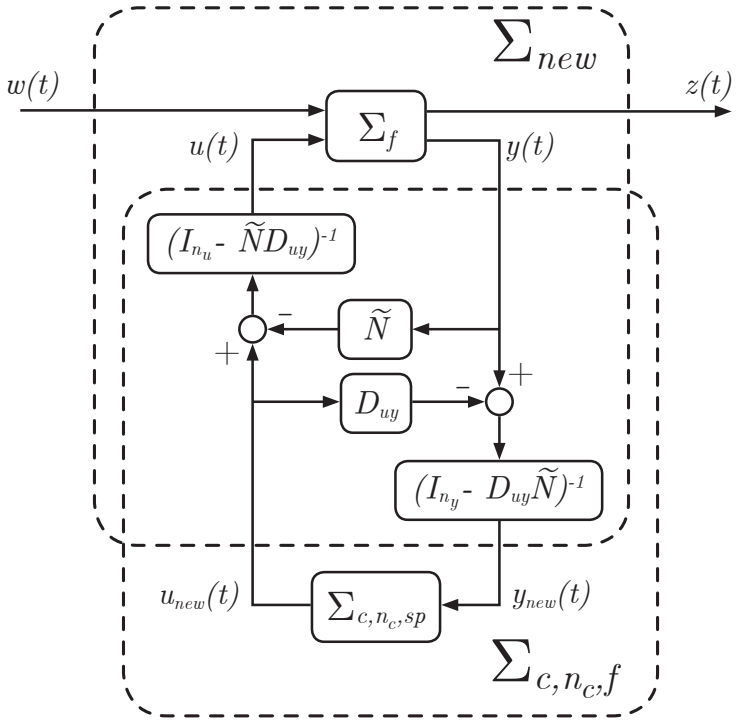

Figure A.1: A block scheme that visualises the proof for Lemma 2.18.

Proof for Corollary 2.24:

The aim is to design a state feedback $u(t) = F_u x(t)$ for Σ (2.14), which does not satisfy assumption 2.2. We can define a new input signal $v(t)$ that relates to the

original input as $u(t) = F_a x(t) + G_a v(t)$, with $F_a = -(D_{uz}^\top D_{uz})^{-1} D_{uz}^\top C_z$ and $G_a = -(D_{uz}^\top D_{uz})^{\frac{1}{2}}$. By considering the input signal $v(t)$, we obtain the system

$$\Sigma_v = \begin{cases} \dot{x}(t) = \Big(A + B_u F_a\Big) x(t) + B_u G_a u(t) + B_w w(t) \\ z(t) = \Big(C_z + D_{uz} F_s\Big) x(t) + D_{uz} G_a u(t). \end{cases}$$

A state feedback $v(t) = F_v x(t)$ is now designed for Σ_v, which implies that the feedback F_u for Σ (2.14) is parametrised as $F_u = F_a + G_a F_v$. By observing that G_a is full rank, it can be concluded that this specific parametrisation is non-restrictive—i.e. any mapping F_u can be created through F_v. The design of F_u for Σ (2.14) can therefore be replaced by the design of F_v for Σ_v. The reason for designing F_v instead, is that Σ_v does satisfy items 1a, 2a and 3a in assumption 2.1 and item 1 in assumption 2.2; therefore the results that were obtained with these assumptions can directly be used to design F_v.

The ARE in (2.18) for Σ_v is equal to the ARE in (2.21). Furthermore, an H_2 optimal state feedback for Σ_v is given by $v(t) = -G_a B_u^\top P^+ x(t)$. This implies that an optimal state feedback for Σ (2.14) is given by $u(t) = -G_a^2 (B_u^\top P^+ + D_{uz}^\top C_z)$, which is the presented state feedback. □

Proof for Lemma 2.27:

The procedure as discussed in this proof is visualised in figure A.2. In this figure, $\Sigma_{e,n_e,f}$ denotes the estimator for Σ_f (2.11), which can directly be derived from the estimator $\Sigma_{e,n_e,sp}$ that is designed for a system of the form Σ'_{new} as defined below.

By considering $J = A + LC_y$, $K = -L$, $M = C_z - NC_y$ and $e(t) = x(t) - x_e(t)$ we obtain the error system $\Sigma_{\epsilon,o} =$

$$\begin{cases} \dot{e}(t) = \Big(A + LC_y\Big) e(t) + \Big(B_u + LD_{uy} - K_u\Big) u(t) + \Big(B_w + LD_{wy}\Big) w(t) \\ \epsilon_z(t) = \Big(C_z - NC_y\Big) e(t) + \Big(D_{uz} - ND_{uy} - N_u\Big) u(t) + \Big(D_{wz} - ND_{wy}\Big) w(t). \end{cases} \tag{A.1}$$

For this system, there always exists a mapping N_u such that $D_{uz,\epsilon} = 0$. Under assumption 2.1, there also exists a mapping L such that $\lambda(A + LC_y) \subseteq \mathbb{C}_-$, which implies that the stability requirement can also be met. Therefore, the existence of a mapping N such that $D_{wz,\epsilon} = 0$ is a sufficient and necessary condition on the existence of an H_2-admissible estimator for Σ_f (2.11).

With the mapping N such that $D_{wz} - ND_{wy} = 0$, let us define the new outputs $y_{new}(t) = y(t) - D_{uy} u(t)$ and $z_{new} = z(t) - N y_{new}(t)$ to obtain the system

$$\Sigma'_{new} = \begin{cases} \dot{x}(t) = Ax(t) + B_u u(t) + B_w w(t) \\ y_{new}(t) = C_y x(t) + D_{wy} w(t) \\ z_{new}(t) = \Big(C_z - NC_y\Big) x(t) + D_{uz} u(t). \end{cases}$$

Σ'_{new} is indeed similar in form to Σ (2.14) and it satisfies items 1b, 2b and 3b in assumption 2.1. Finally, with these assumptions an H_2-admissible estimator $\Sigma_{e,n_e,sp}$ for Σ'_{new} must utilise the mapping $N = 0$. □

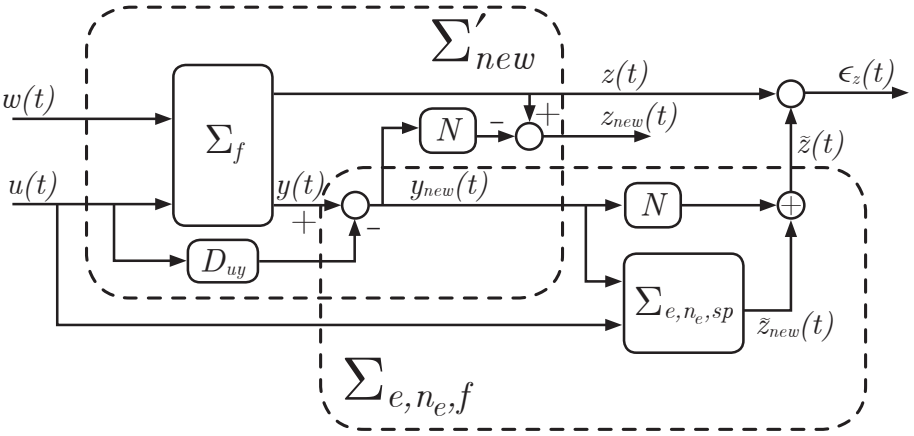

Figure A.2: A block scheme that visualises the proof for Lemma 2.27.

Proof for Corollary 2.30:

The aim is to design an estimator Σ_{e,n_e} (2.22) for Σ (2.14), which does not satisfy assumption 2.2. The estimation problem is essentially transformed into a control problem by considering the dual system $\Sigma^\top$ (2.26), for which an appropriate dual input signal $y'(t)$ must be created with the dual estimator $\Sigma^\top_{e,n_e}$ (2.27). We can define a new dual input $v'(t)$ which relates to the original dual input as $y'(t) = L_a^\top x(t) + H_a^\top v'(t)$; with $L_a = -B_w D_{wy}^\top (D_{wy} D_{wy}^\top)^{-1}$ and $H_a = -(D_{wy} D_{wy}^\top)^{\frac{1}{2}}$. By observing that H_a is full rank, it can be concluded that any signal $y'(t)$ can be created through $v'(t)$. Therefore the design of a a dual estimator $\Sigma^\top_{e,n_e,v}$ for

$$\Sigma_v^\top = \begin{cases} \dot{x}'(t) = \left(A + L_a C_y\right)^\top x'(t) + C_y^\top H_a^\top y'(t) + C_z^\top z'(t) \\ w'(t) = \left(B_w + L_a D_{wy}\right)^\top x'(t) + D_{wy}^\top H_a^\top y'(t), \end{cases}$$

can be considered instead—again, when the input $u(t)$ is omitted. It is easy to show that Σ_v does satisfy items 1b, 2b and 3b in assumption 2.1 and item 2 in assumption 2.2; therefore the results that were obtained with these assumptions can directly be used to design $\Sigma_{e,n_e,v}$.

The ARE in (2.28) for Σ_v is equal to the ARE in (2.32), which completes the first part of the proof.

Then consider the dual state and dual input trajectories for the interconnection

between $\Sigma_v^\top$ and $\Sigma_{e,n_e,v}^\top$ as a result of impulses on each dual disturbance $\epsilon_z'(t)$ as:

$$\begin{pmatrix} X'(t) \\ X_e'(t) \end{pmatrix} = e^{\begin{pmatrix} (A+L_aC_y)^\top & C_y^\top H_a^\top K^\top \\ 0 & J^\top \end{pmatrix} t} \begin{pmatrix} C_z^\top \\ -M^\top \end{pmatrix}, \quad V'(t) = K^\top X_e'(t)$$

to—by using $Y'(t) = L_a^\top X'(t) + H_a^\top V'(t)$—obtain $C_z Q^+ C_z^\top =$

$$\begin{aligned} & \int_{t=0}^{\infty} \tfrac{d}{dt} \left(X'(t)^\top Q^+ X'(t) \right) dt \\ = \; & \int_{t=0}^{\infty} \left[(D_{wy} D_{wy}^\top)^{-\frac{1}{2}} (C_y Q^+ + D_{wy} B_w^\top) X'(t) + (D_{wy} D_{wy}^\top)^{\frac{1}{2}} Y'(t) \right]^\top \\ & \qquad \left[(D_{wy} D_{wy}^\top)^{-\frac{1}{2}} (C_y Q^+ + D_{wy} B_w^\top) X'(t) + (D_{wy} D_{wy}^\top)^{\frac{1}{2}} Y'(t) \right] dt \\ & \quad - \int_{t=0}^{\infty} (B_w^\top X'(t) + D_{wy}^\top Y'(t))^\top (B_w^\top X'(t) + D_{wy}^\top Y'(t)) dt. \end{aligned}$$

This, by observing the similarity to Theorem 2.28, completes the proof. □

Proof for Proposition 2.32:

An external input signal $u(t)$ can equivalently be interpreted as a disturbance that affect the system, but which is directly available to the estimator through $y(t)$. In this way, an extended disturbance and measurement

$$w_{ext}(t) = \begin{pmatrix} w(t) \\ u(t) \end{pmatrix}, \quad y_{ext}(t) = \begin{pmatrix} y(t) \\ u(t) \end{pmatrix}$$

can be defined in order to obtain an extended system

$$\Sigma_{ext} = \left\{ \begin{array}{rcl} \dot{x}(t) & = & Ax(t) + \begin{pmatrix} B_w & B_u \end{pmatrix} w_{ext}(t) \\ y_{ext}(t) & = & \begin{pmatrix} C_y \\ 0 \end{pmatrix} x(t) + \begin{pmatrix} D_{wy} & 0 \\ 0 & I_{n_u} \end{pmatrix} w_{ext}(t) \\ z(t) & = & C_z x(t) + \begin{pmatrix} 0 & D_{uz} \end{pmatrix} w_{ext}(t). \end{array} \right.$$

For this system, the extended estimator

$$\Sigma_{e,n_e,ext} = \left\{ \begin{array}{rcl} \dot{x}_e(t) & = & Jx_e(t) + \begin{pmatrix} K & K_u \end{pmatrix} y_{ext}(t) \\ \tilde{z}(t) & = & Mx_e(t) + \begin{pmatrix} N & N_u \end{pmatrix} y_{ext}(t). \end{array} \right.$$

is designed. An H_2-admissible estimator for Σ_{ext} satisfies $N = 0$ and $N_u = D_{uz}$, while the mappings J, K, M and M_u are designed to obtain the H_2 optimal performance $\gamma_{H_2,e}^\star(\Sigma \text{ (2.14)})$.

Now, it is easy to show that the ARE in (2.32) for Σ_{ext} is equal to the ARE in (2.32) for Σ (2.14). The latter of which was derived by assuming that $u(t) = 0$ and therefore no conditions were imposed on the mapping K_u. Because $\gamma_{H_2,e}^\star(\Sigma \text{ (2.14)})$ does not change by considering an input signal $u(t) \neq 0$, it can be concluded that $\epsilon_z(t)$ can, in addition, be made independent of $u(t)$ by the appropriate selection of K_u. □

A.2 Proofs for Chapter 3

Proof for Proposition 3.4:

As established in Theorem 3.3, the function $f_{u,g}$ is a weighted sum of two modular functions. It must therefore be shown that the weighted sum of modular functions is modular.

For this purpose, let us consider the set functions $f_s, f_1, f_2 : 2^{\mathrm{card}(V)} \to \mathbb{R}$ and the parameters $\alpha_1, \alpha_2 \in \mathbb{R}$ to define $f_s = \alpha_1 f_1 + \alpha_2 f_2$. Furthermore, let the functions f_1 and f_2 be modular. This implies—according to section 2.1.6—for the subsets $\mathbb{V}_j, \mathbb{V}_k \subseteq \mathbb{V}$ that

$$f_i(\mathbb{V}_j) + f_i(\mathbb{V}_k) = f_i(\mathbb{V}_j \cup \mathbb{V}_k) + f_i(\mathbb{V}_j \cap \mathbb{V}_k), \quad \text{where } i = 1, 2.$$

We therefore get that

$$\begin{aligned} f_s(\mathbb{V}_j) + f_s(\mathbb{V}_k) &= \alpha_1 f_1(\mathbb{V}_j) + \alpha_1 f_1(\mathbb{V}_k) + \alpha_2 f_2(\mathbb{V}_j) + \alpha_2 f_2(\mathbb{V}_k) \\ &= \alpha_1 f_1(\mathbb{V}_j \cup \mathbb{V}_k) + \alpha_1 f_1(\mathbb{V}_j \cap \mathbb{V}_k) + \alpha_2 f_2(\mathbb{V}_j \cup \mathbb{V}_k) \\ &\qquad + \alpha_2 f_2(\mathbb{V}_j \cap \mathbb{V}_k) \\ &= f_s(\mathbb{V}_j \cup \mathbb{V}_k) + f_s(\mathbb{V}_j \cap \mathbb{V}_k), \end{aligned}$$

which implies that f_s is indeed modular. □

Proof for Theorem 3.9:

In section 2.4 it is shown for an ARE-admissible subset $\mathbb{Y}_f$ that

$$\gamma^\star_{H_2}(\Sigma\ (3.4), \mathbb{U}_{n_u}, \mathbb{Y}_f) = \mathrm{tr}(C_z Q^+ C_z^\top) + \gamma^\star_{H_2}(\Sigma_Q\ (3.35), \mathbb{U}_{n_u}, \mathbb{Y}_{ft}),$$

where $\mathbb{Y}_{ft} = \left\{ \left(C_{yf}, (D_{wyf} D_{wyf}^\top)^{\frac{1}{2}}, 0 \right) \right\}$ is a transformed sensor configuration.

Minimising the set function $\gamma^\star_{H_2}(\Sigma\ (3.4), \mathbb{U}_{n_u}, \mathbb{Y}_f)$ is therefore equivalent to minimising $\gamma^\star_{H_2}(\Sigma_Q\ (3.35), \mathbb{U}_{n_u}, \mathbb{Y}_{ft})$. Furthermore, we can conclude that $\mathbb{U}^\star_{n_u} = \mathbb{U}^\star_{n_u,F}$ if it is proven that $\gamma^\star_{H_2}(\Sigma_Q\ (3.35), \mathbb{U}_{n_u}, \mathbb{Y}_{ft}) = \gamma^\star_{H_2,F}(\Sigma_Q\ (3.35), \mathbb{U}_{n_u})$. In other words, it is proven that both problems have the same solution if the objective functions are equal.

To prove this equivalence, let us consider any subset $\mathbb{U}_{n_u} \subseteq \mathbb{U}$—and the corresponding matrices as defined for Σ (3.4)—in combination with $\mathbb{Y}_{ft}$ in order to construct a controller of the form

$$\Sigma_{c,sp} = \begin{cases} \dot{\tilde{x}}(t) = \left(A + B_u F + L_f C_{yf} \right) \tilde{x}(t) - L_f y_f(t) \\ u(t) = F \tilde{x}(t). \end{cases}$$

Then, let us apply this controller to Σ_Q (3.35)—and to which the same actuators are added—in order to obtain the closed-loop system

$$\Sigma_{Q,cl,sp} = \left\{ \begin{array}{rcl} \begin{pmatrix} \dot{x}(t) \\ \dot{e}(t) \end{pmatrix} &=& \begin{pmatrix} A + B_u F & -B_u F \\ 0 & A + L_f C_{yf} \end{pmatrix} \begin{pmatrix} x(t) \\ e(t) \end{pmatrix} + \begin{pmatrix} \bar{B}_w \\ \bar{B}_w + L_f D_{y,f}^{\frac{1}{2}} \end{pmatrix} w(t) \\ z(t) &=& \begin{pmatrix} C_z + D_{uz} F & -D_{uz} F \end{pmatrix} \begin{pmatrix} x(t) \\ e(t) \end{pmatrix} + \begin{pmatrix} 0 \end{pmatrix} w(t), \end{array} \right.$$

with $e(t) = x(t) - \tilde{x}(t)$, $\bar{B}_w = (Q^+ C_{yf}^\top + B_w D_{wyf}^\top)(D_{wyf} D_{wyf}^\top)^{-\frac{1}{2}}$ and $D_{y,f} = \begin{pmatrix} D_{\widetilde{w}yf} & D_{w_yf} \end{pmatrix} \begin{pmatrix} D_{\widetilde{w}yf} & D_{w_yf} \end{pmatrix}^\top$.

The best achievable H_2 (squared) performance with this type of controller is described as

$$\gamma^\star_{H_2}(\Sigma_Q \ (3.35), \mathbb{U}_{n_u}, \mathbb{Y}_{ft}) = \min_{F, L_f} \|\Sigma_{Q,cl,sp}\|^2_{H_2} \\ \text{s.t. } \lambda(A + B_u F) \subset \mathbb{C}_-, \ \lambda(A + L_f C_{yf}) \subset \mathbb{C}_-.$$

Then for any subspace $\mathbb{U}_{n_u}$ we can observe that the optimal observer gain is given by $L_f^\star = (Q^+ C_{yf}^\top + B_w D_{wyf}^\top)(D_{wyf} D_{wyf}^\top)^{-1}$. Namely, $L_f^\star$ will make the state observation errors $e(t)$ independent of the disturbance $w(t)$, which implies that $e(t)$ has no contribution towards the norm of $\Sigma_{Q,cl,sp}$.

Because $\lambda(A + L_f^\star C_{yf}) \subset \mathbb{C}_-$ as well, we can therefore observe that

$$\gamma^\star_{H_2}(\Sigma_Q \ (3.35), \mathbb{U}_{n_u}, \mathbb{Y}_{ft}) = \min_{F} \|\Sigma_{Q,cl,F}\|^2_{H_2} \\ \text{s.t. } \lambda(A + B_u F) \subset \mathbb{C}_-,$$

with

$$\Sigma_{Q,cl,F} = \begin{cases} \dot{x}(t) \ = \ \Big(A \ + \ B_u F \Big) x(t) + \bar{B}_w w(t) \\ z(t) \ = \Big(C_z + D_{uz} F \Big) x(t). \end{cases}$$

Finally, by observing that this expression is equivalent to (3.15), it can indeed concluded that $\gamma^\star_{H_2}(\Sigma_Q \ (3.35), \mathbb{U}_{n_u}, \mathbb{Y}_{ft}) = \gamma^\star_{H_2,F}(\Sigma_Q \ (3.35), \mathbb{U}_{n_u})$, which completes the proof. □

A.3 Proofs for Chapter 5

Proof for Proposition 5.2:

The problem of designing an estimator Σ_{e,n_e} (5.2) for the system Σ (5.1) is equivalent to the problem of designing a controller

$$\Sigma'_{c,n_c} = \begin{cases} \dot{x}_c(t) \ = \ J x_c(t) + \begin{pmatrix} K & K_u \end{pmatrix} y'(t) \\ u'(t) \ = M x_c(t) + \begin{pmatrix} N & N_u \end{pmatrix} y'(t) \end{cases} \tag{A.2}$$

for the system

$$\Sigma' = \begin{cases} \dot{x}(t) \ = & A \ x(t) & + & \begin{pmatrix} B_w & B_u \end{pmatrix} w'(t) \\ y'(t) \ = & \begin{pmatrix} C_y \\ 0 \end{pmatrix} x(t) & + & \begin{pmatrix} D_{wy} & 0 \\ 0 & I_{n_u} \end{pmatrix} w'(t) \\ z'(t) \ = & C_z x(t) - I_{n_z} u'(t) + & & \begin{pmatrix} 0 & D_{uz} \end{pmatrix} w'(t). \end{cases} \tag{A.3}$$

Namely, if we consider $\epsilon_z(t)$ of Σ_{ϵ,n_e} (5.3) and $z'(t)$ of the closed-loop interconnection of Σ' (A.3) with Σ'_{c,n_c} (A.2), then it is easy to show that $\epsilon_z(t) = z'(t)$ for any pair $(w(t), u(t))$ by observing that $w'(t) = \begin{pmatrix} w(t) \\ u(t) \end{pmatrix}$.

Stoorvogel and van der Woude [1991, Thm. 2.2] did show that the closed-loop interconnection of Σ' (A.3) with Σ'_{c,n_c} (A.2) can be disturbance decoupled and be made internally $\mathbb{C}_g$-stable if and only if $\lambda(A) \subseteq \mathbb{C}_g$, (C_y, A) is $\mathbb{C}_g$-detectable and

(a) $\operatorname{im} \begin{pmatrix} B_w & B_u \end{pmatrix} \subseteq \mathcal{V}_g^\star$.

(b) $\mathcal{S}_g^\star \cap \begin{pmatrix} C_y \\ 0 \end{pmatrix}^{-1} \operatorname{im} \begin{pmatrix} D_{wy} & 0 \\ 0 & I_{n_u} \end{pmatrix} \subseteq \ker(C_z)$.

(c) $\mathcal{S}_g^\star \subseteq \mathcal{V}_g^\star$.

For Σ' (A.3) it can be observed that $\mathcal{V}_g^\star = \mathcal{X}$; condition (a) and (c) are therefore by construction satisfied for Σ' (A.3). In addition, it can be observed that condition (b) is equivalent to $\mathcal{S}_g^\star \cap C_y^{-1}\operatorname{im}(D_{wy}) \subseteq \ker(C_z)$.

Then, it must be noted that—unlike the problem as investigated by Stoorvogel and van der Woude [1991, Thm. 2.2]—internal stability is not required for the DDEPS. In Theorem 5.5 it will be shown that it is sufficient and necessary to consider the subspace $\mathcal{S}_g^\star$, while it is not required that $\lambda(A) \subseteq \mathbb{C}_g$ and that (C_y, A) is $\mathbb{C}_g$-detectable.

Finally, in Theorem 5.5 it will be shown that an observer of the form Σ_o (5.4) can indeed be considered. □

Proof for Theorem 5.5:

An observer can be designed for Σ (5.1) by using any equivalent system; a representation of the form $\Sigma^{T_{e,g}}$ (5.8) can therefore be considered. Applying Σ_o (5.4) to $\Sigma^{T_{e,g}}$ (5.8) results in the error system $\Sigma_\epsilon^{T_{e,g}}$ (5.9).

In the proof of Proposition 5.2 it is shown that the design of an estimator Σ_{e,n_e} (5.2) for the system Σ (5.1) is equivalent to the problem of designing a controller Σ'_{c,n_c} (A.2) for the system Σ' (A.3). Stoorvogel and van der Woude [1991, Thm. 2.2 and Cor. 2.3] did show for this latter problem that there exists a mapping N such that $(C_z + NC_y)\mathcal{S}_g = 0$ and $ND_{wy} = 0$.

($\Leftarrow$) In (5.10), the requirements on L can by construction be met for a subspace $\mathcal{S}_g \in \mathbb{S}_g$. These requirements imply for $\Sigma_\epsilon^{T_{e,g}}$ (5.9) that there exists a mapping L_2 such that the mappings in bold font vanish within A^ϵ and B_w^ϵ and that $\lambda(A_{22} + L_2C_{y2}) \subseteq \mathbb{C}_g$. For example, the requirement $(A + LC_y)\mathcal{S}_g \subseteq \mathcal{S}_g$ is for $\Sigma^{T_{e,g}}$ (5.8) described as $(A + LC_y)\mathcal{X}_1 \subseteq \mathcal{X}_1$, which implies that $A_{21} + L_2C_{y1} = 0$. The other requirements can be interpreted in a similar fashion

The mapping N can—as explained above—by construction satisfy $C_{z1} - NC_{y1} = 0$ and $ND_{wy} = 0$. All requirements on N and M are therefore met by additionally considering $M_1 = 0$ and $M_2 = C_{z2} - NC_{y2}$, which implies for $\Sigma_\epsilon^{T_{e,g}}$ (5.9) that all mappings in bold font have vanished.

For $\Sigma_\epsilon^{T_{e,g}}$ (5.9) we can now see that the states $x(t)$ and state observation errors $e_1(t)$ are reachable through $w(t)$ and unobservable in $\epsilon_z(t)$. $e_2(t)$ is observable in $\epsilon_z(t)$

on the other hand, but not reachable through $w(t)$. This implies for the original system Σ (5.1) that $e(t) \in \mathcal{S}_g$ for all $t \geq 0$ and for any triple $(x(t), u(t), w(t))$, provided that $e(0) = e_0 \in \mathcal{S}_g$ and that $\epsilon_z(t)$ is independent of $u(t)$ and $w(t)$. Finally, only $e_2(t)$ is observable in $\epsilon_z(t)$ and the stability requirement is met by imposing $\lambda(A_{22} + L_2 C_{y2}) \subseteq \mathbb{C}_g$.

($\Rightarrow$) Stability and the requirement that $e(t) \in \mathcal{S}_g$ for all $t \geq 0$ and for any triple $(x(t), u(t), w(t))$, provided that $e(0) = e_0 \in \mathcal{S}_g$, implies for $\Sigma_\epsilon^{T_{e,g}}$ (5.9) that the mappings in bold font vanish within A^ϵ and B_w^ϵ and that $(A_{22} + L_2 C_{y2}) \subseteq \mathbb{C}_g$.

Now, the states observation errors $e_1(t)$ and, under assumption 5.1, all states $x(t)$ are reachable through $u(t)$ and $w(t)$. $\epsilon_z(t)$ can therefore only become independent of these signals when the remaining mappings in bold font vanish as well.

Making these mappings vanish—in combination with $\lambda(A_{22} + L_2 C_{y2}) \subseteq \mathbb{C}_g$—is equivalent to the requirements in (5.10), which completes the proof. □

Proof for Corollary 5.6:

($\Rightarrow$) The problem can be solved when there exist mappings L, M and N such that all conditions in Definition 5.4 are met.

First, the requirement that $e(t) \in \mathcal{S}_g$ for all $t \geq 0$ and for any triple $(x(t), u(t), w(t))$, provided that $e(0) = e_0 \in \mathcal{S}_g$, implies that $(A + LC_y)\mathcal{S}_g \subseteq \mathcal{S}_g$ and that $\mathrm{im}(B_w + LD_{wy}) \subseteq \mathcal{S}_g$.

Then in order to make $\epsilon_z(t)$ independent of $u(t)$ and $w(t)$ it is required that all states $x^\epsilon(t)$ of Σ_ϵ (5.5), which are reachable through $u(t)$ and $w(t)$, should be unobservable in $\epsilon_z(t)$. In addition, there cannot be a direct mapping from $w(t)$ to $\epsilon_z(t)$. Under assumption 5.1 this implies that $C_z - NC_y - M = 0$, $M\mathcal{S}_g = 0$ and $ND_{wy} = 0$. Finally, only the state observation errors $e(t) \in (\mathcal{X} \bmod \mathcal{S}_g)$ will be observable in $\epsilon_z(t)$, which requires that $\lambda((A + LC_y)|(\mathcal{X} \bmod \mathcal{S}_g)) \subseteq \mathbb{C}_g$.

In order to meet the requirements on L, an input-containing $\mathbb{C}_g$-detectability subspace $\mathcal{S}_g$ must be considered. The requirements on M and N can be solved when there exists a mapping N such that $(C_z + NC_y)|\mathcal{S}_g = 0$ and that $ND_{wy} = 0$. Stoorvogel and van der Woude [1991, Cor. 2.3] did show that these requirements are equivalent to requiring that $\mathcal{S}_g \in \mathbb{S}_g$.

($\Leftarrow$) In Theorem 5.5 it is shown for a subspace $\mathcal{S}_g \in \mathbb{S}_g$, that there exists an observer that solves the DDEPS for (Σ (5.1), $\mathcal{S}_g$, $\mathbb{C}_g$). □

Proof for Theorem 5.8:

An observer can be designed for Σ (5.1) by using any equivalent system; a representation of the form $\Sigma^{T_{e,g}}$ (5.8) can therefore be considered. Applying $\widehat{\Sigma}_o^{T_{e,g}}$ (5.12) to $\Sigma^{T_{e,g}}$ (5.8) results in the error system $\widehat{\Sigma}_\epsilon^{T_{e,g}}$ (5.13).

Similar to the proof of Theorem 5.5, it can be shown that the conditions in (5.14) imply for $\widehat{\Sigma}_\epsilon^{T_{e,g}}$ (5.13) that the bold-font mappings vanish and that $\lambda(A_{22}+L_2C_{y2}) \subseteq \mathbb{C}_g$. This causes $x_1(t)$, $x_2(t)$ to be reachable through $u(t)$, $w(t)$ and unobservable in $\epsilon_z(t)$. The state observation error $e_2(t)$ is not reachable through $w(t)$, but it is

observable in $\epsilon_z(t)$. The stability requirement is met because and $\lambda(A_{22}+L_2C_{y2}) \subseteq \mathbb{C}_g$. Finally, $\epsilon_z(t)$ is not affected by $w(t)$ with a direct mappings, which implies that $\epsilon_z(t)$ is independent of $w(t)$. $\widehat{\Sigma}_o$ (5.11) therefore solves the DDEPS-CO for (Σ (5.1), n_e, $\mathbb{C}_g$). □

Proof for Theorem 5.9:

In the proof of Proposition 5.2 it is shown that the design of an estimator Σ_{e,n_e} (5.2) for Σ (5.1) is equivalent to the problem of designing a controller Σ'_{c,n_c} (A.2) for Σ' (A.3). Stoorvogel and van der Woude [1991] state that the controller order for this control problem is characterised by the subspaces $\mathcal{S}_g$ and $\mathcal{V}_g$ that satisfy

(a) $\operatorname{im}\begin{pmatrix} B_w & B_u \end{pmatrix} \subseteq \mathcal{V}_g$.
(b) $\mathcal{S}_g \cap C_y^{-1}\operatorname{im}(D_{wy}) \subseteq \ker(C_z)$.
(c) $\mathcal{S}_g \subseteq \mathcal{V}_g$.

For Σ' (A.3), we get under assumption 5.1 that only the subspace $\mathcal{V}_g = \mathcal{X}$ can satisfy requirement (a), while any subspace $\mathcal{S}_g \in \mathbb{S}_g$ can be considered. Therefore, according to Schumacher [1980, Thm. 3.1] we get that

$$n^\star_{e,g} = \min_{\mathcal{S}_g \in \mathbb{S}_g, \mathcal{V}_g = \mathcal{X}} \dim(\mathcal{V}_g) - \dim(\mathcal{S}_g),$$

which completes the first part of the proof.

Finally, in Theorem 5.8 it is demonstrated that an estimator of order $n^\star_e$ can solve the problem for a given subspace $\mathcal{S}_g \in \mathbb{S}_g$ with $n^\star_e = \dim(\mathcal{X}) - \dim(\mathcal{S}_g)$. □

Proof for Proposition 5.12:

The problem of designing a state feedback $u(t) = Fx(t)$ for the system Σ (5.1) is equivalent to the problem of designing a controller

$$\Sigma''_{c,n_c} = \begin{cases} \dot{x}_c(t) &= Jx_c(t) + Ky''(t) \\ u(t) &= Mx_c(t) + Ny''(t) \end{cases} \tag{A.4}$$

for the system

$$\Sigma'' = \begin{cases} \dot{x}(t) &= Ax(t) + B_u u(t) + B_w w(t) \\ y''(t) &= I_{n_x} x(t) \\ z(t) &= C_z x(t) + D_{uz} u(t). \end{cases} \tag{A.5}$$

Namely, the state feedback design problem is equivalent to an output feedback design problem when all states are available as measured output.

Stoorvogel and van der Woude [1991, Thm. 2.2] did show that the closed-loop interconnection of Σ'' (A.5) with Σ''_{c,n_c} (A.4) can be disturbance decoupled and internally stabilised if and only if (A, B_u) is $\mathbb{C}_g$-stabilisable, (I_{n_x}, A) is $\mathbb{C}_g$-detectable and

(a) $\operatorname{im}(B_w) \subseteq \mathcal{V}^\star_g + B_u \ker(D_{uz})$.
(b) $\mathcal{S}^\star_g \cap \operatorname{im}(0) \subseteq \ker(C_z)$.

(c) $\mathcal{S}_g^\star \subseteq \mathcal{V}_g^\star$.

For Σ'' (A.5), it is easy to show that $\mathcal{S}_g^\star = \mathrm{im}(B_w)$ and therefore that conditions (b) and (c) are by construction satisfied for Σ'' (A.5). Finally, the pair (I_{n_x}, A) is by definition $\mathbb{C}_g$-detectable for any stability domain $\mathbb{C}_g$. □

Proof for Theorem 5.17:

A controller can be designed for Σ (5.1) by utilising any equivalent system; a representation of the form Σ^{T_c} (5.29) can therefore be considered. Applying Σ_c (5.25) to Σ^{T_c} (5.29) results in the closed-loop system $\Sigma_{cl}^{T_c}$ (B.1). Note that all mappings in bold-font can vanish by construction, which will be used throughout the proof.

($\Leftarrow$) The first 6 requirements of (5.30)—in combination with $F = \tilde{F} - NC_y$—imply for $\Sigma_{cl}^{T_c}$ (B.1) that the mappings in bold-font vanish, except for $-B_{u3}F_1$ and $-D_{uz}F_1$. For example, the requirement $(A + LC_y)\mathcal{S}_g \subseteq \mathcal{S}_g$ is for Σ^{T_c} (5.29) described as $(A + LC_y)\mathcal{X}_1 \subseteq \mathcal{X}_1$, which implies that $A_{21} + L_2C_{y1} = 0$ and $A_{31} + L_3C_{y1} = 0$. The other 5 requirements can be interpreted in a similar fashion.

The inclusion $(A + B_uNC_y)\mathcal{S}_g \subseteq \mathcal{V}_g$ implies that $A_{31} + B_{u3}NC_{y1} = 0$, which combined with $A_{31} + B_{u3}(F_1 + NC_{y1}) = 0$ implies that $-B_{u3}F_1 = 0$. In a similar fashion $(C_z + D_{uz}NC_y)\mathcal{S}_g = 0$ implies that $-D_{uz}F_1 = 0$.

The conditions in (5.30) therefore imply for $\Sigma_{cl}^{T_c}$ (B.1) that all mappings in bold-font will vanish and, therefore, that conditions (a) and (b) in Definition 5.16 are satisfied. It can also be concluded that all states and state observation errors of $\Sigma_{cl}^{T_c}$ (B.1), which are reachable through $w(t)$ are unobservable in $z(t)$. Finally, the DDPMS is fully solved by imposing the last requirement in (5.30): $\lambda(A^{cl}) \subseteq \mathbb{C}_g$, which by construction of the subspaces $\mathcal{S}_g$ and $\mathcal{V}_g$ can be achieved in combination with the other requirements.

($\Rightarrow$) Conditions (a) and (b) in Definition 5.16 imply for $\Sigma_{cl}^{T_c}$ (B.1) that the mappings in bold-font within A^{cl} and B_w^{cl} vanish. The states $x_1(t)$, $x_2(t)$ and observation error $e_1(t)$ are therefore reachable through $w(t)$. Therefore, $z(t)$ can only become independent of $w(t)$ when the remaining mappings in bold-font vanish as well.

Making these mappings vanish—in combination with closed-loop stability—is equivalent to the requirements in (5.30), which completes the proof. □

Proof for Corollary 5.18:

($\Rightarrow$) In Proposition 5.14 it is shown that the problem can be solved when there exists mappings L, F and N, which uniquely define $\tilde{F} = F + NC_y$, such that all conditions in Definition 5.16 are satisfied.

First, $\lambda(A^{cl}) \subseteq \mathbb{C}_g$ for Σ_{cl} (5.26), requires that Σ (5.1) is $\mathbb{C}_g$-stabilisable and $\mathbb{C}_g$-detectable. Conditions (a) and (b) in Definition 5.16 imply that

$$(A + LC_y)\mathcal{S}_g \subseteq \mathcal{S}_g, \quad \mathrm{im}(B_w + LD_{wy}) \subseteq \mathcal{S}_g,$$
$$(A + B_u\tilde{F})\mathcal{V}_g \subseteq \mathcal{V}_g, \quad \mathrm{im}(B_w + B_uND_{wy}) \subseteq \mathcal{V}_g, \quad (A + B_uNC_y)\mathcal{S}_g \subseteq \mathcal{V}_g.$$

Then, in order to make $z(t)$ independent of $w(t)$ it is required that all states $x^{cl}(t)$ of Σ_{cl} (5.26) that are reachable through $w(t)$ should be unobservable in $z(t)$, while

there cannot be a direct mapping from $w(t)$ to $z(t)$. This implies the remaining conditions in (5.30). Finally, it is shown in [Stoorvogel and van der Woude, 1991, Thm. 2.2] that these conditions can only be satisfied when $(\mathcal{S}_g, \mathcal{V}_g) \in \mathbb{T}_g$.

($\Leftarrow$) In Theorem 5.17 it is shown that for a $\mathbb{C}_g$-stabilisable and $\mathbb{C}_g$-detectable system combined with a pair $(\mathcal{S}_g, \mathcal{V}_g) \in \mathbb{T}_g$, there exists a controller that solves the DDPMS for (Σ (5.1), $\mathcal{S}_g$, $\mathcal{V}_g$, $\mathbb{C}_g$) and therefore the problem can be solved. □

Proof for Theorem 5.20:

A controller can be designed for Σ (5.1) by utilising any equivalent system; a representation of the form Σ^{T_c} (5.29) can therefore be considered. Applying $\widehat{\Sigma}_c^{T_c}$ (5.32) to Σ^{T_c} (5.29) results in a closed-loop system $\widehat{\Sigma}_{cl}^{T_c}$ (B.2). Note that all mappings in bold-font can vanish by construction, which will be used throughout the proof.

The conditions in (5.33) imply for $\widehat{\Sigma}_{cl}^{T_c}$ (B.2) that the bold-font mappings vanish. This causes $x_1(t)$ and $x_2(t)$ to be reachable through $w(t)$ and unobservable in $z(t)$. Furthermore, $x_3(t)$ and $e_2(t)$ are observable in $z(t)$ and not reachable through $w(t)$. Finally, $w(t)$ does not affect $z(t)$ with a direct mapping, which implies that $z(t)$ is independent of $w(t)$. $\widehat{\Sigma}_c$ (5.31) therefore solves the DDPM-CO for (Σ (5.1), n_c). □

Proof for Theorem 5.24:

A controller can be designed for Σ (5.1) by utilising any equivalent system, which is created with a state transformation $T_{c,g}$ that transforms Σ (5.1) into $\Sigma^{T_{c,g}}$ (B.3); a representation of the form $\Sigma^{T_{c,g}}$ (B.3) can therefore be considered. Applying $\widehat{\Sigma}_{c,g}^{T_{c,g}}$ (B.4) to $\Sigma^{T_{c,g}}$ (B.3) results in a closed-loop system $\widehat{\Sigma}_{cl,g}^{T_{c,g}}$ (B.5).

The use of $(F, N) \in \underline{M}_g(\mathcal{S}_g, \mathcal{V}_g)$ implies that $T_{c,g}F = \begin{pmatrix} 0 & F_{12} & F_2 & F_{31} & 0 \end{pmatrix}$. We therefore get that $F_{m,g} = \begin{pmatrix} F_{12} & F_2 & F_{31} \end{pmatrix}$. Inserting this mapping into $\widehat{\Sigma}_{cl,g}^{T_{c,g}}$ (B.5) implies that all mappings in bold-font that depend on F and N vanish. Furthermore, with these mappings we get that

$$\lambda \begin{pmatrix} A_{1111} + B_{u11}NC_{y11} & A_{1112} + B_{u11}\tilde{F}_{12} & A_{112} + B_{u11}\tilde{F}_2 \\ A_{1211} + B_{u12}NC_{y11} & A_{1212} + B_{u12}\tilde{F}_{12} & A_{122} + B_{u12}\tilde{F}_2 \\ A_{211} + B_{u2}NC_{y11} & A_{212} + B_{u2}\tilde{F}_{12} & A_{22} + B_{u2}\tilde{F}_2 \end{pmatrix} \subseteq \mathbb{C}_g,$$

$$\lambda \begin{pmatrix} A_{3131} + B_{u31}\tilde{F}_{31} & A_{3132} + B_{u31}NC_{y32} \\ A_{3231} + B_{u32}\tilde{F}_{31} & A_{3232} + B_{u32}NC_{y32} \end{pmatrix} \subseteq \mathbb{C}_g,$$

for $\tilde{F}_{12} = F_{12} + NC_{y12}$, $\tilde{F}_2 = F_2 + NC_{y2}$ and $\tilde{F}_{31} = F_{31} + NC_{y31}$.

The use of subspaces $\mathcal{S}_1$ and $\mathcal{S}_3$ implies for $\widehat{\Sigma}_{cl,g}^{T_{c,g}}$ (B.5) that also all mappings in bold-font which depend on L can vanish by construction, while rendering the closed-loop system stable. The remaining requirements in (5.36) achieve this vanishing, together with

$$\lambda \begin{pmatrix} A_{1212} + L_{12}C_{y12} & A_{122} + L_{12}C_{y2} & A_{1231} + L_{12}C_{y31} \\ 0 & A_{22} + L_2C_{y2} & A_{231} + L_2C_{y31} \\ 0 & A_{312} + L_{31}C_{y2} & A_{3131} + L_{31}C_{y31} \end{pmatrix} \subseteq \mathbb{C}_g.$$

Inserting these mappings into $\widehat{\Sigma}_{cl,g}^{T_{c,g}}$ (B.5) causes $x_{11}(t)$, $x_{12}(t)$, $x_2(t)$ and $e_{12}(t)$ to be reachable through $w(t)$, while they are unobservable in $z(t)$. Furthermore, $x_{31}(t)$, $x_{32}(t)$, $e_2(t)$ and $x_{31}(t)$ are observable in $z(t)$, but not reachable through $w(t)$. $w(t)$ does not affect $z(t)$ with a direct mapping, which implies that $z(t)$ is independent of $w(t)$. Finally, observe that $\widehat{\Sigma}_{cl,g}^{T_{c,g}}$ (B.5) is $\mathbb{C}_g$-stable as well, which implies that $\widehat{\Sigma}_{c,g}$ (5.35) solves the DDPMS-CO for (Σ (5.1), n_c, $\mathbb{C}_g$). □

Proof for Theorem 5.27:

We will use the solution to the DDPM as a starting point for the proof. A controller can be designed for Σ (5.1) by utilising any equivalent system; a representation of the form Σ^{T_c} (5.29) can therefore be considered for a given pair $(\mathcal{S}, \mathcal{V}) \in \mathbb{T}$. Let us first apply a *full order* controller Σ_c (5.25) to Σ^{T_c} (5.29), which results in the closed-loop system $\Sigma_{cl}^{T_c}$ (B.1). Note that the solution to the DDPM requires that all mappings in bold-font vanish.

With the conditions on D_{wy} and D_{uz}, it can be shown that this is the case if and only if $F_1 = 0$, $L_3 = 0$ and $N = 0$. For these specific mappings, the requirements $\lambda((A + B_uF)|\mathcal{V}) \subseteq \mathbb{C}_g$ and $\lambda((A + LC_y)|(\mathcal{X} \bmod \mathcal{S})) \subseteq \mathbb{C}_g$ are equivalent to

$$\lambda \begin{pmatrix} A_{11} & A_{12} + B_{u1}F_2 \\ A_{21} & A_{22} + B_{u2}F_2 \end{pmatrix} \subseteq \mathbb{C}_g, \quad \lambda \begin{pmatrix} A_{22} + L_2C_{y2} & A_{23} + L_2C_{y3} \\ A_{32} & A_{33} \end{pmatrix} \subseteq \mathbb{C}_g.$$

The minimal controller order is characterised in Theorem 5.25 for the DDPM-CO (i.e. without closed-loop stability) on the basis of the subspaces $(\mathcal{S}, \mathcal{V}) \in \mathbb{T}$. Now, let a *reduced order* controller $\widehat{\Sigma}_c^{T_c}$ (5.32) be applied to Σ^{T_c} (5.29), which results in the closed-loop system $\widehat{\Sigma}_{cl}^{T_c}$ (B.2).

The conditions on D_{wy} and D_{uz} imply that $N = 0$ and $-B_{u3}F_2 = A_{32}$. The inclusion of stability for $\widehat{\Sigma}_{cl}^{T_c}$ (B.2) is, as a consequence, equivalent to additionally requiring for $(\mathcal{S}, \mathcal{V}) \in \mathbb{T}$ that $\lambda((A+B_uF)|\mathcal{V}) \subseteq \mathbb{C}_g$ and $\lambda((A+LC_y)|(\mathcal{X} \bmod \mathcal{S})) \subseteq \mathbb{C}_g$, which is equivalent to the condition $(\mathcal{S}, \mathcal{V}) \in \mathbb{T}_g$.

The minimal controller order is therefore characterised for the DDPMS-CO by considering the subspaces $(\mathcal{S}_g, \mathcal{V}_g) \in \mathbb{T}_g$ in Theorem 5.25, which completes the proof. □

Proof for Theorem 5.32:

In Corollary 2.25 it is shown for a given H_2-admissible state feedback $u(t) = Fx(t)$ that

$$\gamma_{H_2,F}(\Sigma \text{ (5.1)}, F) = \operatorname{tr}\left(B_w^\top P^+ B_w\right) + \gamma_{H_2,F}(\Sigma_P \text{ (5.53)}, F).$$

Furthermore, an H_2 optimal feedback achieves $\gamma^\star_{H_2,F}(\Sigma \text{ (5.1)}) = \operatorname{tr}\left(B_w^\top P^+ B_w\right)$.

($\Rightarrow$) An H_2 optimal state feedback $u(t) = Fx(t)$ for Σ (5.1) will therefore achieve $\lambda(A + B_uF) \subset \mathbb{C}_-$ and $\gamma_{H_2,F}(\Sigma_P \text{ (5.53)}, F) = 0$. These conditions directly imply that the state feedback $u(t) = Fx(t)$ is H_2-admissible for Σ_P (5.53) and that $\Sigma_{cl,P,F}$ is disturbance decoupled.

($\Leftarrow$) An H_2-admissible state feedback $u(t) = Fx(t)$ for Σ_P (5.53) that achieves disturbance decoupling on $\Sigma_{cl,P,F}$ obtains $\gamma_{H_2,F}(\Sigma_P\ (5.53), F) = 0$ and $\lambda(A + B_uF) \subset \mathbb{C}_-$. This implies—as explained at the beginning of the proof—that the state feedback must be H_2 optimal for Σ (5.1). □

Proof for Proposition 5.33:

(i) $\Leftrightarrow$ (ii): It has been established for both systems that $\mathcal{V}_-^\star = \mathcal{X}$, which by definition satisfies $\mathrm{im}(B_w) \subseteq \mathcal{X}$ and $\mathrm{im}(B'_w) \subseteq \mathcal{X}$; this implies that $\mathcal{X} \in \mathbb{V}_-(\Sigma_P\ (5.53))$ and that $\mathcal{X} \in \mathbb{V}_-(\Sigma'_P)$. Finally, the requirements on F to solve the DDPS with this subspace are equivalent for both systems, because they are independent of B_w and B'_w.

(i) $\Rightarrow$ (iii): By observing that $\mathcal{V}_-^\star = \mathcal{X}$, the requirements on the mapping F to solve the DDPS for (Σ_P (5.53), $\mathcal{V}_-^\star$, $\mathbb{C}_-$) are $(A + B_uF)\mathcal{X} \subseteq \mathcal{X}$, $((D_{uz}^\top D_{uz})^{-\frac{1}{2}}(B_u^\top P^+ + D_{uz}^\top C_z) + (D_{uz}^\top D_{uz})^{\frac{1}{2}}F)\mathcal{X} = 0$ and $\lambda(A + B_uF) \subset \mathbb{C}_-$. The second requirement uniquely defines $F = -(D_{uz}^\top D_{uz})^{-1}(B_u^\top P^+ + D_{uz}^\top C_z)$, while the other requirements are satisfied with this state feedback as well.

(iii) $\Rightarrow$ (i): By observing that $\mathcal{V}_-^\star = \mathcal{X}$, it is easy to show for the given mapping F that the requirements $(A + B_uF)\mathcal{X} \subseteq \mathcal{X}$, $((D_{uz}^\top D_{uz})^{-\frac{1}{2}}(B_u^\top P^+ + D_{uz}^\top C_z) + (D_{uz}^\top D_{uz})^{\frac{1}{2}}F)\mathcal{X} = 0$ and $\lambda(A + B_uF) \subset \mathbb{C}_-$ are satisfied, which completes the proof. □

Proof for Theorem 5.37:

It easy to show that an estimator Σ_{e,n_e} (5.2) is H_2-admissible for Σ (5.1) if and only if it is H_2-admissible for Σ_Q (5.55).

In Corollary 2.30 it is shown for a given H_2-admissible estimator Σ_{e,n_e} (5.2) that

$$\gamma_{H_2,e}(\Sigma\ (5.1), \Sigma_{e,n_e}\ (5.2)) = \mathrm{tr}\left(C_zQ^+C_z^\top\right) + \gamma_{H_2,e}(\Sigma_Q\ (5.55), \Sigma_{e,n_e}\ (5.2)).$$

Furthermore, an H_2 optimal estimator achieves $\gamma^\star_{H_2,e}(\Sigma\ (5.1)) = \mathrm{tr}\left(C_zQ^+C_z^\top\right)$ in combination with the stability requirement.

($\Rightarrow$) An H_2 optimal estimator Σ_{e,n_e} (5.2) for Σ (5.1) will therefore achieve $\gamma_{H_2,e}(\Sigma_Q\ (5.55), \Sigma_{e,n_e}\ (5.2)) = 0$. This condition implies that $\Sigma_{\epsilon,n_e,Q}$ is disturbance decoupled, while the estimator must be H_2-admissible for Σ_Q (5.55).

($\Leftarrow$) An H_2-admissible estimator Σ_{e,n_e} (5.2) for Σ_Q (5.55) that achieves disturbance decoupling on $\Sigma_{\epsilon,n_e,Q}$ obtains $\gamma_{H_2,e}(\Sigma_Q\ (5.55), \Sigma_{e,n_e}\ (5.2)) = 0$ and is H_2-admissible for Σ (5.1). This implies—as explained at the beginning of the proof—that the estimator must be H_2 optimal for Σ (5.1). □

Proof for Proposition 5.38:

(i) $\Leftrightarrow$ (ii): It has been established for both systems that $\mathcal{S}_-^\star = 0$, which by definition satisfies $0 \subseteq \ker(C_z)$ and $0 \subseteq \ker(C'_z)$; this implies that $0 \in \mathbb{S}_-(\Sigma_Q\ (5.55))$ and that $0 \in \mathbb{S}_-(\Sigma'_Q)$. Finally, the requirements on L to solve the DDEPS with this subspace are equivalent for both systems, because they are independent of C_z, D_{uz}, C'_z and D'_{uz}.

(i) $\Rightarrow$ (iii): By observing that $\mathcal{S}_-^\star = 0$, the requirements on the mapping L to solve the DDEPS for (Σ_Q (5.55), $\mathcal{S}_-^\star$, $\mathbb{C}_-$) are $(A + LC_y)0 \subseteq 0$, $((Q^+C_y^\top + B_wD_{wy}^\top)(D_{wy}D_{wy}^\top)^{-\frac{1}{2}} + L(D_{wy}D_{wy}^\top)^{\frac{1}{2}}) \subseteq 0$ and $\lambda(A + LC_y) \subset \mathbb{C}_-$. The second requirement uniquely defines $L = -(Q^+C_y^\top + B_w^\top D_{wy})(D_{wy}D_{wy}^\top)^{-1}$, while the other requirements are satisfied with this observer gain L as well.

(iii) $\Rightarrow$ (i): By observing that $\mathcal{S}_-^\star = 0$, it is easy to show for the given mapping L that the requirements $(A + LC_y)0 \subseteq 0$, $((Q^+C_y^\top + B_wD_{wy}^\top)(D_{wy}D_{wy}^\top)^{-\frac{1}{2}} + L(D_{wy}D_{wy}^\top)^{\frac{1}{2}}) \subseteq 0$ and $\lambda(A+LC_y) \subset \mathbb{C}_-$ are satisfied, which completes the proof. □

Proof for Lemma 5.42:

(a) It has been proven by Stoorvogel and van der Woude [1991, Cor 2.4] that the conditions $\mathrm{im}(B_w) \subseteq \mathcal{V}_- + B_u \ker(D_{uz})$, $\mathcal{S}_- \cap C_y^{-1}\mathrm{im}(D_{wy}) \subseteq \ker(C_z)$ and $\mathcal{S}_- \subseteq \mathcal{V}_-$ are replaced by $\mathcal{S}_- \subseteq \ker(C_z)$, $\mathrm{im}(B_w) \subseteq \mathcal{V}_-$ and $A\mathcal{S}_- \subseteq \mathcal{V}_-$, when a controller Σ_c (5.25) with $N = 0$ is considered.

Assumption 5.2 implies for Σ_{PQ} (5.56) that $(D_{uz}^\top D_{uz})^{\frac{1}{2}} N (D_{wy}D_{wy}^\top)^{\frac{1}{2}} = 0$ if and only if $N = 0$. A controller with $N = 0$ must therefore be considered for the DDPMS, which implies that the set in (5.27) is indeed described by $\mathbb{T}_-(\Sigma_{PQ}$ (5.56)) as defined above.

(b) and (c) follow directly from Lemmas 5.31 and 5.36, when it is observed that $A0 \subseteq \mathcal{X}$

(c) It has been shown by Saberi et al. [1995b, Sec. 3.2] that the conditions $\mathcal{S}_- \subseteq \ker(\tilde{C}_z)$ and $A\mathcal{S}_- \subseteq \mathcal{V}_-$ imply that $\mathcal{S}_- \subseteq \mathcal{V}_-$. □

Proof for Theorem 5.43:

It easy to show that a controller Σ_{c,n_c} (5.21) is H_2-admissible for Σ (5.1) if and only if it is H_2-admissible for Σ_{PQ} (5.56).

In Corollary 2.34 it is shown for a given H_2-admissible controller Σ_{c,n_c} (5.21) that
$\gamma_{H_2}(\Sigma$ (5.1), Σ_{c,n_c} (5.21)) $= \mathrm{tr}(B_w^\top P_r^+ B_w) + \mathrm{tr}(B_u^\top P_r^+ Q_r^+ P_r^+ B_u)$
$+ \gamma_{H_2}(\Sigma_{PQ}$ (5.56), Σ_{c,n_c} (5.21)).
Furthermore, an H_2 optimal controller achieves closed-loop stability in combination with $\gamma_{H_2}^\star(\Sigma$ (5.1)) $= \mathrm{tr}(B_w^\top P_r^+ B_w) + \mathrm{tr}(B_u^\top P_r^+ Q_r^+ P_r^+ B_u)$.

($\Rightarrow$) An H_2 optimal controller for Σ (5.1) will therefore achieve $\gamma_{H_2}(\Sigma_{PQ}$ (5.56), Σ_{c,n_c} (5.21)) $= 0$. This condition implies that $\Sigma_{cl,PQ}$ is disturbance decoupled, while the controller must be H_2-admissible for Σ_{PQ} (5.56).

($\Leftarrow$) An H_2-admissible controller Σ_{c,n_c} (5.21) for Σ_{PQ} (5.56) that achieves disturbance decoupling on $\Sigma_{cl,PQ}$ obtains $\gamma_{H_2}(\Sigma_{PQ}$ (5.56), Σ_{c,n_c} (5.21)) $= 0$ and is H_2-admissible for Σ (5.1). This implies—as explained at the beginning of the proof—that the controller must be H_2 optimal for Σ (5.1). □

Someone told me that each equation I included in the book would halve the sales.

Stephen Hawking

B

Additional Equations for Chapter 5

$$
\Sigma_{cl}^{T_c} = \left\{ \begin{array}{rl}
\begin{pmatrix} \dot{x}_1(t) \\ \dot{x}_2(t) \\ \dot{x}_3(t) \\ \hline \dot{e}_1(t) \\ \dot{e}_2(t) \\ \dot{e}_3(t) \end{pmatrix} = & \left(\begin{array}{ccc|ccc} A_{11}+B_{u1}(F_1+NC_{y1}) & A_{12}+B_{u1}(F_2+NC_{y2}) & A_{13}+B_{u1}(F_3+NC_{y3}) & -B_{u1}F_1 & -B_{u1}F_2 & -B_{u1}F_3 \\ A_{21}+B_{u2}(F_1+NC_{y1}) & A_{22}+B_{u2}(F_2+NC_{y2}) & A_{23}+B_{u2}(F_3+NC_{y3}) & -B_{u2}F_1 & -B_{u2}F_2 & -B_{u2}F_3 \\ \mathbf{A_{31}+B_{u3}(F_1+NC_{y1})} & \mathbf{A_{32}+B_{u3}(F_2+NC_{y2})} & A_{33}+B_{u3}(F_3+NC_{y3}) & \mathbf{-B_{u3}F_1} & -B_{u3}F_2 & -B_{u3}F_3 \\ \hline 0 & 0 & 0 & A_{11}+L_1C_{y1} & A_{12}+L_1C_{y2} & A_{13}+L_1C_{y3} \\ 0 & 0 & 0 & \mathbf{A_{21}+L_2C_{y1}} & A_{22}+L_2C_{y2} & A_{23}+L_2C_{y3} \\ 0 & 0 & 0 & \mathbf{A_{31}+L_3C_{y1}} & A_{32}+L_3C_{y2} & A_{33}+L_3C_{y3} \end{array}\right) \begin{pmatrix} x_1(t) \\ x_2(t) \\ x_3(t) \\ \hline e_1(t) \\ e_2(t) \\ e_3(t) \end{pmatrix} \\
& + \begin{pmatrix} B_{w1}+B_{u1}ND_{wy} \\ B_{w2}+B_{u2}ND_{wy} \\ \mathbf{B_{w3}+B_{u3}ND_{wy}} \\ \hline B_{w1}+L_1D_{wy} \\ \mathbf{B_{w2}+L_2D_{wy}} \\ \mathbf{B_{w3}+L_3D_{wy}} \end{pmatrix} w(t) \\
z(t) \quad = & \left(\mathbf{C_{z1}+D_{uz}(F_1+NC_{y1})} \;\; \mathbf{C_{z2}+D_{uz}(F_2+NC_{y2})} \;\; C_{z3}+D_{uz}(F_3+NC_{y3}) \middle| \mathbf{-D_{uz}F_1} \;\; -D_{uz}F_2 \;\; -D_{uz}F_3\right) \begin{pmatrix} x(t) \\ \hline e(t) \end{pmatrix} \\
& + \left(\mathbf{D_{uz}ND_{wy}}\right) w(t).
\end{array} \right. \tag{B.1}
$$

$$
\widehat{\Sigma}_{cl}^{T_c} = \left\{ \begin{array}{rl}
\begin{pmatrix} \dot{x}_1(t) \\ \dot{x}_2(t) \\ \dot{x}_3(t) \\ \hline \dot{e}_2(t) \end{pmatrix} = & \left(\begin{array}{ccc|c} A_{11}+B_{u1}NC_{y1} & A_{12}+B_{u1}(F_2+NC_{y2}) & A_{13}+B_{u1}NC_{y3} & -B_{u1}F_2 \\ A_{21}+B_{u2}NC_{y1} & A_{22}+B_{u2}(F_2+NC_{y2}) & A_{23}+B_{u2}NC_{y3} & -B_{u2}F_2 \\ \mathbf{A_{31}+B_{u3}NC_{y1}} & \mathbf{A_{32}+B_{u3}(F_2+NC_{y2})} & A_{33}+B_{u3}NC_{y3} & -B_{u3}F_2 \\ \hline \mathbf{A_{21}+L_2C_{y1}} & 0 & A_{23}+L_2C_{y3} & A_{22}+L_2C_{y2} \end{array}\right) \begin{pmatrix} x_1(t) \\ x_2(t) \\ x_3(t) \\ \hline e_2(t) \end{pmatrix} + \begin{pmatrix} B_{w1}+B_{u1}ND_{wy} \\ B_{w2}+B_{u2}ND_{wy} \\ \mathbf{B_{w3}+B_{u3}ND_{wy}} \\ \hline \mathbf{B_{w2}+L_2D_{wy}} \end{pmatrix} w(t) \\
z(t) \quad = & \left(\mathbf{C_{z1}+D_{uz}NC_{y1}} \;\; \mathbf{C_{z2}+D_{uz}(F_2+NC_{y2})} \;\; C_{z3}+D_{uz}NC_{y3} \middle| -D_{uz}F_2\right) \begin{pmatrix} x(t) \\ \hline e_2(t) \end{pmatrix} + \left(\mathbf{D_{uz}ND_{wy}}\right) w(t)
\end{array} \right. \tag{B.2}
$$

$$\Sigma^{T_{c,g}} = \begin{cases} \begin{pmatrix} \dot{x}_{11}(t) \\ \dot{x}_{12}(t) \\ \dot{x}_{2}(t) \\ \dot{x}_{31}(t) \\ \dot{x}_{32}(t) \end{pmatrix} = \begin{pmatrix} A_{1111}\, A_{1112}\, A_{112}\, A_{1131}\, A_{1132} \\ A_{1211}\, A_{1212}\, A_{122}\, A_{1231}\, A_{1232} \\ A_{211}\;\; A_{212}\;\; A_{22}\;\; A_{231}\;\; A_{232} \\ A_{3111}\, A_{3112}\, A_{312}\, A_{3131}\, A_{3132} \\ A_{3211}\, A_{3212}\, A_{322}\, A_{3231}\, A_{3232} \end{pmatrix} \begin{pmatrix} x_{11}(t) \\ x_{12}(t) \\ x_{2}(t) \\ x_{31}(t) \\ x_{32}(t) \end{pmatrix} + \begin{pmatrix} B_{u11} \\ B_{u12} \\ B_{u2} \\ B_{u31} \\ B_{u32} \end{pmatrix} u(t) + \begin{pmatrix} B_{w11} \\ B_{w12} \\ B_{w2} \\ B_{w31} \\ B_{w32} \end{pmatrix} w(t) \\ y(t) = \begin{pmatrix} C_{y11}\, C_{y12}\, C_{y2}\, C_{y31}\, C_{y32} \end{pmatrix} x(t) + D_{wy}\, w(t) \\ z(t) = \begin{pmatrix} C_{z11}\, C_{z12}\, C_{z2}\, C_{z31}\, C_{z32} \end{pmatrix} x(t) + D_{uz}\, u(t) \end{cases} \tag{B.3}$$

$$\widehat{\Sigma}_{c,g}^{T_{c,g}} = \begin{cases} \begin{pmatrix} \dot{\tilde{x}}_{12}(t) \\ \dot{\tilde{x}}_{2}(t) \\ \dot{\tilde{x}}_{31}(t) \end{pmatrix} = \begin{pmatrix} A_{1212} + B_{u12}F_{12} + L_{12}C_{y12} & A_{122} + B_{u12}F_2 + L_{12}C_{y2} & A_{1231} + B_{u12}F_{31} + L_{12}C_{y31} \\ A_{212} + B_{u2}F_{12} + L_2C_{y12} & A_{22} + B_{u2}F_2 + L_2C_{y2} & A_{231} + B_{u2}F_{31} + L_2C_{y31} \\ A_{3112} + B_{u31}F_{12} + L_{31}C_{y12} & A_{312} + B_{u31}F_2 + L_{31}C_{y2} & A_{3131} + B_{u31}F_{31} + L_{31}C_{y31} \end{pmatrix} \begin{pmatrix} \tilde{x}_{12}(t) \\ \tilde{x}_{2}(t) \\ \tilde{x}_{31}(t) \end{pmatrix} + \begin{pmatrix} B_{u12}N - L_{12} \\ B_{u2}N - L_2 \\ B_{u31}N - L_{31} \end{pmatrix} y(t) \\ u(t) = \begin{pmatrix} F_{12} & F_2 & F_{31} \end{pmatrix} \begin{pmatrix} \tilde{x}_{12}(t) \\ \tilde{x}_{2}(t) \\ \tilde{x}_{31}(t) \end{pmatrix} + N\, y(t) \end{cases} \tag{B.4}$$

$$
\widehat{\Sigma}_{cl,g}^{T_{c,g}} =
\left\{
\begin{array}{l}
\begin{pmatrix} \dot{x}_{11}(t) \\ \dot{x}_{12}(t) \\ \dot{x}_{2}(t) \\ \dot{x}_{31}(t) \\ \dot{x}_{32}(t) \\ \hline \dot{e}_{12}(t) \\ \dot{e}_{2}(t) \\ \dot{e}_{31}(t) \end{pmatrix}
= \left(\begin{array}{ccccc|c}
A_{1111}+B_{u11}NC_{y11} & A_{1112}+B_{u11}(F_{12}+NC_{y12}) & A_{112}+B_{u11}(F_2+NC_{y2}) & A_{1131}+B_{u11}(F_{31}+NC_{y31}) & A_{1132}+B_{u11}NC_{y32} & \cdots \\
A_{1211}+B_{u12}NC_{y11} & A_{1212}+B_{u12}(F_{12}+NC_{y12}) & A_{122}+B_{u12}(F_2+NC_{y2}) & A_{1231}+B_{u12}(F_{31}+NC_{y31}) & A_{1232}+B_{u12}NC_{y32} & \cdots \\
A_{211}+B_{u2}NC_{y11} & A_{212}+B_{u2}(F_{12}+NC_{y12}) & A_{22}+B_{u2}(F_2+NC_{y2}) & A_{231}+B_{u2}(F_{31}+NC_{y31}) & A_{232}+B_{u2}NC_{y32} & \cdots \\
\mathbf{A_{3111}+B_{u31}NC_{y11}} & \mathbf{A_{3112}+B_{u31}(F_{12}+NC_{y12})} & \mathbf{A_{312}+B_{u31}(F_2+NC_{y2})} & A_{3131}+B_{u31}(F_{31}+NC_{y31}) & A_{3132}+B_{u31}NC_{y32} & \cdots \\
\mathbf{A_{3211}+B_{u32}NC_{y11}} & \mathbf{A_{3212}+B_{u32}(F_{12}+NC_{y12})} & \mathbf{A_{322}+B_{u32}(F_2+NC_{y2})} & A_{3231}+B_{u32}(F_{31}+NC_{y31}) & A_{3232}+B_{u32}NC_{y32} & \cdots \\ \hline
\mathbf{A_{1211}+L_{12}C_{y11}} & 0 & 0 & 0 & A_{1232}+L_{12}C_{y32} & \cdots \\
\mathbf{A_{211}+L_2C_{y11}} & 0 & 0 & 0 & \mathbf{A_{232}+L_2C_{y32}} & \cdots \\
\mathbf{A_{3111}+L_{31}C_{y11}} & 0 & 0 & 0 & \mathbf{A_{3132}+L_{31}C_{y32}} & \cdots
\end{array}\right)
\begin{pmatrix} x_{11}(t) \\ x_{12}(t) \\ x_2(t) \\ x_{31}(t) \\ x_{32}(t) \\ \hline e_{12}(t) \\ e_2(t) \\ e_{31}(t) \end{pmatrix}
+ \left(\begin{array}{c|c}
B_{w11}+B_{u11}ND_{wy} & \cdots \\
B_{w12}+B_{u12}ND_{wy} & \cdots \\
B_{w2}+B_{u2}ND_{wy} & \cdots \\
\mathbf{B_{w31}+B_{u31}ND_{wy}} & \cdots \\
\mathbf{B_{w32}+B_{u32}ND_{wy}} & \cdots \\ \hline
B_{w12}+L_{12}D_{wy} & \cdots \\
\mathbf{B_{w2}+L_2D_{wy}} & \cdots \\
\mathbf{B_{w31}+L_{31}D_{wy}} & \cdots
\end{array}\right) w(t) \\
\qquad\qquad \cdots \left|\begin{array}{ccccc}
-B_{u11}F_{12} & -B_{u11}F_2 & -B_{u11}F_{31} & \cdots \\
-B_{u12}F_{12} & -B_{u12}F_2 & -B_{u12}F_{31} & \cdots \\
-B_{u2}F_{12} & -B_{u2}F_2 & -B_{u2}F_{31} & \cdots \\
\mathbf{-B_{u31}F_{12}} & -B_{u31}F_2 & -B_{u31}F_{31} & \cdots \\
\mathbf{-B_{u32}F_{12}} & -B_{u32}F_2 & -B_{u32}F_{31} & \cdots \\ \hline
A_{1212}+L_{12}C_{y12} & A_{122}+L_{12}C_{y2} & A_{1231}+L_{12}C_{y31} & \cdots \\
\mathbf{A_{212}+L_2C_{y12}} & A_{22}+L_2C_{y2} & A_{231}+L_2C_{y31} & \cdots \\
\mathbf{A_{3112}+L_{31}C_{y12}} & A_{312}+L_{31}C_{y2} & A_{3131}+L_{31}C_{y31} & \cdots
\end{array}\right| \\
z(t) = \left(\mathbf{C_{z11}+D_{uz}NC_{y11}} \quad \mathbf{C_{z12}+D_{uz}(F_{12}+NC_{y12})} \quad \mathbf{C_{z2}+D_{uz}(F_2+NC_{y2})} \quad C_{z31}+D_{uz}(F_{31}+NC_{y31}) \quad C_{z32}+D_{uz}NC_{y32}\right) \left|\begin{array}{c} \cdots \\ \hline \cdots \end{array}\right. \\
\qquad\qquad \cdots \left|\begin{array}{c} -\mathbf{D_{uz}F_{12}} \quad -D_{uz}F_2 \quad -D_{uz}F_{31} \end{array}\right| \begin{pmatrix} x(t) \\ \hline e_{12}(t) \\ e_2(t) \\ e_{31}(t) \end{pmatrix} + \left(\mathbf{D_{uz}ND_{wy}}\right) w(t)
\end{array}
\right. \tag{B.5}
$$

Bibliography

F. D. Adegas, I. B. Sonderby, M. H. Hansen, and J. Stoustrup. Reduced-Order LPV Model of Flexible Wind Turbines from High Fidelity Aeroelastic Codes. In *International Conference on Control Applications*, pages 424–429, Hyderabad, India, 2013. IEEE. ISBN 978-1-4799-1559-0. doi: 10.1109/CCA.2013.6662786.

H. Aling and J. M. Schumacher. A Nine-Fold Canonical Decomposition for Linear Systems. *International Journal of Control*, 39(4):779–805, 1984. ISSN 0020-7179. doi: 10.1080/00207178408933206.

Amcoss. Amcoss, facilitating innovation, 2019. URL `https://amcoss.com/en/componentsrefurbishment/lithography/refurbishment-of-canon-stepper-chucks-and-asml-wafer-tables/`. [June 11, 2019].

A. C. Antoulas. *Approximation of Large-Scale Dynamical Systems*. SIAM, 2005. ISBN 978-0-89871-529-3. doi: 10.1137/1.9780898718713.

A. Argha, S. W. Su, and A. Savkin. Optimal Actuator/Sensor Selection Through Dynamic Output Feedback. In *Conference on Decision and Control*, pages 3624–3629, Las Vegas, NV, USA, 2016. IEEE. ISBN 978-1-5090-1837-6. doi: 10.1109/CDC.2016.7798814.

D. Arzelier, G. Georgia, S. Gumussoy, and D. Henrion. Multiobjective Robust Control with HIFOO 2.0. In *Symposium on Robust Control Design*, Haifa, Israël, 2009. IFAC. URL `https://cs.nyu.edu/overton/papers/pdffiles/hifoo-haifa.pdf`.

D. Arzelier, G. Georgia, S. Gumussoy, and D. Henrion. H_2 for HIFOO. In *International Conference on Control and Optimization with Industrial Applications*, Ankara, Turkey, 2011. URL `https://arxiv.org/abs/1010.1442`.

S. Banholzer, E. Makarov, and S. Volkwein. *POD-Based Multiobjective Optimal Control of Time-Variant Heat Phenomena*. Springer, 2019. doi: 10.1007/978-3-319-96415-7_83.

G. Basile and G. Marro. *Controlled and Conditioned Invariants in Linear Systems Theory*. Prentice Hall, 1992. ISBN 0131729748.

K. J. Bathe. *Finite Element Procedures*. Prentice Hall, 1996. ISBN 9780133496970. URL `http://web.mit.edu/kjb/www/Books/FEP_2nd_Edition_4th_Printing.pdf`.

P. Benner, S. Gugercin, and K. Willcox. A Survey of Projection-Based Model Reduction Methods for Parametric Dynamical Systems. *SIAM Review*, 57(4): 483–531, 2015. ISSN 0036-1445. doi: 10.1137/130932715.

P. Benner, T. Mitchell, and M. L. Overton. Low-Order Control Design using a Reduced-Order Model with a Stability Constraint on the Full-Order Model. In *Conference on Decision and Control*, pages 3000–3005, Miami Beach, FL, USA, 2018. IEEE. ISBN 978-1-5386-1395-5. doi: 10.1109/CDC.2018.8619449.

D. S. Bernstein. Sequential Design of Decentralized Dynamic Compensators using the Optimal Projection Equations. *International Journal of Control*, 46(5):1569–1577, 1987. ISSN 0020-7179. doi: 10.1080/00207178708933995.

C. Bikcora, S. Weiland, and W. M. J. Coene. Thermal Deformation Prediction in Reticles for Extreme Ultraviolet Lithography Based on a Measurement-Dependent Low-Order Model. *IEEE Transactions on Semiconductor Manufacturing*, 27(1):104–117, 2014. ISSN 0894-6507. doi: 10.1109/TSM.2014.2298360.

O. H. Bosgra, H. Kwakernaak, and G. Meinsma. Design Methods for Control Systems, 2007. URL `http://wwwhome.math.utwente.nl/~meinsmag/dmcs/dmcs0708.pdf`.

S. Boyd. Distributed Optimization and Statistical Learning via the Alternating Direction Method of Multipliers. *Foundations and Trends in Machine Learning*, 3(1):1–122, 2010. ISSN 1935-8237. doi: 10.1561/2200000016.

M. Campi, A. Lecchini, and S. Savaresi. Virtual Reference Feedback Tuning: a Direct Method for the Design of Feedback Controllers. *Automatica*, 38(8):1337–1346, 2002. ISSN 00051098. doi: 10.1016/S0005-1098(02)00032-8.

A. Candeo and F. Dughiero. Numerical FEM Models for the Planning of Magnetic Induction Hyperthermia Treatments With Nanoparticles. *IEEE Transactions on Magnetics*, 45(3):1658–1661, 2009. ISSN 0018-9464. doi: 10.1109/TMAG.2009.2012769.

L. F. O. Chamon, G. J. Pappas, and A. Ribeiro. The Mean Square Error in Kalman Filtering Sensor Selection is Approximately Supermodular. In *Conference on Decision and Control*, pages 343–350, Melbourne, Australia, 2017. IEEE. ISBN 978-1-5090-2873-3. doi: 10.1109/CDC.2017.8263688.

B. M. Chen. Linear Systems Toolkit, 2018. URL `http://uav.ece.nus.edu.sg/~bmchen/linsyskit/index.html`. [May 9, 2018].

B. M. Chen, Z. Lin, and Y. Shamash. *Linear Systems Theory*. Springer, 2004. ISBN 978-1-4612-7394-3. doi: 10.1007/978-1-4612-2046-6.

R. Choroszucha and J. Sun. Empirical Riccati Covariance Matrices for Closed-Loop Model Order Reduction of Nonlinear Systems by Balanced Truncation. In *American Control Conference*, pages 3476–3482, Seattle, WA, USA, 2017. IEEE. ISBN 978-1-5090-5992-8. doi: 10.23919/ACC.2017.7963484.

COMSOL Multiphysics. COMSOL Multiphysics, 2019. URL http://www.comsol.com.

G. E. Davis. Scattering of Light by an Air Bubble in Water. *Journal of the Optical Society of America*, 45(7):572, 1955. ISSN 0030-3941. doi: 10.1364/JOSA.45.000572.

N. K. Dhingra, M. R. Jovanovic, and Z.-Q. Luo. An ADMM Algorithm for Optimal Sensor and Actuator Selection. In *Conference on Decision and Control*, pages 4039–4044, Los Angeles, CA, USA, 2014. IEEE. ISBN 978-1-4673-6090-6. doi: 10.1109/CDC.2014.7040017.

J. Doyle. Guaranteed Margins for LQG Regulators. *IEEE Transactions on Automatic Control*, 23(4):756–757, 1978. ISSN 0018-9286. doi: 10.1109/TAC.1978.1101812.

M. Drapeau, V. Wiaux, E. Hendrickx, S. Verhaegen, and T. Machida. Double Patterning Design Split Implementation and Validation for the 32nm Node. In *Advanced Lithography*, page 652109, San Jose, CA, USA, 2007. SPIE. doi: 10.1117/12.712139.

H. El-Zobaidi and I. Jaimoukha. Robust Control and Model and Controller Reduction of Linear Parameter Varying Systems. In *Conference on Decision and Control*, volume 3, pages 3015–3020, Tampa, FL, USA, 1998. IEEE. ISBN 0-7803-4394-8. doi: 10.1109/CDC.1998.757952.

S. Formentin, M. Corno, S. M. Savaresi, and L. Del Re. Direct Data-Driven Control of Linear Time-Delay Systems. *Asian Journal of Control*, 14(3):652–663, 2012a. ISSN 15618625. doi: 10.1002/asjc.387.

S. Formentin, A. Karimi, and S. M. Savaresi. On Input Design for Direct Data-Driven Controller Tuning. *IFAC Proceedings Volumes*, 45(16):1466–1471, 2012b. ISSN 14746670. doi: 10.3182/20120711-3-BE-2027.00305.

G. F. Franklin, J. D. Powell, and A. Emami-Naeini. *Feedback Control of Dynamical Systems*. Pearson, 2015. ISBN 9780133496598. URL https://www.pearson.com/us/higher-education/program/Franklin-Feedback-Control-of-Dynamic-Systems-8th-Edition/PGM1653583.html.

W. Gawronski and K. B. Lim. Balanced Actuator and Sensor Placement for Flexible Structures. *International Journal of Control*, 65(1):131–145, 1996. ISSN 0020-7179. doi: 10.1080/00207179608921690.

D. Georges. The Use of Observability and Controllability Gramians or Functions for Optimal Sensor and Actuator Location in Finite-Dimensional Systems. In *Conference on Decision and Control*, volume 4, pages 3319–3324, New Orleans, LA, USA, 1995. IEEE. ISBN 0-7803-2685-7. doi: 10.1109/CDC.1995.478999.

P. J. Goddard. *Performance-Preserving Controller Approximation*. Ph.d. dissertation, Cambridge, 1995. URL http://citeseerx.ist.psu.edu/viewdoc/download?doi=10.1.1.9.1949&rep=rep1&type=pdf.

V. Gold. Evaporation. In *Compendium of Chemical Terminology*. IUPAC, 2014. doi: 10.1351/goldbook.E02227.

M. Grant and S. Boyd. CVX: Matlab Software for Disciplined Convex Programming, version 2.1, 2014. URL `http://cvxr.com/cvx`.

M. C. Grant and S. P. Boyd. Graph Implementations for Nonsmooth Convex Programs. In *Recent Advances in Learning and Control*, pages 95–110. Springer, 2008. doi: 10.1007/978-1-84800-155-8Ω_.

C. Grimholt and S. Skogestad. Optimization of Fixed-Order Controllers using Exact Gradients. *Journal of Process Control*, 71:130–138, 2018. ISSN 09591524. doi: 10.1016/j.jprocont.2018.09.001.

S. Gugercin and A. C. Antoulas. A Survey of Model Reduction by Balanced Truncation and Some New Results. *International Journal of Control*, 77(8):748–766, 2004. ISSN 0020-7179. doi: 10.1080/00207170410001713448.

M. Habets, R. Merks, S. Weiland, and W. Coene. A Multiphysics Modeling Approach for Thermal Aberration Prediction and Control in Extreme Ultraviolet Lithography. In *Imaging and Applied Optics*, page AOM4B.2, Washington D.C., USA, 2015. OSA. ISBN 978-1-943580-00-2. doi: 10.1364/AOMS.2015.AOM4B.2.

A. Hać and L. Liu. Sensor And Actuator Location In Motion Control Of Flexible Structures. *Journal of Sound and Vibration*, 167(2):239–261, 1993. ISSN 0022460X. doi: 10.1006/jsvi.1993.1333.

J. Hanema. *Anticipative Model Predictive Control for Linear Parameter-Varying Systems*. Ph.d. dissertation, Eindhoven Univeristy of Technology, 2018. URL `https://research.tue.nl/en/publications/anticipative-model-predictive-control-for-linear-parameter-varyin`.

M. Hautus. (A, B)-Invariant and Stabilizability Subspaces : A Frequency Domain Description with Applications. Technical report, Eindhoven University of Technology, Eindhoven, 1979. URL `https://research.tue.nl/en/publications/ab-invariant-and-stabilizability-subspaces-a-frequency-domain-des`.

D. Henrion and D. Arzelier. LMIs in Systems and Control, State-Space Methods and Stability Analysis, 2004. URL `http://homepages.laas.fr/henrion/courses/edsys04/edsys04_7.pdf`. [April 21, 2019].

G. Hilhorst. *Design of Fixed-Order Feedback Controllers for Mechatronic Systems*. Ph.d. dissertation, KU Leuven, 2015. URL `https://lirias.kuleuven.be/retrieve/346059`.

C. Hol. *Structured Controller Synthesis for Mechanical Servo-Systems*. Ph.d. dissertation, Delft University of Technology, 2006. URL `https://repository.tudelft.nl/islandora/object/uuid:8eff9ef1-b509-4f3d-b1f7-7d1357c53ff8/datastream/OBJ`.

T. C. Ionescu and A. Astolfi. Moment Matching for Linear Systems. *IFAC Proceedings Volumes*, 44(1):12739–12744, 2011. ISSN 14746670. doi: 10.3182/20110828-6-IT-1002.02406.

T. Ito and S. Okazaki. Pushing the Limits of Lithography. *Nature*, 406(6799): 1027–1031, 2000. ISSN 0028-0836. doi: 10.1038/35023233.

T. Iwasaki and R. Skelton. All Controllers for the General H_∞ Control Problem: LMI Existence Conditions and State Space Formulas. *Automatica*, 30(8):1307–1317, 1994. ISSN 00051098. doi: 10.1016/0005-1098(94)90110-4.

C. Jia, D. Reuter, Z. Wen, M. Baum, M. Wiemer, and T. Gessner. FEM Simulation and its Application in MEMS Design. In *Semiconductor Conference*, pages 1–4, Dresden, Germany, 2011. IEEE. ISBN 978-1-4577-0431-4. doi: 10.1109/SCD.2011.6068759.

E. Jonckheere and L. Silverman. A New Set of Invariants for Linear Systems–Application to Reduced Order Compensator Design. *IEEE Transactions on Automatic Control*, 28(10):953–964, 1983. ISSN 0018-9286. doi: 10.1109/TAC.1983.1103159.

M. R. Jovanović and N. K. Dhingra. Controller Architectures: Tradeoffs Between Performance and Structure. *European Journal of Control*, 30:76–91, 2016. ISSN 09473580. doi: 10.1016/j.ejcon.2016.05.003.

E. Kreyszig. *Introductory Functional Analysis with Applications*. John Wiley & Sons, 1989. ISBN 0471504599. URL `https://www.wiley.com/en-us/Introductory+Functional+Analysis+with+Applications-p-9780471504597`.

D. C. Lay and S. R. Lay. *Linear Algebra and its Applications*. Pearson, 2015. ISBN 9781292092232. URL `https://www.pearson.com/us/higher-education/product/Lay-Linear-Algebra-and-Its-Applications-4th-Edition/9780321385178.html`.

B. J. Lin. Innovating from History. In *Advanced Lithography*, page 1058402, San Jose, CA, USA, 2018. SPIE. URL `https://www.spiedigitallibrary.org/conference-proceedings-of-spie/10584/1058402/Innovating-from-History/10.1117/12.2305526.full`.

F. Lin, M. Fardad, and M. R. Jovanovic. Sparse Feedback Synthesis via the Alternating Direction Method of Multipliers. In *American Control Conference*, pages 4765–4770, Montreal, Canada, 2012. IEEE. ISBN 978-1-4577-1096-4. doi: 10.1109/ACC.2012.6315694.

F. Lin, M. Fardad, and M. R. Jovanovic. Design of Optimal Sparse Feedback Gains via the Alternating Direction Method of Multipliers. *IEEE Transactions on Automatic Control*, 58(9):2426–2431, 2013. ISSN 0018-9286. doi: 10.1109/TAC.2013.2257618.

F. Lin, M. Fardad, and M. R. Jovanović. LQRSP Toolbox, 2014. URL `http://people.ece.umn.edu/~mihailo/software/lqrsp/index.html`. [May 21, 2019].

F. Liu, Y. Li, Y. Cao, J. She, and M. Wu. A Two-Layer Active Disturbance Rejection Controller Design for Load Frequency Control of Interconnected Power System. *IEEE Transactions on Power Systems*, 31(4):3320–3321, 2016. ISSN 0885-8950. doi: 10.1109/TPWRS.2015.2480005.

S. Liu, M. Fardad, S. Kar, and P. K. Varshney. On Optimal Sensor Collaboration Topologies for Linear Coherent Estimation. In *International Symposium on Information Theory*, pages 2624–2628, Honolulu, HI, USA, 2014. IEEE. ISBN 978-1-4799-5186-4. doi: 10.1109/ISIT.2014.6875309.

L. Ljung. *System Identification: Theory for the User*. Prentice Hall, 1999. ISBN 9780136566953. URL `https://books.google.nl/books?id=nHFoQgAACAAJ`.

J. Löfberg. YALMIP : A Toolbox for Modeling and Optimization in MATLAB. In *Conference on Robotics and Automation*, pages 284–289, New Orleans, LA, USA, 2004. IEEE. doi: 10.1109/CACSD.2004.1393890.

S. N. Lordejani, B. Besselink, M. Abbasi, G.-O. Kaasa, W. Schilders, and N. van de Wouw. Model Order Reduction for Managed Pressure Drilling Systems based on a Model with Local Nonlinearities. *IFAC-PapersOnLine*, 51(8):50–55, 2018. ISSN 24058963. doi: 10.1016/j.ifacol.2018.06.354.

T. Luspay, T. Peni, and B. Vanek. Control Oriented Reduced Order Modeling of a Flexible Winged Aircraft. In *Aerospace Conference*, pages 1–9, Big Sky, MT, USA, 2018. IEEE. ISBN 978-1-5386-2014-4. doi: 10.1109/AERO.2018.8396496.

C. Mack. *Fundamental Principles of Optical Lithography*. John Wiley & Sons, 2007. ISBN 9780470723876. doi: 10.1002/9780470723876.

C. A. Mack and B. J. Lin. Understanding Focus Effects in Submictron Optical Lithography. In *Symposium on Microlithography*, pages 135–148, Santa Clara, CA, USA, 1988. SPIE. doi: 10.1117/12.968408.

G. Marro. Geometric Approach, 2018. URL `http://www3.deis.unibo.it/Staff/FullProf/GiovanniMarro/geometric.htm`. [May 9, 2018].

H. Megens. Overlay. Technical report, ASML, Veldhoven, the Netherlands, 2007. URL `https://staticwww.asml.com/doclib/productandservices/images/asml_overlay_images_fall07.pdf`.

N. Mehrabi. *Dynamics and Model-Based Control of Electric Power Steering Systems*. Ph.d. dissertation, University of Waterloo, 2014. URL `https://uwspace.uwaterloo.ca/handle/10012/8887`.

R. W. H. Merks and S. Weiland. Constrained Order Controller Design for the Disturbance Decoupling Problem with Dynamic Measurement Feedback and Stability. submitted to *IEEE Transactions on Automatic Control*, 2019a.

R. W. H. Merks and S. Weiland. On the Non-Optimality of Linear Quadratic Gaussian Balanced Truncation for Constrained Order Controller Design. In *European Control Conference*, Napels, Italy, 2019b. IEEE.

R. W. H. Merks, E. M. M. Kivits, and S. Weiland. Constrained Order Observer Design for Disturbance Decoupled Output Estimation. *IEEE Control Systems Letters*, 3(1):49–54, 2019. ISSN 2475-1456. doi: 10.1109/LCSYS.2018.2851539.

G. E. Moore. Cramming More Components Onto Integrated Circuits. *IEEE Solid-State Circuits Society Newsletter*, 38(8):114–117, 1965. doi: 10.1109/N-SSC.2006.4785860.

G. E. Moore. Progress in Digital Integrated Electronics. In *International Electron Device Meeting*, pages 11–13, Washington D.C., USA, 1975. IEEE. doi: 10.1109/N-SSC.2006.4804410.

M. Morari and G. Stephanopoulos. Studies in the Synthesis of Control Structures for Chemical Processes: Part II: Structural Aspects and the Synthesis of Alternative Feasible Control Schemes. *Advancements in Chemical Engineering*, 26(2): 232–246, 1980. ISSN 0001-1541. doi: 10.1002/aic.690260206.

D. Mustafa. Reduced-Order Robust Controllers: H_∞-Balanced Truncation and Optimal Projection. In *Conference on Decision and Control*, pages 488–493 vol.2, Honolulu, HI, USA, 1990. IEEE. doi: 10.1109/CDC.1990.203646.

M. Mutsaers. *Control Relevant Model Reduction and Controller Synthesis for Complex Dynamical Systems*. Ph.d. dissertation, Eindhoven University of Technology, 2012. URL `https://pure.tue.nl/ws/files/3694274/734624.pdf`.

M. Mutsaers and S. Weiland. A Model Reduction Scheme with Preserved Optimal Performance. In *Conference on Decision and Control and European Control Conference*, pages 7176–7181, Orlando, FL, USA, 2011. IEEE. ISBN 978-1-61284-801-3. doi: 10.1109/CDC.2011.6161379.

G. L. Nemhauser, L. A. Wolsey, and M. L. Fisher. An Analysis of Approximations for Maximizing Submodular Set Functions—I. *Mathematical Programming*, 14 (1):265–294, 1978. ISSN 0025-5610. doi: 10.1007/BF01588971.

G. Obinata and B. D. O. Anderson. *Model Reduction for Control System Design*. Springer, 2001. ISBN 978-1-4471-1078-1. doi: 10.1007/978-1-4471-0283-0.

M. Opmeer, F. Wubs, and S. van Mourik. Model Reduction for Controller Design for Infinite-Dimensional Systems: Theory and an Example. In *Conference on Decision and Control*, pages 2469–2474, Seville, Spain, 2005. IEEE. ISBN 0-7803-9567-0. doi: 10.1109/CDC.2005.1582533.

T. Oyvang, J. K. Noland, G. J. Hegglid, and B. Lie. Online Model-Based Thermal Prediction for Flexible Control of an Air-Cooled Hydrogenerator. *IEEE Transactions on Industrial Electronics*, 66(8):6311–6320, 2019. ISSN 0278-0046. doi: 10.1109/TIE.2018.2875637.

L. Pernebo and L. Silverman. Model Reduction via Balanced State Space Representations. *IEEE Transactions on Automatic Control*, 27(2):382–387, 1982. ISSN 0018-9286. doi: 10.1109/TAC.1982.1102945.

D. Picard, J. Drgoňa, M. Kvasnica, and L. Helsen. Impact of the Controller Model Complexity on Model Predictive Control Performance for Buildings. *Energy and Buildings*, 152:739–751, 2017. ISSN 03787788. doi: 10.1016/j.enbuild.2017.07.027.

J. W. Polderman and J. C. Willems. *Introduction to Mathematical Systems Theory*, volume 26. Springer, 1998. ISBN 978-1-4757-2955-9. doi: 10.1007/978-1-4757-2953-5.

K. J. Åström and R. M. Murray. *Feedback Systems. An Introduction for Scientists and Engineers*. Princeton University Press, 2012. ISBN 978-0-691-13576-2. URL `https://press.princeton.edu/titles/8701.html`.

M. Renardy and R. C. Rogers. *An Introduction to Partial Differential Equations*. Springer, 2004. ISBN 0-387-00444-0. doi: 10.1007/b97427.

Y. Saad. *Iterative Methods for Sparse Linear Systems*. SIAM, 2003. ISBN 978-0-89871-534-7. doi: 10.1137/1.9780898718003.

Y. Saad. *Numerical Methods for Large Eigenvalue Problems*. SIAM, 2011. ISBN 978-1-61197-072-2. doi: 10.1137/1.9781611970739.

J. Saak, M. Köhler, and P. Benner. M.E.S.S.-1.0.1 — The Matrix Equations Sparse Solvers library, 2019. URL `www.mpi-magdeburg.mpg.de/projects/mess`. [April 27, 2019].

A. Saberi, P. Sannuti, and B. M. Chen. *H_2 Optimal Control*. Prentice Hall, 1995a. ISBN 9780134897820. URL `https://books.google.nl/books?id=VvlfQgAACAAJ`.

A. Saberi, Zongli Lin, and A. Stoorvogel. H_2 Almost Disturbance Decoupling Problem with Internal Stability. In *American Control Conference*, volume 5, pages 3414–3418, Seattle, WA, USA, 1995b. IEEE. ISBN 0-7803-2445-5. doi: 10.1109/ACC.1995.532245.

A. Saberi, P. Sannuti, and A. A. Stoorvogel. H_2 Optimal Controllers with Measurement Feedback for Continuous-Time Systems—Flexibility in Closed-Loop Pole Placement. *Automatica*, 32(8):1201–1209, 1996. ISSN 00051098. doi: 10.1016/0005-1098(96)00052-0.

S. Salakij, N. Yu, S. Paolucci, and P. Antsaklis. Model-Based Predictive Control for Building Energy Management. I: Energy Modeling and Optimal Control. *Energy and Buildings*, 133:345–358, 2016. ISSN 03787788. doi: 10.1016/j.enbuild.2016.09.044.

C. Scherer and S. Weiland. Linear Matrix Inequalities in Control, 2015. URL `https://www.imng.uni-stuttgart.de/mst/files/LectureNotes.pdf`.

W. H. A. Schilders, H. A. van der Vorst, and J. Rommes. *Model Order Reduction: Theory, Research Aspects and Applications*, volume 13. Springer, 2008. ISBN 978-3-540-78840-9. doi: 10.1007/978-3-540-78841-6.

S. Schuler, P. Li, J. Lam, and F. Allgöwer. Design of Structured Dynamic Output-Feedback Controllers for Interconnected Systems. *International Journal of Control*, 84(12):2081–2091, 2011. ISSN 0020-7179. doi: 10.1080/00207179.2011.634029.

J. Schumacher. Compensator Synthesis Using (C, A, B)-Pairs. *IEEE Transactions on Automatic Control*, 25(6):1133–1138, 1980. ISSN 0018-9286. doi: 10.1109/TAC.1980.1102515.

Semiconductor Industry Association. The Final International Technology Roadmap for Semiconductors, 2015. URL `https://www.semiconductors.org/wp-content/uploads/2018/06/0_2015-ITRS-2.0-Executive-Report-1.pdf`.

P. Singh, M. Chen, L. Carlone, S. Karaman, E. Frazzoli, and D. Hsu. Supermodular Mean Squared Error Minimization for Sensor Scheduling in Optimal Kalman Filtering. In *American Control Conference*, pages 5787–5794, Seattle, WA, USA, 2017. IEEE. ISBN 978-1-5090-5992-8. doi: 10.23919/ACC.2017.7963857.

T. Singh, J. Swevers, and G. Pipeleers. Concurrent H_2/H_∞ Feedback Control Design with Optimal Sensor and Actuator Selection. In *International Workshop on Advanced Motion Control*, pages 223–228, Tokyo, Japan, 2018. IEEE. ISBN 978-1-5386-1946-9. doi: 10.1109/AMC.2019.8371092.

A. Stoorvogel and J. van der Woude. The Disturbance Decoupling Problem with Measurement Feedback and Stability for Systems with Direct Feedthrough Matrices. *Systems & Control Letters*, 17(3):217–226, 1991. ISSN 01676911. doi: 10.1016/0167-6911(91)90067-O.

A. A. Stoorvogel. The H_∞ Control Problem: A State Space Approach, 2000. URL `http://wwwhome.math.utwente.nl/~stoorvogelaa/book2.pdf`.

H. Subawalla, V. P. Paruchuri, A. Gupta, H. G. Pandit, and R. R. Rhinehart. Comparison of Model-Based and Conventional Control: A Summary of Experimental Results. *Industrial & Engineering Chemistry Research*, 35(10):3547–3559, 1996. ISSN 0888-5885. doi: 10.1021/ie950686h.

T. Summers. Actuator Placement in Networks Using Optimal Control Performance Metrics. In *Conference on Decision and Control*, pages 2703–2708, Las Vegas, NV, USA, 2016. IEEE. ISBN 978-1-5090-1837-6. doi: 10.1109/CDC.2016.7798670.

T. H. Summers, F. L. Cortesi, and J. Lygeros. On Submodularity and Controllability in Complex Dynamical Networks. *IEEE Transactions on Control of Network Systems*, 3(1):91–101, 2016. ISSN 2325-5870. doi: 10.1109/TCNS.2015.2453711.

J. A. Taylor, N. Luangsomboon, and D. Fooladivanda. Allocating Sensors and Actuators via Optimal Estimation and Control. *IEEE Transactions on Control Systems Technology*, 25(3):1060–1067, 2017. ISSN 1063-6536. doi: 10.1109/TCST.2016.2575799.

H. Thompson and K. Vogiatzis. Heat Balance and Thermal Management of the TMT Observatory. In *Astronomical Telescopes + Instrumentation*, page 915012, Montreal, Canada, 2014. SPIE. doi: 10.1117/12.2057152.

Top Gear. Richard Hammond Drives a F1 Car, 2007. URL `https://www.youtube.com/watch?v=EGUZJVY-sHo`. [January 21, 2019].

C. Toumazou, G. Moschytz, B. Gilbert, and G. Kathiresan. *Trade-Offs in Analog Circuit Design*. Springer, 2002. ISBN 978-1-4020-7037-2. doi: 10.1007/b117184.

H. L. Trentelman, A. A. Stoorvogel, and M. Hautus. *Control Theory for Linear Systems*. Springer, 2001. ISBN 978-1-4471-1073-6. doi: 10.1007/978-1-4471-0339-4.

U. Vaidya and M. Fardad. On Optimal Sensor Placement for Mitigation of Vulnerabilities to Cyber Attacks in Large-Scale Networks. In *European Control Conference*, pages 3548–3553, Zurich, Switzerland, 2013. IEEE. ISBN 978-3-033-03962-9. doi: 10.23919/ECC.2013.6669723.

M. van de Wal and B. de Jager. A Review of Methods for Input/Output Selection. *Automatica*, 37(4):487–510, 2001. ISSN 00051098. doi: 10.1016/S0005-1098(00)00181-3.

M. van den Brink. Litho Today, Litho Tomorrow, 2016. URL `http://staticwww.asml.com/doclib/investor/investor_day/asml_20161031_03_Investor_Day_2016_Litho_today_-_Litho_tomorrow_MvdBrink.pdf`.

D. van den Hurk, S. Weiland, and K. van Berkel. Modeling and Localized Feedforward Control of Thermal Deformations Induced by a Moving Heat Load. In *International Symposium on Control Systems*, pages 171–178, Tokyo, Japan, 2018. IEEE. ISBN 978-4-9077-6458-6. doi: 10.23919/SICEISCS.2018.8330172.

A. Varga and B. Anderson. Accuracy Enhancing Methods for the Frequency-Weighted Balancing Related Model Reduction. In *Conference on Decision and Control*, pages 3659–3664, Orlando, FL, USA, 2001. IEEE. ISBN 0-7803-7061-9. doi: 10.1109/CDC.2001.980430.

K. W. Verkerk. *Improved Accuracy of Flexible Systems by State Estimation: Applied to High-Precision Motion Systems*. Ph.d. dissertation, Eindhoven Univeristy of Technology, 2018. URL `https://research.tue.nl/en/publications/improved-accuracy-of-flexible-systems-by-state-estimation-applied`.

P. T. M. Vermeulen, A. W. Heemink, and J. R. Valstar. Inverse Modeling of Groundwater Flow using Model Reduction. *Water Resources Research*, 41(6), 2005. ISSN 00431397. doi: 10.1029/2004WR003698.

Q.-G. Wang. *Decoupling Control*, volume 285. Springer, Berlin, 2006. ISBN 978-3-540-44128-1. doi: 10.1007/3-540-46151-5.

Y.-S. Wang, N. Matni, and J. C. Doyle. Localized LQR Optimal Control. In *Conference on Decision and Control*, pages 1661–1668, Los Angeles, CA, USA, 2014. IEEE. ISBN 978-1-4673-6090-6. doi: 10.1109/CDC.2014.7039638.

Wikipedia. 7 nanometer, 2018a. URL `https://en.wikipedia.org/wiki/7_nanometer`. [December 12, 2018].

Wikipedia. Moore's Law, 2018b. URL `https://en.wikipedia.org/wiki/Moores_law`. [December 4, 2018].

W. M. Wonham. *Linear Multivariable Control*. Springer, 1985. ISBN 978-1-4612-7005-8. doi: 10.1007/978-1-4612-1082-5.

P. Wortelboer. *Frequency-Weighted Balanced Reduction of Closed-Loop Mechanical Servo-Systems: Theory and Tools*. Ph.d. dissertation, Delft University of Technology, 1994.

P. Wortelboer and O. Bosgra. Generalized Frequency Weighted Balanced Reduction. In *Conference on Decision and Control*, pages 2848–2849, Tucson, AZ, USA, 1992. IEEE. ISBN 0-7803-0872-7. doi: 10.1109/CDC.1992.371294.

P. M. R. Wortelboer, M. Steinbuch, and O. H. Bosgra. Iterative Model and Controller Reduction using Closed-Loop Balancing, with Application to a Compact Disc Mechanism. *International Journal of Robust and Nonlinear Control*, 9(3):123–142, 1999. ISSN 1049-8923. doi: 10.1002/(SICI)1099-1239(199903)9:3<123::AID-RNC396>3.0.CO;2-T.

C. Yang, W. Wang, and H. Xie. An Efficiency Model and Optimal Control of the Vehicular Diesel Exhaust Heat Recovery System using an Organic Rankine Cycle. *Energy*, 171:547–555, 2019. ISSN 03605442. doi: 10.1016/j.energy.2018.12.219.

J. Yang, H. Cui, S. Li, and A. Zolotas. Optimized Active Disturbance Rejection Control for DC-DC Buck Converters With Uncertainties Using a Reduced-Order GPI Observer. *IEEE Transactions on Circuits and Systems*, 65(2):832–841, 2018. ISSN 1549-8328. doi: 10.1109/TCSI.2017.2725386.

L. Zhao, Y. Yang, Y. Xia, and Z. Liu. Active Disturbance Rejection Position Control for a Magnetic Rodless Pneumatic Cylinder. *IEEE Transactions on Industrial Electronics*, 62(9):5838–5846, 2015. ISSN 0278-0046. doi: 10.1109/TIE.2015.2418319.

K. Zhou, J. C. Doyle, and K. Glover. *Robust and Optimal Control*. Pearson, 1996. ISBN 9780134565675. URL `https://www.pearson.com/us/higher-education/program/Zhou-Robust-and-Optimal-Control/PGM17767.html`.

K. Zhou, G. Salomon, and E. Wu. Balanced Realization and Model Reduction for Unstable Systems. *International Journal of Robust and Nonlinear Control*, 9(3):183–198, 1999. ISSN 1049-8923. doi: 10.1002/(SICI)1099-1239(199903)9:3<183::AID-RNC399>3.0.CO;2-E.

J. Ziegler, N. Nicholds, and N. Rochester. Optimum Settings for Automatic Controllers. *American Society of Mechanical Engineers*, 1942. URL `https://staff.guilan.ac.ir/staff/users/chaibakhsh/fckeditor_repo/file/documents/OptimumSettingsforAutomaticControllers(ZieglerandNichols,1942).pdf`.

List of Publications

Journal Articles

Peer-Reviewed — Published

- R. Merks, E. Kivits and S. Weiland. Constrained Order Observer Design for Disturbance Decoupled Output Estimation. *IEEE Control Systems Letters*, 3(1):49-54,2019. ISSN 2475-1456 doi: 10.1109/LCSYS.2018.2851539

Submitted

- R. Merks and S. Weiland. Constrained Order Controller Design for the Disturbance Decoupling Problem with Dynamic Measurement Feedback and Stability. Submitted to *IEEE Transactions on Automatic Control*.

In Preparation for Submission

- R. Merks and S. Weiland. Constrained Order H_2 Optimised Controller Design: Improvements to Control Relevant Order Reduction.
- R. Merks and S. Weiland. A Geometric Characterisation of the Minimal Controller Order for the H_2 Optimal Control Problem.

Conference Proceedings

Peer-Reviewed — Published

- R. Merks, E. Kivits and S. Weiland. Constrained Order Observer Design for Disturbance Decoupled Output Estimation. In *Conference on Decision and Control*, Miami Beach, FL, USA, 2018. IEEE. [Note: Published as the journal article above]
- M. Habets et al.. A Multiphysics Modeling Approach for Thermal Aberration Prediction and Control in Extreme Ultraviolet Lithography. In *Imaging and Applied Optics*, page AOM4B.2, Washington, D.C., USA, 2015. OSA. doi: 10.1364/AOMS.2015.AOM4B.2
- B. Milne et al.. Verification of Sinusoidal Steady State System Identification of a Phantom Omni Haptic Device using Data Driven Modeling. In *International Conference on Automation, Robotics and Applications*, pages 283-288, Queenstown, New Zealand, 2015. IEEE. doi: 10.1109/ICARA.2015.7081161

Peer-Reviewed — Accepted

- R. W. H. Merks, M. Mirzakhalili and S. Weiland. On the Non-optimality of Linear Quadratic Gaussian Balanced Truncation for Constrained Order Controller Design. In *European Control Conference*, Napels, Italy, 2019.

Abstracts

Not Peer-Reviewed — Published

- R. Merks and S. Weiland. Reduced Order Controller Design for Disturbance Decoupling Problems. In *Benelux Meeting on Systems and Control*, Soesterberg, the Netherlands, 2018.
- R. Merks and S. Weiland. Measures of Controllability and Observability for Large-scale Systems. In *Benelux Meeting on Systems and Control*, Spa, Belgium, 2017.
- R. Merks, M. Habets and S. Weiland. Thermal Control in Wafer Scanners using High Complexity Models. in *Benelux Meeting on Systems and Control*, Soesterberg, the Netherlands, 2016.
- R. Merks, M. Habets, S. Weiland and W. Coene. Irradiance Models for Projection Optics. In *Benelux Meeting on Systems and Control*, Lommel, Belgium, 2015.
- M. Habets, R. Merks, S. Weiland and W. Coene. Woofer-tweeter Adaptive Optics for EUV Lithography. In *Benelux Meeting on Systems and Control*, Lommel, Belgium, 2015.

Acknowledgements/Dankwoord

Het is heel gek, maar nu ik dit laatste stukje van mijn proefschrift aan het schrijven ben, begin ik pas echt te beseffen dat er een einde gaat komen aan een fantastisch avontuur. In het begin lijkt vier jaar aan individueel onderzoek een lange tijd, vooral als je nog niet precies weet welke richting je wilt inslaan. Achteraf gezien moet ik toch echt concluderen dat de tijd gevlogen is, maar ook dat het afronden van mijn proefschrift alles behalve een individuele prestatie geweest is. Ik ben daarom aan velen mijn dank verschuldigd—sommigen voor hun technische bijdrage en anderen voor hun gezelligheid, steun en toeverlaat—en hier heb ik gelukkig de kans om er een aantal specifiek in het zonnetje zetten.

Allereerst wil ik mijn eerste promotor, Siep Weiland, bedanken. Onze samenwerking begon iets meer dan vijf jaar geleden tijdens mijn afstudeeronderzoek dat, net als dit project, een samenwerking was tussen de TU/e en ASML. Op zowel technisch als op mentaal vlak zijn onze meetings, die vaak volgens een NS-achtig dienstschema verliepen, voor mij van onschatbare waarde geweest om dit proefschrift te maken tot wat het is. Het vertrouwen dat je mij hebt gegeven en de vrijheid die je me gegund hebt—zelfs toen ik na anderhalf jaar nog geen flauw idee had wat ik nu echt wilde onderzoeken—zijn met zekerheid de belangrijkste factoren geweest, om op dit moment met trots te kunnen kijken naar het resultaat van mijn eigen onderzoek. Al moet natuurlijk ook met trots gezegd worden dat jouw kritische vragen en het betwisten van “de typische aannames” ertoe geleid hebben dat dit boekje een aanzienlijke (en zeer gezonde) hoeveelheid Siep-visie uitstraalt. Siep, ik wil je daarom ontzettend bedanken voor alles!

Verder wil ik ook mijn promotor Hans Butler bedanken. Jouw kritische en frisse blik op het einde van het project hebben een zeer positieve invloed gehad op dit proefschrift.

I would like to extend my sincere gratitude towards the members of my committee: prof.dr.ir. Van de Wouw, prof.dr.ir. Heemink, prof.dr.ir. Stoustrup, dr.ir. Besselink and dr.ir. Mutsaers. Thank you for participating in the defence and for your efforts in reading my thesis during the summer holiday period. In particular, I would like to thank dr.ir. Besselink and dr.ir. Mutsaers for providing extensive (and extremely useful) feedback that has had a significant impact on the thesis.

In de richting van ASML ben ik de grootste dank verschuldigd aan Fokke. Het voelt voor mij als een voorrecht dat ik een praktisch georiënteerd onderzoek heb mogen uitvoeren, waarbij ik ook de vrijheid heb gekregen om mijn ogen wat verder op de horizon te houden. Verder wil ik Alex, Hans en Kees bedanken voor het feit dat ze altijd klaarstonden om ondersteuning te verlenen aan de persoon die

op het einde omschreven werd als “trouwens, er is er ook nog eentje op de TU/e”. Ook wil ik Jim en Dennis bedanken voor het delen van hun kennis met betrekking tot de BES-toepassing en de bijbehorende uitdagingen. Tot slot ben ik veel dank verschuldigd aan Marc, die te allen tijde een kritische blik bleef werpen op de koers die ik aan het varen was. Zonder al jullie hulp was het zeker niet gelukt om ergens tussen theorie en praktijk te landen.

Binnen mijn persoonlijke kringen wil ik allereerst mijn paranimf Henrik bedanken. Het feit dat ik dit stukje tijdens de introductieweek aan het schrijven ben, betekent dat we elkaar nu welgeteld elf jaar (plus minus een paar dagen) kennen. Terugdenkend aan deze periode komen er ongelofelijk veel mooie herinneringen in mij op, waarin vele liters koffie genuttigd zijn, we de nodige verhuizingen hebben meegemaakt, er natuurlijk genoeg geklaagd is; en boven alles, waarin we veel gelachen hebben. Maar, zonder enige twijfel is de reis naar Nieuw-Zeeland voor mij het hoogtepunt geweest binnen een vriendschaap waar ik ontzettend veel waarde aan hecht. Het feit dat jij straks het avontuur opzoekt in Australië—en dus geen paranimf meer kan zijn—is voor mij dan ook één van de drijfveren geweest om dit proefschrift op tijd af te krijgen. Ik wil jou en Ayla oprecht heel veel geluk wensen aan de andere kant van de wereld, al wil ik jullie niet in de waan laten dat zo’n afstand genoeg is om volledig aan mij te ontkomen. Nogmaals, heel veel plezier gewenst!

I would like to thank my master graduation students Lizan, Mahmood and Joshua who all had a significant impact on this thesis. Lizan, I am grateful that I was able to participate in your master graduation project, which mainly encouraged me to step out of my comfort zone and to step up my game on a theoretical level. You are a talented researcher and I am certain that you have a promising career ahead of you. Mahmood, I know that taking compliments is not really your thing, but it has been an honour and a pleasure to collaborate with you. You should be proud of your work and its results, which have already raised the eyebrows of several renowned experts. Joshua, it has been a joy to support you in your practical project at ASML and it was amazing to see how quickly you transformed my weird theoretical ideas into concrete results. I would like to wish you, your wife and the youngest member of your family all the best for the future.

Then, I would like to thank all the members of the CS group who, as a whole, made me feel at home since the first day of my master graduation project. We have shared a lot of good moments—and exchanged a great number of laughs—in the office, at conferences, in plenty of bars and at the particularly famous poker nights. There are too many people to thank—and I am certain that I will forget a few—but that will not stop me from trying. Thank you: David, Dhruv, Pepijn, Ruxandra, Rian, Feye, Jurre, Constantijn, Alina, Will, Tom, (my ex-neighbour) Henk Jan, Xiaodong, Patrick, Bahadir, Koen, Henrik (again), Michel, Sofie, Tuan, Giuseppe, Paul (2x), Daming, Amritam, Harm, Siep, Ioannis, Hans, Mircea, Veaceslav, Giulio, Maarten, Yutao and Tijs. I do, however, want to particularly extend my gratitude to the secretariat: Barbara(†), Diana, Hiltje and Lucia. I enjoyed the chats that we had, and I highly appreciate the continuous support that I received from you throughout my entire PhD project (also, I am voluntarily saying this and have not been bribed with candy)!

Verder wil ik de TU/e studiegenoten app-groep bedanken: Bas, Niels, Ruud, Henrik en Bart. Na vele pogingen om dingen te ondernemen (zoals skiën, poolen en een escape room), hebben we allemaal moeten concluderen dat onze kwaliteiten beter tot hun recht komen aan een tafel met wat drankjes erop. En ondanks onze drukke levens, hoop ik dat we elkaar nog jaren blijven zien en dat we ooit aan onze winter barbecue gaan toekomen!

Daarnaast wil ik ook Ayla bedanken, allereerst voor het feit dat je het Brabantse "Guus-uitje" geïntroduceerd hebt, maar daarnaast ook voor de gezelligheid die jouw opgewekte persoonlijkheid met zich meebrengt. Ik wil je—samen met Henrik—veel plezier in Australië wensen en daarnaast ook veel succes wensen met je verdediging, al ben ik er zeker van dat je dat niet nodig gaat hebben!

Als vrienden die ik ongeveer mijn halve leven ken, wil ik Robert en Bianca heel erg bedanken voor alle leuke, gezellige, maar vaak ook late avonden. Daarnaast wil ik Robert ook ontzettend bedanken voor het kaftontwerp van dit proefschrift (en de gezellige avonden die ik daarbij cadeau kreeg). Ik weet niet hoe je het voor elkaar gekregen hebt, maar het is compleet anders geworden dan ik dacht, en tegelijkertijd precies geworden wat ik wenste.

Ook ben ik veel dank verschuldigd aan mijn huisgenoten Tim en Koen. Na een lange dag schrijven aan dit proefschrift is er niets fijner dan lekker thuis te mogen komen, om in goed gezelschap te kunnen eten. De mate van gezelligheid is dan ook vaak te meten aan de ietwat grote porties die op onze borden belanden. Ik ben heel erg dankbaar voor jullie mentale steun en afleiding tijdens de laatste maanden van dit project. Maar ook ben ik dankbaar voor het feit dat jullie—bij wijze van extreme uitzondering—niet te erg oordeelden als ik doordeweeks een biertje voor het slapen deed.

Een dankwoord is natuurlijk niet compleet zonder ook mijn familie te bedanken. Omdat het kleinste foutje nog lang tegen mij gebruikt kan—en zal—worden (met een knipoog), durf ik me er alleen niet aan te wagen om jullie individueel te bedanken. Allereerst wil ik daarom de gehele familie in Best bedanken voor alle steun en gezelligheid gedurende mijn hele leven. Daarnaast ben ik natuurlijk net zoveel dank verschuldigd aan mijn familie in de Achterhoek. Ondanks dat ik jullie de laatste jaren minder heb gezien dan ik zou willen, ben ik oprecht heel blij dat ik dit speciale moment ook met jullie mag delen! Tot slot wil ik mijn bedankje aan jullie graag eindigen met een tegeltjeswijsheid: "Familie kan je misschien niet kiezen, maar het zijn wel degenen die er altijd voor je zijn".

Brenda, tot een paar jaar geleden kon ik jou nog als mijn kleine zusje zien, maar tegenwoordig zie ik niets anders meer dan een sterke en volwassen dame. Als broer en zus hebben wij veel momenten gedeeld, maar tot nu toe is onze reis naar de Verenigde Staten voor mij het absolute hoogtepunt. Ik had die reis met niemand anders willen maken en kijk er nog vaak met veel plezier op terug. Tot slot wil ik je veel geluk toewensen, samen met je vriend Tjeerd—die op de tennisbaan beter bekend staat als "The Hammer". Ik ben echt ongelofelijk trots en blij dat ik jou mijn zus en paranimf mag noemen!

Maar boven alles ben ik natuurlijk de meeste dank verschuldigd aan mijn ouders. Zonder jullie onvoorwaardelijke steun en aanmoediging gedurende mijn hele leven, was ik nooit de persoon geworden die ik vandaag de dag ben. Wel moet ik (met een knipoog) bekennen dat mijn eigenzinnigheid—of was het nou eigenwijsheid, ik haal die twee altijd door elkaar—waarschijnlijk tot meer grijze haren heeft geleid dan jullie aanvankelijk gepland hadden. Lieve mam en pap, ik ben ongelofelijk dankbaar dat ik te allen tijde in het Frisopark welkom geweest ben—en hopelijk zal blijven—om een gezonde (Brabantse) hoeveelheid warmte en gezelligheid te ontvangen. Ik wil jullie nogmaals ontzettend bedanken voor alles!

Ruben Merks
Eindhoven, augustus 2019

About the Author

Ruben Merks was born on June 26, 1990 in Eindhoven, the Netherlands. After completing pre-university education in 2008 at Pleincollege Bisschop Bekkers in Eindhoven, he studied Electrical Engineering at Eindhoven University of Technology.

In 2015 he finished his master thesis on the topic "Thermal control for projection optics in extreme ultraviolet lithography" with a final grade of 10. The graduation project was performed in the control systems group, in collaboration with the company ASML. In the control systems group he started a PhD project directly after graduation; the results of which are presented in this dissertation. The PhD project is part of the Impuls 1 research program and is financed by ASML.

Currently he is a teacher and postdoctoral researcher in the Dynamics and Control group in the department of Mechanical Engineering at Eindhoven University of Technology.